VOLUME 104 PART A NUMBER 14 APRIL 1957

The Proceedings

OF

THE INSTITUTION OF ELECTRICAL ENGINEERS

FOUNDED 1871: INCORPORATED BY ROYAL CHARTER 1921

PART A

POWER ENGINEERING

SAVOY PLACE · LONDON W.C.2

Price Ten Shillings

THE INSTITUTION OF ELECTRICAL ENGINEERS

FOUNDED 1871 INCORPORATED BY ROYAL CHARTER 1921

PATRON: HER MAJESTY THE QUEEN

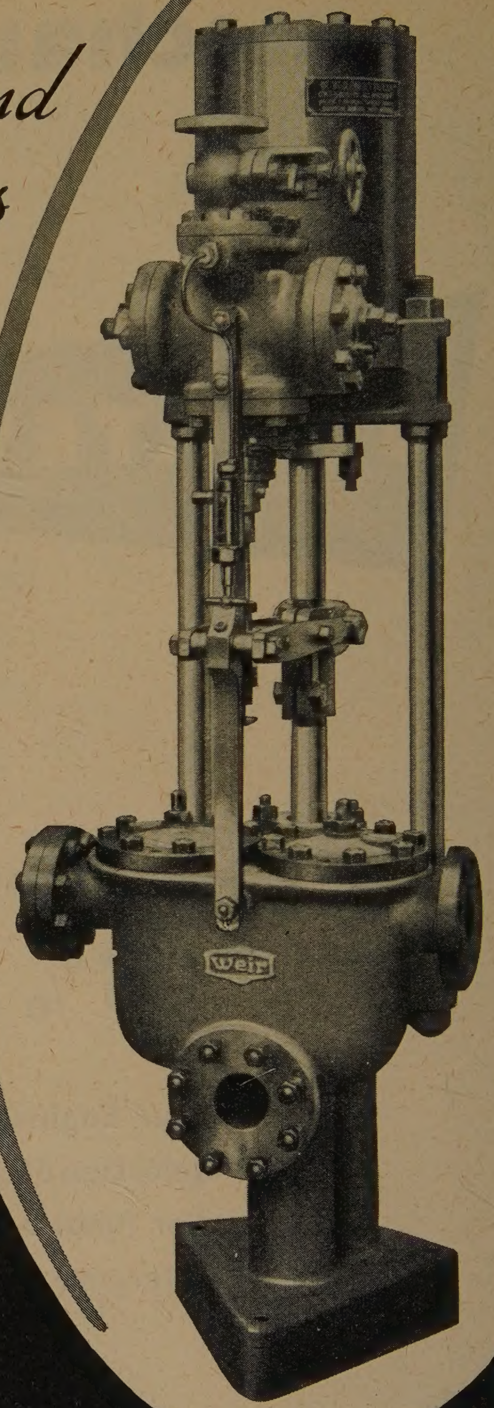

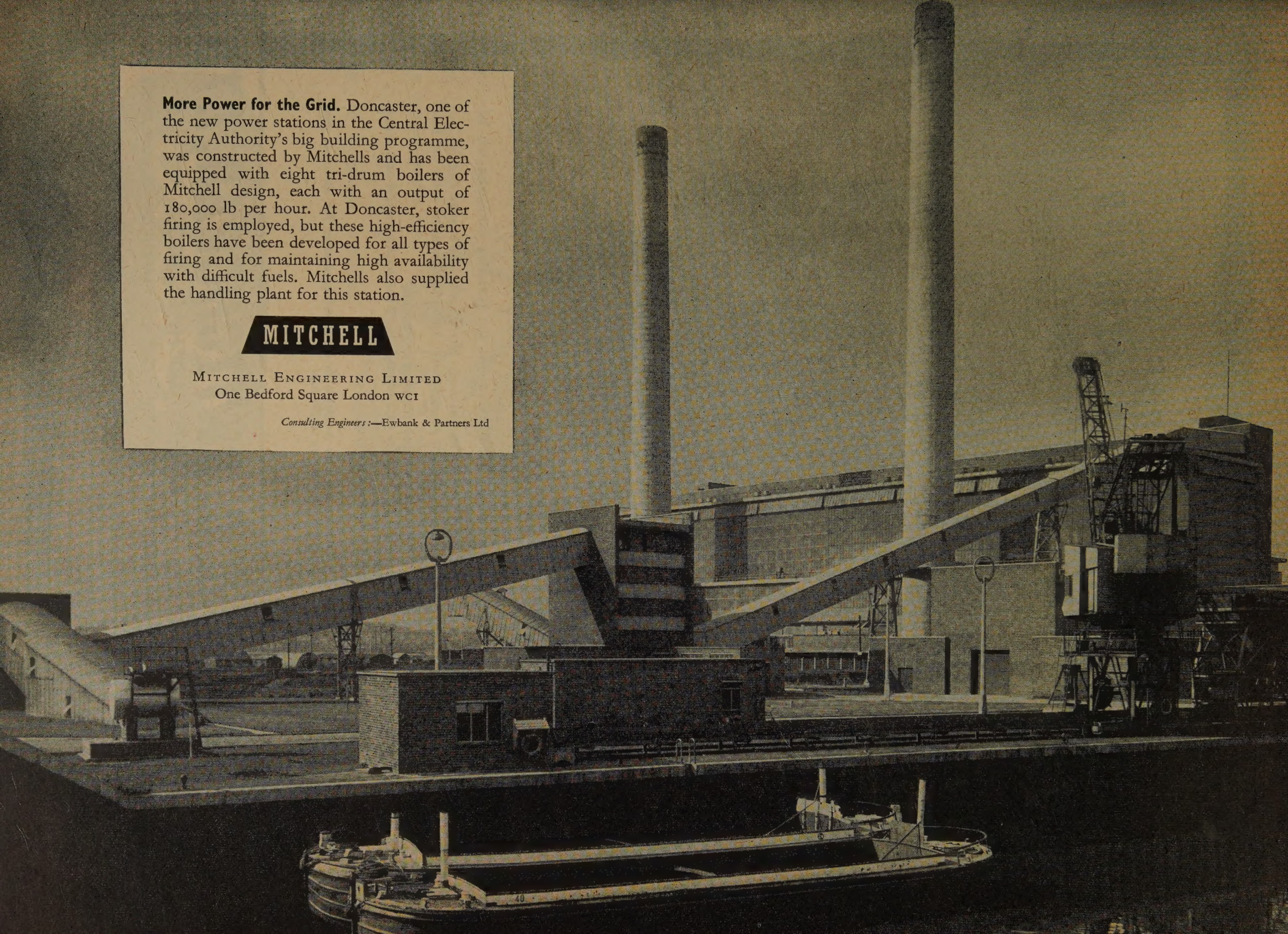
More Power for the Grid. Doncaster, one of the new power stations in the Central Electricity Authority's big building programme, was constructed by Mitchells and has been equipped with eight tri-drum boilers of Mitchell design, each with an output of 180,000 lb per hour. At Doncaster, stoker firing is employed, but these high-efficiency boilers have been developed for all types of firing and for maintaining high availability with difficult fuels. Mitchells also supplied the handling plant for this station.
MITCHELL
MITCHELL ENGINEERING LIMITED
One Bedford Square London WC1
Consulting Engineers:—Ewbank & Partners Ltd

FLAMEPROOF DIRECT-ON STARTER 150 h.p. 3·3 k.v.

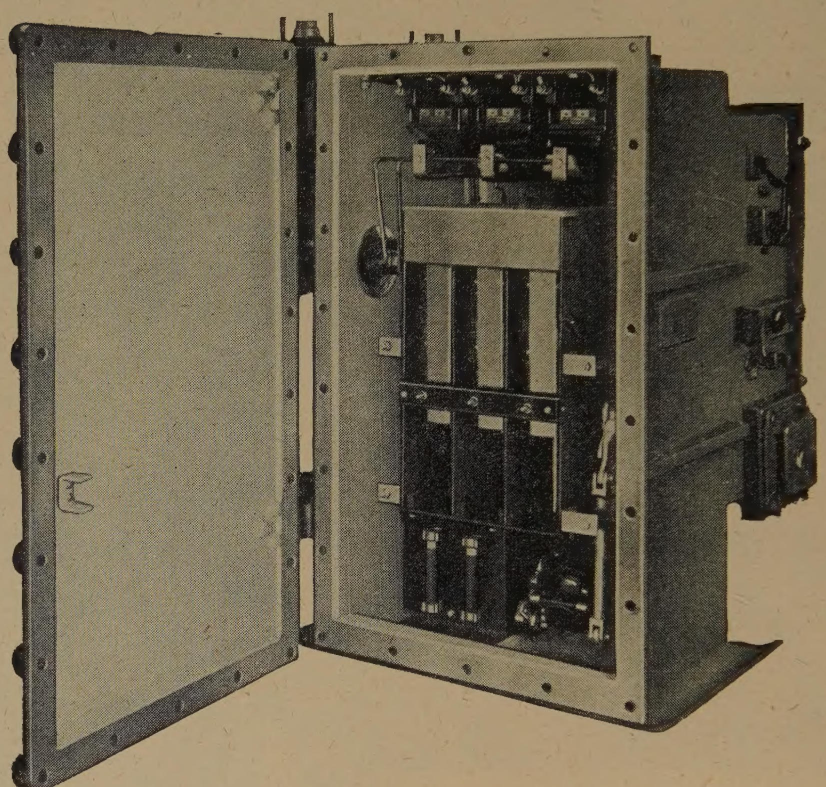

In addition to the basic components the following auxiliaries can be provided.

Control circuit 110 volt; alternatively, intrinsically safe control circuit.

Earth leakage protection; alternatively, *Sentryfugue* control relay for belt slip protection.

Brake Control Unit with overcurrent protection.

500 v.a. supply available for external lighting when brake control unit is not included.

Automatic sequence starting.

Ammeter.

3·3 k.v. Starters are also available in industrial enclosures for direct-on and stator/rotor starting up to 200 h.p.

M. & C. SWITCHGEAR, LTD.

KIRKINTILLOCH, GLASGOW.

LONDON OFFICE, 36 VICTORIA ST., S.W.1. SHEFFIELD OFFICE, OLIVE GROVE RD.

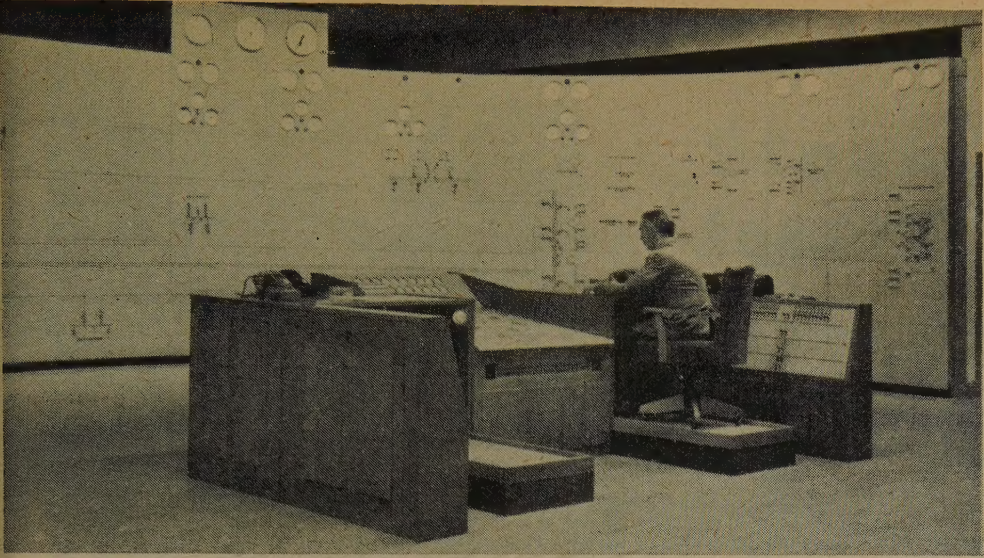

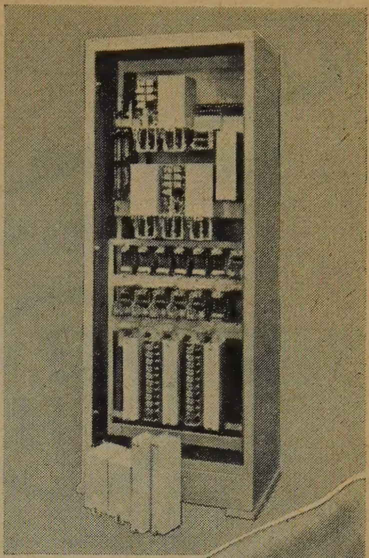

A typical G.E.C. remote supervisory control room, with (right) a typical private automatic exchange unit. G.E.C. remote supervisory control provides the power engineer with the means of controlling power distribution from a central control room, and with speech facilities, long-range meter readings, and state-of-switchgear indications.

It's a small world . . .

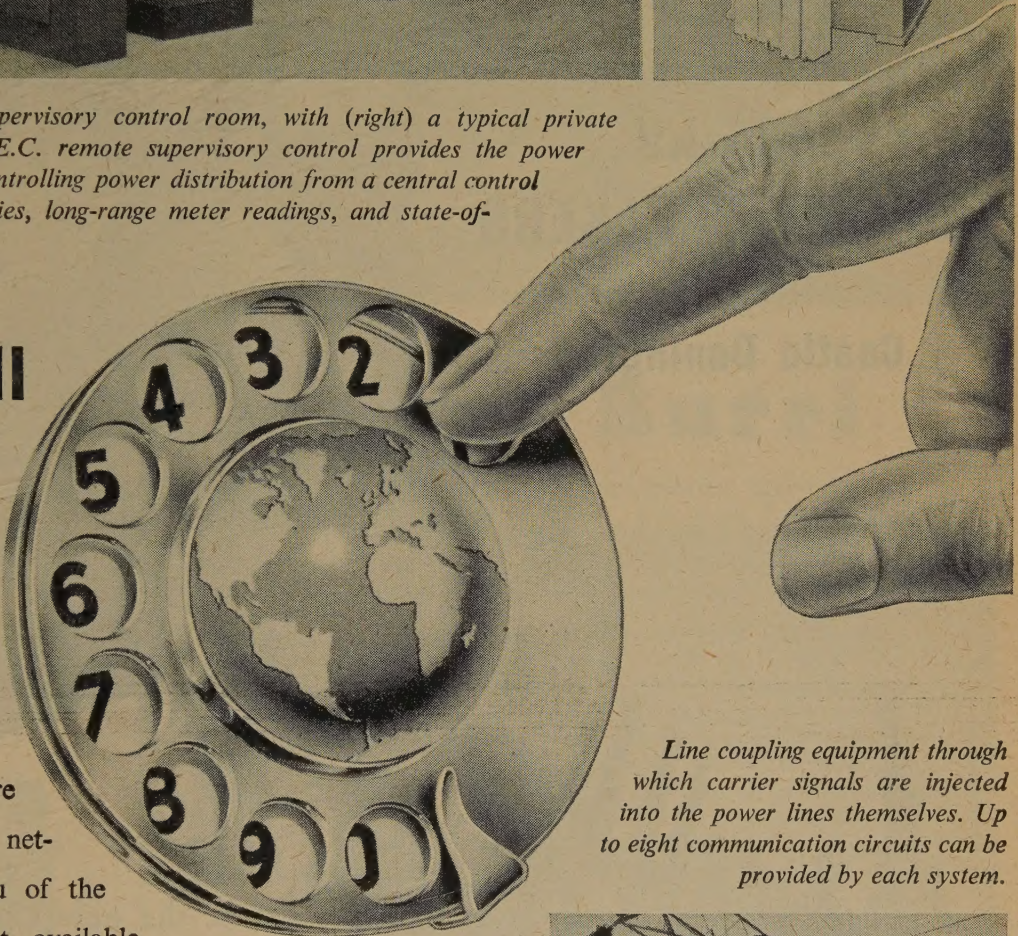

G.E.C. telecommunication systems bridge the seas, span deserts, level mountain ranges. If you want a private intercommunication system, or are planning a comprehensive network, let G.E.C. tell you of the wide range of equipment available.

Line coupling equipment through which carrier signals are injected into the power lines themselves. Up to eight communication circuits can be provided by each system.

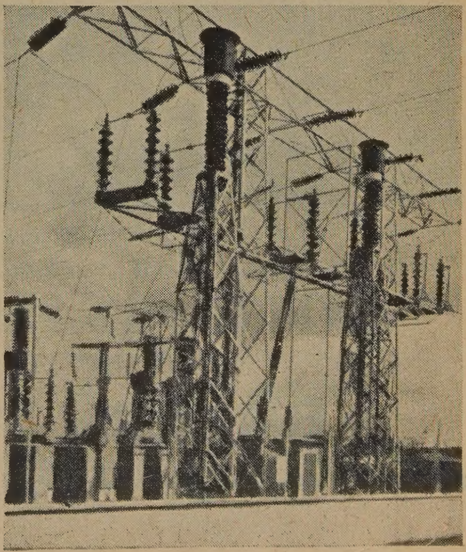

G.E.C.

THE GENERAL ELECTRIC COMPANY LTD. OF ENGLAND

TELEPHONE, RADIO AND TELEVISION WORKS, COVENTRY

B T-H

275-kV CIRCUIT-BREAKERS at Castle Donington

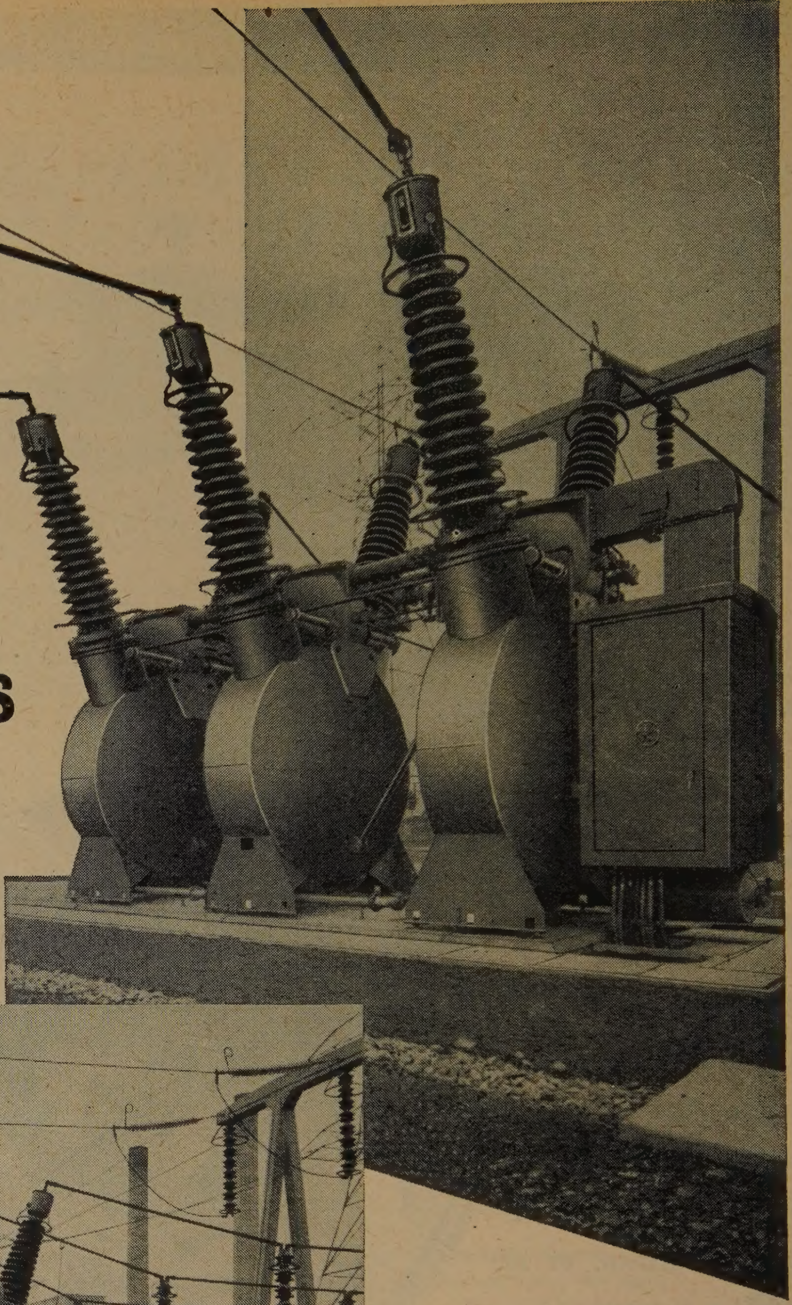

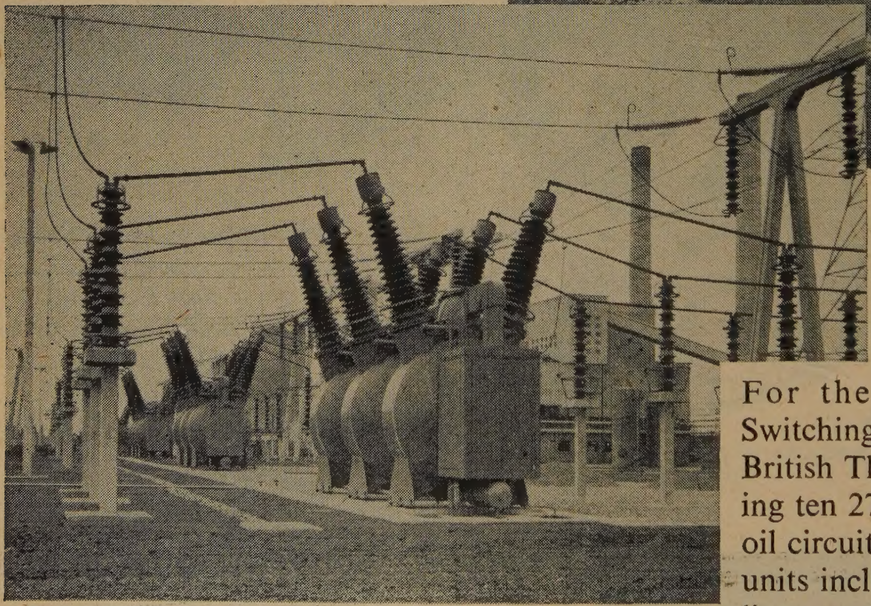

Some of the BTH circuit-breakers on site at Castle Donington, C.E.A. East Midlands Division.

For the new C.E.A. Super Grid Switching Station at Castle Donington, British Thomson-Houston are supplying ten 275-kV, 7,500 MVA lenticular oil circuit-breakers. Each phase of the units includes four breaks shunted by linear resistors which ensure an equal distribution of voltage between breaks and effectively control switching overvoltages.

BRITISH THOMSON-HOUSTON

THE BRITISH THOMSON-HOUSTON COMPANY LIMITED · WILLESDEN · ENGLAND

Member of the AEI group of companies

A5107

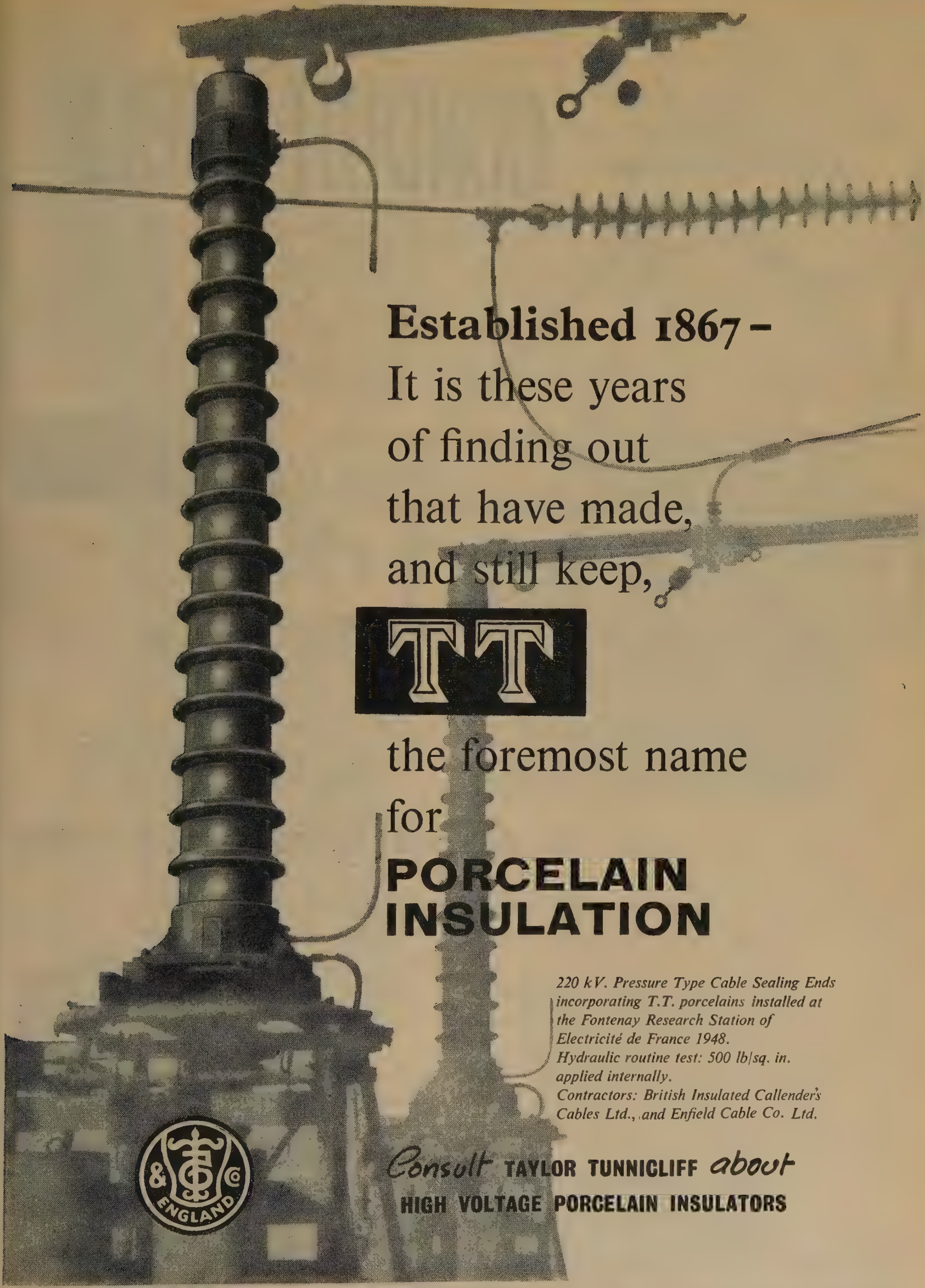
Established 1867 –
It is these years
of finding out
that have made,
and still keep,
TT
the foremost name
for
PORCELAIN
INSULATION
220 kV. Pressure Type Cable Sealing Ends incorporating T.T. porcelains installed at the Fontenay Research Station of Electricité de France 1948.
Hydraulic routine test: 500 lb/sq. in. applied internally.
Contractors: British Insulated Callender's Cables Ltd., and Enfield Cable Co. Ltd.
T & Co ENGLAND
Consult TAYLOR TUNNICLIFF about
HIGH VOLTAGE PORCELAIN INSULATORS

In the production of these insulated shrouds and for potting transformers, South Wales Switchgear Ltd. use 'Araldite' casting resins. For every branch of electrical engineering, 'Araldite' offers advantages which make it invaluable. These include remarkable adhesion to metals and ceramics, excellent electrical properties, stability and resistance to moisture. The two units illustrated are an insulated shroud for a 33kV switchgear earthing device and a 3-phase voltage transformer, ratio 6600/110V, 200VA.

Earth... and potting

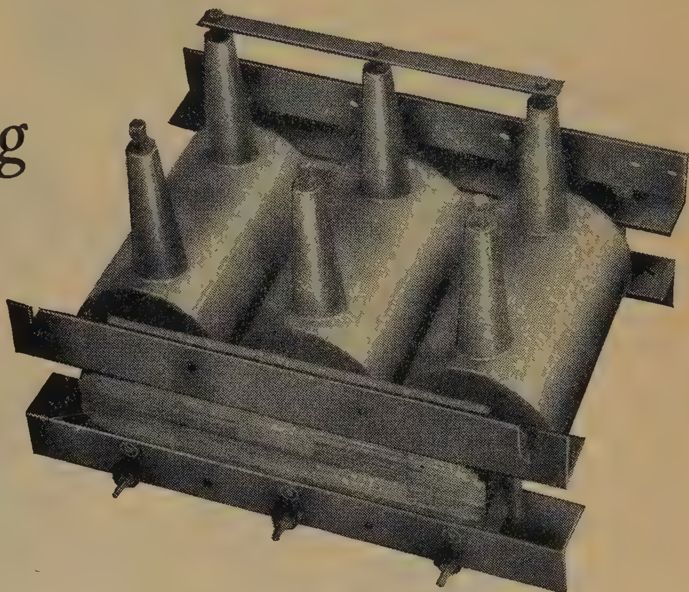

'Araldite' epoxy resins have a remarkable range of characteristics and uses:

They are used

* **for bonding metals, porcelain, glass, etc.**
* **for casting high grade solid insulation**
* **for impregnating, potting or sealing electrical windings and components**
* **for producing glass fibre laminates**
* **for producing patterns, models, jigs and tools**
* **as fillers for sheet metal work**
* **as protective coatings for metal, wood and ceramic surfaces**

'Araldite' *epoxy resins*

'Araldite' is a registered trade name

Aero Research Limited *A Ciba Company. Duxford, Cambridge. Tel: Sawston 2121*

AP. 264-233

INDEX OF ADVERTISERS

THE PROCEEDINGS OF
THE INSTITUTION OF ELECTRICAL ENGINEERS

EDITED UNDER THE SUPERINTENDENCE OF W. K. BRASHER, C.B.E., M.A., M.I.E.E., SECRETARY

VOL. 104. PART A. No. 14. APRIL 1957

621.313.333 : 621.34.677.01

Paper No. 1988 U
Feb. 1956

A SELF-OSCILLATING INDUCTION MOTOR FOR SHUTTLE PROPULSION

By E. R. LAITHWAITE, M.Sc., Associate Member, and P. J. LAWRENSON, B.Sc., Student.

(*The paper was first received* 22*nd July, and in revised form* 27*th October*, 1955. *It was published in February*, 1956, *and was read before the* UTILIZATION SECTION 15*th November, and the* NORTH-WESTERN UTILIZATION GROUP 11*th December*, 1956, *and the* NORTH MIDLAND UTILIZATION GROUP 19*th February*, 1957.)

SUMMARY

An induction motor can be constructed in such a way as to produce a magnetic field travelling in a straight line. Such a device can be used to propel a shuttle across a loom. A stator arrangement is described by which the shuttle can be caused to oscillate without the use of switches. With suitable design there is an inherently stable condition. Expressions are derived for the amplitude and period of this oscillation, for an unloaded motor, and for a motor operating against a constant load force. These are used to derive theoretical curves and phase-plane diagrams which are compared with those obtained in practice. Proposed practical schemes are discussed.

LIST OF PRINCIPAL SYMBOLS

v_s = Synchronous speed.
p = Pole pitch.
f = Stator supply frequency.
x_1 and x_2 = Distances of "rotor" from centre of oscillation.
v_1 and v_2 = Particular velocities attained.
v = Velocity at any position.
R = Rotor resistance.
X = Rotor leakage reactance.
$n = R/X$.
a_m = Maximum motor acceleration.
σ = Fractional slip.
a = "Rotor" acceleration.
a' = "Rotor" deceleration.
s_1 = Distance travelled during acceleration.
s_2 = Distance travelled during deceleration.
v' = Velocity at centre for stable oscillation.
t_1 and t_2 = Time periods corresponding to s_1 and s_2 respectively.
β = Loading factor.

(1) INTRODUCTION

If the stator of a conventional induction motor could be cut open along one side and unrolled, as shown in Fig. 1, the arrangement of the stator windings remaining otherwise unaltered, the resulting stator would produce a *travelling* magnetic field, instead of the *rotating* field of the original machine. The speed of the field v_s would be given by

$$v_s = 2pf$$

where p is the pole pitch and f the frequency of the stator supply.

If electrically conducting material were placed in such a field it would be accelerated towards the speed v_s and the arrangement could be said to constitute a "linear" induction motor.

In recent years such devices have been used for accelerating aircraft on take-off[1] and for pumping liquid metal.[2] It has also been proposed to use the linear motor for propelling a shuttle across a loom.[3,4] Such a system would clearly utilize one of the inherent advantages of an induction motor, that of requiring no connections to the moving part.

(2) SHUTTLE PROPULSION

In the earliest form of hand-loom the shuttle carrying the weft was pushed from side to side through the shed formed by the warp threads. The invention of the "flying shuttle" introduced the idea of striking the shuttle at each side of the loom in turn. In this case the shuttle is given a high acceleration over a short distance. During this operation enough energy is imparted to it to carry it through the shed against the friction of the warp threads, so that it arrives at the other side before a certain specified time. One such traverse of the shed is called a "pick." In order to guarantee the arrival of the shuttle, which must inevitably work against a load which varies as between one pick and the next, it is necessary to begin with far more energy than is needed to overcome friction. This means that the shuttle emerges with considerable velocity and has to be brought to rest in a short distance.

The disadvantages of this system are as follows:

(*a*) The spool of weft being carried by the shuttle breaks up if subjected to too high an acceleration. This sets an upper limit to the weaving speed for a given type of spool.

(*b*) The wear of parts because of the impulsive nature of the drive and stop is considerable.

(*c*) If the shuttle is improperly struck it may fail to enter the shed.

An alternative method of propulsion consists in having a cylinder at each side of the loom from which the shuttle is

Mr. Laithwaite and Mr. Lawrence are in the Electrical Engineering Department, University of Manchester.

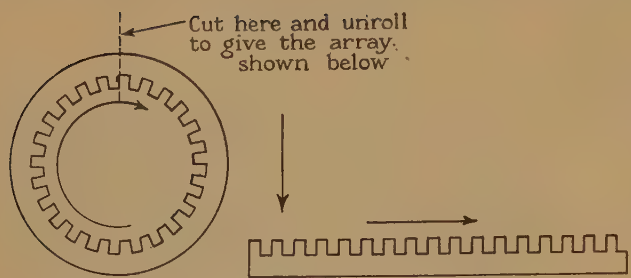

Fig. 1.—Development of a travelling magnetic field.

expelled by compressed air. By this method acceleration and deceleration can be effected over a rather greater distance, but higher accuracy in directing the shuttle is demanded than in the mechanical-impulse method, because the shuttle must enter each cylinder properly at the end of its travel and, by the very nature of the system, the shuttle must fit fairly closely into the cylinder.

The use of induction-motor propulsion is an attempt to obtain three advantages: first, continuous acceleration and deceleration of the shuttle over the entire length of its travel, thus reducing accelerations to a relatively low value; secondly, very little wearing of parts; and thirdly, at the start of the travel the shuttle is travelling at its slowest and is not likely to cause much damage if it fails to enter the shed.

In the reference already mentioned[3] the reversal of the direction of motion of the shuttle was effected by reversing two phases of the supply to the stator at the appropriate time. This appears to impose a serious limitation on the device, since the switching arrangement is called upon to perform between 100 and 200 operations per minute continuously. It must also be borne in mind that, since the "rotor" of the motor—in this case the shuttle—only occupies a small fraction of the stator, the stator current will be mainly magnetizing and heavily lagging.

The present paper describes a method of connection of the stator coils so that a continuous oscillation of stable amplitude is possible without any switching whatsoever.

(3) METHOD OF OBTAINING SELF-OSCILLATION

The stator windings may be arranged in two halves as shown in Fig. 2, so that the travelling field produced by each half is directed towards the centre of the stator. For the motor to oscillate with a stable amplitude, it is necessary for it to have a speed/force characteristic of the form shown in Fig. 3; i.e. the leakage-reactance/resistance ratio should be such as to produce a maximum in the force at a speed greater than zero.

Fig. 2.—Arrangement of the travelling fields.

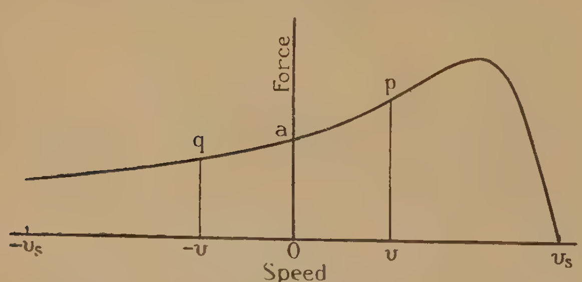

Fig. 3.—Speed/force characteristic of the motor.

Suppose the "rotor" to be at rest at position A, Fig. 2, distance x_1 from the centre. During its acceleration time from A to the centre it will be operating on the part *ap*, say, of the speed/force characteristic, as shown in Fig. 3. It will therefore have attained a speed v before it crosses the centre line. On entering the reverse field, it is immediately operating at point q on the characteristic and will be brought to rest by operation along the portion *qa*. Since its decelerating force is always less than its accelerating force, it will come to rest at a point B (Fig. 2) such that $x_2 > x_1$.

Thus, each successive run will produce a rest position further from the centre until some point is reached where the rotor attains a speed very close to the synchronous speed v_s, beyond which no further increase in amplitude can result. The rotor will now oscillate with stable amplitude. The action can be summarized by a diagram such as Fig. 4, in which the left-hand half of Fig. 3 is drawn as a mirror image about the vertical axis.

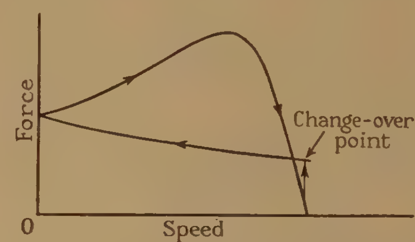

Fig. 4.—Cycle of operation for a stable amplitude on no-load.

So far, it has been assumed that (*a*) the characteristics of the motor under the transient conditions required for this type of operation are essentially of the same form as the steady-state characteristics, (*b*) the characteristics of a motor of the form described with a short rotor inside a long stator are of similar form to those for a conventional induction motor, and (*c*) the motor is operating on no-load.

(3.1) Oscillation of a Loaded Motor

The characteristic of the load against which a shuttle operates is almost certainly non-linear and is probably variable as between one pick and the next. In order to form some idea of the behaviour of the linear induction motor under working conditions, it is assumed that the load consists of a constant force at all speeds whose direction is opposite to the velocity. Thus, if the speed/force characteristic of the motor is of the form shown by the continuous lines of Fig. 5(*a*), on the acceleration portion of the curve the load force must be subtracted from the motor characteristic, yielding a net accelerating force/speed curve shown (broken) at AB. During deceleration the corresponding curve will be shown at CD, obtained by adding the load force to the motor braking force.

The resulting operating characteristic is shown in Fig. 5(*b*), from which the general behaviour of the system may be predicted as follows: If the rotor starts from rest a distance from the centre such that it fails to reach a velocity v_1 [Fig. 5(*b*)] by the time it has reached the centre, it must produce a damped oscillation, since, during each pick, it is undergoing deceleration of a greater value than the corresponding acceleration. However, if the rotor starts from rest at a greater distance from the centre than the one above, it will reach a velocity v_2, greater than v_1. There should be a value of v_2 above which build-up of oscillation, as described in the unloaded case, will occur, culminating in a stable cycle of operations as shown by the arrows in Fig. 5(*b*). This value of v_2 will always be obtainable provided that the load force is not a large proportion of the total available accelerating force of the machine.

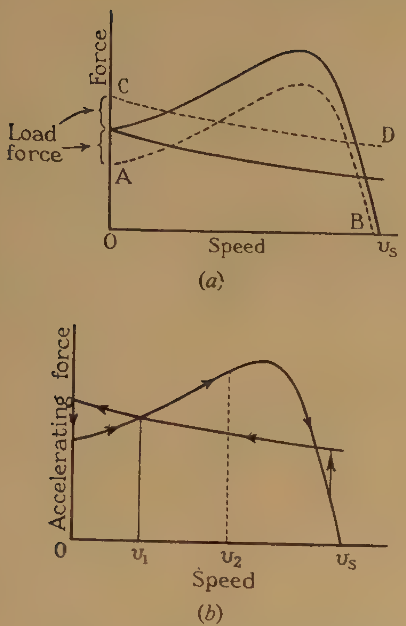

Fig. 5.—Operation against a load.

(a) Resultant force/speed characteristics with a constant friction load.
(b) Cycle of operation for a stable amplitude.

(4) APPLICATION TO WEAVING

The linear motor operating without switches in the manner described will set up its own amplitude and frequency of oscillation. The requirements of the loom are that the amplitude of oscillation of the shuttle shall be somewhat greater than the width of the finished cloth; that the shuttle shall be outside the shed whilst various other functions are performed, principally heald changing and beat-up; and that the frequency shall be that required to give the desired weaving speed.

This type of shuttle propulsion therefore makes a demand upon the design of a loom to the extent that the shuttle shall be the mechanism from which all other functions are timed. Before the device can be applied to a loom, however, it must be modified to ensure that the amplitude of oscillation is not dependent on the possible changes in load. It is therefore necessary to investigate the variation of the stable amplitude with load.

The quantities which will affect the amplitude and frequency are the R/X ratio of the motor, the maximum accelerating force available, the synchronous speed of the field, and the magnitude of the load force.

Accordingly it was decided to carry out a more detailed investigation of the nature of the oscillations. The prime points of interest were, first, the ability of the designer to fix the amplitude and period of the oscillation by suitable choice of values of v_s and R/X; secondly, that it might be possible to obtain fine control of amplitude by varying the supply voltage, so that in the weaving of a thicker cloth where the average load force would be higher, the supply voltage could be adjusted to give the required stable amplitude; and thirdly, to investigate the effect of load upon the stable amplitude and frequency as mentioned earlier.

(5) THEORETICAL INVESTIGATIONS

Since the transient behaviour of induction motors is extremely complex, and since the period of the proposed oscillation is very long compared with that of a normal a.c. supply, it was decided to begin the investigation by considering the motor to be working under steady-state conditions at all times. This being so, it is possible to use the simple steady-state formula for the speed/force characteristic and to compare the results with those obtained in practice.

The formula for the acceleration produced by the induction motor at speed v is therefore assumed to be

$$a = \frac{2a_m(n\sigma)}{(n^2 + \sigma^2)} \quad . \quad . \quad . \quad . \quad . \quad . \quad . \quad (1)$$

where a_m is the maximum acceleration, n is the R/X ratio and σ is the fractional slip, equal to $(1 - v/v_s)$.

(5.1) No-Load Running

Eqn. (1) refers to the accelerating part of the cycle shown in Fig. 4. The decelerating portion is given by the equation

$$a' = 2a_m\left[\frac{n(2-\sigma)}{n^2 + (2-\sigma)^2}\right] \quad . \quad . \quad . \quad . \quad (2)$$

Thus, for the cross-over point beyond which stable running occurs, $a = a'$, whence

$$\sigma = 1 - \sqrt{(1 - n^2)} \text{ or } v = v_s\sqrt{\left[1 - \left(\frac{R}{X}\right)^2\right]} \quad . \quad (3)$$

During acceleration, the distance travelled, s_1, is given by

$$s_1 = \int_0^{v'} \frac{v}{a}dv \quad . \quad . \quad . \quad . \quad . \quad . \quad . \quad (4)$$

where v' is the velocity attained at the centre. For the distance, s_2, traversed during deceleration

$$s_2 = -\int_{v'}^{0} \frac{v}{a'}dv \quad . \quad . \quad . \quad . \quad . \quad . \quad . \quad (5)$$

Stable running will occur when $s_1 = s_2$.

Evaluation of s_1 and s_2 from eqns. (4) and (5) using the expressions for a and a' from eqns. (1) and (2) yields the equation for v' as follows:

$$\frac{1}{n^2}\left(\frac{v'}{v_s}\right)^3 + 3\left(\frac{v'}{v_s}\right) = 3 \text{ arc tanh}\left(\frac{v'}{v_s}\right) \quad . \quad . \quad . \quad (6)$$

Fig. 6 shows a graph of v'/v_s plotted against n, and it can be seen that for $R/X < 1/2$ synchronous speed is almost attained at the centre point for stable running.

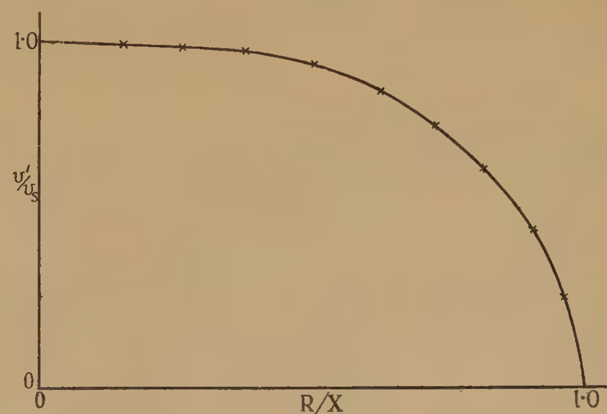

Fig. 6.—Speed at centre as a function of R/X [from eqn. (6)].

The total amplitude $(s_1 + s_2)$ evaluated from eqns. (4) and (5) is given by

$$s_1 + s_2 = \frac{v_s^2}{2a_m}\left\{\frac{1}{n}\left(\frac{v'}{v_s}\right)^2 - n\log\left[1 - \left(\frac{v'}{v_s}\right)^2\right]\right\}$$

Direct substitution from eqn. (6) is not possible, but eqn. (6) can be used to reduce the expression for $(s_1 + s_2)$ to a form in which approximation can be used. Thus, the stable amplitude can be shown to be

$$s_1 + s_2 = \frac{v_s^2}{2a_m}\left\{\frac{1}{n}\left(\frac{v'}{v_s}\right)^2 - 2n\log\left[1 + \left(\frac{v'}{v_s}\right)\right] + \frac{2}{3n}\left(\frac{v'}{v_s}\right)^3 + 2n\left(\frac{v'}{v_s}\right)\right\} \quad . \quad . \quad . \quad . \quad (7)$$

and for $R/X < 1/2$ we can write $v'/v_s = 1$ and eqn. (7) becomes

$$s_1 + s_2 = \frac{v_s^2}{2a_m}\left(\frac{1\cdot67}{n} + 0\cdot614n\right)$$

Of the two terms $1\cdot67/n$ and $0\cdot614n$, the second is clearly much smaller than the first, since $n < 1/2$ and we may write

$$s_1 + s_2 \simeq \frac{5}{6}\frac{v_s^2}{na_m} \quad . \quad . \quad . \quad . \quad . \quad . \quad (8)$$

The time occupied during acceleration, t_1, is given by

$$t_1 = \int_0^{v'} \frac{dv}{a} \quad . \quad . \quad . \quad . \quad . \quad . \quad . \quad (9)$$

and similarly the time, t_2, for deceleration is given by

$$t_2 = \int_{v'}^{0} -\frac{dv}{a'} \quad . \quad . \quad . \quad . \quad . \quad . \quad . \quad (10)$$

Thus, the total time $(t_1 + t_2)$ can be shown to be

$$t_1 + t_2 = \frac{v_s}{2a_m}\left[\frac{2}{n}\left(\frac{v'}{v_s}\right) + n\log\left(\frac{v_s + v'}{v_s - v'}\right)\right]$$

Again using eqn. (6), this equation can be reduced to

$$t_1 + t_2 = \frac{v_s}{2a_m}\left[2\left(n + \frac{1}{n}\right)\left(\frac{v'}{v_s}\right) + \frac{2}{3n}\left(\frac{v'}{v_s}\right)^3\right] \quad . \quad (11)$$

and for $R/X < 1/2$, we can write $v'/v_s = 1$ and

$$t_1 + t_2 = \frac{v_s}{2a_m}\left(\frac{8}{3n} + 2n\right)$$

Again assuming $2n \ll 8/3n$, which is true for $n < 1/2$, we can write

$$t_1 + t_2 \simeq \frac{8}{6}\frac{v_s}{na_m} \quad . \quad . \quad . \quad . \quad . \quad . \quad (12)$$

Thus, the average speed of the rotor, end to end, is seen to be given by

$$\frac{s_1 + s_2}{t_1 + t_2} \simeq \frac{5}{8}v_s \quad . \quad . \quad . \quad . \quad . \quad . \quad . \quad (13)$$

This may be an interesting design feature, since, if true in practice, it would imply that for a given width of loom, the weaving speed is simply set by v_s—i.e. by the pole pitch—for a given frequency, and is independent of a_m and R/X provided that the latter is less than 1/2.

It remains to be investigated, using the simple steady-state theory, whether load conditions differ to any great extent from the no-load conditions.

(5.2) Running on Load

When running on load, the load will be represented as a fraction of the maximum accelerating force, producing deceleration a_m/β, so that for the accelerating portion of the movement we can write

$$a = 2a_m\left(\frac{n\sigma}{n^2 + \sigma^2} - \frac{1}{2\beta}\right) \quad . \quad . \quad . \quad . \quad (14)$$

and for the decelerating portion,

$$a' = 2a_m\left[\frac{n(2-\sigma)}{n^2 + (2-\sigma)^2} + \frac{1}{2\beta}\right] \quad . \quad . \quad (15)$$

With the same technique as before, the expressions for s_1 and s_2 can be shown to be

$$s_1 = \frac{v_s^2\beta}{a_m}\left[2\beta n\left(\frac{v'}{v_s}\right) - \frac{1}{2}\left(\frac{v'}{v_s}\right)^2 + \frac{2\beta n}{(1-p_1^2)}\left\{\left(1 - \frac{n}{p_1}\right)\log\left[1 - \frac{\left(\frac{v'}{v_s}\right)}{\left(1 - \frac{n}{p_1}\right)}\right] - p_1^2(1 - np_1)\log\left[1 - \frac{\left(\frac{v'}{v_s}\right)}{(1 - np_1)}\right]\right\}\right] \quad . \quad . \quad . \quad . \quad (16)$$

$$s_2 = \frac{v_s^2\beta}{a_m}\left[-2\beta n\left(\frac{v'}{v_s}\right) + \frac{1}{2}\left(\frac{v'}{v_s}\right)^2 + \frac{2\beta n}{(1-p_2^2)}\left\{\left(1 - \frac{n}{p_2}\right)\log\left[1 + \frac{\left(\frac{v'}{v_s}\right)}{\left(1 - \frac{n}{p_2}\right)}\right] - p_2^2(1 - np_2)\log\left[1 + \frac{\left(\frac{v'}{v_s}\right)}{(1 - np_2)}\right]\right\}\right] \quad . \quad . \quad . \quad . \quad (17)$$

where $p_1 = \beta + \sqrt{(\beta^2 - 1)}$

and $p_2 = -\beta + \sqrt{(\beta^2 - 1)}$

Similarly the times t_1 and t_2 can be calculated, giving

$$t_1 = \frac{v_s\beta}{a_m}\left[-\left(\frac{v'}{v_s}\right) + \frac{2\beta n}{(1-p_1^2)}\left\{\log\left[1 - \frac{\left(\frac{v'}{v_s}\right)}{\left(1 - \frac{n}{p_1}\right)}\right] - p_1^2\log\left[1 - \frac{\left(\frac{v'}{v_s}\right)}{(1 - np_1)}\right]\right\}\right] \quad . \quad . \quad . \quad . \quad (18)$$

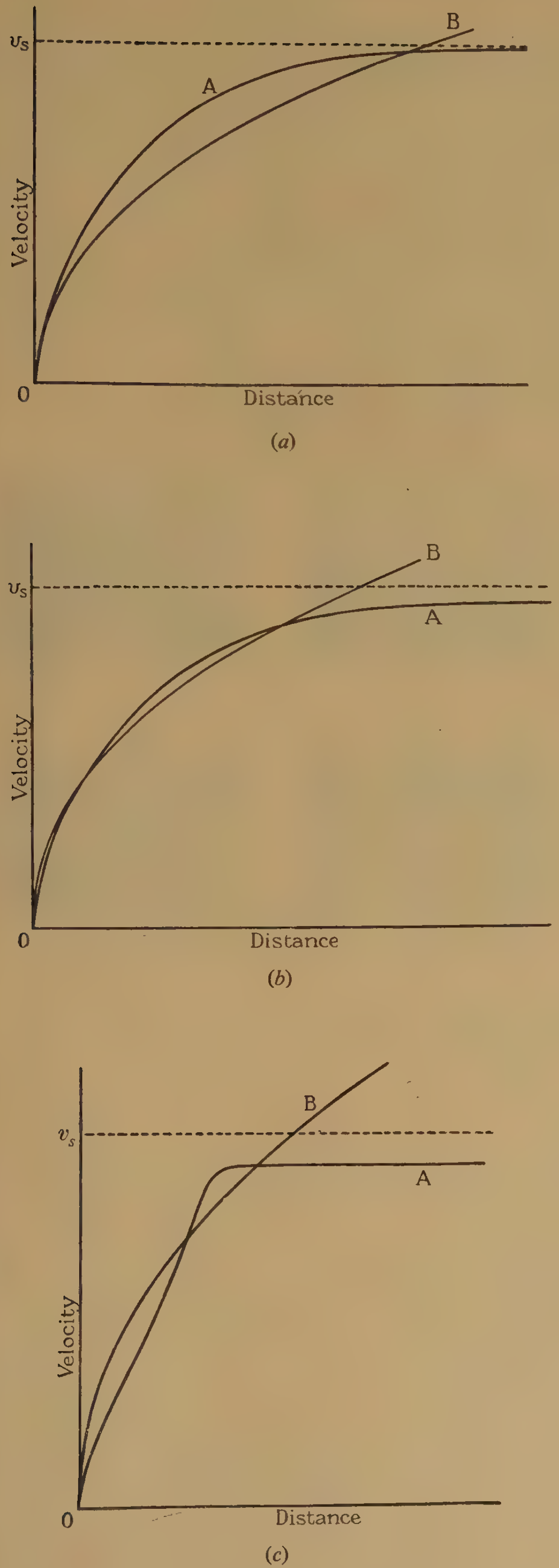

Fig. 7.—Velocity/distance relationships for varying loads.

(a) No load ($\beta = \infty$).
(b) $\beta = 10$.
(c) $\beta = 8$.

$$t_2 = \frac{v_s\beta}{a_m}\left[\left(\frac{v'}{v_s}\right) - \frac{2\beta n}{(1-p_2^2)}\left\{\log\left[1+\frac{\left(\frac{v'}{v_s}\right)}{\left(1-\frac{n}{p_2}\right)}\right] - p_2^2\log\left[1+\frac{\left(\frac{v'}{v_s}\right)}{(1-np_2)}\right]\right\}\right] \quad . \quad . \quad . \quad . \quad (19)$$

In each case v' is the velocity at the centre. These expressions are so complex as to render further algebraic analysis almost impossible. The behaviour of the motor is predictable, however, from the above equations by use of the phase-plane technique.

Fig. 7 shows the results of eqns. (16) and (17) plotted for different values of β and n. If contours are cut for any one of these pairs of curves, say for $\beta = 10$, $n = 1/2$, a phase-plane diagram may be constructed as follows:

If contour A [Fig. 7(*b*)] represents eqn. (16) and contour B represents eqn. (17), we can begin at any point P on the *s*-axis (Fig. 8) and use contour A to determine the speed v_1 attained at

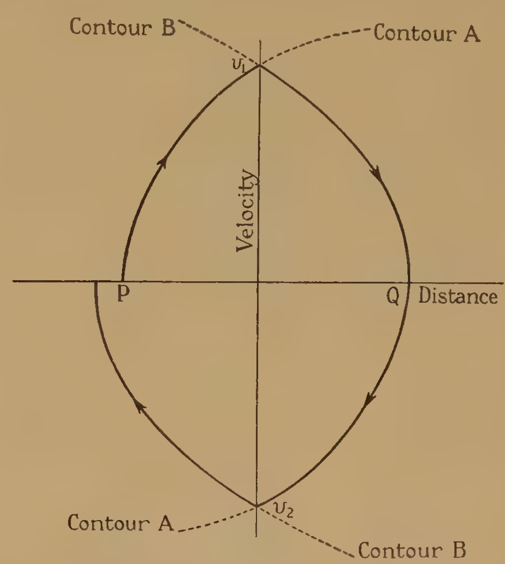

Fig. 8.—Construction of phase-plane diagrams.

the centre. Then, using contour B reversed, we can find the point Q to which the rotor will move starting with speed v_1. Contour A inverted will then determine point v_2 and so on, using contour A in quadrants 1 and 3 and contour B in quadrants 2 and 4. In this way the behaviour of the machine may be predicted for any starting point P.

Fig. 9 shows a phase-plane analysis of a machine for the three conditions to which Fig. 7 refers. Fig. 9(*a*) is the unloaded phase-plane diagram illustrating the stable nature of the contour PQRS and the approach to this contour from any starting position. Fig. 9(*b*) shows a second contour P′Q′R′S′, for which the oscillation is clearly in a condition of unstable equilibrium, for a slight departure from this curve results in either a build-up to the stable contour PQRS or a decay to the origin.

Fig. 9(*c*) shows how increase in load brings the stable and unstable contours closer together, until in the limit there is clearly a load for which the machine can never oscillate in a stable manner.

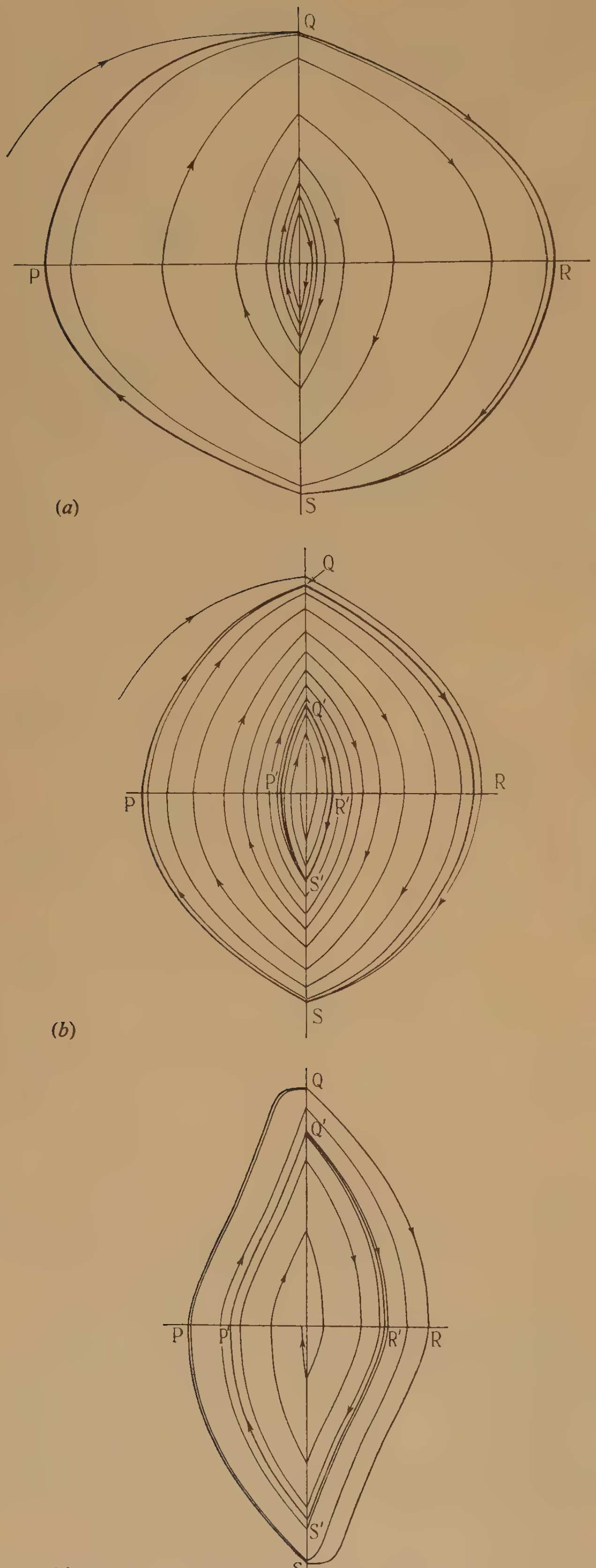

Fig. 9.—Theoretical phase-plane diagrams.
(a) No load ($\beta = \infty$). (b) $\beta = 10$. (c) $\beta = 8$.

(6) PRACTICAL RESULTS

A linear motor was constructed to test the simple theory of Section 3. The choice of v_s and a_m, at this stage, was quite arbitrary. The synchronous speed chosen was 50 ft/sec on a 50 c/s supply. The motor was found to have a maximum acceleration of 16g and the stator was 4 ft long. The rotor was found to oscillate such that a stop had to be provided at each end to limit the amplitude. This was not surprising in the light of the later calculations shown in Section 5, which predict a stable amplitude of over 10 ft (eqn. (8)].

It is not convenient to vary the rotor resistance in a machine of this type for purposes of experiment, since a new rotor is required for each value of R/X. Accordingly it was decided to perform the experiments on a conventional rotary machine with slip-rings, using a relay-operated change-over switch to correspond to the centre point of the linear stator. In this way, infinite amplitude is available in each direction.

Fig. 10 shows phase-plane diagrams obtained from an oscillo-

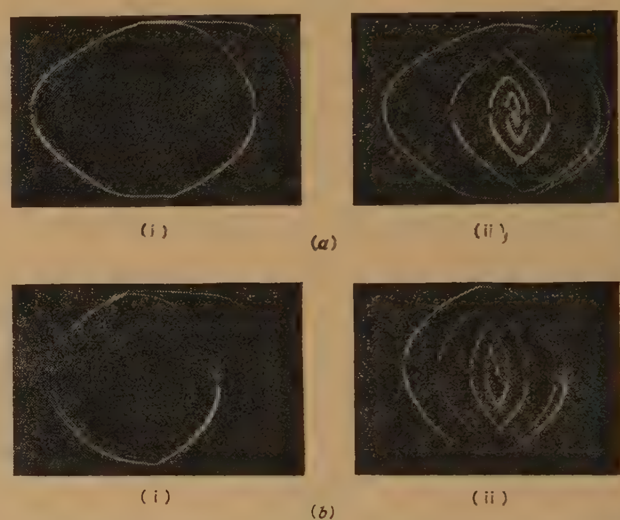

Fig. 10.—Photographed phase-plane diagrams, no load.

(a) $R/X = 0{\cdot}35$.
(i) and (ii) showing reduction and build-up respectively to the stable amplitude.
(b) $R/X = 0{\cdot}57$.
(i) and (ii) as in (a).

graph, the method employed being to connect the X-plates to a geared potentiometer driven from the motor shaft, and the Y-plates to a d.c. tachometer-generator, also driven by the motor.

Fig. 10(a) part (i) shows clearly that the approximation $v'/v_s = 1$ is justified for $R/X = 0{\cdot}35$, as can be seen by the incursion from a remote point when running-light speed is sure to be attained. Fig. 10(b) for $R/X = 0{\cdot}57$ shows the amount by which v' falls short of v_s and is certainly less than 5%.

An experiment was then performed to test eqns. (7) and (11). Fig. 11(a) shows the comparison between theory and practice for variation in a_m at a fixed R/X value of $0{\cdot}7$, and the two are seen to be in agreement. Fig. 11(b) shows a similar comparison for R/X variations, and here there is some discrepancy, particularly for the larger values of R/X. It should be noted that the relative effect of backlash is greater for large R/X values where the amplitude is smaller. If, however, the measured value of v'/v_s is used in eqns. (7) and (11), instead of that computed from eqn. (6), better agreement is obtained as is seen in Fig. 11(b).

In order to vary v_s and still use the same machine, the frequency of the supply must be varied. However, this involves changes in R/X also, and if the frequency is varied whilst keeping the supply

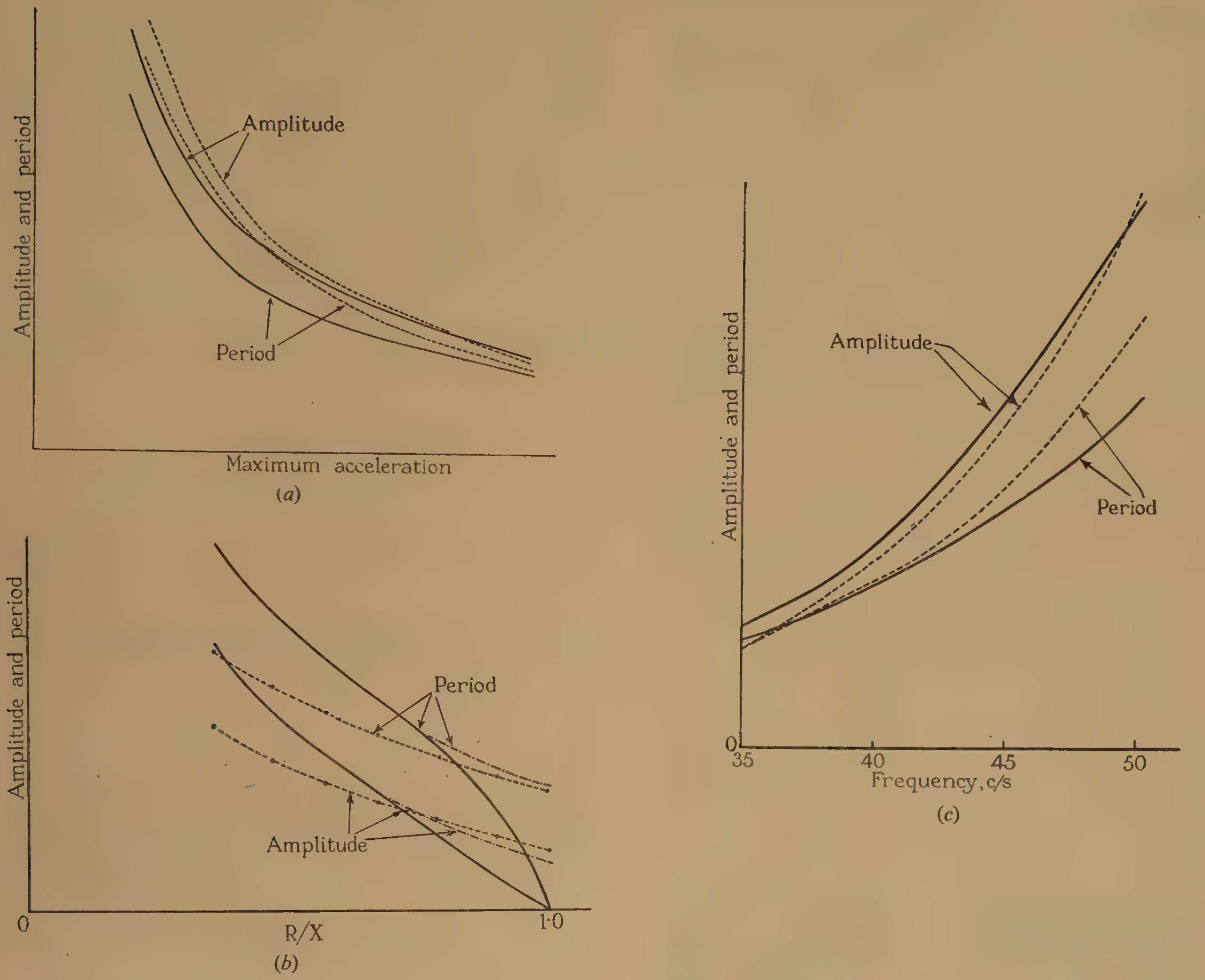

Fig. 11.—Comparison of amplitude and time periods in theory and in practice.

———— Theoretical curves.
– – – – Practical curves.
—·—·— Theoretical curves using measured values of v'/v_s.

(a) For variations in a_m.
(b) For variations in R/X.
(c) For variations in v_s.

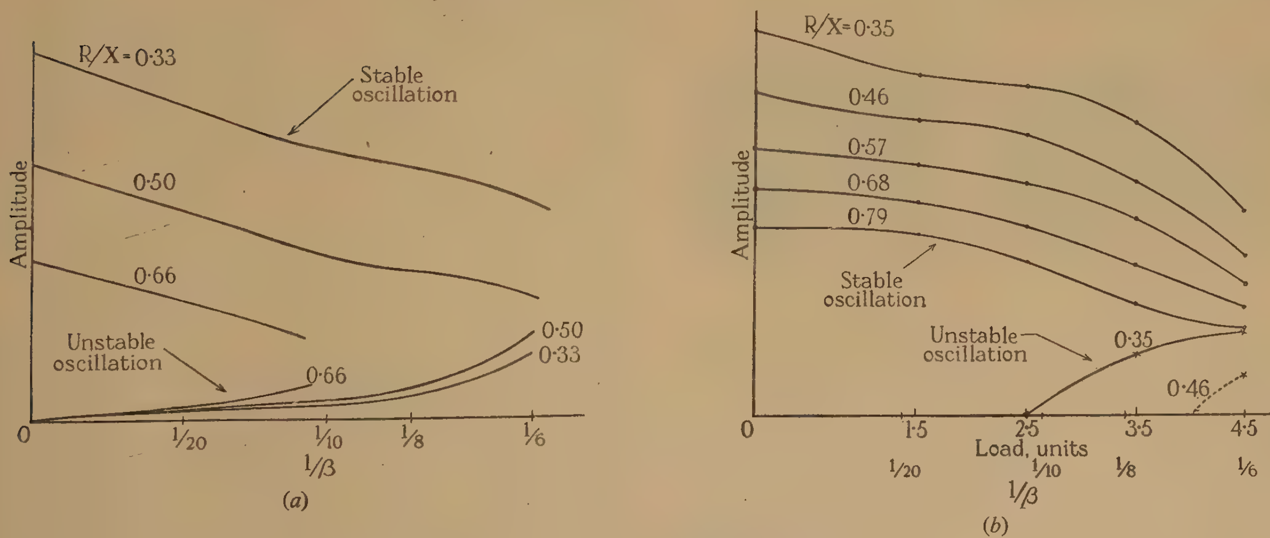

Fig. 12.—Variation in amplitude with load.

(a) Theoretical curves.

(b) Curves obtained in practice.

voltage constant $\left(a_m \propto \frac{1}{f^2}\right)$, eqn. (8) shows the amplitude to be proportional to the fifth power of the frequency.

Fig. 11(c) shows the comparison for frequency variation.

If the three assumptions set out in Section 3 are borne in mind, and allowance is made for experimental error, these results show a fairly close agreement, and it seemed worth while to proceed with the theory for the loaded case, making the same assumptions. Accordingly, pairs of curves, as shown in Fig. 7, were computed to enable the stable and unstable crossing points to be read off, and Fig. 12(a) shows the theoretical curve for the stable and unstable amplitudes as a function of the load factor. Some difficulty was encountered in finding a suitable type of brake which would operate for both directions of rotation. The most successful type consisted of a friction band-brake carrying two spring-balances as shown in Fig. 13. Fig. 12(b) shows the

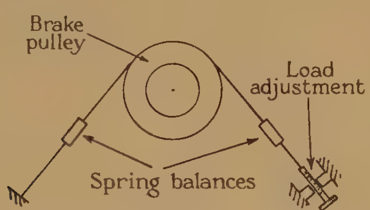

Fig. 13.—Type of brake used for two-way operation.

practical results obtained, and it appears that there is an optimum value of R/X which minimizes changes in amplitude with load.

Fig. 14 shows phase-plane diagrams for two loaded conditions. These illustrate the decrease in amplitude with load, and Fig. 14(b) part (ii) shows the unstable limit.

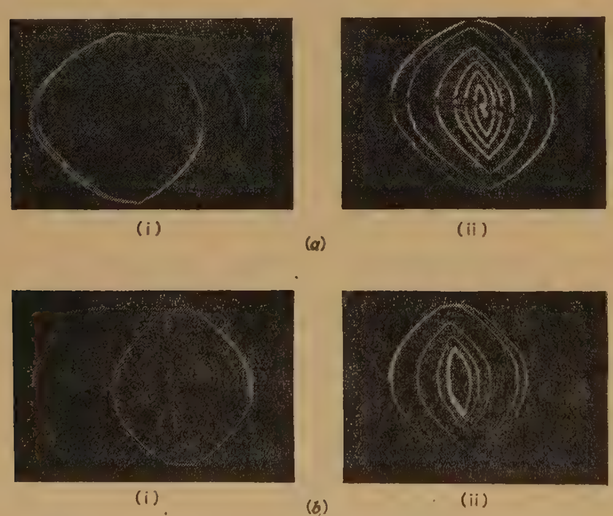

Fig. 14.—Phase-plane diagrams for loaded conditions: $R/X = 0{\cdot}35$.
(a) $\beta = 18$.
(i) and (ii) Show respectively the reduction and build-up to the stable amplitude.
(b) $\beta = 8$.
(i) Reduction to stable amplitude.
(ii) Build-up from unstable to stable amplitude.

(7) DEVELOPMENT OF A SYSTEM TO MEET PRACTICAL REQUIREMENTS

Having established the principle of operation both in theory and by experiment, it remains to be established that a workable system can be devised, which will meet all the requirements of weaving technique.

(7.1) Vertical Transverse Stabilization

One of the features of the linear motor which appears at first sight to render the device impracticable is the magnetic attraction between rotor and stator. In the model described the rotor was fitted with ball-races as wheels and ran on rails which enabled a constant air-gap to be maintained between stator and rotor. It seems difficult to identify such a system with a "flying shuttle," whose name implies that it follows a free flight through space as it traverses the shed. In fact, however, the shuttles of most types of loom in use to-day do not fly freely through the shed, but rather they slide on the sley which is usually made of wood, or are in fact often forced between the tunnel of threads which serves to effect transverse stabilization, as shown in Fig. 15(a). The lower threads are then forced against the sley,

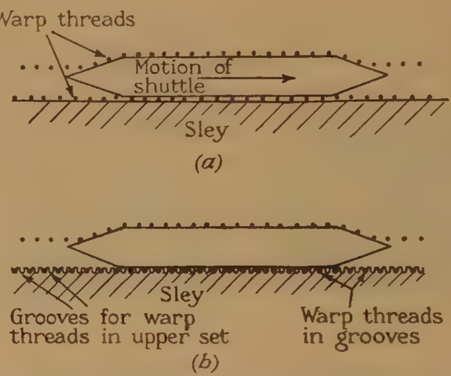

Fig. 15.—Motion of shuttle through shed.

not only by the weight of the shuttle, but also by the tension in the upper threads. The friction between the lower threads and the shuttle sides does not break the threads because the shuttle sides are highly polished and because the warp threads are continually being absorbed into the finished cloth so that the shuttle does not repeatedly touch the same piece of warp.

Examination of the sley of a loom which has been used for weaving the same type of cloth for some considerable time reveals grooves worn in the wood where each warp thread has been forced against it. The shuttles of such looms are then supported purely by the sley, the warp threads fitting into their own individual grooves, as shown in Fig. 15(b).

If magnetic attraction between rotor and stator proved so great that the roller bearings supporting the shuttle damaged the warp threads, then it would become necessary to fit on to the stator track a thin layer of material containing the necessary number of pre-formed grooves for the particular cloth being woven. Such a system is suggested in Reference 4.

A double-sided system employing a stator track above and below could be used to reduce the downward magnetic pull, the rotor being located somewhat nearer to the upper stator, to attempt to balance out the weight of the shuttle also.

A development of the double-sided system which appears to have attractive possibilities consists of a rotor which contains only non-ferrous conducting material moving between a double track. Owing to leakage flux, the rotor will tend to occupy a mid-position between the stators and would, for the most part of its travel, be propelled freely through the air. The practical difficulties of such a system would be, first, that unless the rotor were fairly thin the stator currents would be called upon to drive flux across a very large air-gap, and the size and weight of the whole device would be large; and secondly, as the result of tests on a number of shapes and sizes of rotor, it appears that the R/X ratio of rotors containing no iron is unsuited to power

frequencies so far as self-oscillation is concerned. Nevertheless, the design of a non-ferrous rotor to operate in the manner just described may well prove to be physically possible and—in fact—the best working system.

(7.2) Horizontal Transverse Stabilization

The standard practice for obtaining horizontal transverse stabilization consists in firing the shuttle against a curved "reed" or comb, as shown in Fig. 16(*a*), and relying upon centrifugal

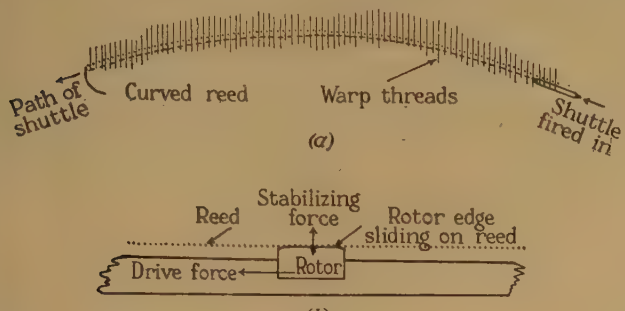

Fig. 16.—Methods of effecting horizontal transverse stabilization.

force to hold it against the reed throughout its travel. A similar method is possible with the type of rotor used in the model, with the possible modification of roller bearings between shuttle and reed.

An interesting point to note is that non-ferrous rotors, if they could be made practicable in other respects, would be the easiest to stabilize in the horizontal direction, since they could be offset from the stator, as shown in Fig. 16(*b*), when they could experience at all times a component of force at right angles to the reed, which could therefore be made straight.

(7.3) Location at Ends of Travel

Fig. 12(*a*) indicates that the change in the stable amplitude with load is not large provided that the factor β is greater than 10, whilst the practical results of Fig. 12(*b*) suggest that the theory is even pessimistic in this respect. It is necessary to ensure that the shuttle shall clear the shed at each end of its travel, and, therefore, the stable amplitude should be calculated for the maximum load which it is reasonable to expect for a given type of cloth. Thus, for most of the time the shuttle may be expected to oscillate with an amplitude a little in excess of this. In order to avoid excessively long portions of useless track to accommodate such overshoots, some form of amplitude limiter is necessary. This could take the form of a simple spring which would increase the acceleration from the standstill point up to, say, the peak acceleration, or even higher, since the latter is probably a hundred times smaller than that for a mechanically propelled shuttle.

Alternatively, d.c. magnetic clamps could be arranged at each end of the track to provide a strong permanent field to act on a

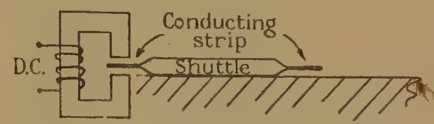

Fig. 17.—Arrangement of d.c. clamps.

slab of conducting material on the rotor, as shown in Fig. 17. The travelling field would be able to extract the rotor from the clamp for the return pick. Such an arrangement would have the effect of causing the rotor to spend rather longer in the shuttle-boxes, which might prove to be a desirable feature.

(8) CONCLUSIONS

The nature of the oscillations obtained is such as to render mathematical treatment extremely difficult, and only by making sweeping assumptions can any formulation of the equations of motion be attempted. The experimental results, however, show that such treatment gives at least a qualitative appreciation of the mode of operation. One of the main experimental difficulties lay in reducing backlash in the rotary system. This made assessment of the unstable limit extremely unreliable. It should further be mentioned that the rotary machine does not represent a true equivalent of the linear case, where the end effects of the "rotor" must play a part in shaping the speed/force characteristic. Recent work has, in fact, led to the belief that such end-effects tend to produce a characteristic which has a maximum at a fixed value of slip, independent of the R/X ratio. Certainly, the most recent experiments on the linear motor have shown that stable oscillation is difficult to obtain with a rotor whose length is less than two pole-pitches, but the theoretical considerations of this phenomenon are as yet unexplored. So far as the application of the device to weaving is concerned, it seems possible that a workable system can be evolved even though most of Section 7 is speculation rather than the result of experiment. Whether such a device demands too great a change in the design of a loom for it to be of value is a question which the authors are not competent to answer at the present time.

(9) REFERENCES

(1) "A Wound-Rotor Motor 1 400 ft long," *Westinghouse Engineer*, 1946, **6**, p. 160.
(2) Reece, A. B. J.: "Power Production in Nuclear Reactors," *Students' Quarterly Journal*, 1954, **25**, p. 7.
(3) Eisselt, G.: British Patent No. 483816. April, 1938.
(4) Filter, W.: British Patent No. 709299. May, 1954.

[The discussion on the above paper will be found on page 118.]

621.313.333

Paper No. 2097 U
June 1956

BRUSHLESS VARIABLE-SPEED INDUCTION MOTORS

By Professor F. C. WILLIAMS, O.B.E., D.Sc., D.Phil., F.R.S., Member, E. R. LAITHWAITE, M.Sc., Associate Member, and L. S. PIGGOTT, M.Sc., Associate Member.

(*The paper was first received* 22*nd October*, 1955, *and in revised form* 21*st February*, 1956. *It was published in June*, 1956, *and was read before the* UTILIZATION SECTION 15*th November*, 1956.)

SUMMARY

The first part of the paper describes experiments performed on a spherical machine. These experiments show that speed ranges up to 5·5 : 1 can be obtained, and that the speed range obtained depends markedly on the ratio of pole width to pole pitch. They also show that the losses in the machine cannot be accounted for by conventional induction-motor theory. It is shown, however, that the extra losses are due to the fact that the stator is 'short' in that it is not continuous round the machine; they are not due to the variable-speed feature.

The second part is devoted to a theoretical analysis of the properties of short-stator machines, in the first place without reference to variable-speed properties. Equations are developed which permit the formulation of the salient external characteristics of such machines, it being shown in particular that high efficiencies can be obtained provided there are four or more poles on the 'short' stator. This general theory is then applied to the variable-speed case. The theoretical findings are supported by numerous experimental results.

Broad design criteria are laid down, but since one of these is that the machine should be large it has not yet been possible to make and test a properly designed machine.

(1) INTRODUCTION

In a recent paper[1] the authors described a new type of variable-speed brushless induction motor. The principle on which the motor is based is that when a piece of conducting material is placed in a moving magnetic field it can be caused to move at a speed in excess of the speed of the field by constraining it to move at an angle θ to the direction of motion of the field. The paper described a disc type of machine which sufficed to demonstrate the principle involved, but which was so inefficient that no reasonable idea of the practicability of the device could be formed. The paper closed with the suggestion that higher efficiencies would be possible with a barrel type of construction, but that this would require the use of a spherical barrel rather than the more conventional cylindrical barrel. The form of construction envisaged is as shown in Fig. 1, several stator blocks similar to the one shown being fitted round the rotor.

The present paper describes an experimental machine of this kind. The investigation is not yet complete, but a point has been reached where the salient properties of such machines can be described and broad design criteria laid down. Since some considerable time will necessarily elapse before further experimental machines can be constructed, it is thought to be appropriate to present an interim report at this stage.

(2) EXPERIMENTAL SPHERICAL MACHINE

(2.1) Rotor Design

As indicated in the earlier paper, the main practical difficulty with this type of machine is the fact that it is essentially multipolar so that the pole pitch tends to be small, with all the attendant difficulties as regards leakage inductance, excessive copper loss and high magnetizing current. These difficulties are obviously minimized by making the machine as large as possible. The maximum size of rotor that could be conveniently turned with

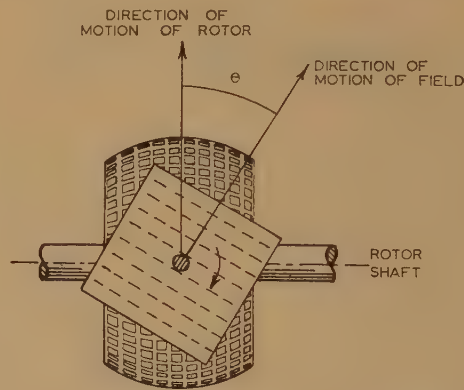

Fig. 1.—Arrangement of rotor and stator in a spherical machine.

available plant was 14 in diameter, and this size was therefore chosen.

The rotor was made up of stampings stacked in the conventional manner, but four different diameters were used, as shown in Fig. 2, to provide a 'stepped' approximation to a sphere.

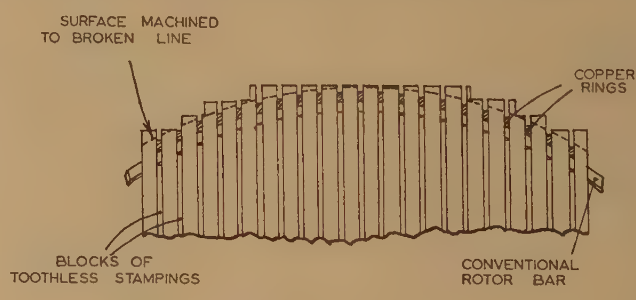

Fig. 2.—Details of rotor construction.

The rotor stampings had 150 semi-closed slots 0·6 in deep by 0·2 in wide with a slot opening of 0·1 in. Stacks of these were interleaved with stacks of 'toothless' stampings to provide 21 peripheral slots as indicated. The rotor was wound with a number of separate wires of No. 20 s.w.g. tinned copper. A layer of these was laid in each conventional slot, through the slot openings, then a layer of wire was bound round the peripheral slots, then more wires were laid in the conventional slots, and so on. In this way a matrix of wires was set up, interlaced in the conventional and peripheral directions. During this winding, resin-cored solder wires replaced copper wires in the proportion of 1 to 5. When the winding was complete the whole rotor was

Prof. Williams and Messrs. Laithwaite and Piggott are in the Electrical Engineering Department, University of Manchester.

heated to the melting point of the solder so as to ensure good soldered joints at all crossing points. Plumber's lead was then hammered into the slot openings to make a solid mechanical job. The effective cross-section of the copper in each slot was 1/40 in^2. The rotor was then turned spherical using a template.

The rotor length, l, was made equal to the radius for a reason connected with the stator design, which will now be considered.

(2.2) Stator Design

The overriding consideration in the design of the stator is to get the largest possible pole pitch consistent with the rotor radius and the proper performance of the machine. The earlier paper showed that best results were obtained with a large value of W/p, where W is the pole width and p the pole pitch. This fact suggests that the number of poles on a stator block needs to be in excess of the minimum value of 2, and it was therefore decided to provide slotting for up to eight poles per stator block.

At the minimum speed ($\theta = 0°$ in Fig. 1) the stator block will correspond with a section of the stator of a conventional machine, except for its spherical shape. At the setting for maximum speed, the stator block will be turned through an angle approaching 90°. It is desirable that the fraction of the rotor covered by each stator block should be approximately the same in the two conditions—first for constructional reasons, so that clearances between blocks remain similar, and secondly for experimental reasons, so that results at different angles will correspond with equal areas of active surface. A circular stator would meet these requirements best, but for ease of construction a square shape was adopted, as shown in Fig. 1. For maximum pole pitch, therefore, the rotor should be as long as possible. However, the longer the rotor is made the greater will be the difference in surface speed between middle and edge, and ideally the whole rotor surface should travel at the same speed. A reasonable compromise seems to be to make $l = r$, at which value the speed at the edge is only 12% lower than that at the middle.

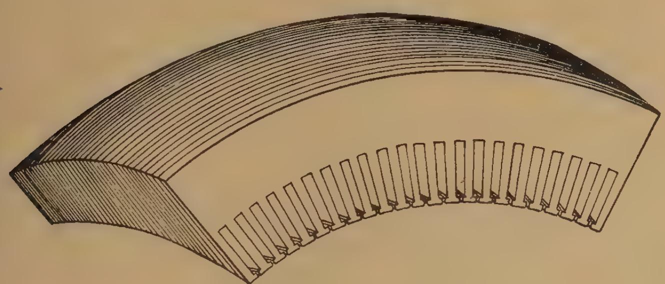

Fig. 3.—Details of stator construction.

Fig. 3 shows details of the stator actually used. It was made up of segmental stampings of thin high-quality iron having 22 slots in an arc length of 8 in. The stampings were all of the same radius, but were clamped together and 'bumped down' on the rotor to give the best fit. This approximately spherical shape was then turned spherical using a template. It was wound with a conventional double-layer 3-phase winding. The complete experimental stator assembly is shown in Fig. 4. Only one stator block has been used, but it may be seen that there is space for four such blocks.

The speed of the travelling field can be calculated from the formula $u_s = 2pf$, where p is the pole pitch and f the supply frequency, whence the angular synchronous speed ω_s at $\theta = 0$ is given by $\omega_s = 2pf/r$. With a 4-pole winding in the stator block described this produces a value for synchronous speed of 300 r.p.m. at 50 c/s.

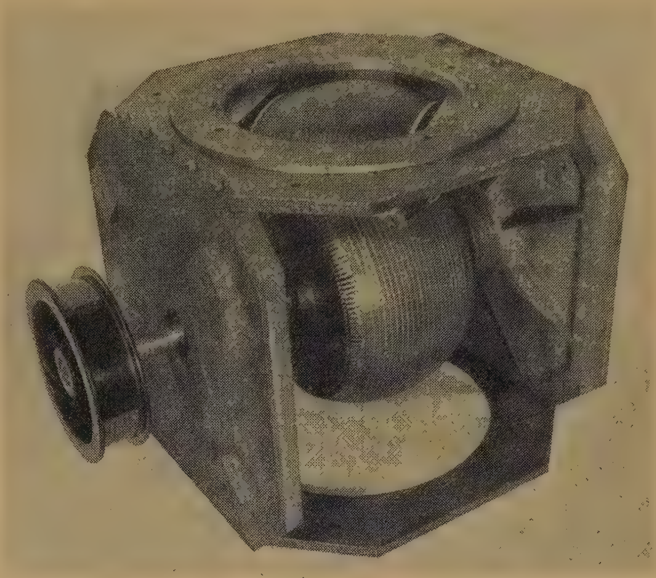

(a)

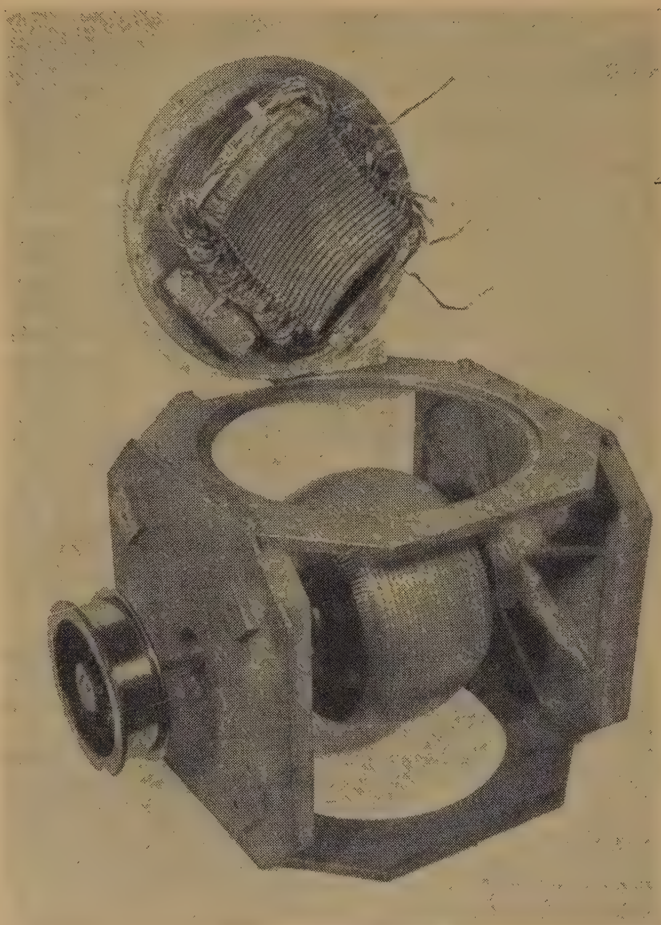

(b)

Fig. 4.—The experimental machine.

(a) One stator block in position.
(b) Stator block removed to show construction.

(2.3) Experimental Results

The speed range available with this equipment was investigated first. In the earlier paper some curves were given, calculated to show the expected speed range in the case of a purely resistive rotor. Owing to the inclusion of iron in the rotor, the new machine exhibits some rotor reactance. It was not expected, therefore, that accurate agreement with the predictions would be obtained. All attempts to include leakage reactance in a similar analysis had failed, however, so the experimental approach was the only one available. Some results are shown in Fig. 5 relating

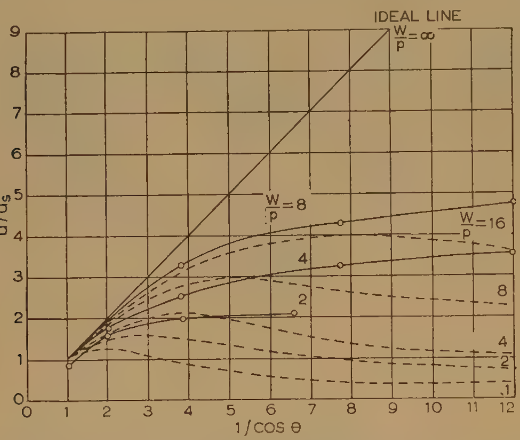

Fig. 5.—Speed variation obtained with the experimental machine.

——— Experimental curves.
– – – Curves plotted from the simple theory of Reference 1.

to 2-, 4- and 8-pole windings, for which the corresponding values of W/p were 2, 4 and 8. From these it may be seen that the behaviour is superior to expectation. Evidently, rotor inductance is a helpful feature. The theoretical curves show that the greater the value of W/p the greater is the maximum speed range attained and the more nearly does the curve conform to the ideal line (where $u/u_s = 1/\cos\theta$) at the lower values of $1/\cos\theta$. The practical results are seen to substantiate these predictions qualitatively.

At the higher speeds, due allowance was made for friction and windage, so that the speeds plotted are true 'running light' speeds, rather than actual speeds. It should, however, be noted that at 50 c/s, with eight poles, an actual speed over five times the minimum speed was reached. It should also be noted that whereas the 4- and 8-pole structures exhibit the expected speed at $\theta = 0°$, the 2-pole structure achieves only 90% of this speed. No explanation has yet been found for this discrepancy, but its existence has been established beyond doubt.

After it was thus established that the spherical version of the variable-speed machine works in practice, and is in fact superior to the disc machine, attention was turned to an investigation of load characteristics. Many measurements were taken with various numbers of poles, various values of θ, and at several frequencies. Space will not permit of their reproduction here but the salient findings are illustrated in Fig. 6. The curves relate to a 4-pole structure operated at 200 c/s on constant voltage with $\theta = 0$. From curve (f) it may be seen that for this case the efficiency η is less than 50%. It was found that the efficiency fell as the number of poles was reduced. The efficiency also fell as θ was increased, but the fall was not catastrophic until θ had been increased to a value corresponding approximately with a 10% departure of the running-light speed from the ideal value (see Fig. 5). Thus, if a significant speed range is required, at least four poles are needed, and more are preferable.

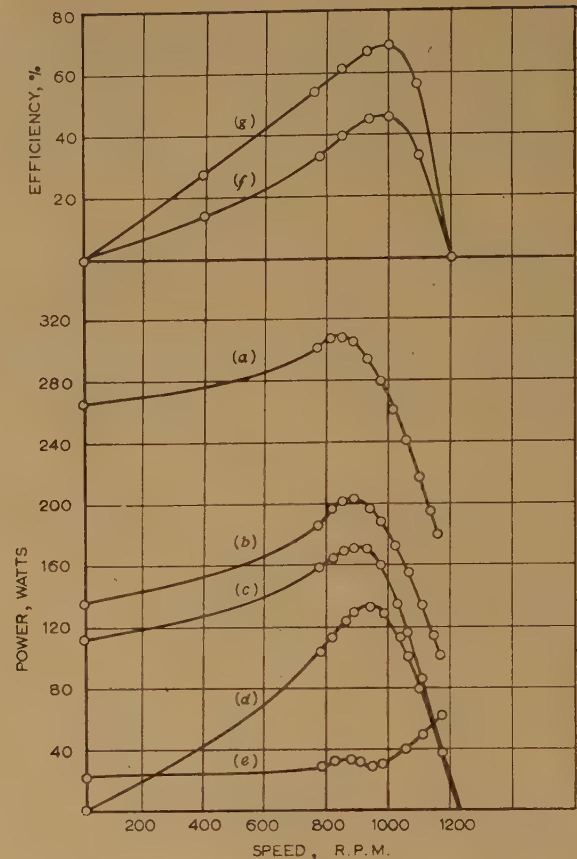

Fig. 6.—Analysis of losses for $\theta = 0$, $W/p = 4$, at 200 c/s.

(a) Input power.
(b) Input power less stator I^2R loss.
(c) Synchronous watts, ($T\omega_s$).
(d) Output power.
(e) = (b) − (c).
(f) Overall efficiency.
(g) Efficiency neglecting stator I^2R loss.

However, even at $\theta = 0$ the efficiency was not acceptable and attention was therefore directed to an analysis of losses.

(2.4) Analysis of Losses

The only losses in this machine that are readily calculable are the stator copper losses. Friction and windage losses were measured and added to the measured torque. The quantities plotted in Fig. 6 against actual speed, are:

(a) Total input power, watts.
(b) (Input power) − (stator copper loss).
(c) Torque × synchronous speed (expressed in watts) i.e.

$$\text{Torque in pound-feet} \times \frac{pf}{\pi r}\frac{2\pi \times 746}{550}$$

(d) Mechanical power output (including friction and windage), i.e. (c) × ω_r/ω_s
(e) (b) − (c).

Of these, (a) and (b) are self-explanatory, (c) − (d) would be the rotor copper loss in a normal induction motor, and is therefore referred to as 'legitimate' rotor copper loss. Curve (e) should be the iron loss and stray load loss, which should be small.

The first thing to note from Fig. 6 is that the stator copper loss is excessive, but at this stage little attention need be given to this, since the theoretical cure is obvious, although it may prove extremely inconvenient practically. The peak overall efficiency is 44% and the peak efficiency neglecting stator copper loss is 68%.

The second and more important thing is that (e) is so large and varies with speed in such an unusual manner that it cannot be dismissed as iron loss. This curve in fact became known as the 'missing watts' curve and was the starting point of a long series of experiments, all designed to discover what became of the missing power. Nearly all these experiments proved abortive and are best forgotten.

With a view to detailed investigations numerous search coils were incorporated in the stator blocks. In particular, a set of four was included across the face of a 4-pole block at intervals of one pole pitch in the direction of motion of the field. These provided the first real clue to the source of the missing power. Fig. 7 shows the voltages measured on these search coils when at

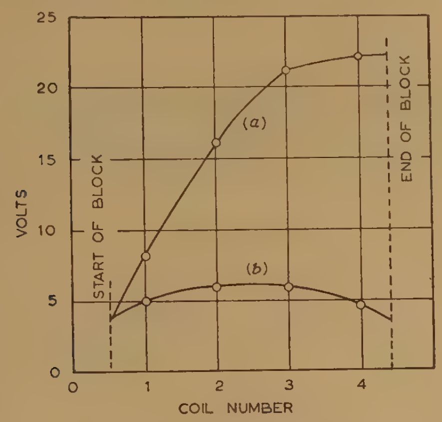

Fig. 7.—Search-coil voltages.

(a) Running light.
(b) At standstill.

standstill and running light with a 100 c/s supply. For these measurements, the current supplied to the machine was held constant. At standstill, as would be expected, the search coils yielded similar voltages, any differences being presumably due to small variations in size, or in the effective gap. With the machine running light the coils showed a progressive increase in voltage as the distance from the point of entry into the field increased. At entry the flux was apparently independent of whether the machine was running or not.

The running-light curve suggests an exponential rise of flux during the time a particular rotor element is under the stator structure. In order to establish that the effect was time-dependent rather than space-dependent, the experiment was repeated at a number of frequencies. The results were then corrected to a common time scale, and expressed as flux densities. The results are shown in Fig. 8, where the ordinate is proportional to flux density and the abscissa represents time. The stator current was held constant throughout. Various frequencies between 12·5 and 300 c/s were used. The curve shown is the empirical curve $V = 4 + 24(1 - \varepsilon^{-50t})$. These results show that the effect is time-dependent, and that, in fact, the flux rises with time from an initial value, equal to the standstill value, and approaches exponentially a value some six times as high. Calculation shows that this final value is approximately the flux that would obtain if the rotor contained no conductors.

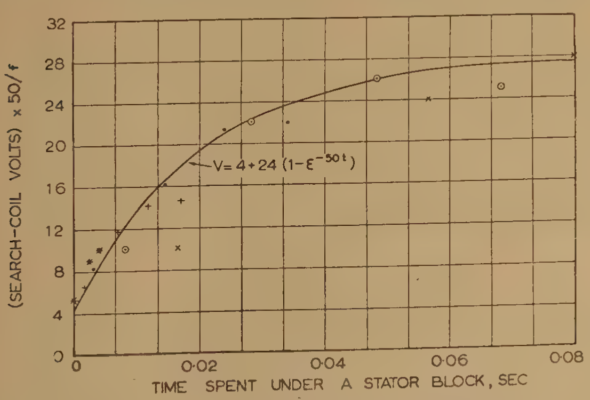

Fig. 8.—Flux build-up under a stator block.

× 12·5 c/s.
⊙ 25 c/s.
● 50 c/s.
+ 100 c/s.
✱ 300 c/s.

It was now apparent that conventional induction-motor theory would have to be abandoned, but with this experimental information it became possible to formulate a theory of the behaviour of the machine, and an exposition of this now follows.

(3) THEORETICAL CONSIDERATIONS

Attention will be confined, in the first instance, to operation with $\theta = 0$, but it will be shown in Section 6 that the results obtained relate also to operation at any angle. To simplify the theoretical approach to the problem a model, as shown in Fig. 9,

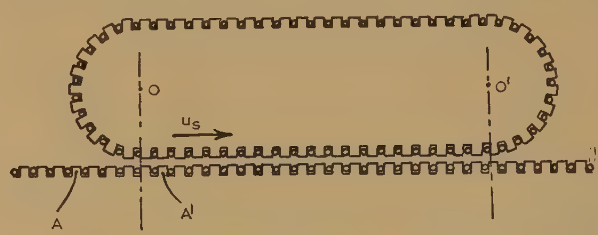

Fig. 9.—Theoretical representation of a short-stator machine.

will first be considered. The stator has been represented in the model by a caterpillar arrangement of conductors moving around the centres 0, 0′. These conductors carry constant direct currents whose values have a sinusoidal distribution along the caterpillar track. The rotor of the machine takes the form of an infinitely long 'squirrel cage' of conducting bars, moving under the track of the caterpillar at the same speed as the caterpillar, corresponding with running light. The tooth pitches on rotor and stator are equal and are assumed to be in register. Magnetic locking effects are assumed to be absent.

Consider any rotor tooth A outside the stator but about to enter it. If fringing effects are neglected, the flux in this tooth will be zero and the current in the bars surrounding it will also be zero.

Now consider the same tooth a short time t_e later, when it has reached the position A′ just inside the stator. Let the flux now in the tooth, due to the action of the stator currents, be Φ. The average rate of change of flux through the tooth during the motion is Φ/t_e, and this must be the average voltage round the conducting loop surrounding it during the motion from A to A′. If the resistance and leakage inductance of the rotor bars were zero, there could be no voltage in the loop round the tooth for any finite value of current; hence, for this case, $\Phi/t_e = 0$, and therefore $\Phi = 0$. If Φ is to be zero in all such teeth as A′, there must be induced in the rotor bars currents equal and opposite to those facing them on the stator, and there will then be no flux anywhere in the gap.

Consider now rotor bars with some finite resistance, but still with no leakage reactance. There will, in general, be a resistive voltage, e_r, round the loop surrounding a tooth, since the

currents differ from bar to bar. Flux can now build up in the tooth at the rate

$$\frac{d\Phi}{dt} = -e_r$$

Φ will therefore still be zero at entry but will build up with time, and since the tooth considered is moving from left to right the gap flux will increase in this direction. Provided that t_e is small, the initial value of Φ, when the tooth has just entered, will be substantially zero, i.e. gap flux density will be zero at entry.

(3.1) Analysis

With these ideas in mind the more general case will now be considered.

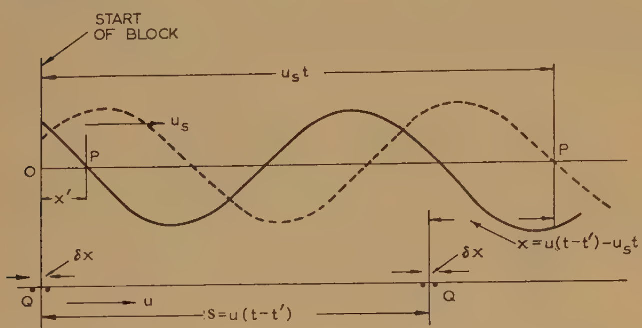

Fig. 10.—Conditions when a coil Q is entering the gap under the stator and when it is at a distance s from the point of entry.

In Fig. 10 the sine curve represents a wave of current density travelling along a stator block from left to right at velocity u_s. Expressed as a surface density at any instant, using the point P which moves with the wave as the origin of x, we have

$$j_s = -J_s \sin\frac{\pi x}{p} \quad . \quad . \quad . \quad . \quad . \quad . \quad (1)$$

Let the instant $t = 0$ be chosen when P is just entering the block which begins at O. Then the continuous curves of Fig. 10 relate to time t' where the position x' of O relative to P is given by $x' = -u_st'$. At this instant let an elementary coil Q on the rotor be just entering the gap under the block, and let it be travelling at speed u from left to right. Then, at time t conditions are as shown by the broken curve. P has moved until it is a distance u_st from O, while Q has moved through a distance $s = u(t - t')$ to the position S. Q is now displaced from P by an amount x given by

$$x = u(t - t') - u_st \quad . \quad . \quad . \quad . \quad . \quad (2)$$

Consider now the resistive voltage round the coil due to the rotor current density. If rotor surface current-density, j_r, at this instant is a function of x, the difference in current density in the two sides of the coil Q of width δx is

$$\delta x\frac{\partial j_r}{\partial x}$$

and the resistive voltage round the loop is

$$\rho_r\delta x\frac{\partial j_r}{\partial x}$$

where ρ_r is the surface resistivity of the rotor. This voltage must be balanced by an induced voltage owing to the rate of change of flux through the coil, i.e.

$$\delta x\frac{db}{dt} = \rho_r\delta x\frac{\partial j_r}{\partial x} \quad . \quad . \quad . \quad . \quad . \quad . \quad (3)$$

where b is the flux density through the coil Q.

Hence
$$b = \int_{t'}^{t} \rho_r\frac{\partial j_r}{\partial x}dt + b_0' \quad . \quad . \quad . \quad . \quad . \quad (4)$$

where b_0' is the value of flux density at entry and is a constant for this coil, but may be a function of x', the displacement of the coil at entry.

For a given value of t' this is the flux density through the coil at any subsequent time. Alternatively, if $t - t'$ is held constant and t' is treated as a variable, it describes the time variations of flux density at a fixed point a distance s from O, such that $s = (t - t')u$ from the entry point; hence at S

$$b_s = \int_{t'}^{t'+s/u} \frac{\partial j_r}{\partial x}dt \quad . \quad . \quad . \quad . \quad . \quad . \quad . \quad (5)$$

where b_s is the flux density in the coil Q as it passes S. The flux density at entry being zero the constant of integration is zero.

For comparison, the time variation of stator current-density as the coil passes S can be derived as follows:

$$j_s = -J_s \sin\frac{\pi x}{p}$$

and from Fig. 10

$$x = u(t - t') - u_st$$

At S the value of $(t - t')$ is always s/u, so that

$$x = s - u_st$$
$$= -u_st' - \left(\frac{u_s}{u} - 1\right)s$$

whence

$$j_s = -J_s \sin\left[-\frac{\pi u_st'}{p} - \frac{\pi s}{p}\left(\frac{u_s}{u} - 1\right)\right]$$
$$= J_s \sin\left[\omega t' + \frac{\pi s}{p}\left(\frac{u_s}{u} - 1\right)\right] = J_s \sin\omega t''$$

where
$$t'' = t' + \frac{\pi}{p\omega}\left(\frac{u_s}{u} - 1\right)s \quad . \quad . \quad . \quad . \quad . \quad (6)$$

Relating these equations to the particular case, it may be noted that rotor current-density can differ from stator current-density only to the extent necessary to set up the flux density. The difference is, in fact, the magnetizing current. In the first instance this will be neglected. It follows that

$$j_r = -j_s = J_s \sin\frac{\pi x}{p}$$

whence, following the general argument,

$$\frac{\partial j_r}{\partial x} = \frac{\pi}{p}J_s \cos\frac{\pi x}{p}$$

and from Fig. 10, at the instant t,

$$x = (u - u_s)t - ut'$$

Hence
$$b_s = \int_{t'}^{t'+(s/u)} \rho_r\frac{\partial j_r}{\partial x}dt = \int_{t'}^{t'+(s/u)} \frac{\rho_rJ_s\pi}{p}\cos\frac{\pi}{p}[(-u_s + u)t - ut']dt \quad . \quad . \quad . \quad . \quad (7)$$

Integrating and expressing eqn. (7) in terms of t'' from eqn. (6) yields

$$b_s = \frac{\rho_rJ_s}{u_s - u}\left\{\sin\omega t'' - \sin\left[\omega t'' - \frac{\pi}{p}\left(\frac{u_s}{u} - 1\right)s\right]\right\} \quad . \quad (8)$$

This equation can be expressed as

$$b_s = B_p \sin \omega t'' + B_q \cos \omega t'' \quad . \quad . \quad . \quad . \quad (9)$$

where B_p and B_q are functions of s, and are the peak values of components of flux density at position S in time phase and in time quadrature with j_s at S, and are given by

$$B_p = \frac{\rho_r J_s}{u_s - u}\left[1 - \cos\frac{\pi s}{p}\left(\frac{u_s}{u} - 1\right)\right] \text{ (in phase)} \quad . \quad (10)$$

$$B_q = \frac{\rho_r J_s}{u_s - u}\sin\frac{\pi s}{p}\left(\frac{u_s}{u} - 1\right) \quad \text{(in quadrature)} \quad . \quad (11)$$

Consider first the values of these quantities when $u_s = u$. B_p is of the form $(1 - \cos \alpha A)/A$ with $A \to 0$. This tends to zero for all finite values of α.

B_q can be rewritten,

$$B_q = \frac{\rho_r J_s \dfrac{\pi s}{p}}{u\left(\dfrac{u_s}{u} - 1\right)\dfrac{\pi s}{p}} \sin\frac{\pi s}{p}\left(\frac{u_s}{u} - 1\right)$$

which as $$\left(\frac{u_s}{u} - 1\right) \to 0$$

yields $$B_q = \frac{\rho_r J_s \pi s}{u_s p} \quad . \quad . \quad . \quad . \quad . \quad . \quad . \quad (12)$$

Hence B_q increases linearly with s.

Consider now a point fixed on the rotor at a point of current zero. As this point passes S a current zero is observed, and since B_q is in quadrature with j_s a flux maximum must be observed. Such a point therefore corresponds with a maximum in the space distribution of the flux in the gap, and at this point B_q has the value given by eqn. (12). This is illustrated by Fig. 11(*a*), where B_q is plotted against s/p which is distance from the entry point expressed in pole pitches. If it is desired to remain at this fixed point on the rotor, for which $s = u_s t$, where $t = 0$ when $s = 0$, then

$$B_q = \frac{\rho_r J_s \pi t}{p}$$

i.e. the flux at such a point increases linearly with time as already indicated.

If we now return to the case of $u \neq u_s$, Fig. 11(*a*) also shows B_p and B_q for a slip of 1/9, Fig. 11(*b*) is for $\sigma = 1/5$, and Fig. 11(*c*) for $\sigma = 1/3$. The end point of the graph will of course depend on the number of poles in the block.

The information contained in Fig. 11 is summarized in Fig. 12, where ordinates and abscissae have been given the most convenient forms, but with some loss of physical significance. For any given slip the abscissa is a measure of distance in pole pitches to some scale, but the scale, and therefore the end-point of any given block, is a function of slip. The less the slip, the nearer the end-point approaches the origin.

These results can be explained alternatively as follows.

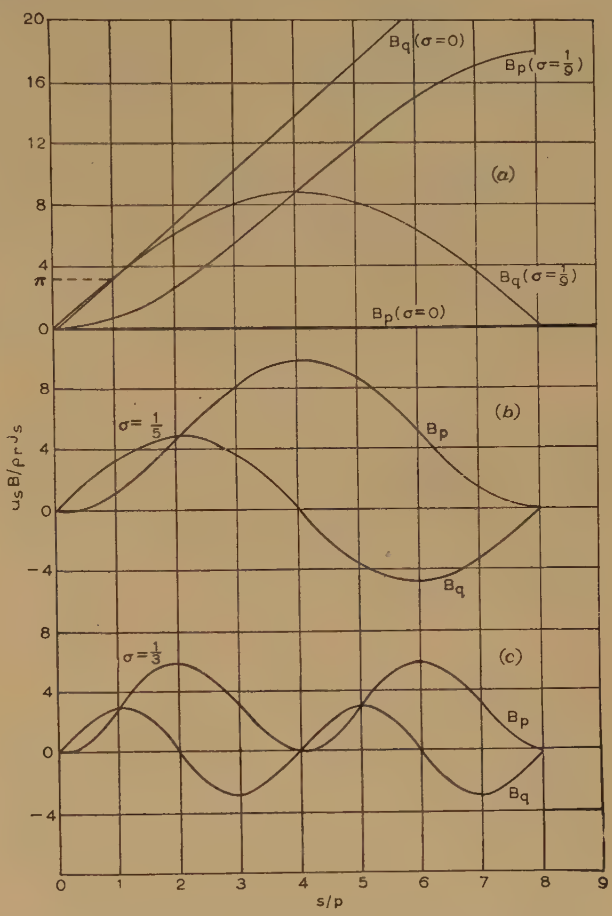

Fig. 11.—Theoretical flux distribution for different values of σ.

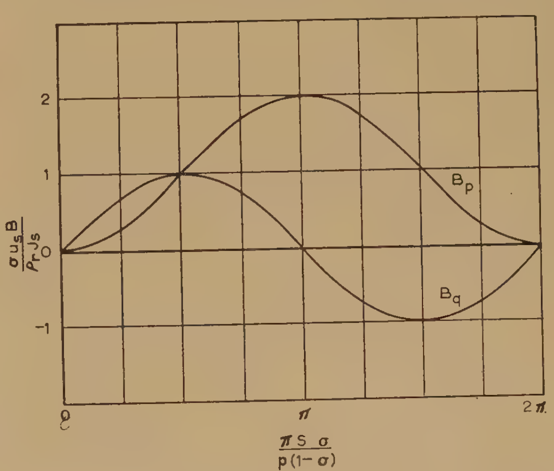

Fig. 12.—Summary graph of theoretical flux distribution.

(3.2) Alternative Approach

The case for $u_s = u$ will be considered first. The flux in the gap may be regarded as being made up of two components acting in opposition. The first component is due to stator currents and the second to rotor currents. The stator sets up a travelling wave of flux of constant amplitude which produces at all points a time variation of flux in quadrature with the current variations at that point. It is assumed that each element of rotor conductor, as it enters the block, acquires a current of magnitude equal to, but opposing, the stator current which it faces. If this current were maintained, the rotor would produce an equal and opposite travelling wave of flux. However, there is no slip and therefore no mechanism by which currents can be maintained indefinitely in the rotor. The current at a particular point in the rotor therefore decays with time. It has an initial value at entry into the block equal and opposite to that of the stator current it faces, but it decays from this value as the bar proceeds away from the

start. Since the rotor structure is an inductive circuit with resistance (the stator, being current fed, can be regarded simply as iron) the decay is exponential and of the form $J_r = J_0 \varepsilon^{-t/\tau}$. These currents produce a travelling flux wave which, at entry, is equal and opposite to the stator flux wave, but which thereafter decays as $\varepsilon^{-t/\tau}$. The final flux wave, being the sum of the two, has the form $K(1-\varepsilon^{-t/\tau})$, where K is the value of the flux that would be set up by the stator currents acting alone at the point S distant s from the entry point, and t is the time taken for a rotor bar to move from the entry point to S, i.e. $t = s/u_s$.

Whence,
$$B_q = K\left(1 - \varepsilon^{-s/\tau u_s}\right)$$

If $u_s\tau/s \gg 1$
$$B_q = \frac{Ks}{\tau u_s}$$

K can be evaluated exactly, since it is a steady-state flux, and this has been done in Section 12.1. The rigorous evaluation of τ presents greater difficulty, since it depends on the flow lines of rotor current, and these are not known unless τ is known and constant. However, τ is evaluated in Section 12.2 for a special case, and if this value is inserted

$$B_q = \frac{\pi\rho_r J_s s}{p u_s}$$

which agrees exactly with eqn. (12).

That this approach yields an exponential subsidence to a steady value, whereas the earlier approach gave an indefinite linear rise, results from the fact that magnetizing current was neglected in the earlier and more rigorous approach which corresponds with $u_s\tau/s \gg 1$ in the second approach. The degree of agreement suggests that the extension provided by the less rigorous second approach can be accepted as substantially true.

This second approach can also be applied to the case of $u \neq u_s$ and provides a corresponding extension. It also provides some physical insight into the reasons for the rather peculiar behaviour of B_q and B_p. In this case the flux is again regarded as due to two components, but now the first component is due to the stator current acting in concert with that part of the rotor current that can be maintained indefinitely by the agency of slip. This flux is, in fact, the final steady-state flux at points remote from the start, and corresponds exactly with the flux in a conventional machine of equal dimensions as regards gap, pole pitch, ρ_r, and so on. This component will contain a small element B_q corresponding with input magnetizing current and a large element B_p corresponding with input load current.

The second component is equal and opposite to the first at the point of entry, but is due to transient currents induced in the rotor which cannot be maintained and which therefore die away with time-constant τ, thus causing the second flux wave to decay from its initial value equal and opposite to the first component. However, this component now differs from the first one not only in the respect that it decays, but also in the respect that, being a rotor transient, it travels at rotor speed u, whereas the first component travels at u_s.

If the decay is ignored for a moment, i.e. $u_s\tau/s \gg 1$, because of the different speeds, the two waves build up a phase difference as the point in question on the rotor proceeds further from the start. Initially, the difference is mainly in quadrature with the two waves, but when one wave has 'slipped' one half-wave relative to the other, the fluxes, which were initially in opposition, become additive, yielding an amplitude of twice the steady-state amplitude. At this point the 'quadrature difference' is zero; beyond it the waves move towards opposition again, with quadrature difference increasing but with reversed sign. After a whole wavelength of slip the initial conditions are reinstated; thereafter the cycle described is repeated indefinitely. This behaviour is consistent with that derived from the earlier analysis and depicted in Figs. 11 and 12.

A detailed analysis which, however, is not rigorous because of the doubts about τ, but which includes the effects of decay and finite magnetizing current, is given in Section 12.3. It shows that

$$B_p = \frac{\rho_r J_s \sigma u_s}{(\sigma u_s)^2 + \left(\frac{\rho_r g}{4p\mu_0}\right)^2}\left\{1 - \exp\left[\frac{-\pi\rho_r g s}{4p^2\mu_0 u_s(1-\sigma)}\right]\right.$$
$$\left.\left[\cos\frac{\pi\sigma s}{p(1-\sigma)} + \frac{\rho_r g}{4p\mu_0\sigma u_s}\sin\frac{\pi\sigma s}{p(1-\sigma)}\right]\right\} \quad . \quad (13)$$

$$B_q = \frac{\rho_r J_s\left(\frac{\rho_r g}{4p\mu_0}\right)}{(\sigma u_s)^2 + \left(\frac{\rho_r g}{4p\mu_0}\right)^2}\left\{1 - \exp\left[\frac{-\pi\rho_r g s}{4p^2\mu_0 u_s(1-\sigma)}\right]\right.$$
$$\left.\left[\cos\frac{\pi\sigma s}{p(1-\sigma)} - \frac{4p\mu_0\sigma u_s}{\rho_r g}\sin\frac{\pi\sigma s}{p(1-\sigma)}\right]\right\} \quad . \quad (14)$$

These equations are depicted in Fig. 13 for the particular case of $\sigma = 1/3$, and $\tau = 1{\cdot}25/f$. The main differences between these

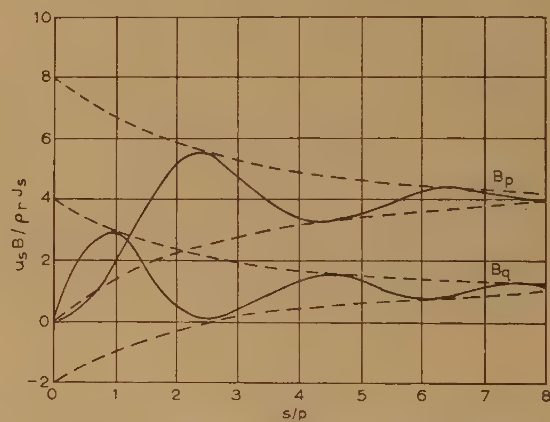

Fig. 13.—Flux distribution with finite air-gap.

curves and those in Fig. 11(c) are that now the oscillation about the mean level gradually decays and the mean level, particularly that of B_q, is shifted.

The presence of a finite value of B_q in the steady state indicates that part of the stator current, which has been used as a reference throughout, must be regarded as magnetizing current.

These curves have been included to illustrate the general effect of magnetizing current, but in the interests of simplicity the remainder of the discussion will be based on the simpler curves of Fig. 12. The important feature of eqns. (13) and (14) is the time-constant $\tau = 4p^2\mu_0/\pi\rho_r g$, since this must be known if $u_s\tau/s$ is to be made large compared with unity, so that Fig. 12 applies to a fair degree of approximation.

(4) EXPERIMENTAL RESULTS

The somewhat unexpected results of the preceding Sections have been tested experimentally with the spherical machine. An 8-pole winding was used with seven search coils arranged at intervals of one pole pitch on the stator surface. The coils were confined to the middle third of the pole width to avoid excessive variation of u_s due to the spherical shape. The voltages

rom these were amplified, and their r.m.s. values measured. The amplifier output was also fed to the Y-plates of an oscillo- graph, the X-plates of which were fed with a voltage of variable phase derived from the supply by means of a Magslip resolver, itted with a scale. The phase was measured by adjusting the Magslip until a straight line was obtained on the oscillograph. Care was taken always to use settings of the Magslip within one quadrant, so that the readings were actually very close together, the search coils being 180° apart. In this way Magslip errors were made negligible.

A small resistance was inserted in series with the connection of one of the stator phases to the star point and the potential difference across this, proportional to stator current, was used as a phase reference.

Measurements were made at standstill, while running light and with a variety of values of slip.

Columns (i)–(iv) of Table 1 show the results at standstill and for $\sigma = 12\frac{1}{2}\%$.

Table 1

Coil No.	(i) V_1	(ii) ξ_1	(iii) V_σ	(iv) ξ_σ	(v) V_L	(vi) ξ_L	(vii) kB_q	(viii) kB_p
	volts	deg	volts	deg	volts	deg	volts	volts
1	21·6	31·0	25·5	25·0	21·4	24·5	4·1	0·2
2	28·2	26·0	36·0	22·0	28·0	19·5	7·9	1·5
3	31·8	22·5	41·6	22·0	31·6	16·0	9·8	4·4
4	30·0	30·5	40·6	33·0	29·8	24·0	10·4	6·4
5	30·1	17·0	40·7	21·0	29·9	10·5	10·2	7·4
6	29·0	25·0	38·4	34·0	28·8	18·5	8·3	10·2
7	29·8	20·0	36·2	30·0	29·6	13·5	5·2	10·3

The phase angles have an arbitrary zero but are related to the phase of the stator current. Fig. 14 illustrates the method used in calculating B_p and B_q.

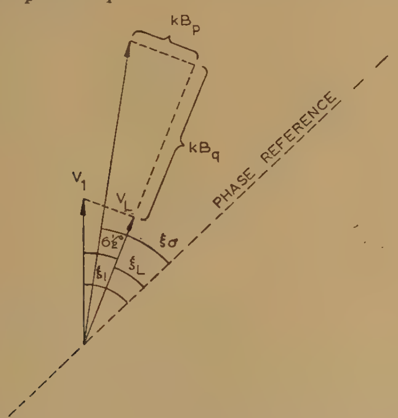

Fig. 14.—Vector diagram for search-coil measurements.

The standstill results include a major contribution from rotor leakage flux, which is not included in the theory. If there were no rotor leakage inductance, this flux would be substantially zero, so the results of Table 1 require correction before compari- son with theory. To do this it has been assumed that, for a given stator current, rotor leakage flux is independent of slip, and this assumption will be valid provided that the space configuration of rotor currents is substantially independent of slip, as it will be if the coupling is good.

To evaluate the rotor leakage flux it is necessary to resolve the observed search-coil voltage at standstill into its in-phase and quadrature components, and for this purpose the rotor time- constant was used. This was deduced from Fig. 8, where it will be noted that the coupling time-constant is $\frac{1}{50}$ sec. The initial ordinate of this curve is an approximate measure of rotor leakage inductance to the same scale as the final ordinate is a measure of coupled inductance plus leakage inductance. The rotor leakage time-constant is therefore $\frac{4}{28} \times 0{\cdot}02$ sec (approximately 0·003 sec) yielding a rotor phase angle of $83\frac{1}{2}°$ at 500 c/s.

In Table 1 the reactive components of column (i) are shown in column (v), and the phase angles of these components relative to the arbitrary zero are shown in column (vi). The phase angles of column (vi) were taken as defining the phase corresponding with quadrature flux B_q and were used to resolve the search-coil voltages defined by columns (iii) and (iv) into B_q and B_p com- ponents, as shown in columns (vii) and (viii), leakage flux, shown in column (v), being subtracted to obtain B_q.

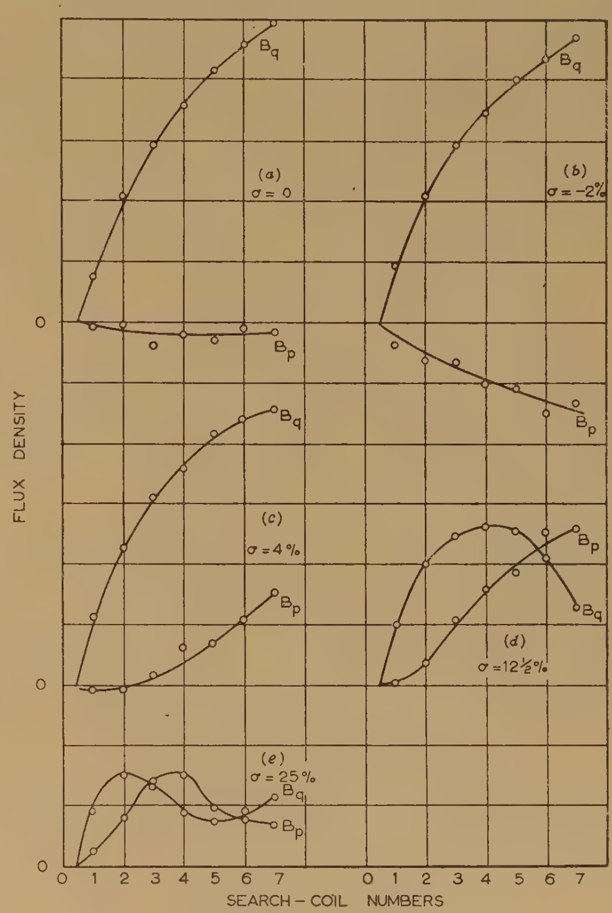

Fig. 15.—Experimental results for flux distribution.

Fig. 15 shows the results of a set of experiments analysed in this way. A high frequency (480 c/s) was used to reduce the effects of decrement, i.e. $\tau u_s/s = 4{\cdot}8$. Fig. 15(*a*) shows the performance at synchronous speed, and exhibits a fairly linear rise of B_q, with B_p substantially equal to 0, as expected from eqns. (10), (11) and (12).

Figs. 15(*b*) and 15(*c*) show the effects of small values of negative slip and positive slip. B_q is little changed, but B_p now enters with its sign dependent on slip [see eqn. (10)]. None of these curves exhibits any oscillatory tendency, since the slip is so small that

$$\frac{\sigma}{1-\sigma}\frac{\pi s}{p} \ll \pi$$

[see eqns. (10) and (11)] for the whole length. At the end of the block, $s = np$, the values are $-0\cdot16\pi$ and $+0\cdot33\pi$.

The oscillatory form is brought out by the curves (*d*) and (*e*) for $\sigma = \frac{1}{8}$ and $\sigma = \frac{1}{4}$ for which the values of $\pi\sigma s/p(1-\sigma)$ are $8\pi/7$ and $8\pi/3$, respectively, for the end of the block. The wavelength of the oscillations is therefore seen to be approximately of the expected value, and there is evidence of the decrement required by eqns. (13) and (14). It may also be seen that the vertical dimension of the diagrams decreases as slip increases, as in Fig. 11. The agreement between Fig. 15(*e*) and Fig. 13 is very striking.

This degree of agreement is regarded as indicating that the theoretical treatment is sufficiently near the truth to form a sound basis for design purposes at this stage in the development of these machines. Agreement in greater detail can hardly be expected, if one bears in mind the many manipulations involved in completing Table 1, which shows that leakage flux is responsible for a major part of most of the measured voltages. More detailed comparison of theory and practice must await the construction of a more suitable test machine in which leakage inductance is kept relatively lower by the use of a larger pole pitch.

Several other sets of curves of B_p and B_q have, in fact, been taken, some for a 4-pole stator. In all cases reasonable agreement with theory was obtained.

(5) ENGINEERING SIGNIFICANCE OF THE THEORETICAL RESULTS

The theory has been developed on the assumption that the supply current is held constant; as a result the terminal voltage is a function of slip. However, provided that this terminal voltage can be calculated as a function of slip it is quite simple to scale the other quantities so as to yield the constant-voltage characteristics.

From the design engineer's point of view the factors of first importance are the external characteristics of the machine in respect of supply voltage, load current, efficiency, torque/speed characteristics, power factor and so on. In deriving these quantities the most important items in the theory are eqns. (10), (11) and (34) and Fig. 12. The importance of eqn. (34) lies only in establishing that in a proposed design $\tau u_s/s$ will be much greater than unity so that eqns. (10) and (11) apply approximately.

(5.1) Torque and Output Power

The average force exerted on a rotor element of length ds and unit width in a direction perpendicular to the plane of the paper in Fig. 10, and situated at S, is

$$dF = fds\int_0^{1/f} j_s b_p dt = \frac{J_s B_p}{2}ds$$

The force on a strip of rotor of unit width and of length equal to the length of the stator block, np, is therefore

$$F = \int_0^{np} dF = \frac{J_s}{2}\int_0^{np} B_p ds = \frac{\rho_r J_s^2}{2\sigma u_s}\left[np - \frac{p(1-\sigma)}{\pi\sigma}\sin\frac{\pi\sigma n}{1-\sigma}\right]$$

or

$$Fu_s = \frac{\rho_r J_s^2}{2\sigma}\left[np - \frac{p(1-\sigma)}{\pi\sigma}\sin\frac{\pi\sigma n}{1-\sigma}\right] \quad . \quad . \quad (15)$$

expressed as 'synchronous watts'. The torque will be the force F multiplied by the appropriate radius. The power output from the strip is

$$P_0 = Fu = \frac{np\rho_r J_s^2(1-\sigma)}{2\sigma}\left(1 - \frac{1-\sigma}{\pi n\sigma}\sin\frac{n\pi\sigma}{1-\sigma}\right) \quad . \quad (16)$$

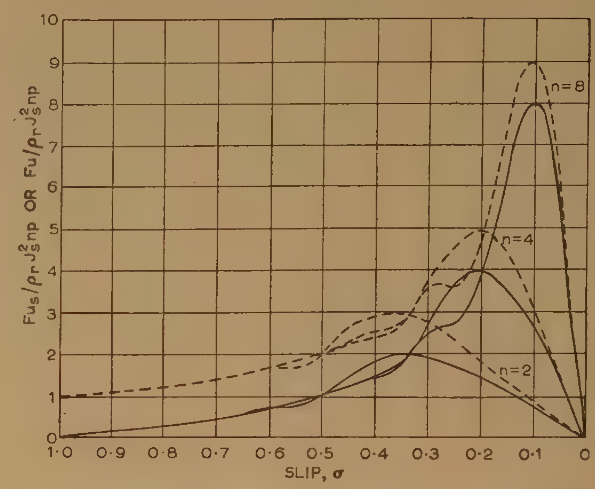

Fig. 16.—Theoretical speed/torque curves at constant current.

Eqn. (16) is plotted in Fig. 16 for two, four and eight poles wound on blocks of equal size. The broken curves show the corresponding 'synchronous watts', Fu_s, from eqn. (15). Fig. 17 shows experimental results at 200 c/s for four and eight poles wound on similar blocks with the same current

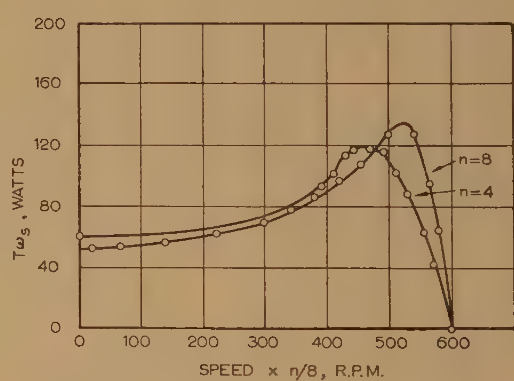

Fig. 17.—Experimental speed/torque curves.

Torque expressed as synchronous watts.

per slot. It may be seen that the general shape is in accordance with expectation, and the peak torques occur at about the right values. On the other hand, in the experimental results, the standstill torque is a much larger fraction of the peak torque than the theory predicts. There are two probable reasons for this. The peak observed torque will be less than the theoretical value because, in the practical case, there is some decrement [see Fig. 15(*a*)], which means that the flux density at exit is less than the expected value. Secondly, the effective rotor resistance is probably higher at standstill than during running, owing to skin effects.

It has been verified that skin effects are significant by comparing standstill rotor and stator copper losses at various frequencies, and it is found that the rotor losses increase relatively at the higher frequencies, the resistance being apparently nearly twice as high at 300 c/s as at 100 c/s. Similar effects probably explain the failure of the ratio of the peaks to reach the expected value, although mechanical differences between the two blocks might contribute to this discrepancy.

(5.2) Rotor Copper Loss

The copper loss per unit square of rotor is $\rho_r(J_r^2/2)$.
So for the strip considered above

$$P_r = \tfrac{1}{2}\int_0^{np} \rho_r J_r^2 ds$$

and if J_r is assumed uniform along the strip, as it will be provided that $\tau u_s/s$ is much greater than unity,

$$P_r = \tfrac{1}{2}\rho_r J_r^2 np \quad . \quad . \quad . \quad . \quad . \quad . \quad (17)$$

(5.3) Stator Copper Loss

Clearly
$$P_s = \frac{\rho s}{\rho r} P_r \quad . \quad . \quad . \quad . \quad . \quad . \quad (18)$$

if $J_s = J_r$ and if rotor leakage inductance is neglected.

(5.4) Efficiency

If iron loss, friction, windage, etc., are ignored, eqns. (16), (17) and (18) permit evaluation of the efficiency as

$$\eta = \frac{P_o}{P_o + P_r + P_s} \quad . \quad . \quad . \quad . \quad . \quad . \quad (19)$$

where P_o is the power output and P_r and P_s are the rotor and stator copper losses respectively. Before evaluating this quantity, reference will be made to Fig. 12. For any given value of slip, the abscissa of the graph is proportional to distance travelled under the stator block from the point of entry. For short distances travelled, i.e. abscissae less than, say, $\pi/4$, copper losses, both rotor and stator, accumulate in proportion to distance, but output power, being proportional to B_p, accumulates at a very low rate compared with the mean rate for a very long stator, which is measured by the mean value of B_p, which itself is the value B_p would have in a conventional machine with similar pole pitch, gap, windings, etc.

It follows that if the end of the stator block were at a distance corresponding to an abscissa of, say, $\pi/4$, the rotor copper loss would be vastly in excess of that appropriate to a conventional machine developing the same output power. On the other hand, if the block was of length corresponding to π, in the equivalent length between $\pi/2$ and π the flux density B_p (and therefore the output power) exceeds the mean by as much as it falls short of the mean between 0 and $\pi/2$, and a block of length corresponding to π would have rotor copper loss exactly appropriate in conventional terms to its power output.

A block length corresponding to $3\pi/2$ would appear to do better than a conventional machine; this has yet to be investigated, but it may be noted that there is no fundamental objection to this result since no exact value can be ascribed to the velocity of the field—which increases in size and changes phase as it travels.

A block length corresponding to 2π might appear ideal. The average value of B_q is 0, so the power factor is unity (discounting magnetizing current and leakage reactance this would always be true in a conventional machine), the average of B_p is that appropriate to a conventional machine, and the flux density at entry to and exit from the block is zero.

However, reference to Fig. 16 shows that $P_o = Fu$ has a maximum value near $\sigma = 1/(n+1)$. Since this is a constant-current graph both P_r and P_s will be constant, and it follows from eqn. (19) that the efficiency has a maximum near $\sigma = 1/(n+1)$.

Further discussion of numerical efficiency will be found in Section 8, it being sufficient to note here that a possible explanation of the 'missing watts' has been exposed.

(5.5) 'Excess' Rotor Copper Losses

If 'excess' rotor copper losses, P_e, are defined as actual copper losses minus the copper losses appropriate to the power output and slip of a conventional machine,

$$P_e = \tfrac{1}{2}\rho_r J_s^2 np - \frac{\sigma}{1-\sigma} P_o$$

Substituting for P_o from eqn. (16) yields

$$P_e = \tfrac{1}{2}\rho_r J_s^2 np - \frac{\sigma}{1-\sigma}\left\{\frac{\rho_r J_s^2 u}{2\sigma u_s}\left[np - \left(\frac{1-\sigma}{\sigma}\right)\frac{p}{\pi}\sin\frac{n\pi\sigma}{1-\sigma}\right]\right\}$$

or
$$P_e = \frac{\rho_r J_s^2 np}{2}\left[\frac{\sin\dfrac{n\pi\sigma}{1-\sigma}}{\dfrac{n\pi\sigma}{1-\sigma}}\right] \quad . \quad . \quad . \quad . \quad (20)$$

or
$$P_e = \tfrac{1}{2}\rho_r J_s^2 np\left(\frac{\sin\psi}{\psi}\right)$$

where $\psi = n\pi\sigma/(1-\sigma)$. Eqn. (20) is plotted in Fig. 18 for the particular cases of two, four and eight poles.

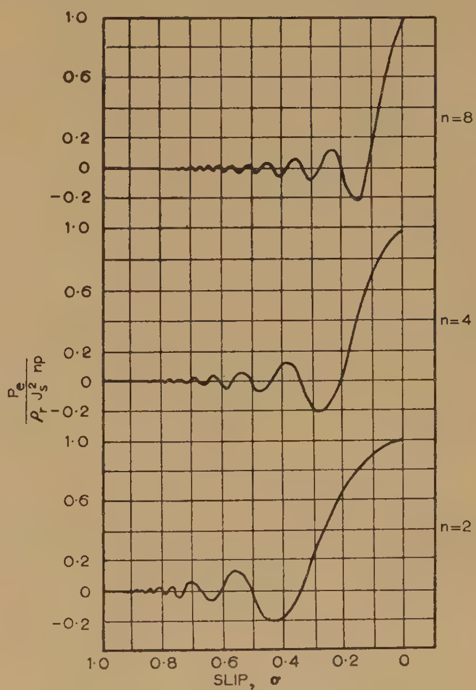

Fig. 18.—Theoretical curves for excess rotor copper loss.

If the missing-power curve of Fig. 6 is replotted at constant current with ordinates $P_m/N^2J_s^2$, where N is the stator-to-rotor turns ratio, the result is as in Fig. 19, curve (*b*); curve (*a*), which is similar, is for an 8-pole structure. Since the curves of Fig. 19 represent total untraced power, which includes iron loss and any stray load losses, and since the ordinates represent only about 20% of the total input, the general agreement with Fig. 18 is thought to be satisfactory. The drop in $P_m/N^2J_s^2$ between synchronous speed and $\sigma = 1/(n+1)$ is about the same in the two cases, as is required by the theory.

(5.6) Terminal Voltage

Because the flux wave in the gap is a complicated function of s and σ, terminal voltage cannot be assessed by the simple process

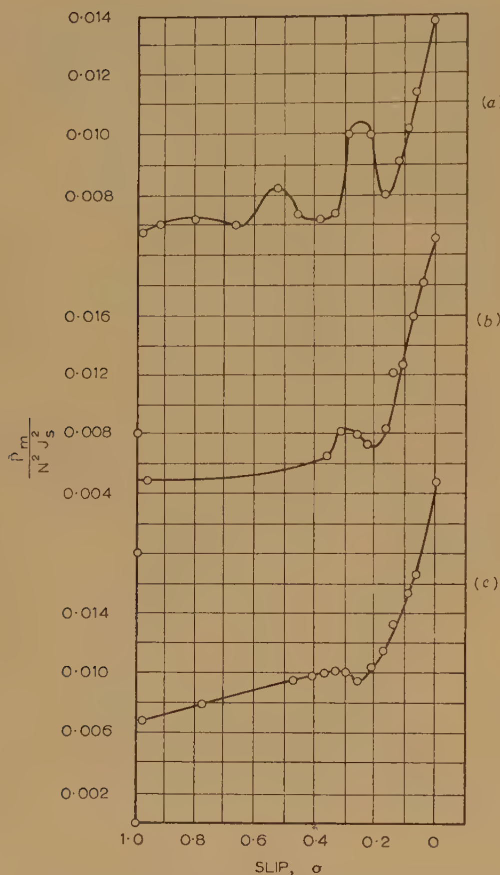

Fig. 19.—Experimental missing-power curves.

(a) 8-pole block.
$\theta = 0$
$n = 8$

(b) 4-pole block.
$\theta = 0$
$n = 4$

(c) 8-pole block.
$\theta = 60°$
n (equivalent) $= 4$.

of ascribing a velocity to the field and using the flux-cutting rule. The apparent-power intake can, however, be calculated by other means, and this has been done in Section 12.4, which shows that, for a strip of unit width and length np,

$$P_i = \rho_r J_s^2 p\left[\frac{n}{\sigma} - \frac{1}{\pi}\left(\frac{1-\sigma}{\sigma}\right)^2 \sin\psi\right] \quad . \quad . \quad (21)$$

$$Q_i = \rho_r J_s^2 p\left[\frac{1}{\pi}\left(\frac{1-\sigma}{\sigma}\right)^2 - \frac{1}{\pi}\left(\frac{1-\sigma}{\sigma}\right)^2 \cos\psi\right] \quad . \quad (22)$$

In these expressions J_s is the surface current density, and in a practical machine would be replaced by βI_a, where I_a is the actual line current and β is a factor depending on the winding arrangement, i.e. slots per pole, conductors per slot and so on. To find the phase voltage it is then necessary to divide P_i and Q_i by I_a and multiply by the pole width, W. For the present purpose it will suffice to divide P_i and Q_i by J_s, so obtaining a figure proportional to terminal voltage. The constant of proportionality K_1 is dependent on β and W but independent of slip,

hence $$V_p = K_1\rho_r J_s p\left[\frac{n}{\sigma} - \frac{1}{\pi}\left(\frac{1-\sigma}{\sigma}\right)^2 \sin\frac{n\pi\sigma}{1-\sigma}\right] \quad . \quad (23)$$

$$V_q = K_1\rho_r J_s p\left[\frac{1}{\pi}\left(\frac{1-\sigma}{\sigma}\right)^2 - \frac{1}{\pi}\left(\frac{1-\sigma}{\sigma}\right)^2 \cos\frac{n\pi\sigma}{1-\sigma}\right] \quad (24)$$

The total terminal voltage is $\sqrt{(V_p^2 + V_q^2)}$ and the power factor is $V_p/\sqrt{(V_p^2 + V_q^2)}$. These quantities are plotted in Figs. 20 and 21 as functions of slip for $n = 2$, 4 and 8. The broken

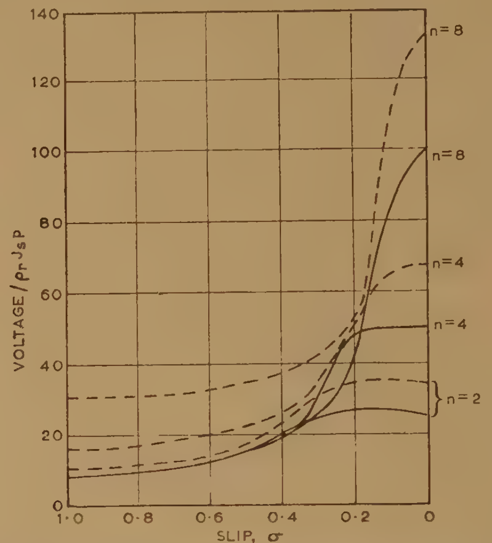

Fig. 20.—Theoretical voltage/slip curves at constant J_s.

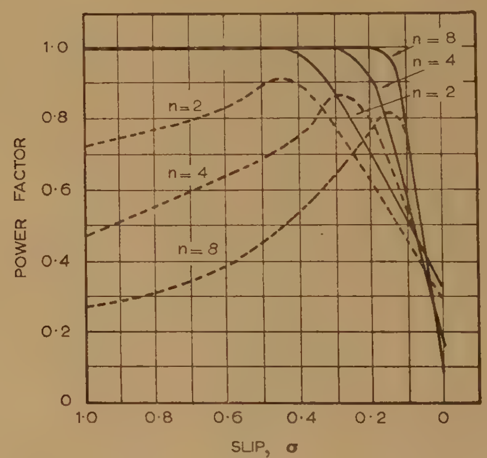

Fig. 21.—Theoretical power-factor/slip curves.

curves relate to cases including leakage inductance L where $L\omega_s = 30K_1\rho_r p$, the effect of which is simply to add $L\omega_s J_s$ numerically to V_q. There will, of course, be a corresponding degeneration of power factor on Fig. 21, as shown by the broken curves.

From Fig. 21 it may be seen that the power factor is satisfactory for all values of σ in excess of $1/(n + 1)$, but rapidly becomes unacceptable at lower values of slip.

The interesting feature of the voltage curve is that it enables the torque curves in Fig. 16 to be redrawn on a constant-voltage basis. This has been done in Fig. 22, where it may be seen that the peak at $1/(n + 1)$ has vanished and there is a steady rise of torque (and, of course, of load current) as slip increases. Here again the continuous curves relate to zero leakage inductance, and the broken curves to the same leakage inductance as that

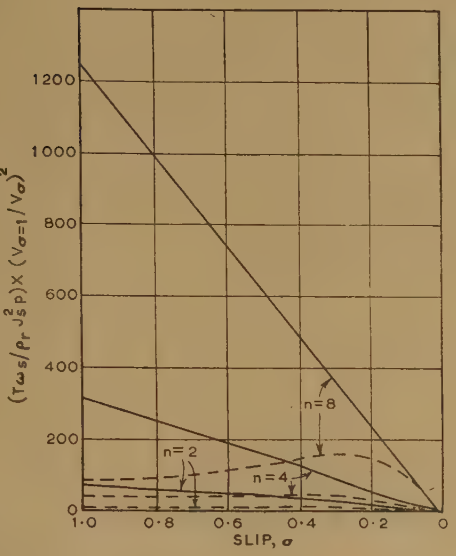

Fig. 22.—Theoretical speed/torque curves at constant voltage.

used for the broken curves in Figs. 20 and 21. The practical difficulty is to reduce the inherent leakage to an acceptable value; no experimental values are given since the experimental machine had excessive leakage.

(6) OPERATION AT AN ANGLE

When the stator block is turned through an angle θ from the 0° position, as shown in Fig. 23, rotor elements such as those considered in Section 2 cannot proceed along the line of motion of the field, but only in directions parallel to OO′. Such elements will, however, have a component of velocity u_r along the direction of the field, acting in conjunction with a component $u_q = u_r \tan\theta$ at right angles to the direction of motion of the field. From Fig. 10 and the associated analysis it appears that the formulae deduced would not be invalidated if the entire diagrams were given a velocity at right angles to the paper, corresponding with

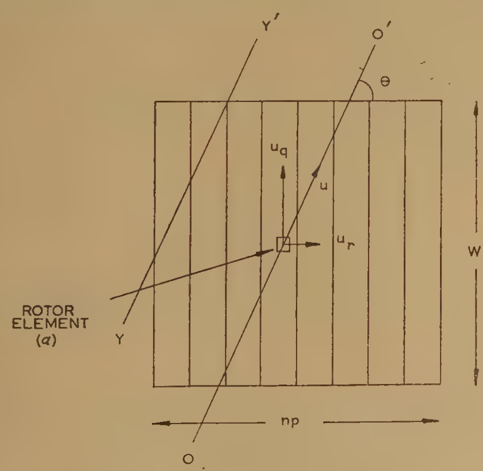

Fig. 23.—Operation at an angle θ.

u_q in Fig. 23. The only effect in Fig. 10 is that the time spent under the block by an element such as (*a*) in Fig. 23 is reduced from

$$\frac{np}{u_r}$$

at $\theta = 0$ to

$$\frac{W}{u_q} = \frac{W}{u_r \tan\theta} = \frac{np}{u_r \tan\theta}$$

(for a square block) at any other value of θ.

This factor can be incorporated in the formulae by substituting $W/\tan\theta$ for the block length. Calculated torques will require multiplication by $\cos\theta$ and calculated speeds by $1/\cos\theta$. Slip values will be unchanged.

These arguments apply quantitatively only to strips formed by elements of the rotor crossing the stator along paths such as O–O′ in Fig. 23. Paths such as Y–Y′ yield a different and variable value of block length. However, for large values of θ, say $\theta > 60°$, most paths will be of the O–O′ kind.

The detailed implications of this equivalence will not be discussed further, it being sufficient now to note that the effect of greatest importance is the reduction of the effective number of poles in a square block from n to $n/\tan\theta$, with the attendant change in the optimum slip, which now becomes

$$\sigma = \frac{1}{\dfrac{n}{\tan\theta} + 1}$$

Similar results can be obtained alternatively by redefining Fig. 10 so that it represents a section through OO′ or YY′ on Fig. 23 instead of a section along the direction of u_r. To do this it is necessary to write $p/\cos\theta$ for p in the equation for the travelling wave, so that the apparent pole-pitch increases as θ increases. The analysis can then proceed as before, and actual values of rotor speed will enter throughout, but in order to calculate torque and terminal voltage it will be necessary to correct for the fact that now the sides of the elementary coil do not emerge perpendicularly from the paper, but at an angle θ to it.

The validity of this approach has been tested by comparing the performance of a 4-pole stator at 60° with two of those four poles at 0°. To obtain common abscissae the measured speeds at 0° were doubled, and the observed torques and input powers were also doubled to compensate for the fact that one-half of the block was then inactive. Both sets of curves are plotted on Fig. 24. The agreement is good and both curves show the

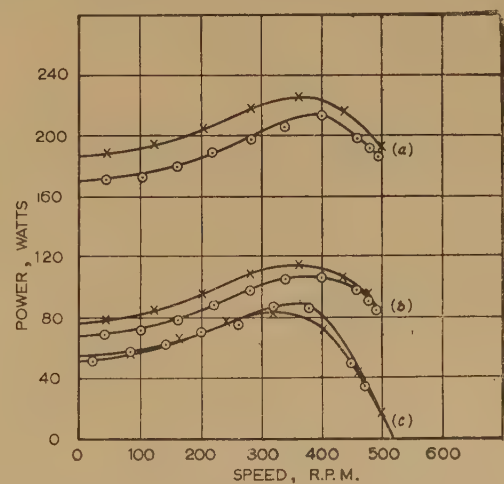

Fig. 24.—Comparison between 4-pole stator at 60° and 2-pole stator at 0°.

○○○ 4-pole 60°.
××× 2-pole 0°.
(*a*) Input power.
(*b*) Input power less stator copper loss.
(*c*) Synchronous watts, $T\omega_s$.

typical peak in the vicinity of $\sigma = 1/3$. Additional confirmation is supplied by curve (c) in Fig. 19, which shows missing power for eight poles at 60°; this may be seen to have the shape appropriate to a 4-pole structure.

It is believed that with sufficient development this approach could explain the shape of the speed/$(1/\cos\theta)$ curves in Fig. 5, but it would also be necessary to discover the cause of the failure of 2-pole blocks to produce the calculated speed at 0°. This is believed to be connected with the fact that on exit from the block the rotor is energized and carries energy away from the block continuously, but no quantitative agreement between observation and speculation has yet been obtained.

(7) STATOR END-EFFECTS

The preceding theory takes no account of events at the exit end of the stator block; the entry end is taken into account in the requirement that $b = 0$ there. Similar considerations suggest that b must retain its value, b_x, at exit even after the particular rotor element considered has left the block. This is illustrated in Fig. 25. Here the iron structure of the stator is

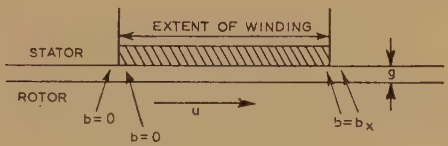

Fig. 25.—Stator end-effects.

shown as continuous, but the stator winding is of limited length. The flux density immediately beyond the winding must be b_x; otherwise there would be an instantaneous change in flux through the short-circuited rotor conductors at exit. Since there is now no stator current there will be rotor current sufficient to produce this flux. The flux will decay exponentially as the rotor element moves on, owing to dissipation in the rotor resistance. The r.m.s. value of b_x at exit will be

$$\frac{B_x}{\sqrt{2}} = \sqrt{\left(\frac{B_{px}^2 + B_{qx}^2}{2}\right)}$$

where B_{px} and B_{qx} are the values obtained by putting $s = np$ in eqns. (10) and (11).

The average magnetic energy carried away from the stator in this way is $\frac{1}{2}B_x^2\,\frac{1}{8\pi\mu_0}g$ per unit square of rotor surface leaving the stator. The corresponding rate of energy loss per unit length of stator edge perpendicular to the paper in Fig. 25 is

$$P_x = \frac{1}{2}B_x^2\,\frac{1}{8\pi\mu_0}gu \quad . \quad . \quad . \quad . \quad . \quad (25)$$

Both u and B_x have their greatest values at $u = u_s$, when $B_x = B_{qx} = \frac{\pi}{p}\rho_r J_s \frac{s}{u_s}$ [eqn. (11)].

Therefore $$P_{x(max)} = \frac{1}{2}\,\frac{g}{8\pi\mu_0}\,\frac{\pi^2}{p^2}\rho_r^2 J_s^2 \frac{s^2}{u_s^2}u_s$$

where $s = np$,

or $$P_{x(max)} = \frac{1}{2}\rho_r J_s^2 pn\left(\frac{1}{2}\,\frac{np}{u_s\tau}\right) \quad . \quad . \quad . \quad . \quad (26)$$

where τ is evaluated from eqn. (34), and is the time-constant of decay of the rotor currents producing b_x.

It is a design requirement that $u_s\tau/s > 1$, and it follows that in the circumstances of Fig. 25,

$$P_{x(max)} < \tfrac{1}{4}\rho_r J_s^2 np$$

which is the rotor copper loss. If this were the whole stor stator end-effect could be neglected. Unfortunately, it is n the whole story: the iron of the stator does not continue beyon the winding, and even if it conveniently could, the flux carrie away by the rotor must be dissipated somehow before the roto re-enters a stator block, if the entry condition $b = 0$ is not to t vitiated. Again, when the stator block is turned through a angle, rotor speed increases and magnetic energy is transporte at a greater rate. All these factors indicate that this effect mu be examined fully, but this has not yet been done. Some simila work appears to have been done in Russia in connection wit 'arch'-type motors,[2,3,4,5] and this is currently under examinatio

One way of dissipating the flux fairly quickly would be t continue the stator iron beyond the end of the winding, but wit the gap increased by a factor γ so as to replace τ by τ/γ. If th interval between stators were equal to stator length, then $\frac{\gamma}{\tau}\,\frac{np}{u_s} =$ might suffice. $P_{x(max)}$ would then be one-half of the rotor coppe loss. The stator iron is not continued in the experimenta machines, but there is, of course, some rotor inductance eve when the rotor is outside the stator block. Since it may be see from Fig. 11 that B_x falls fairly quickly as slip increases, an since this 'edge' loss is proportional to B_x^2, it is not unreasonabl to assume for the present that the effect is not dominant a working speeds. It is thought, however, that it may well explai the failure of 2-pole machines to reach full speed, and also th strange flatness of the curves of Fig. 5 at high values of θ.

(8) DESIGN PROCEDURE

It was shown in Section 5.4 that maximum efficiency occu when $\sigma = 1/(n+1)$, whilst reference to Fig. 21 shows that th power factor with $\sigma = 1/(n+1)$ is about 87%, which is regarde as acceptable, bearing in mind that it would be necessary t double the slip to get a power factor of unity, discounting mag netizing current and leakage effects. The fact that $\sigma = 1/(n+1$ corresponds with a peak on Fig. 16 need not deter us fro choosing this as a maximum load condition, because thes curves are for constant current. Fig. 22 shows that there is n corresponding peak in the constant-voltage curve.

The design will be discussed in the first place in terms c constant-current supply, the implications of the necessary chang to constant-voltage conditions being discussed separately late It will also be assumed that operation will be designed to occu in a range where the decrement of the fluxes can be neglecte since this is simplest, and will suffice to bring out the salie points in the design of this new type of machine. This require that

$$\frac{\tau u_s}{np} = \frac{2\tau f}{n} = \frac{8p^2\mu_0 f}{\pi\rho_r g n} > 1 \quad . \quad . \quad . \quad . \quad (27$$

for all designs.

Eqn. (19) states the efficiency, neglecting iron loss, as

$$\eta = \frac{P_o}{P_o + P_r + P_s}$$

Eqns. (17) and (18) give P_r and P_s, and inserting $\sigma = 1/(n+1$ in eqn. (16) yields

$$[P_o]_{\sigma=\frac{1}{n+1}} = n\left(\frac{\rho_r J_s np}{2}\right) = n \times \text{(rotor copper loss)}$$

Hence $$\eta = \frac{n}{n + 1 + \dfrac{\rho_s}{\rho_r}} \quad . \quad . \quad . \quad . \quad . \quad (2$$

From this equation it may be seen that n should be large,

would be expected from the fact that in a conventional machine n is effectively infinite.

Similarly, ρ_s should be small, as expected. What is perhaps unexpected is the fact that ρ_r should not be made too small; it should in fact be made greater than ρ_s, particularly if n, as is likely, is not very large. This means that, in general, the rotor slotting will be made much smaller than the stator slotting.

In a conventional machine ρ_r is commonly made very small, and its relation to ρ_s is not particularly significant; this is because in a conventional machine the slip at full load is proportional to ρ_r, whereas in variable-speed machines full-load slip is set by other considerations.

The requirement that n should be large is not easily met, for the larger it is made the smaller the pole pitch becomes, and the more difficult it is to achieve high efficiency even in a conventional machine. If one assumes as a round figure a stator block occupying one-quarter of the periphery of the rotor, it will be found that with $n = 8$ (the equivalent conventional machine has 32 poles) the limiting efficiency from eqn. (28) will be 88%, even if $\rho_r \gg \rho_s$. Thirty-two-pole conventional machines with efficiencies of this order can be made only with large diameters; it may therefore be better to use $n = 4$ and accept a limiting efficiency of 80%. If it is borne in mind, however, that with square blocks a 2 : 1 increase in speed will involve an effective 2 : 1 reduction in n, it seems likely that where speed ranges of 2 : 1 or greater are required, $n = 8$ should be used.

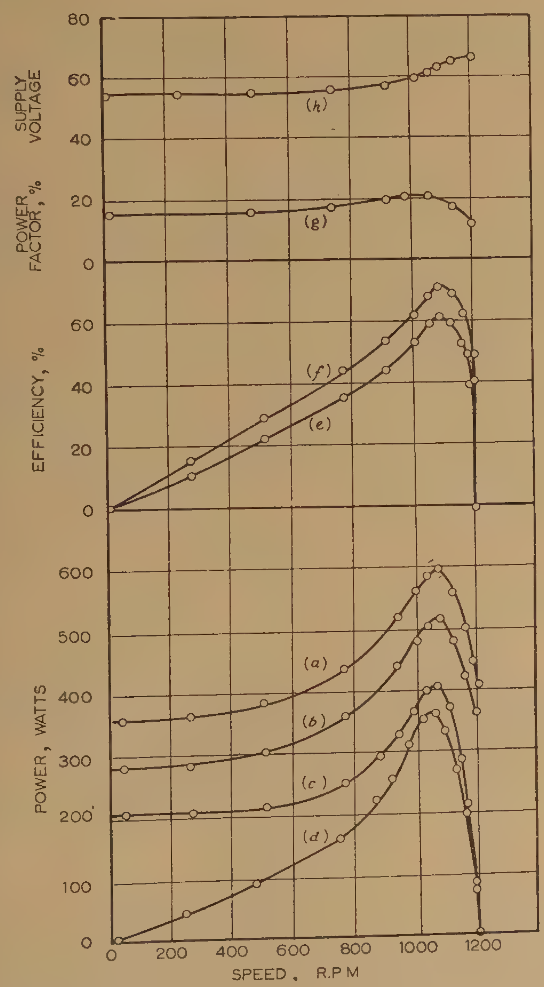

Fig. 26.—Results of brake test with 8-pole stator at 0°, 400 c/s.

(a) Input power.
(b) Input power less stator copper loss.
(c) Synchronous watts, $T\omega_s$.
(d) Output power.
(e) Overall efficiency.
(f) Efficiency neglecting stator copper loss.
(g) Power factor.
(h) Supply voltage.

Since square blocks will not necessarily always be used, this design criterion should probably be restated thus: 'The number of effective poles should not fall much below four at any speed where high efficiency is required'.

The other design criteria emerging from this discussion are that rotor resistance should exceed stator resistance, which itself should be made as small as possible, and that the full-load slip should be $1/(n + 1)$ where n is the number of stator poles presented to a rotor element as it traverses the stator. It is also necessary that the rotor should be able to dissipate as heat $1/n$ of the output power required.

It has not yet been possible to build a new machine incorporating these principles. The present machine can be criticized in several respects. Thus, with reference to Fig. 6, it is clear that ρ_s/ρ_r is not sufficiently small, the ratio at standstill being about 1 : 1. It is also apparent from Fig. 8 that the time-constant τ is too small for satisfactory operation at 50 c/s. The situation cannot be improved by adjustment of ρ_r since to improve ρ_s/ρ_r requires an increase of ρ_r, and to increase τ requires a reduction of ρ_r. On the other hand, increased size would permit both reduction of ρ_s and increase of τ without change of ρ_r. This course is not immediately possible. All that can be done now is to record the best result that has been achieved so far with the present machine. For this purpose a high frequency was used. This has a twofold effect: first the required value of τ is reduced, and secondly, the apparent value of ρ_r is increased by skin effects.

Fig. 26 relates to the experimental machine run at 400 c/s. The standstill values now show $\rho_s \simeq \frac{1}{3}\rho_r$, but this will not be maintained under running conditions. In spite of this the importance of stator copper loss has been reduced, although at the expense of a relative increase in iron loss as represented by the difference between curves (b) and (c) at standstill. The overall efficiency is now 61%.

However, in achieving this fairly high efficiency, the importance of leakage inductance has been emphasized by the high frequency; the power factor is therefore poor and the change in terminal voltage is small, the bulk of the terminal voltage arising from voltage drop across the stator leakage inductance.

(9) CONCLUSIONS

The most important general conclusion drawn from the work described is that the general theoretical approach contained in Sections 3 and 5 is substantially correct. With the help of this theoretical insight it should now be possible to investigate fully the performance that can be expected from this type of machine in most circumstances. The salient characteristics have already been described, but much remains to be done, particularly as regards estimating leakage inductance effects and the investigation and control of stator exit-edge losses.

On the practical side it appears that efficient machines can be made only in large sizes, and that for 50 c/s operation over a substantial speed range, say 2 or 3 to 1, the rotor diameter would need to be at least 24 in. This appears to be consistent with Russian practice in arch motors, where the power levels are in the megawatt range.[6] Improved mechanical design may permit some reduction below this figure, but it seems improbable that it will be very great.

Much smaller machines can, of course, be made and they can have extensive speed ranges—5·5 : 1 has in fact been achieved—but efficiency and power factor are then rather poor.

The theory discussed in Sections 3 and 5, which applies to all short-stator machines irrespective of whether the field is 'angled' or not, is of general application; for instance, it applies to liquid metal pumps,[7] shuttle propulsion schemes,[8] aircraft launchers,[9] arch motors and so on. Furthermore, it may be that some process of loss comparable to that described in the theory may exist in conventional machines owing to variation of air-gap around the periphery; the short-stator machine is merely an extreme case.[10] It may prove possible to explain some part of the so-called 'stray load losses' of conventional machines in this way.

Further work on this subject is proceeding along two main lines. A rather larger spherical machine on a different mechanical plan permitting increased pole pitch is being designed using the principles described in the paper. When this has been tested it should be possible to make a fair assessment of the practicability of the spherical machine. The second line of development lies in replacing the mechanical adjustment of skew used in the spherical machine by an equivalent electrical adjustment on a cylindrical machine using phase-shifting transformers. It has already been established that speed ranges in excess of 3 : 1 can be obtained in this way, but experiments have not yet proceeded far enough for the efficiency to be predicted.

Although attention in theory and experiments has been concentrated on the performance of the machine as a motor, it is clear that similar principles govern its behaviour as a generator.

(10) ACKNOWLEDGMENTS

The authors are indebted to the Metropolitan-Vickers Electrical Co. Ltd., for help in making the experimental machines; to Mr. Arthur Gledson for his invaluable help in the mechanical design and construction of the machines, and to the staff of the Manchester University Electrical Engineering Department for much useful discussion.

(11) REFERENCES

(1) WILLIAMS, F. C., and LAITHWAITE, E. R.: 'A Brushless Variable-Speed Induction Motor', *Proceedings I.E.E.*, Paper No. 1737 U, November, 1954 (**102** A, p. 203).

(2) SHTURMAN, G. I.: 'An Induction Motor with an Open Magnetic Circuit', *Elektrichestvo*, 1946, No. 10, p. 43.

(3) SHTURMAN, G. I., and ARONOV, R. L.: '"Edge Effect" in Induction Motors with Open Magnetic Field', *ibid.*, 1947, No. 2, p. 54.

(4) REZIN, M. G.: 'Armature Reaction Effects and the Mechanical Characteristics of a Motor with an Arc-Shaped Stator', *ibid.*, 1950, No. 2, p. 51.

(5) REZIN, M. G.: 'Some Peculiarities of the Electromagnetic Phenomena in a Motor with an Arc-Shaped Stator', *ibid.*, 1951, No. 6, p. 25.

(6) FRIDKIN, P. A.: *Engineer's Digest*, 1945, **6**, p. 281.

(7) REECE, A. B. J.: 'Power Production in Nuclear Reactors', *Students' Quarterly Journal*, 1954, **25**, p. 7.

(8) LAITHWAITE, E. R., and LAWRENSON, P. J.: 'A Self-Oscillating Induction Motor for Shuttle Propulsion', *Proceedings I.E.E.*, 1956 (to be published).

(9) 'A Wound-Rotor Motor 1 400 feet Long', *Westinghouse Engineer*, 1946, **6**, p. 160.

(10) KIKLEVICH, N. A.: 'The Influence of Non-Uniform Airgap on the Characteristics and Reliable Operation of Induction Motors', *Elektrichestvo*, 1949, No. 12, p. 15.

(12) APPENDICES

(12.1) Calculation of Steady-State Flux Density

For steady-state conditions all flux and current distributions are sinusoidal and it is permissible to integrate over a pole pitch in order to evaluate the magnetizing current required to set up a given flux density. The flux distribution will, of course, be in space quadrature with the current distribution.

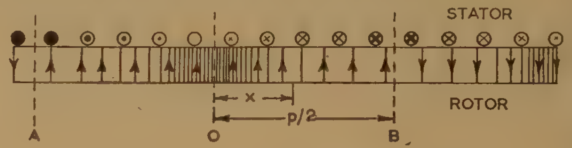

Fig. 27.—Flux and current distributions.

The peak flux density at O (Fig. 27) is calculable from a knowledge of the effective m.m.f. from A to B, i.e.

$$4\pi \int_0^{p/2} j_m ds = \frac{Bg}{\mu_0}$$

where g is the gap length and μ_0 the gap permeability, and j_m can be expressed as $J_m \sin(\pi s/p)$ with reference to O. Therefore

$$B = \frac{4\pi\mu_0 J_m}{g} \int_0^{p/2} \sin\frac{\pi s}{p} ds = \frac{4p\mu_0}{g} J_m \quad . \quad . \quad . \quad (29)$$

whence, $b = B \cos \pi s/p$ since it is in space quadrature with j_m.

For $u = u_s$ the stator current j_s would in the steady state be wholly magnetizing and would produce a flux density $\frac{4p\mu_0}{g}J_s$ in space quadrature with J_s.

For $u \neq u_s$ the rotor bars cut the flux at velocity σu_s thereby acquiring a voltage $b\sigma u_s$ per unit length at right angles to the plane of the paper in Fig. 27. The flux distribution is now not wholly in space quadrature with J_s. It can therefore be resolved into components $b'_p = B'_p \sin \pi s/p$ in space phase with J_s and $b'_q = B'_q \cos \pi s/p$ in space quadrature with it. The magnetizing currents necessary to set up b'_p and b'_q are accordingly, from eqn. (29),

$$j_{mp} = \frac{gB'_q}{4p\mu_0} \sin\frac{\pi s}{p}$$

and

$$j_{mq} = -\frac{gB'_p}{4p\mu_0} \cos\frac{\pi s}{p}$$

The difference between stator and rotor current at any point is the magnetizing current. Hence, the rotor current-density may be represented as two components j_{rp} and j_{rq} given by

$$j_{rp} = j_s - j_{mp} = \left(J_s - \frac{gB'_q}{4p\mu_0}\right) \sin\frac{\pi s}{p} \quad . \quad . \quad (30)$$

$$j_{rq} = \frac{gB'_p}{4p\mu_0} \cos\frac{\pi s}{p} \quad . \quad . \quad . \quad . \quad . \quad . \quad (31)$$

These components give rise to voltage components $\rho_r j_{rp}$ and $\rho_r j_{rq}$, owing to resistance drop, and these voltages must be balanced by the induced voltages due to the slip.

Slipping through flux b'_p produces a voltage $\sigma u_s b'_p$ in phase with b'_p, and the equations correlating b'_p and b'_q can therefore be written

$$\sigma u_s b'_p = \rho_r j_{rp}$$

$$\sigma u_s b'_q = \rho_r j_{rq}$$

i.e. from eqns. (30) and (31)

$$\sigma u_s B_p' = \rho_r\left(J_s - \frac{gB_q'}{4p\mu_0}\right)$$

$$\sigma u_s B_q' = \frac{\rho_r g B_p'}{4p\mu_0}$$

Solving for B_p', B_q' yields

$$B_p' = \frac{\rho_r J_s \sigma u_s}{(\sigma u_s)^2 + \left(\frac{\rho_r g}{4p\mu_0}\right)^2} \quad . \quad . \quad . \quad . \quad (32)$$

$$B_q' = \frac{\rho_r J_s\left(\frac{\rho_r g}{4p\mu_0}\right)}{(\sigma u_s)^2 + \left(\frac{\rho_r g}{4p\mu_0}\right)^2} \quad . \quad . \quad . \quad . \quad (33)$$

(12.2) Calculation of Rotor Time-Constant, τ

Fig. 28 shows a half-wavelength of the flux density b, where $b = B\cos\pi x/p$ and x is measured from O.

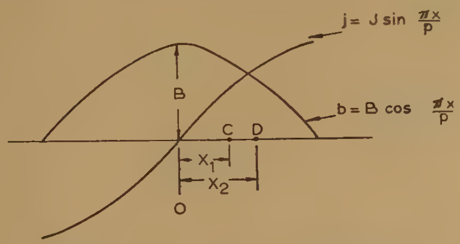

Fig. 28.—Flux and current relationship.

The total flux Φ contained within a loop such as CD is seen to be

$$\Phi = \int_{x_1}^{x_2} B\cos\frac{\pi x}{p}dx$$

$$= \frac{p}{\pi}B\left(\sin\frac{\pi x_2}{p} - \sin\frac{\pi x_1}{p}\right)$$

The current j_m which sets up b produces a resistive voltage-drop $\rho_r(j_d - j_c)$ around the loop CD.

This voltage drop is seen to be

$$\rho_r J_m\left(\sin\frac{\pi x_2}{p} - \sin\frac{\pi x_1}{p}\right)$$

which must therefore balance $d\Phi/dt$, and the time-constant of decay of i_r will be

$$\tau = \Phi\Big/\frac{d\Phi}{dt} = \frac{pB}{\pi\rho_r J_m}$$

which is independent of x_1 and x_2 so that it is fair to assume that the currents decay without changing their flow lines.

From eqn. (29) of Section 12.1

$$J_m = \frac{Bg}{4p\mu_0}$$

whence

$$\tau = \frac{4p^2\mu_0}{\pi\rho_r g} \quad . \quad . \quad . \quad . \quad . \quad . \quad . \quad (34)$$

(12.3) Evaluation of Flux Density at Slip σ including Finite Air-Gap

With reference to Fig. 10, the time elapsed between the elementary coil Q entering the stator and reaching the point S is $t - t'$.

The decaying transient is of the form

$$b'' = A_o\varepsilon^{-(t-t')/\tau}$$

where A_o is a function of the time of entry and $t - t'$ is the time since entry equal to s/u, so that transients have the form

$$b'' = A_o\varepsilon^{-s/\tau u} \quad . \quad . \quad . \quad . \quad . \quad . \quad (35)$$

Section 12.1 evaluates the steady-state flux density as in-phase and quadrature components. These can each be expressed as waves travelling with velocity u_s, i.e.

$$b_p' = B_p'\sin\omega\left(t - \frac{s}{u_s}\right)$$

$$= B_p'\sin\left(\omega t - \frac{\pi s}{p}\right)$$

and similarly $\quad b_q' = B_q'\cos\left(\omega t - \frac{\pi s}{p}\right)$

At $s = 0$ these components must each be cancelled by a transient wave travelling at rotor velocity u, i.e

$$b_p'' = -B_p'\varepsilon^{-s/\tau u}\sin\omega\left(t - \frac{s}{u}\right)$$

$$= -B_p'\varepsilon^{-s/\tau u}\sin\left(\omega t - \frac{\pi s}{p}\frac{u_s}{u}\right)$$

$$= -B_p'\varepsilon^{-s/\tau u}\sin\left(\omega t - \frac{\pi s}{p} - \frac{\sigma}{1-\sigma}\frac{\pi s}{p}\right)$$

and similarly

$$b_q'' = -B_q\varepsilon^{-s/\tau u}\cos\left(\omega t - \frac{\pi s}{p} - \frac{\sigma}{1-\sigma}\frac{\pi s}{p}\right)$$

The total flux at any point is the sum of the steady-state and transient waves,

i.e.

$$b = b_p' + b_p'' + b_q' + b_q''$$

$$b = B_p'\left[\sin\left(\omega t - \frac{\pi s}{p}\right) - \varepsilon^{-s/\tau u}\sin\left(\omega t - \frac{\pi s}{p} - \frac{\sigma}{1-\sigma}\frac{\pi s}{p}\right)\right]$$

$$+ B_q'\left[\cos\left(\omega t - \frac{\pi s}{p}\right) - \varepsilon^{-s/\tau u}\cos\left(\omega t - \frac{\pi s}{p} - \frac{\sigma}{1-\sigma}\frac{\pi s}{p}\right)\right]$$

By expanding the second term in each bracket, and grouping in $\sin(\omega t - \pi s/p)$ and $\cos(\omega t - \pi s/p)$ terms, we obtain

$$b_p = B_p'\sin\left[\omega t - \frac{\pi s}{p}\right]$$

$$\left[1 - \varepsilon^{-s/\tau u}\left(\cos\frac{\sigma}{1-\sigma}\frac{\pi s}{p} + \frac{B_q'}{B_p'}\sin\frac{\sigma}{1-\sigma}\frac{\pi s}{p}\right)\right]$$

and $\quad b_q = B_q'\cos\left[\omega t - \frac{\pi s}{p}\right]$

$$\left[1 - \varepsilon^{-s/\tau u}\left(\cos\frac{\sigma}{1-\sigma}\frac{\pi s}{p} - \frac{B_p'}{B_q'}\sin\frac{\sigma}{1-\sigma}\frac{\pi s}{p}\right)\right]$$

The amplitudes of these travelling waves, if the values of B'_p, B'_q and τ are substituted from eqns. (32), (33) and (34), are:

$$B_p = \frac{p_r J_s \sigma u_s}{(\sigma u_s)^2 + \left(\frac{\rho_r g}{4p\mu_0}\right)^2}$$

$$\left\{1 - \exp\left[\frac{-\pi\rho_r g s}{4p^2\mu_0 u_s(1-\sigma)}\right]\left[\cos\frac{\sigma}{1-\sigma}\frac{\pi s}{p} + \frac{\rho_r g}{4p\mu_0\sigma u_s}\sin\frac{\sigma}{1-\sigma}\frac{\pi s}{p}\right]\right\} \quad . \quad . \quad . \quad . \quad (36)$$

$$B_q = \frac{\rho_r J_s\left(\frac{\rho_r g}{4p\mu_0}\right)}{(\sigma u_s)^2 + \left(\frac{\rho_r g}{4p\mu_0}\right)^2}$$

$$\left\{1 - \exp\left[\frac{-\pi\rho_r g s}{4p^2\mu_0 u_s(1-\sigma)}\right]\left[\cos\frac{\sigma}{1-\sigma}\frac{\pi s}{p} - \frac{4p\mu_0\sigma u_s}{\rho_r g}\sin\frac{\sigma}{1-\sigma}\frac{\pi s}{p}\right]\right\} \quad . \quad . \quad . \quad . \quad (37)$$

The modifications introduced into Fig. 12 by the more complete theory are illustrated in Fig. 13 by a pair of curves for B_p and B_q for the particular case of $\sigma = 1/3$ and $\tau = 1{\cdot}25/f$ showing the decay of B_p to the steady-state power flux and the decay of B_q to the steady-state magnetizing flux.

(12.4) Calculation of Terminal Voltage for Constant Current

The flux wave in the gap has been calculated for the simple case in Section 3.1, and it is expressed in terms of components b_p and b_q in eqns. (10) and (11). The travelling wave of flux density may therefore be written:

$$b = B_p \sin\left(\omega t - \frac{\pi s}{p}\right) + B_q \cos\left(\omega t - \frac{\pi s}{p}\right)$$

where B_p and B_q are functions only of s.

For an elementary strip of the stator surface of length δs and unit width in the direction at right angles to the direction of motion of the fields, the electric force E is such that

$$\frac{\partial E}{\partial s}\delta s = -\frac{\partial b}{\partial t}\delta s$$

or

$$\frac{\partial E}{\partial s} = -\frac{\partial b}{\partial t} = -B_p\omega\cos\left(\omega t - \frac{\pi s}{p}\right) + B_q\omega\sin\left(\omega t - \frac{\pi s}{p}\right) \quad (38)$$

By substitution from eqns. (10) and (11)

$$\frac{\partial E}{\partial s} = \frac{\omega\rho_r J_s}{\sigma u_s}\left[\sin\frac{\sigma}{1-\sigma}\frac{\pi s}{p}\sin\left(\omega t - \frac{\pi s}{p}\right) - \left(1 - \cos\frac{\sigma}{1-\sigma}\frac{\pi s}{p}\right)\cos\left(\omega t - \frac{\pi s}{p}\right)\right]$$

$$= \frac{\omega\rho_r J_s}{\sigma u_s}\left[\cos\left(\omega t - \frac{\pi s}{p} - \frac{\pi s}{p}\frac{\sigma}{1-\sigma}\right) - \cos\left(\omega t - \frac{\pi s}{p}\right)\right]$$

whence

$$E = \frac{\omega\rho_r J_s}{\sigma u_s}\left\{\frac{-p(1-\sigma)}{\pi}\sin\left[\omega t - \frac{\pi s}{p} - \frac{\pi\sigma s}{p(1-\sigma)}\right] + \frac{p}{\pi}\sin\left(\omega t - \frac{\pi s}{p}\right)\right\} = \frac{\omega\rho_r J_s}{\sigma u_s}\left[\frac{p}{\pi}\sin\left(\omega t - \frac{\pi s}{p}\right)\right.$$

$$- \frac{p(1-\sigma)}{\pi}\cos\frac{\pi\sigma s}{p(1-\sigma)}\sin\left(\omega t - \frac{\pi s}{p}\right)$$

$$\left. + \frac{p(1-\sigma)}{\pi}\sin\frac{\pi\sigma s}{p(1-\sigma)}\cos\left(\omega t - \frac{\pi s}{p}\right)\right] \quad . \quad . \quad (39)$$

The power input to the block is given by $\int_0^{np}\frac{E_p J_s}{2}dS$, where E_p is the component of E in phase with J_s.

Thus the power input is given by

$$P_i = \frac{\omega\rho_r J_s^2}{2\sigma u_s}\int_0^{np}\left[\frac{p}{\pi} - \frac{p(1-\sigma)}{\pi}\cos\frac{\pi\sigma s}{p(1-\sigma)}\right]ds$$

$$= \frac{\rho_r J_s^2 p}{2\sigma}\left[n - \frac{(1-\sigma)^2}{\pi\sigma}\sin\frac{\pi\sigma n}{1-\sigma}\right] \quad . \quad . \quad . \quad (40)$$

The reactive power (volt-amperes) Q_i is given by

$$Q_i = \int_0^{np}\frac{E_q J_s}{2}ds$$

where E_q is the component of E in quadrature with J_s, and therefore

$$Q_i = \frac{\omega\rho_r J_s^2}{2\sigma u_s}\int_0^{np}\frac{p(1-\sigma)}{\pi}\sin\frac{\pi\sigma s}{p(1-\sigma)}ds$$

$$= \frac{\rho_r J_s^2 p}{2\pi}\left(\frac{1-\sigma}{\sigma}\right)^2\left(1 - \cos\frac{\pi\sigma n}{1-\sigma}\right) \quad . \quad . \quad (41)$$

The difference between P_i and the output Fu may be confirmed using eqn. (16); it is in fact found to equal the rotor copper loss $\rho_r J_s^2 np/2$.

DISCUSSION ON THE ABOVE TWO PAPERS BEFORE THE UTILIZATION SECTION, 15TH NOVEMBER, 1956

Mr. E. M. Briscoe: I should like more information on this machine with 50 c/s supplies. I appreciate that it has been necessary to use higher frequencies for experimental purposes, but this makes it more difficult to assess its potentialities either as a large machine or as a small variable-speed machine.

It would be interesting to know how the variable-speed machine in a large size would compare, for instance, with a Ward Leonard set. To-day it is necessary not only to have variable speed but also to control the torque at different speeds, which means some form of feedback to keep the desired characteristics: a Ward Leonard system with electronic control would be of great assistance, and I do not see how this could be done with the spherical-rotor machine.

Will the authors amplify their statement that 'the machine should preferably be large', giving the horse-power or frame size they have in mind?

With the rather complicated rotor construction and the method of construction (winding solder round the rings and heating them until it melted), it is not surprising that there are losses which cannot be accounted for; in the fractional-horse-power motor it

s well known that, with die-cast rotor bars, certain things must
ɔe done to the rotor to relieve the extra losses set up by the ntimate contact of the die-cast aluminium and the steel.

Mr. W. Hill: Many applications call for translation rather han rotation, but the latter is used for convenience, e.g. the centrifugal pump and the lift. Indeed every form of modern ransport in some way aims at translatory rather than rotating notion. Real progress was made in air transport when the propeller was replaced by the jet or the rocket engine, which seems essentially a simpler way of getting from A to B. It is herefore possible that the authors' demonstrations will mean to ndustry what the jet engine has meant to air transport: they show a linear motion which could be adopted in many aspects of industrial life.

Would it be possible to use some form of linear accelerator to move trains? Efficiency may not be so important, because steam locomotives have a very low efficiency, but the overhead ransmission lines would be eliminated; all that would be necessary are regularly spaced linear accelerators, and these need not be energized all the time—the approach of the train could easily be arranged to initiate the energizing of the coils.

half-speed effects, have the authors experienced anything of this nature in their linear motor?

If the shuttle motor corresponds broadly to a salient-rotor machine, the variable-speed induction motor could be described as a salient-stator machine; and since some of the difficulties associated with it appear to be due to the end-effects of the linear arrays, there is something to be said for constructing a movable stator which is continuous and can be rotated as a whole. I believe that the authors have considered something similar, and should be interested to learn their experience with such a construction.

Mr. F. Najmabadi: The practical possibilities of this development are best assessed by comparing its performance data with those of other variable-speed combinations, e.g. the Ward Leonard set, the Schrage motor and the a.c. commutator motor. While the Schrage motor gives speed variations in discrete steps, the others, including the spherical motor, have infinitely-variable speed characteristics. Furthermore, the spherical motor should operate at a slip of $1/(n + 1)$ for maximum efficiency, so that if the number of poles is less than 5 or 6, it is virtually a high-slip motor having inevitably a poor efficiency. Table A and Fig. A compare the performance data for a spherical motor with a 14 in rotor, which should develop about 14 h.p. at a middle speed of 500 r.p.m., with other comparable variable-speed sets.

Table A

COMPARISON OF VARIABLE-SPEED DRIVES GIVING 14–7 H.P. AT 750–375 R.P.M.

Type of machine	Efficiency			Power factor			Power/weight ratio	Relative cost
	High speed setting	Middle speed setting	Low speed setting	High speed setting	Middle speed setting	Low speed setting		
	%	%	%				h.p./lb	%
Schrage	79	78	67	0·99	0·77	0·65	0·008 8	380
Ward Leonard	65	63	60	—	—	—	0·008	400
A.C. commutator	76	78	77	0·9	0·75	0·65	0·007 1	450
Spherical	61	68	75	0·84*	0·83*	0·81*	0·010 5	260 + 80†
Squirrel-cage (14 h.p. at 500 r.p.m.)	—	85	—	—	0·71	—	0·018	100

* Taken from Fig. 21 of the paper (at preferred slip, which is probably optimistic). † 80% contingencies.

Dr. R. L. Russell: When two 3-phase supplies of opposed phase rotation are connected to opposite ends of an orthodox 3-phase winding,* a salient-pole rotor, with or without a single-phase winding, will rotate with an angular velocity corresponding to half the difference between the angular frequencies of the two supplies and will thus behave as a differential. If this principle is applied to a linear array one has an example of what, in classical physics, is termed wave interference (indeed the expression $v_s = 2pf$ is, in different guise, simply the familiar relation between the velocity of wave propagation and the product of wavelength and frequency). The shuttle or rotor will move at a difference frequency, or, when the two supply systems have the same frequency, it will be held in a fixed setting determined by their relative phase displacement. The ability to position a linear moving element merely by using a phase-shifter may well be useful.

What the authors have done is not to superimpose the two travelling waves in one array, but to arrange two separate opposed arrays end-to-end. What are the possibilities of using the cylindrical equivalent of this arrangement to give opposed rotating fields in each half of a multi-polar winding and thus to achieve self-sustained angular oscillation? The rotor of such a device would clearly have to be of an unusual shape, and since saliency or asymmetry in cylindrical machines usually leads to

* RUSSELL, R. L., and HODGES, N. W.: 'The Application of Counter-Rotating Fields to Electrical Measuring and Indicating Devices', *Proceedings I.E.E.*, Paper No. 1628 M, April, 1954 (101, Part II, p. 178), Fig. 1.

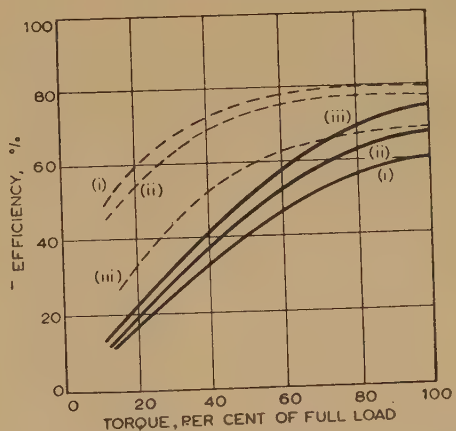

Fig. A.—Comparison of theoretical efficiencies of Schrage and spherical motors.

——— Spherical motor.
– – – – Schrage motor.

(i) Top speed.
(ii) Middle speed.
(iii) Bottom speed.

The formula used to derive the efficiency figures for the spherical motor is

$$\eta = \frac{n \times 100}{n + 1 + \rho_s/\rho_r} - 7\cdot5\%$$

($7\cdot5\%$ for 'torn out' watts, stray load, iron, friction and windage losses).

The decrease in efficiency with increasing speeds need not in itself be an undesirable feature. The high cost of the spherical motor is occasioned by the special manufacturing features, e.g. machining the rotor to a spherical contour, building the stator blocks, mechanism for rotating the stator blocks, etc. However, it compares favourably with other variable-speed combinations for its performance data, superior power/weight ratio and lower cost.

Finally, I would ask the authors to discuss the operation of this motor at constant voltage, which is obviously of great practical importance.

Mr. R. D. Ball: Have the authors reached any further conclusions regarding end-effects from References 2–5?

Whereas the conventional induction motor has a continuous or 'ring' stator, the authors' devices employ a discontinuous or arc stator in which end-effects are produced. Whereas in a ring stator the rotor, after starting, is conditioned continuously into the right phase, in the arc stator the raw unconditioned rotor experiences a transient current and must slip a pole before it does any work; this seems to be the reason why the efficiency is $(n-1)/n$. Fig. B shows a simplified version of Prof. Shturman's[3] calculations, the full line being for the 4-pole arc rotor and the

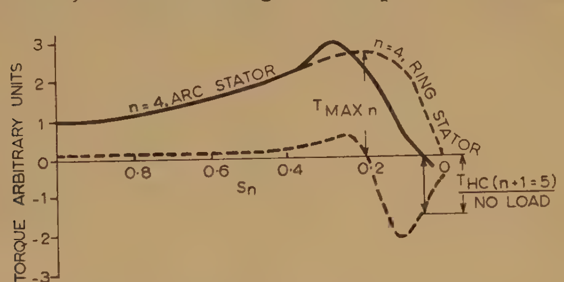

Fig. B.—Approximate speed/torque curves for arc and ring stators.

broken continuation for a 4-pole ring stator; the difference is made up by a distorted 5-pole field which acts as an induction brake at slips below $1/(n + 1)$, giving a no-load slip of $0\cdot05$ and a harmonic torque which is half the maximum fundamental torque.

Fig. C shows backward torques and slips at no-load against the reciprocal of pole number, where the $13\cdot3$-pole point is from Rezin,[4] the 4-pole point from Shturman[3] and the others from the authors' motor, which show that the ratio (backward torque)/(maximum torque) is $2/n$ per pole and the slip is $0\cdot25/n$

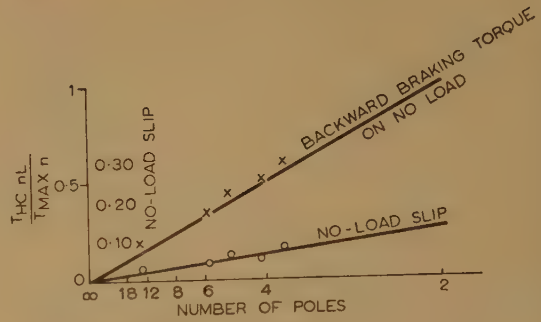

Fig. C.—Backward torque and slip at no load.

per pole and is zero for a ring stator where $n = \infty$. The task wi be to devise means to overcome the end-effects of arc stators.

Have Messrs. Laithwaite and Lawrenson applied their principl to single-phase pendulum clocks?

Mr. B. Adkins: The squirrel-cage motor, although very simpl in operation, offers many possibilities of trouble from suc things as parasitic torques, extra losses, vibrations and lockin phenomena. These matters have been studied extensively, bu even in ordinary motors they are still liable to cause trouble i the design is unusual. Has the authors' design been immun from what may be called the normal troubles of squirrel-cag induction motors? For example, some of the diagrams indicat that the windings have only one slot per pole per phase an would therefore produce fairly large harmonic fluxes.

In order to make the spherical motor work when the angle o the stator is not zero, the rotor must be provided with a numbe of intermediate rings connecting the bars together. This migh give rise to extra losses in a manner similar to that experience in the early days with the cast-aluminium squirrel-cage rotor before the technique of insulating the rotor bars was developed Because the aluminium made more intimate contact with th iron than copper bars normally do, current flowed through the iro between adjacent bars. Apart from the direct losses in the iron there was a non-uniform distribution of current in the main bars and so a loss of torque. Although the motors usually produce a reasonable standstill torque, the torque at low speeds wa greatly reduced, and in some motors the effect was sufficient t prevent their running up to full speed.

Mr. J. C. Hopkins: In the linear acceleration of charge particles use can be made of a travelling wave to increase th energy of a particle, and there is, electrically, no limitation o the ultimate energy which can be obtained. Considering th analogy between this and the machine which has been described what are the electrical limitations to the speed which can b imparted to a rotor of the type the authors have built?

[The authors' reply to the above discussion will be found o page 122.]

NORTH-WESTERN UTILIZATION GROUP AT MANCHESTER, 11TH DECEMBER, 1956*

Mr. R. D. Ball: One of the most outstanding demonstrations given when the paper was read was the oscillating metal plunger within a glass tube surrounded at the lower end by a stack of polyphase coils, the oscillations being almost constant in amplitude and frequency, without the use of switches. The analysis of the performance of this essentially simple apparatus, however, requires rather complex functions of distance and time, which apparently can be solved only by recourse to phase-plane analysis. Did the authors use an electronic calculating machine for this purpose?

* The discussion at Manchester was confined to the first paper (page 93).

The effect of a short rotor (i.e. less than two pole-pitches) i referred to in Section 8. Would this be due to the ratio of roto length to block length or to the fact that it requires at least tw pole-pitches to enable the magnetic circuit to be completed?

The demonstration of the shuttle model suggested that this i arranged for constant speed; since it may be necessary to chang the speed to suit the different materials to be woven, would it b possible to sectionalize the multi-polar track and twist the stato in the manner of the spherical motor for speed control?

Mr. J. G. Winterbottom: The conventional loom is driven b an individual motor through the medium of, say, a V-drive, an

the velocity of the shuttle and thus the number of picks per minute are dependent on the efficiency of the transmission. Any degree of slip will reflect itself in loss of speed of the shuttle, with a consequent reduction in weaving efficiency. The self-oscillating motor-shuttle ensures beyond doubt that the pre-determined picking speed will be maintained throughout the weaving process without variation.

It is noticed that the amplitude and frequency of oscillation are dependent upon V_s and R/X. These variables would provide for different picking speeds and weights of cloth being woven. How can the synchronous speed of the linear stator field be altered at will? Do the authors envisage a self-contained frequency-changer to enable wide ranges of picking speeds to be produced?

Two of the principal motions within a weaving machine are the firing of the shuttle containing the weft thread from one side of the machine to the other, and the beating up of the weft thread after each passage of the shuttle has been completed. With the self-oscillating shuttle design, it is obvious that the beat-up motion will have to be driven by a separate driving unit. Can the beat-up drive be electrically tied to the shuttle propulsion unit to ensure perfect synchronism between these two motions?

Finally, it would appear that, after a period of running under normal load, heating might occur within the shuttle body, and the consequences of a heated element passing across warps of synthetic yarn might be serious. Has this condition been considered, and would not the double-sided system be the answer? Alternatively could there be means of heat insulation within the metal shuttle casing itself?

Dr. D. Morrison: The authors have devised and constructed a mechanism whereby a shuttle may be accelerated and decelerated smoothly over the full length of a track, thus reducing very considerably the acceleration involved for a given distance travelled in a given time. It is still, however, an open question whether this mechanism could be used to increase the running speed of a power loom, since loom speeds depend just as closely on the dynamic difficulties associated with the sley motion as with those associated with the shuttle motion. In a traditional loom, the shuttle passes through the warp threads in approximately one-third of the total time for one cycle. This fraction varies, again by tradition, according to the relative breadth of the loom, and it would appear theoretically possible to establish this relative time as a function of some non-dimensional expression of loom breadth. On general design considerations it would be assumed that, if a method is found of decreasing the difficulty associated with one particular function, the logical way to make use of this would be to decrease the time allowed, and hence the authors should envisage a loom in which the time allowed for shuttle flight is rather less than the one-third of total already in common use. An analogous situation probably arises in the design of a transformer for minimum bulk, where if a core material of higher permissible flux density were made available, the best use would be made of this by decreasing the relative size of the core.

An idealized example could be given showing the values liable to occur in weaving practice, as follow:

Useful length of shuttle travel	60 in
Time for one complete cycle of operation ..	0·3 sec
Time for shuttle to pass through warp	0·1 sec
Shuttle speed through warp	600 in/sec
Shuttle acceleration and deceleration over $7\frac{1}{2}$ in at each end outside useful travel.	

Therefore, average acceleration .. .. $= \dfrac{(600)^2}{2 \times 7\frac{1}{2}}$
$= 24\,000$ in/sec²

Peak acceleration about 1·6 times this (theoretically $\pi/2$).

Therefore, peak acceleration .. .. $= 24\,000 \times 1{\cdot}6$
$= 38\,400$ in/sec²
$= 99{\cdot}4g$

If electromagnetic propulsion permits uniform acceleration and deceleration of the shuttle over the same total distance of 75 in with steady accelerations of $\neq 99{\cdot}4g$, the time for a total travel of 75 in is 0·088 4 sec and the time to travel the central 60 in is 0·048 8 sec. This is a big improvement on the time of shuttle flight, but if the sley motion remains unaltered—and this is optimistic in view of the probably increased sley weight—the total time for one pick is reduced only from 0·3 to 0·2 + 0·048 8 = 0·248 8 sec, which would amount to an increase in weaving speed of just over 20%.

Mr. A. Cotton: Contrary to the authors' view, the high acceleration of a shuttle driven by a picking stick is an advantage, since the function of a loom is to produce cloth quickly and cheaply. In a loom of 48 in reed space weaving at 180 picks/min (which is about normal for an automatic loom) the total time for one pick is 0·33 sec, of which the time for the shuttle in the shed is less than 0·11 sec. If the shuttle accelerates more slowly, a greater time for the passing of the shuttle will be required.

The power taken for the shuttle in this loom would not be more than 0·25 h.p. out of a total of 0·75 h.p. for the complete loom. This compares with the 100 kVA for the model demonstrated and at a power factor which would require a capacitor as large as the loom itself.

Improper striking of the shuttle occurs but infrequently, and is then usually due to some mechanical defect. Against this the authors' loom requires the timing of the various other functions of the loom from the shuttle. This would appear to present a greater problem to ensure perfect synchronism of the heald movement and the beat up of the sley, and to obtain shuttle passage at the correct time. Since the sley and heald movements are oscillatory, perhaps the driving of these parts by self-oscillating induction motors will be considered.

Mr. A. F. M. Ashworth: One point which appears to have been overlooked in the paper is the loss occurring in the shuttle during acceleration and deceleration under the influence of the travelling magnetic fields, as a direct consequence of its inertia. If the shuttle reaches synchronous speed during its travel, the energy loss during acceleration from rest to synchronous speed equals the kinetic energy at synchronous speed and during deceleration from synchronous speed to rest, and the loss is three times this value. If the shuttle weighs 5 lb and the synchronous speed is 50 ft/sec, the energy loss in the shuttle during one pick is 776 lb-ft; and at 200 operations per minute this represents a shuttle loss of 3·51 kW. It is therefore obvious that it will be necessary to minimize the weight of the shuttle and to incorporate an efficient spring system at each end of the track to decelerate and reaccelerate the shuttle and thereby increase the efficiency of the machine.

Mr. Cotton points out that in the conventional 'pick stick' machine the power input is approximately $\frac{1}{4}$ h.p. Can the authors foresee a commercial self-oscillating induction motor which could compete in efficiency with existing systems of shuttle propulsion?

[The authors' reply to the above discussion will be found overleaf.]

THE AUTHORS' REPLY TO THE ABOVE DISCUSSIONS

Prof. F. C. Williams, Messrs. E. R. Laithwaite, P. J. Lawrenson and L. S. Piggott (*in reply*): Much development work has been carried out since the papers were written, and some of the results of this work are particularly relevant to Mr. Briscoe's contribution. We regret that it is impossible to discuss these results in detail in the space available, but Mr. Briscoe's point regarding Ward Leonard systems is answered in part by Mr. Najmabadi.

Train propulsion by the use of linear motors was suggested about 50 years ago but never seems to have found favour. However, Mr. Hill's point that rotary machines are generally used to produce linear motion is quite a profound one, and certainly in connection with the motions in a loom we consider that the linear motor may be advantageous.

Dr. Russell's suggestion regarding linear position control is interesting. We have been able to use a linear motor both as a magslip and as an M-type motor for position control, and see no reason why Dr. Russell's suggestion should not result in a useful device. Self-sustained rotary oscillation is made difficult in small machines, because of the high acceleration necessary to attain synchronous speed from rest in half a revolution. We have so far experienced no half-speed effects with linear machines with short rotors.

We are grateful to Mr. Najmabadi for the work he has put into the production of Table A, which appears to show the spherical motor in quite a favourable light as regards both power/weight ratio and initial cost. Present development work is concerned with constant-voltage operation, but this aspect is too complicated to be discussed here.

The Russian publications, particularly those due to Shturman, derive the properties of short-stator machines in a different way from the present paper, but the results are very similar. Mr. Ball's graph, which shows results from three separate sources, certainly confirms this. While the Russian papers derive their results in a strictly mathematical manner, we believe that our approach to the problem is more likely to lend itself immediately to the design of this type of motor.

With regard to Mr. Ball's suggestions on the oscillating motor, the principle has not yet been applied to clocks. The effect of the short rotor is thought to be due only to magnetic locking phenomena, and a rotor spanning only $\frac{1}{3}$ pole pitch is capable of attaining synchronous speed on a linear track. We did use a digital computer for some of the analysis. The angled-field principle may be applied to linear arrays in the manner suggested by Mr. Ball, and this offers one solution to Mr. Winterbottom's question of variable picking speed. The beat-up problem is complicated and is under investigation at the present time. We consider that the double-sided system can provide an answer to the shuttle-heating problem.

The spherical motor appears to be free from locking phenomena by the very nature of its construction. Some evidence of stray load loss has been found, but not to any serious extent. No serious effect from non-uniform current distribution, such as that described by Mr. Adkins, has so far been observed.

While there is no theoretical limit to the linear velocity of a travelling field, there appears to be some very definite reason why a linear array which has been bent into a circle to join up with itself cannot produce a rotor speed in excess of that produced by a 2-pole machine. This aspect is still under investigation.

Mr. Morrison's contribution appears to answer Mr. Cotton's first point excellently. The main advantages of electromagnetic shuttle propulsion appear to be the reduction of noise and wear, and greater reliability. Speed, as Mr. Morrison shows, is only a secondary advantage. It is fairly clear that linear motors consuming only 1–2 kW can be designed to replace the early demonstration model to which Mr. Cotton refers, and we have for some time been investigating a system using end-springs, as described by Mr. Ashworth, to minimize the rotor energy loss. Such a system also suggests the possibility of driving the heald and beat-up movements from the shuttle itself.

621.618.9

Paper No. 2128 M
Aug. 1956

INSULATION PROPERTIES OF COMPRESSED ELECTRONEGATIVE GASES

By P. R. HOWARD, Ph.D., B.Sc.(Eng.), Associate Member.

(*The paper was first received* 22*nd September*, 1955, *in revised form* 17*th January*, 1956, *and in final form* 9*th April*, 1956. *It was published in August*, 1956, *and was read before the* MEASUREMENT AND CONTROL SECTION 6*th November*, 1956.)

SUMMARY

The electrical insulating properties under pressure of a number of halogenated methane compounds and sulphur hexafluoride are compared; sphere-sphere and point-sphere electrode configurations, and alternating, direct and impulse voltages are used. The influence of irradiation is also investigated. Of tho gases studied, sulphur hexafluoride and difluorodichloromethane (known commercially as Arcton 6) have the most favourable properties for high-voltage insulation, and additional data are provided for the comparison of these two gaseous compounds. This includes (*a*) power-frequency breakdown-voltage characteristics of admixtures with nitrogen in uniform and divergent fields, (*b*) the comparison of the radio and power-frequency uniform-field breakdown voltages at atmospheric pressure, (*c*) the breakdown-voltage characteristics for a number of concentric-cylinder electrodes at various gas pressures with alternating, direct and impulse voltage, (*d*) the surface flashover-voltage/gas-pressure characteristics of solid insulation subjected to various forms of tangential stress.

Data pertaining to electronegative gases are compared with corresponding data for nitrogen under the same conditions and with transformer oil at atmospheric pressure.

Chemical and physical properties, such as decomposition in the presence of electrical discharges and vapour pressure characteristics, and economic factors are considered in assessing the suitability of sulphur hexafluoride and difluorodichloromethane as insulants for high-voltage equipments.

Factors contributing to the high electric strength of some electronegative gases are briefly discussed.

(1) INTRODUCTION

The potentialities of compressed gases for the insulation of electrical apparatus have been appreciated for some time, and there have been a number of practical applications, mainly with air, nitrogen and carbon dioxide. However, the electric strengths of these gases are comparable with those of liquids and solids only when they are subjected to considerable compression. Therefore there has been considerable interest in recent years in the electrical properties of complex chlorinated and fluorinated molecular compounds which, in some cases, possess high electric strengths at relatively low gas pressures. This feature of high electric strength is ascribed to molecular complexity[1] and hence to the greater possibility of inelastic non-ionizing collisions and to negative-ion-forming reactions.[2–6] By the first mechanism such electrons as are created by ionization in the gas are retarded in accumulating energy by the frequent loss of energy on impact. Through the second mechanism the average energy required by free electrons to cause cumulative ionization is increased. Appreciation of the negative-ion-forming reactions and field-modifying mechanisms, particularly in non-uniform fields, has clarified the general picture of breakdown in these gases, but it is too intricate for full quantitative treatment. Because of this complexity, knowledge of breakdown strength depends to a large extent upon experimental determination as a function of pressure and electrode geometry.

Although a fair volume of literature has appeared in America on the electrical properties of electronegative gases, there have been very few data published on the subject in Britain. The paper describes comprehensive sets of experiments which have been carried out to assess the performance and suitability of a number of halogenated methane compounds and sulphur hexafluoride as insulants for high-voltage equipments.

(1.1) Requirements of Gaseous Insulation

The suitability of a gas as an insulant does not entirely depend upon its electric strength; physical and chemical properties, and economic considerations are also relevant. Gases suitable for electrical apparatus should in the main have the following properties:

(*a*) High electric strength at low absolute gas pressures.
(*b*) High saturation vapour pressure at normal room temperatures.
(*c*) Chemical inertness.
(*d*) Negligible toxicity.
(*e*) High thermal conductivity.
(*f*) Availability and cheapness.

(2) COMPOUNDS SELECTED FOR EXAMINATION

Table 1 gives the gases selected, their boiling-points at atmospheric pressure, and a summary of relative electric strengths obtained by different workers for uniform field conditions at atmospheric pressure with nitrogen as the datum.

The gases were obtained in steel cylinders from commercial sources, and Appendix 12.1 gives the probable impurities present in the various compounds.

(3) PRESSURE CHAMBER AND ASSOCIATED EQUIPMENT

A schematic showing the layout of the pressure and vacuum systems is given in Fig. 1. The electrical tests, involving the determination of breakdown and surface flashover characteristics, were carried out in Pyrex glass pressure cylinders having internal diameters of 6 and 3 in and a length of 24 in.

The gases were cleaned of mechanical impurities by chemically-pure glass wool, dried through a column of activated alumina and finally filtered through a porous sintered glass plate with pores measuring $5–10 \times 10^{-4}$ cm before being admitted to the pressure chamber. The complete system could be evacuated to a pressure of less than 0·01 mm Hg by the use of two oil diffusion pumps in series, backed by a standard rotary oil pump. In the pressure system industrial-scale glassware was used with Neoprene gaskets between joints. Freezing traps were incorporated as shown to prevent contamination of the pressure chamber by mercury vapour from the McLeod gauge and oil vapour from the diffusion and rotary pumps.

(4) EXPERIMENTAL PROCEDURE

In making breakdown and surface flashover tests with alternating and direct voltages, the voltage was raised quickly to 80–90% of the expected breakdown value and subsequently in small increments, with a pause at each step, until breakdown occurred. The measurement of breakdown voltage was made

The paper is an official communication from the National Physical Laboratory.

Table 1

RELATIVE ELECTRIC STRENGTH OF GASES IN UNIFORM FIELDS WITH NITROGEN AS DATUM

Gaseous compounds	One atmosphere absolute pressure	
	Boiling-point	Relative electric strength
	°C	
Sulphur hexafluoride SF_6	− 62·0	2·49[7]: 2·3–2·5[8]: 1·86[13]: 1·6[14]: 2·4[21]: 2·45–2·62[19]
Carbon tetrafluoride CF_4 (Arcton 0)	−128·0	1·1[8]: 0·9[13]: 1·0[14]: 2·2[17]
Trifluorochloromethane CF_3Cl (Arcton 3)	− 81·5	1·23[13]: 1·35[14]
Difluorodichloromethane CF_2Cl_2 (Arcton 6)	− 29·8	2·56[7]: 2·4–2·5[8]: 2·0[9]: 2·4[10]: 2·69[11]: 2·5[12]; 2·05[13]: 1·9[14]: 3·0[15]: 2·5[16]: 2·65[20]: 2·65[18]
Monofluorotrichloromethane $CFCl_3$ (Arcton 9)	23·7	4·47[7]: 3–4·4[8]: 3·0[10]: 2·65[13]
Trifluoromethane CHF_3 (Arcton 1)	− 84·0	0·68[14]
Difluoromonochloromethane CHF_2Cl (Arcton 4)	− 40·8	1·0[14]
Monofluorodichloromethane $CHFCl_2$ (Arcton 7)	8·9	1·33[10] References are in brackets.

Spheres or spherically-ended discs were used for References 10–15, 17 and 19–21, and uniform field electrodes for References 7, 16 and 18.
No experimental data were given in (8) and the results in (9) were obtained with plane electrodes with a small hemispherically-ended boss in the centre of the anode plane.

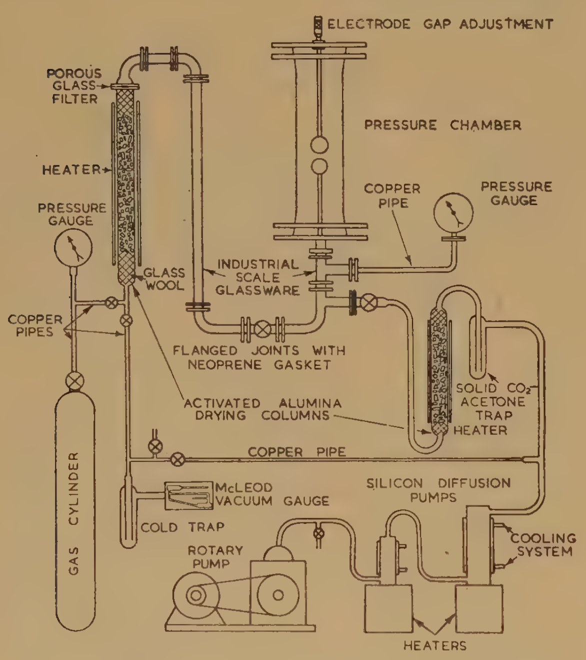

Fig. 1.—Schematic of the pressure and vacuum systems.

directly across the test gap with a 10-megohm resistor between the gap and voltage source to limit the discharge current. A rectified capacitor-current peak-voltmeter was used for alternating voltages; the purity of the waveform was checked by means of an oscillograph, and the accuracy of voltage measurement was considered to be within ±1%. Direct-voltage measurements were made by recording with a substandard microammeter the current at the earthed end of a 1 000-megohm high-stability 100-kV resistor immersed in transformer oil; voltage measurements were considered accurate to within ±1·5%.

With standard 1/50 microsec impulse voltages, the voltage was increased in 1% steps to breakdown from a level 80–90% of the breakdown value obtained in the first instance using greater voltage steps. For the measurement of peak voltage and the determination of waveshape, a sealed-off high-speed cathode-ray oscillograph was used in conjunction with a resistor divider. Resistance was inserted between the external front capacitor of the generator and the test gap to limit the discharge current; the time-constant of this resistance and the gap capacitance was small, and therefore any error in the measured voltage on the gap was negligible. Allowing for the various errors in measurement and recording, the voltage measurements were considered accurate to within ±1%.

The number of breakdowns, taken at ½-min intervals, which were necessary to obtain mean values was generally in the region of 10 when the spread of individual results was small, but it exceeded 40 in certain cases; the breakdown values obtained during the conditioning of electrodes were not included in the averaged values. (Detailed statistical data are not provided in the text, but typical values for coefficients of variation are given for uniform and divergent field measurements.)

For tests involving solid insulation the number of breakdown values that could be obtained on each sample was severely limited through damage to the insulation which occurred sometimes within two or three voltage applications; a mean was therefore obtained by averaging results of a number of samples.

The corona onset voltage for certain electrode arrangements was determined by observing, with an oscillograph, the voltage developed across a resistor inserted in the earth connection of the electrode assembly.

(5) BREAKDOWN OF GASES

Breakdown data were obtained for a number of field configurations as functions both of electrode spacing and absolute gas pressure under normal and irradiated conditions; irradiation was obtained from a capsule containing 0·5 mg of radium placed opposite the electrode gap on the outside surface of the pressure chamber. Temperature measurements were taken during the tests and appropriate corrections were made for changes in gas density.

(5.1) Sphere-Gaps

The electrodes were 5 cm diameter brass spheres with a 'decorative' chrome finish. The large pressure cylinder was used with an earthed copper mesh screen, adjacent to the inner glass surface, to eliminate the risk of charge deposition on the glass and to maintain constant geometry; close proximity of the insulating walls of the test chamber was considered by Nonken[22] to have influenced the results of Camilli and Chapman.[14] However, in the cases of nitrogen and difluorodichloromethane, results were obtained with and without the mesh screen and there was no detectable difference in the sets of breakdown values; the screen was fitted as a precautionary measure.

Breakdown data for the compounds and transformer oil (for comparison) are summarized in Table 2. There was little difference between positive and negative values with either direct or impulse voltages, and therefore only the negative values have been reproduced. With monofluorodichloromethane ($CHFCl_2$) and monofluorotrichloromethane ($CFCl_3$), which have boiling-points above 0° C at atmospheric pressure, the pure gas breakdown-voltage/gap characteristics could be determined only at atmospheric pressure; at other pressures the results were obtained by the addition of nitrogen. Arising from the higher boiling-point of monofluorotrichloromethane, the partial pressure was not maintained with the addition of nitrogen, and liquefaction occurred at total gas pressures in excess of 30 lb/in^2 absolute. For these gases, the results at other than atmospheric pressure are not very significant. Table 3 gives the coefficients of variation for the breakdown values with power frequency, direct and impulse voltages at atmospheric pressure and an irradiated gap of 1 cm.

The electric strengths of the halogen derivatives of methane fall progressively as chlorine atoms are replaced by fluorine atoms in both the CF_yCl_z and CHF_yCl_z families; in the latter series the replacement of a halogen atom by hydrogen causes a marked decrease in the electric strength and an increased tendency to decompose in the presence of discharges. From the results of Table 2 only sulphur hexafluoride (SF_6), difluorodichloromethane (CF_2Cl_2) and monofluorotrichloromethane ($CFCl_3$) have electric strengths well in excess of nitrogen; the last is not a satisfactory compound since it is liquid at standard atmospheric conditions (20° C and 760 mm Hg).

Fig. 2 gives the breakdown-voltage/gas-pressure and break-

Table 2

BREAKDOWN DATA FOR SPHERICAL ELECTRODES
(SPHERE DIAMETER 5 CM)

Compound	Absolute pressure, atmospheres	Breakdown voltage: Power frequency		Negative direct		Negative impulse		Relative electric strength		Impulse ratio	
		Sphere gap, cm: 0·5	1·0	0·5	1·0	0·5	1·0	0·5	1·0	0·5	1·0
		kV	kV	kV	kV	kV	kV				
Transformer oil	1	110·0	218·0			268·0		6·36	6·86	2·44	
SF_6	1	45·0	86·0	44·0	83·5	47·7	91·3	2·6	2·7	1·06	1·06
	2	79·0	161·0			91·0	171·0	2·47	2·87	1·15	1·06
	3	112·5	218·0			134·5	244·0	2·48	2·68	1·19	1·12
	4	143·5	268·0			175·0	309·0	2·47	2·53	1·22	1·15
CF_4 (Arcton 0)	1	18·3	36·5	16·2	32·5	20·5	44·0	1·06	1·14	1·12	1·2
	2	36·6	71·4			41·0	85·0	1·13	1·27	1·13	1·19
	3	55·0	104·5			60·5		1·21	1·28	1·10	
	4	71·6				79·0		1·23		1·10	
CF_3Cl (Arcton 3)	1	25·0	47·2	23·0	46·0	42·5	71·5	1·44	1·48	1·7	1·48
	2	48·5	90·5			70·0		1·52	1·61	1·44	
	3	71·5						1·57			
	4	93·5						1·60			
CF_2Cl_2 (Arcton 6)	1	47·6	90·6	46·3	87·5	50·2	96·0	2·74	2·84	1·05	1·05
	2	89·0	160·0			90·0	167·0	2·78	2·85	1·01	1·04
	3	122·5	228·0			122·5	232·0	2·70	2·80	1·00	1·02
	4	152·0	282·0			152·0	285·0	2·62	2·67	1·00	1·01
$CFCl_3$ (Arcton 9)	1	65·0	129·0	65·0		76·5		3·76	4·05	1·18	
	2*	96·5						3·02			
	3*	119·0						2·62			
CHF_3 (Arcton 1)	1	15·8	28·5	14·8	27·8	18·8	31·0	0·91	0·90	1·19	1·09
	2	29·5	53·5			27·5	52·5	0·92	0·95	0·93	0·98
	3	41·0	78·0			38·0	75·5	0·90	0·97	0·93	0·97
	4	52·0	100·5			49·5	97·5	0·90	0·95	0·95	0·97
CHF_2Cl (Arcton 4)	1	21·7	39·6	21·7	39·8	22·4	39·8	1·25	1·25	1·03	1·00
	2	40·0	74·5			37·5	71·0	1·25	1·33	0·94	0·95
	3	57·7	108·0			54·5		1·27	1·32	0·94	
	4	74·5						1·28			
$CHFCl_2$ (Arcton 7)	1	32·2	63·1	29·7	58·4	43·8	87·0	1·86	1·98	1·36	1·38
	2*	50·0	93·5					1·56	1·67		
	3*	66·5						1·46			
	4*	81·5						1·40			

* Nitrogen added to compound exerting one atmosphere absolute pressure.

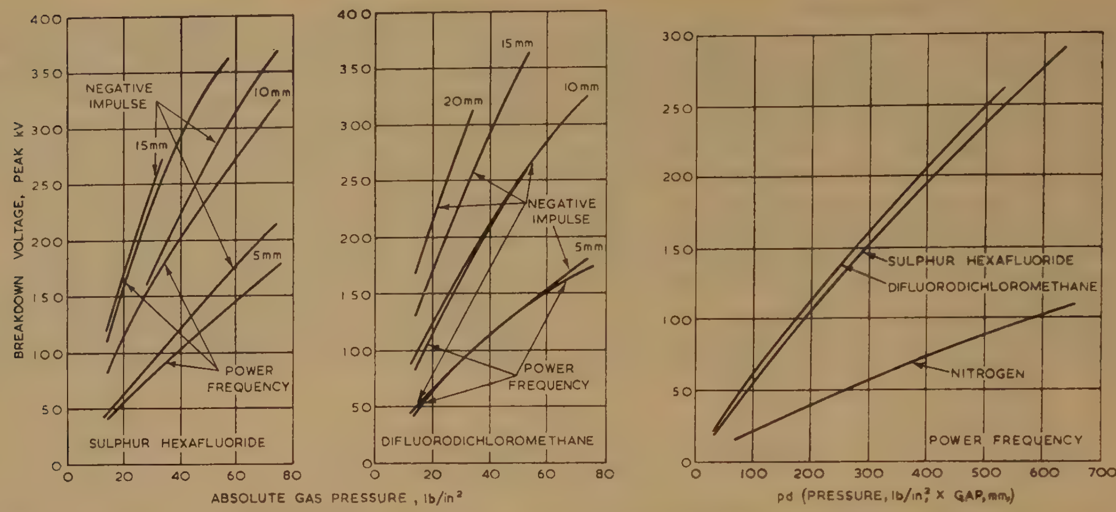

Fig. 2.—Breakdown voltage between 5 cm diameter spheres for sulphur hexafluoride and difluorodichloromethane as functions of gas pressure and *pd* [pressure (lb/in²) × gap (mm)].

Table 3

Coefficient of Variation for Breakdown Values recorded at Atmospheric Pressure with an Irradiated Sphere Gap of 1·0 cm

Compound	Coefficient of variation		
	Power frequency	Negative d.c.	Negative impulse
	%	%	%
SF_6	0·2	0·1	1·8
CF_4 (Arcton 0)	0·5	0·1	4·3
CF_3Cl (Arcton 3)	0·4	0·6	5·5
CF_2Cl_2 (Arcton 6)	0·75	0·8	2·3
$CFCl_3$ (Arcton 9)	0·4*	0·9*	1·9*
CHF_3 (Arcton 1)	0·5	0·9	2·9
CHF_2Cl (Arcton 4)	1·1	0·7	2·2
$CHFCl_2$ (Arcton 7)	0·3	0·4	0·1

* 0·6 cm gap.

down-voltage/*pd* relations, where d = gap separation in millimetres and p = absolute gas pressure in pounds per square inch, for sulphur hexafluoride and difluorodichloromethane.

In Table 4 the results of r.f. measurements (about 1 Mc/s)

Table 4

Radio-Frequency Breakdown Data at Atmospheric Pressure using Spherical Electrodes

Gap	CF_2Cl_2 Breakdown voltage		SF_6 Breakdown voltage	
	Radio frequency	Power frequency	Radio frequency	Power frequency
cm	kV peak	kV peak	kV peak	kV peak
0·3	27·0	29·5	26·4	27·2
0·4	37·9	39·0	34·9	36·1
0·5	46·3	47·6	44·3	45·0

Sphere diameter 5 cm; frequency 980–990 kc/s; radium used.

with sulphur hexafluoride and difluorodichloromethane are recorded with the corresponding power-frequency values for comparison purposes. With difluorodichloromethane, the electrodes rapidly deteriorated during the r.f. measurements, becoming covered with carbon deposits, and sometimes sooty smoke was evolved in the volume of the arc between the electrodes. To obtain consistent results the electrodes had to be frequently cleaned and the pressure chamber filled with fresh gas. With sulphur hexafluoride a white deposit, presumably sulphur, appeared on the electrodes only after prolonged use. The limited number of results support the findings of other workers[23–25] that the r.f. and 50 c/s breakdown voltages of these gases are substantially the same for identical conditions.

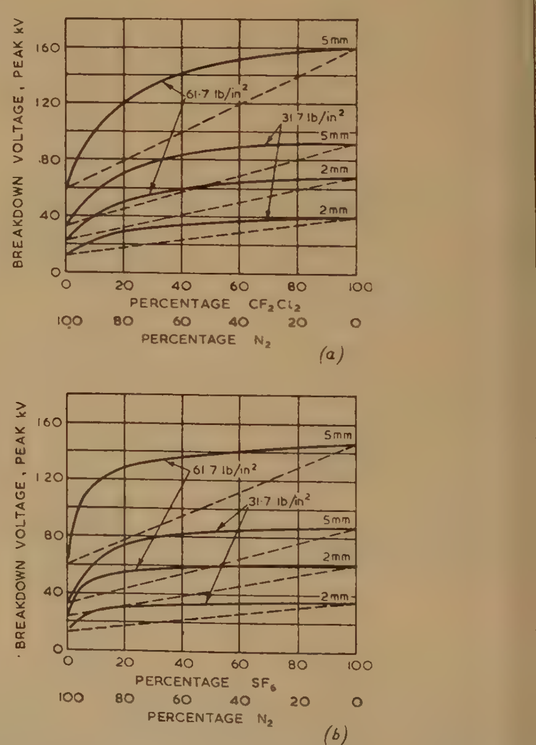

Fig. 3.—Breakdown characteristics between spheres for difluorodichloromethane–nitrogen and sulphur hexafluoride–nitrogen mixtures.

Total gas pressures, 31·7 and 61·7 lb/in²; gaps, 2 and 5 mm.
– – – – Sum of breakdown values for individual constituents.

(5.1.1) Mixtures of Difluorodichloromethane and Sulphur Hexafluoride with Nitrogen.

Gas mixtures were obtained by admitting oxygen-free nitrogen at atmospheric pressure to an evacuated system, adding the required quantity of halogenated compound and then increasing the pressure to the required value with nitrogen.

Fig. 3 gives 50 c/s breakdown voltages for sulphur hexafluoride and difluorodichloromethane as a function of the percentage partial pressure exerted by the gases in admixtures with nitrogen. The electric strength of each mixture is greater than the sum of those of the individual gases exerting their respective partial pressures, and 75–80% of the electric strength of the pure halogen compound is obtained with mixtures containing either 10% by pressure sulphur hexafluoride or 20% by pressure difluorodichloromethane.

(5.2) Point-Sphere Gaps

Non-uniform field conditions frequently prevail in electrical apparatus. For the study of this the breakdown voltage between a hemispherically-ended tungsten cylinder of 0·198 cm diameter and a 5 cm diameter sphere with a 'decorative' chrome finish was measured. The large pressure chamber, fitted with an earthed mesh screen, was used.

Typical curves showing the variation of the power frequency, direct and impulse breakdown voltages with gas pressure at a number of gap settings for sulphur hexafluoride (SF_6), carbon tetrafluoride (CF_4), trifluorochloromethane (CF_3Cl), difluorodichloromethane (CF_2Cl_2) are given in Figs. 4–7. Table 5 gives typical values of coefficients of variation for the breakdown values of these compounds with power frequency, positive point d.c. and impulse voltages; the pressure point selected for

Table 5

Coefficient of Variation for Breakdown Values recorded for Non-Irradiated 1·5 cm Point-Sphere Gap

Compound	Gas pressure	Coefficient of variation		
		Power frequency	Positive d.c.	Positive impulse
	lb/in² absolute	%	%	%
SF_6	31·7	1·3	0·7	3·5
CF_4 (Arcton 0) ..	51·7	0·8	0·3	5·0
CF_3Cl (Arcton 3)	41·7	0·6	0·8*	10·0*
CF_2Cl_2 (Arcton 6)	31·7	0·6	0·6	2·8

* 1·0 cm gap.

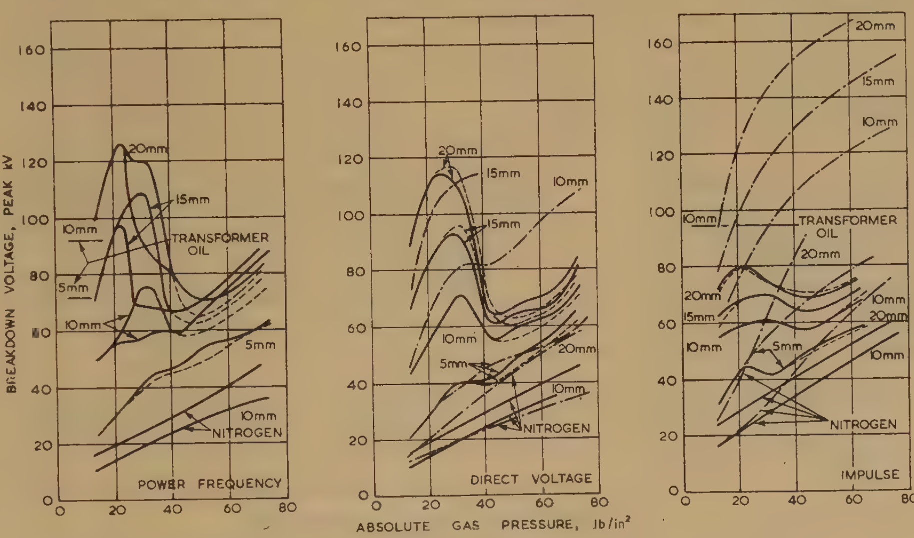

Fig. 4.—Breakdown voltage for sulphur hexafluoride with point-sphere electrodes.

———— Power frequency, positive d.c. and impulse.
— — — — Negative d.c. and impulse.
- - - - - - Positive d.c. and impulse with radium.

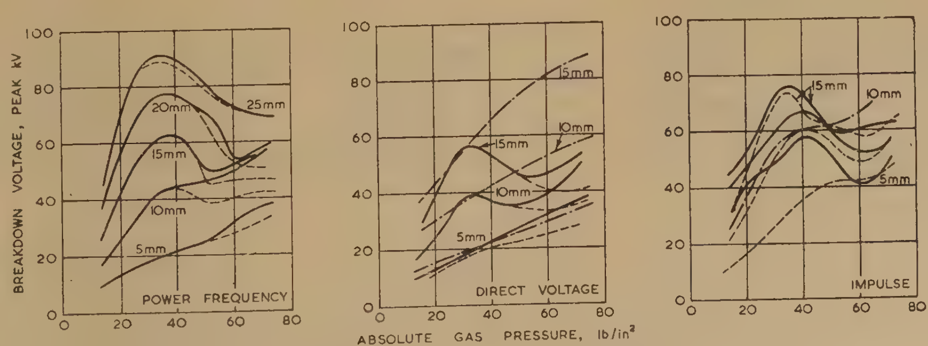

Fig. 5.—Breakdown voltage for carbon tetrafluoride with point-sphere electrodes.

———— Power frequency, positive d.c. and impulse.
— — — — Negative d.c. and impulse.
- - - - - - Power frequency, positive d.c. and impulse with radium.

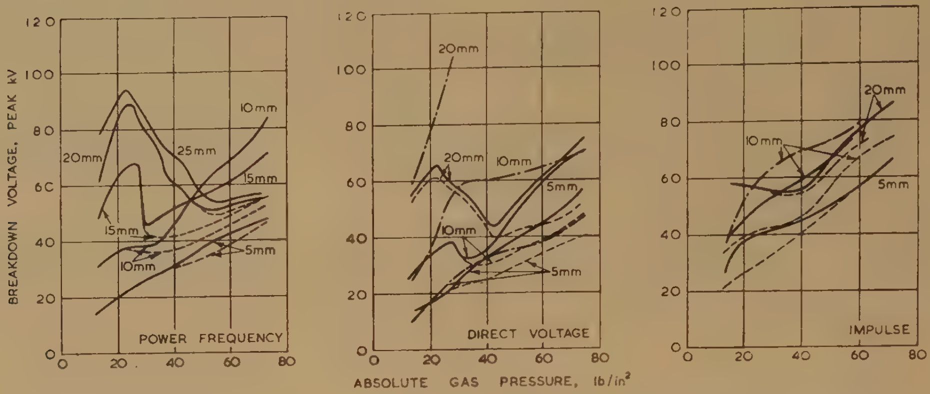

Fig. 6.—Breakdown voltage with trifluorochloromethane and point-sphere electrodes.

——— Power frequency, positive d.c. and impulse.
— — — Negative d.c. and impulse.
- - - - - - Power frequency, positive d.c. and impulse with radium.

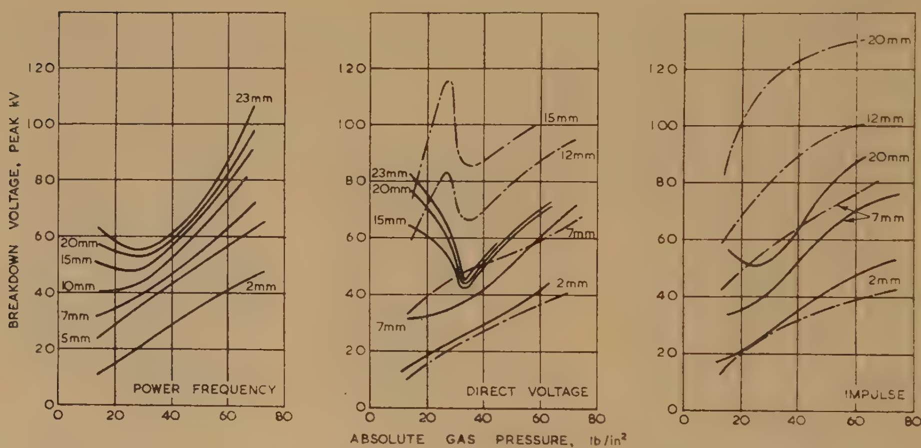

Fig. 7.—Breakdown voltage with difluorodichloromethane and non-irradiated point-sphere electrodes.

——— Power frequency, positive d.c. and impulse.
— — — Negative d.c. and impulse.

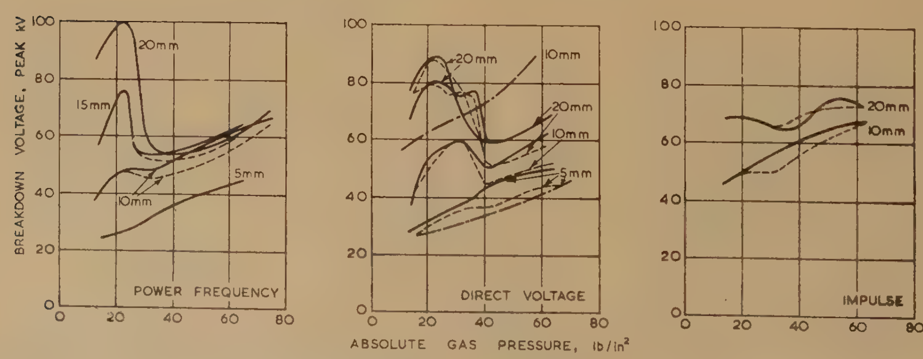

Fig. 8.—Breakdown voltage with point-sphere electrodes for monofluorotrichloromethane at atmospheric pressure and nitrogen added to obtain higher pressure.

——— Power frequency, positive d.c. and impulse.
— — — Negative d.c. and impulse.
- - - - - - Power frequency, positive d.c. and impulse with radium.

each compound is lower than the pressure at which the breakdown voltage is a minimum, i.e. at a point where corona precedes breakdown. Fig. 8 gives the curves for monofluorotrichloromethane to which nitrogen was added to give gas pressures in excess of one atmosphere. Where the results with normal and irradiated conditions coincide or are within 1–2% of each other, the curves corresponding to the unirradiated conditions only have been given. The data for nitrogen and transformer oil are included with the curves for sulphur hexafluoride in Fig. 4. Data for the CHF_yCl_z family of compounds do not show any features which are not present in the other compounds, and so they have not been reproduced.

The region of negative slope in the breakdown voltage curves is characteristic of the electronegative gases, and at pressures lower than that at which the breakdown voltage is a minimum (the critical pressure), visible corona occurs before breakdown

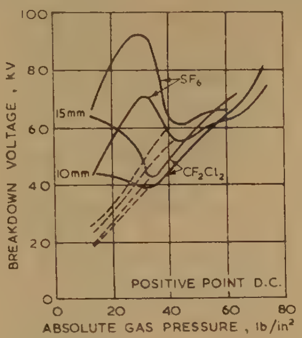

Fig. 9.—Corona inception and breakdown voltage characteristics for difluorodichloromethane and sulphur hexafluoride.
– – – – – Corona inception voltage.

as illustrated by the curves in Fig. 9. At pressures higher than the critical value breakdown coincides with corona inception.

The other significant features of the curves can be summarized as follows:

(*a*) The negative slope, following the voltage maximum, increases with increasing electric strength of the compound.
(*b*) Except with d.c. and impulses of negative polarity, the breakdown voltage increases slowly with electrode separation at pressures above the critical value.
(*c*) For a given compound the critical pressure increases with electrode separation.
(*d*) The effect of irradiation at pressures in the region of and in excess of the critical value is to reduce the breakdown voltage appreciably for gaps in excess of 10 mm; with smaller gaps the breakdown voltage tends to be lower over the whole pressure range.
(*e*) The impulse breakdown voltage is less than the d.c. value, when the point is anode, at pressures below the critical value, for the CF_yCl_z family of compounds and sulphur hexafluoride with the exception of carbon tetrafluoride.
(*f*) The shape of the characteristic for the negative point d.c. is similar to that for the positive point for difluorodichloromethane; unexpected shapes also occur with the curves for trifluorochloromethane and sulphur hexafluoride.

In the case of sulphur hexafluoride (20, 15 and 10 mm gaps) and monofluorochloromethane (20 mm gap) with positive-point d.c. there were two distinct breakdown characteristics for the pressure region below the critical value (see Figs. 4 and 8).

(5.2.1) Mixtures of Compounds including Nitrogen.

Some measurements were made with mixtures of two electronegative gases, the results of which are given in Fig. 10. It is evident from these curves that the performance of these gases can be improved under non-uniform field conditions by utilizing various compound combinations. It is of interest to record that the negative slope could not be eliminated and only one critical pressure region occurred. Detailed consideration

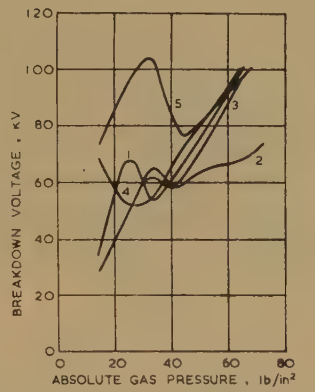

Fig. 10.—Positive point d.c. breakdown voltage for various electronegative gas mixtures.

1. Carbon tetrafluoride at 11 lb/in² with difluorodichloromethane added.
2. As above with carbon tetrafluoride at 14·7 lb/in².
3. As above with carbon tetrafluoride at 25·7 lb/in².
4. Difluorodichloromethane at 14·7 lb/in² with sulphur hexafluoride added.
5. Sulphur hexafluoride at 14·7 lb/in² with difluorodichloromethane added.

of these characteristics is complicated by the varying proportions of constituents with increasing pressure, but the limited number of results indicate that further work on these mixtures would be useful.

Power-frequency characteristics for sulphur hexafluoride/nitrogen and difluorodichloromethane/nitrogen mixtures are given in Fig. 11. The curves for sulphur hexafluoride were obtained

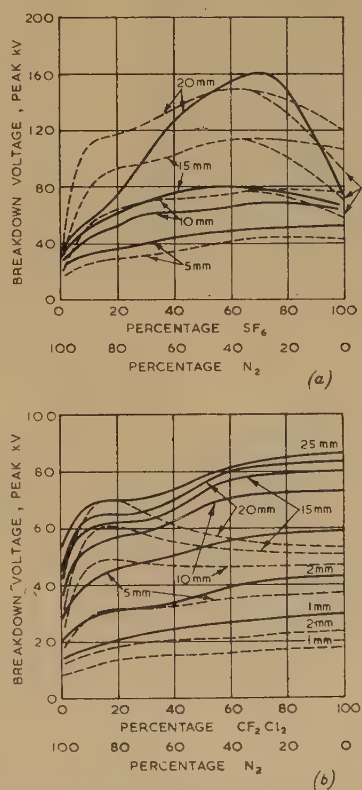

Fig. 11.—Power-frequency breakdown voltage for admixtures with nitrogen and point-sphere electrodes.

(*a*) Sulphur hexafluoride.
——— 46·7 lb/in² absolute.
- - - - - - 31·7 lb/in² absolute. For the pure gas at 31·7 lb/in² there are two stable breakdown values (see Fig. 4).

(*b*) Difluorodichloromethane.
——— 61·7 lb/in² absolute.
- - - - - - 31·7 lb/in² absolute.

at total gas pressures corresponding to the pressure at the voltage maximum (31·7 lb/in²), and the critical gas pressure (46·7 lb/in²) of the pure gas. For difluorodichloromethane, total gas pressures in the region of the critical pressure of the pure gas (31·7 lb/in²) and 61·7 lb/in² were used. These curves provide a further illustration of the useful insulating properties of these gas mixtures in non-uniform fields at certain spacings.

From the electrical data obtained with uniform and divergent field electrode arrangements, only sulphur hexafluoride and difluorodichloromethane appeared to be suitable for use as high-voltage dielectrics; subsequent work was therefore confined to these two gases.

(5.3) Coaxial Cylinders

The breakdown characteristics of concentric-cylinder electrodes are important in high-voltage work through the application of such field forms for compressed-gas capacitors and cables; the electrode arrangement used to obtain these data for the comparison of sulphur hexafluoride (SF_6), difluorodichloromethane (CF_2Cl_2) and nitrogen is shown in Fig. 12. Brass inner electrodes of 20·0, 9·96, 4·94 and 2·61 mm diameter connected by a wire to the top plate of the pressure chamber, and copper electrodes of 1·22 and 0·56 mm diameter (18 and 24 s.w.g.) stretched between the Perspex pillar and the shaft of the micrometer head, were used; these electrodes had ratios of outer diameter, *A* (30 mm), to inner diameters, *a*, 1·5, 3·0, 6·1, 11·5, 24·6 and 53·6.

A lead-through insulator located in the base-plate of the pressure chamber enabled the centre section of the external electrode to be earthed through a resistor for the detection of the corona inception voltage; it also provided means for determining whether breakdown had occurred to the main electrode or to the guard-rings.

Figs. 13–15 give the relation between the breakdown-voltage and the ratio A/a for sulphur hexafluoride, difluorodichloromethane and nitrogen; the complete curves for nitrogen have been included because there are considerable conflicting experimental data for this gas, and much of the published work is not very recent. The most difficult results to obtain were with nitrogen and positive d.c. (inner conductor positive) at ratios of A/a in excess of 11·5. Two completely stable breakdown values could be obtained as illustrated by the curves in Fig. 15; the lower practically coincided with the corona inception voltage; this anomalous behaviour was not associated with either sulphur hexafluoride or difluorodichloromethane.

The main features of the curves are as follows:

(*a*) For small values of A/a the positive d.c. breakdown is higher than the negative, but at larger ratios the curves intersect and the polarity effect is reversed; for nitrogen the point of intersection is not precise. Uhlmann[26] obtained results with air at atmospheric pressure similar to those obtained in the present series of tests for the electro-negative gases; the transition point for air occurred at $A/a = 10$.

(*b*) With the electronegative gases, the power-frequency curves lie between the positive and negative d.c. curves from $A/a = 1 \cdot 5$ approximately up to the transition point and then closely follow the positive. At $A/a = 1 \cdot 5$, the power-frequency breakdown voltages are slightly higher than the d.c. values and as the field approaches uniformity the percentage difference increases.

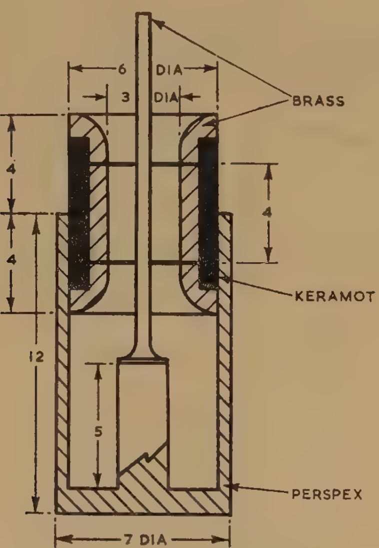

Fig. 12.—Electrode assembly for cylindrical field.

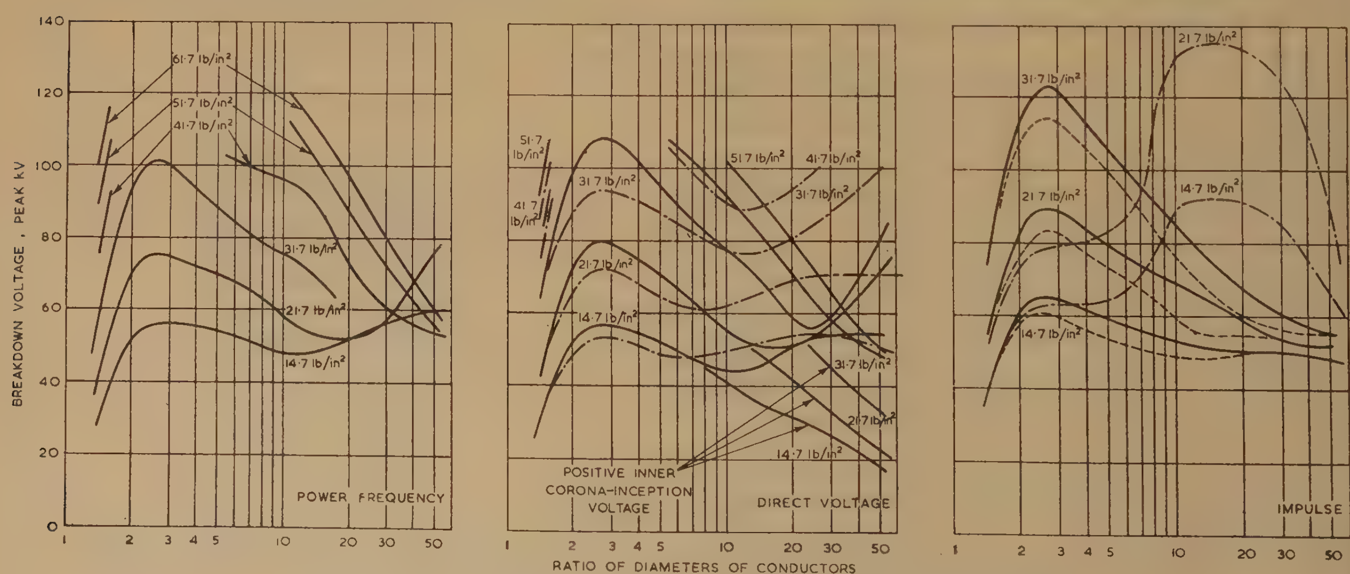

Fig. 13.—Breakdown voltage for sulphur hexafluoride between coaxial cylinders.

——— Power frequency, positive d.c. and impulse.
— — — Negative d.c. and impulse.
- - - - - - Positive impulse with radium.

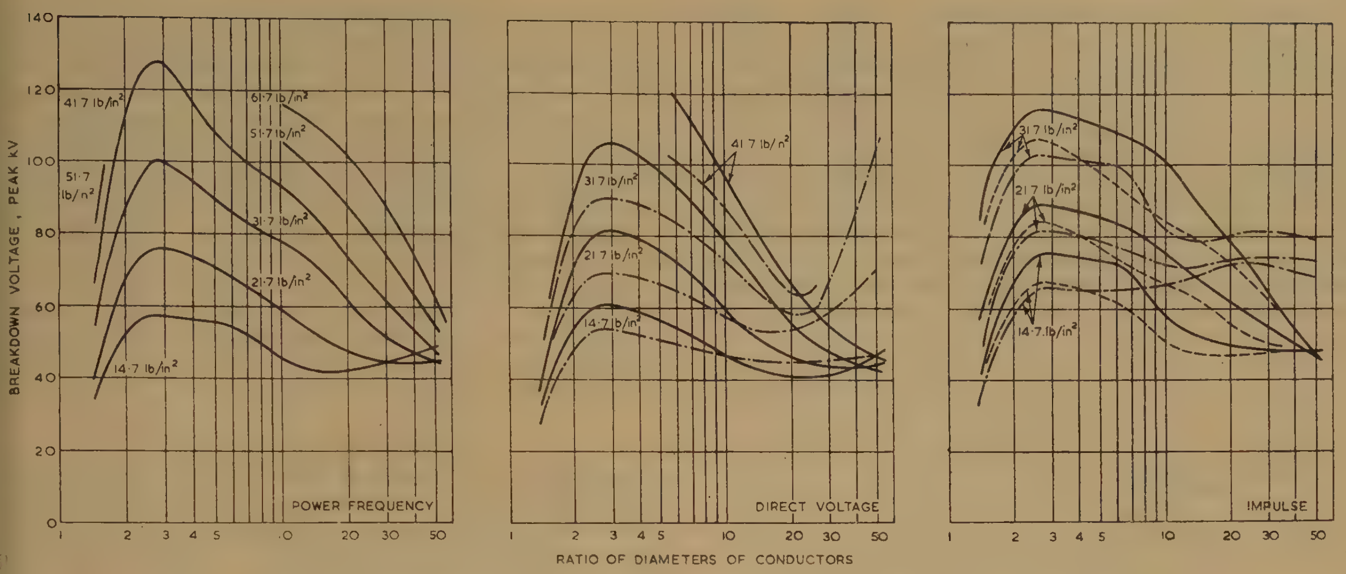

Fig. 14.—Breakdown voltage for difluorodichloromethane between coaxial cylinders.

———— Power frequency, positive d.c. and impulse.
— — — Negative d.c. and impulse.
- - - - - - Positive impulse with radium.

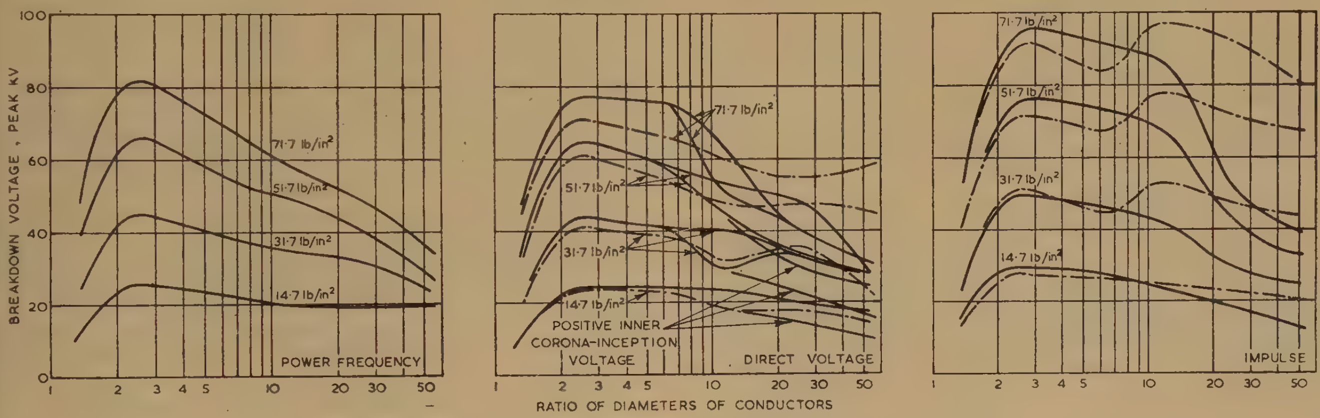

Fig. 15.—Breakdown voltage for nitrogen between coaxial cylinders.

———— Power frequency, positive d.c. and impulse.
—·—·— Negative d.c. and impulse.

(*c*) The intersection of the positive and negative impulse breakdown voltage curves occurs for all three gases.

(*d*) The characteristic negative slope of the breakdown-voltage/gas-pressure curves associated with electronegative gases and point-sphere electrodes is again observed and begins in the region of $A/a = 11 \cdot 5$; at $A/a = 54$ the maximum and minimum in the breakdown-voltage curve for sulphur hexafluoride are very well defined, and impulse ratios which are less than unity occur with a positive point.

(*e*) The corona inception voltage coincides with the breakdown voltage for values of A/a smaller than that at which the positive and negative direct-voltage curves intersect.

Table 6 gives the power-frequency relative electric strengths for the two compounds at atmospheric pressure and for the whole range of A/a values used.

(6) FLASHOVER OF A GASEOUS/SOLID INTERFACE

The use of any electrode system with a gaseous medium must invariably involve solid insulation in some part of the structure; it is therefore of interest to be able to assess the flashover voltage characteristics of this insulation with various electrode forms. The number of possible arrangements is unlimited. Three examples were selected giving different forms of tangential stress on the solid insulation. In series arrangements of solid and gaseous dielectrics, where the total gap is small, the influence of the gaseous medium is not significant. Dielectric combinations involving the puncture of solid insulation were not considered, since only small spacings could be accommodated in the equipment.

Table 6

POWER-FREQUENCY RELATIVE ELECTRIC STRENGTH FOR CONCENTRIC-CYLINDER BREAKDOWN DATA AT ATMOSPHERIC PRESSURE

(Nitrogen as datum)

Conductor ratios ..	1·5	3·0	6·1	11·5	24·6	53·6
Difluorodichloromethane (CF_2Cl_2)	2·36	2·28	2·36	2·25	2·28	2·56
Sulphur hexafluoride (SF_6)	2·27	2·22	2·28	2·43	2·88	3·20

(6.1) Plane Electrodes

The power-frequency flashover-voltage/gas-pressure characteristics were determined for solid porcelain cylinders (10·0 mm long and 15 mm diameter), between plane circular metallic electrodes (70·0 mm diameter) with rounded edges. This arrangement gives a uniform tangential stress along the surface of the porcelain, provided there are no discharges at the ends of the cylinder. To eliminate the difficulties experienced by Trump and Andrias[27] with porcelain in compressed nitrogen and ascribed to imperfect contact between the porcelain and electrodes, the ends of the cylinders were ground flat and coated with graphite. The results are plotted in Fig. 16. The

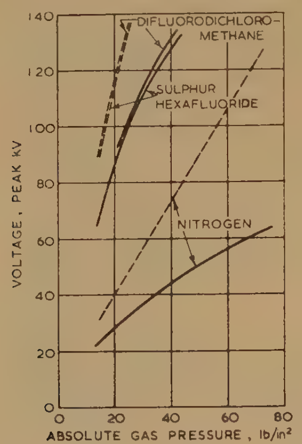

Fig. 16.—Flashover voltage of porcelain cylinders between plane electrodes.

——— Flashover voltage.
- - - - - - Breakdown voltage of gas between plane electrodes.

surface flashover strength benefits substantially from the electric strength of the gaseous medium. If field distortion arising from variations of surface resistivity, surface irregularities, corona discharges at the ends and the presence of bound charges could be eliminated, the flashover voltage would approach the gas value.

(6.2) Foil Electrodes

Samples were formed by wrapping copper foil (0·004 in thick) round ¾ in diameter resin-bonded paper tubes and securing the foil by means of clips. This arrangement gives tangential stresses which are concentrated at the edges of the electrodes.

Curves illustrating the results are given in Fig. 17 for sulphur hexafluoride and difluorodichloromethane; data for nitrogen and transformer oil are included. For comparison, a number of breakdown-voltage values were obtained using the same electrode form without the solid insulation. Sulphur hexafluoride, in spite of the pronounced voltage minimum, has better surface flashover-voltage characteristics than difluorodichloromethane. Both gases give considerably higher flashover voltages than nitrogen, and sulphur hexafluoride at the higher pressures is comparable with transformer oil.

(6.3) Cylindrical-field Electrodes

The third form of tangential stress considered was that provided by an arrangement of concentric electrodes; this gave a higher stress at one electrode. A circular earth plate, which was made from brass 0·125 in thick, had six symmetrically placed holes of 30·0 mm diameter cut near the outer edge. The materials tested were made the same size as the earthed plate; by means of a template, holes were drilled in the insulation to locate the sample in the correct position and to allow six 0·56 mm copper wires to pass through. Extreme care was necessary when drilling the small holes for the inner conductors to ensure that the holes were clean and that no burrs or scratches appeared round the circumferences; when assembled, the inner conductors were concentric with the holes cut in the earthed plate. Studding on the top plate of the structure allowed any slack in the inner conductor to be taken up and the wire put under slight tension; the projecting studding also made it possible, by means of a rotating arm, to select one sample at a time. Test samples were made from laminated Bakelite and Perspex sheets 0·25 in thick.

Both materials were tested with negative and positive impulse and power-frequency voltage in sulphur hexafluoride and difluorodichloromethane; for comparison, Perspex was tested in nitrogen. The surface flashover-voltage/gas-pressure characteristics are given in Fig. 18; breakdown-voltage curves of the gaseous medium alone, obtained with the same electrode sizes

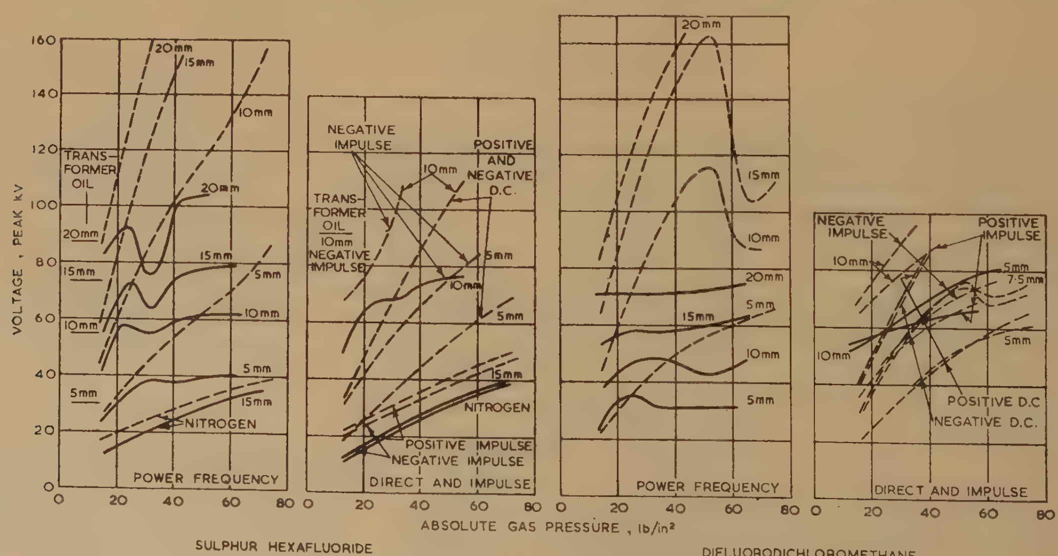

Fig. 17.—Flashover voltage of synthetic-resin bonded-paper tube between foil electrodes.

——— Flashover voltage of solid/gaseous interface.
- - - - - - Breakdown voltage between foil electrodes with the solid insulation removed.

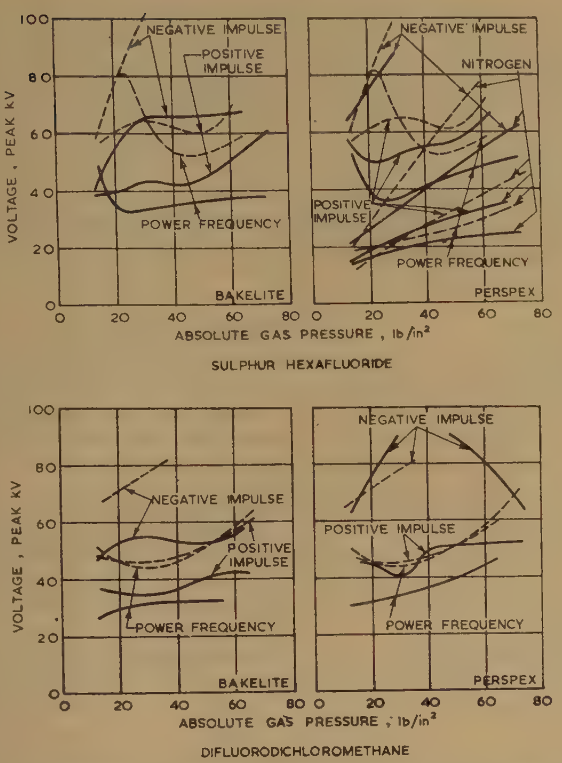

Fig. 18.—Flashover voltage of Bakelite and Perspex between coaxial electrodes.

——— Flashover voltage of solid/gaseous interface.
- - - - - - Breakdown voltage between coaxial electrodes with solid insulation removed.

(Section 5.1.3), are also included although it is to be appreciated that, with the sharp edges on the earth plate of the structure, the two systems are not strictly comparable.

As with foil electrodes, the flashover voltages of both materials are higher in sulphur hexafluoride than in difluorodichloromethane.

(7) CHEMICAL AND PHYSICAL PROPERTIES

(7.1) Stability and Toxicity

Difluorodichloromethane.—At room temperatures there is neither corrosion nor decomposition in the presence of structural metals. Midgeley and Henne[28] have shown that at 175° C the compound is still stable in the presence of carbon steels, aluminium, copper, Monel metal, tin and tin-lead solders, but there is some reaction with phosphor-bronze, brasses and magnesium alloys. Moisture always causes instability at 175° C. The compound is non-toxic. Chlorine is the only toxic element produced by decomposition of the gas by electrical discharges.

Sulphur Hexafluoride.—Constructional materials are unaffected, and the gas is non-inflammable and heat-resisting at temperatures up to 800° C. There is no reaction with water, acid or alkalis, and under the influence of heat the gas is not affected by hydrogen, oxygen, phosphorus, selenium, carbon, copper, silver, etc. The compound is not toxic. However, the commercial product contains small quantities (see Appendix 12.1) of the lower sulphur fluorides, such as disulphur decafluoride (S_2F_{10}), which is extremely toxic. Decomposition of the gas by electrical discharges also produces these toxic compounds.

(7.1.1) Chemical Stability in the Presence of Discharges.

To investigate the dissociation that occurs and the effect of the decomposition products on metallic and non-metallic materials, sulphur hexafluoride and difluorodichloromethane, at atmospheric pressure, were subjected to high-energy discharges.

The tests were carried out in a Pyrex glass cylinder (15 in long and 2·5 in diameter) fitted with tungsten-ended cylindrical electrodes, spaced so that the flashover voltage in the gas to be tested was approximately 70 kV (peak); the materials which were to be subjected to the decomposition products of the gas were placed in the cylinder. When assembled the system was pumped down to approximately 0·1 mm Hg and then filled with the gas to atmospheric pressure. The electrode system was connected through a 40-ohm resistor to a 0·2-μF capacitor which was allowed to charge until the gap in the test cell flashed over; a hundred impulses were applied to each gas sample. Similar tests were carried out in a test cell containing the same materials and activated alumina pellets. The sealed cells were observed over a period of time.

The materials were: copper, brass (one side half-covered with Frigelene and the other half-covered with shellac), mild steel, zinc, aluminium, tinned copper wire, enamelled copper wire, p.v.c.-covered wire, and polythene radio-frequency cable (U.R.39).

Sulphur Hexafluoride.—Decomposition of the gas produces lower-valency fluorides of sulphur,[29] and fluorides of any metals which are exposed to the decomposition products. Copper was the first metal to show signs of attack, and this occurred within forty-eight hours. After eighteen weeks, the samples were taken out of the glass cylinder and examined. The samples showed varying degrees of attack. The metals, in decreasing order of signs of corrosion, were brass, mild steel, copper, zinc, tin (tinned copper) and aluminium; on the last there were no signs of corrosion. Frigelene, shellac and enamel provided adequate protection, and non-metals gave no indication of damage; the corrosion which took place could not be considered serious.

The lower-valency fluorides, sulphur monofluoride (S_2F_2), sulphur difluoride (SF_2), sulphur tetrafluoride (SF_4) and disulphur decafluoride (S_2F_{10}), liberated during dissociation, form acidic substances in the presence of moisture. Activated alumina effectively removed all acidic and oxidizing decomposition products from the gas, since, in the test carried out in the presence of alumina pellets, the metallic samples showed no sign of attack.

Difluorodichloromethane.—The gas partially decomposes producing chlorine, trifluorochloromethane (CF_3Cl), small yields of carbon tetrafluoride and tetrafluorodichloroethane ($C_2F_4Cl_2$).[30] In the presence of the decomposition products, metal chlorides rather than fluorides are formed; this was confirmed by the results obtained, i.e. such readily identified compounds as zinc chloride ($ZnCl_2$) and stannous chloride ($SnCl_2$) were formed.

The copper sample showed signs of attack within a few hours, and after seven days all metallic samples except aluminium showed corrosive effects. After nineteen weeks the cylinder was opened and the samples examined. As far as the metallic materials were concerned, the order of severity of corrosion was the same as that for sulphur hexafluoride, except that the corrosive intensity was greater and the aluminium was affected; Frigelene, etc., again provided protection. Non-metallic materials, except p.v.c., showed no obvious signs of attack; p.v.c. had a waxy feel which was not normal for the compound.

Samples tested in the presence of activated alumina pellets showed no signs of having been affected.

The conclusions to be drawn are that corrosive effects arising from the decomposition products are not serious under the test conditions employed, and that the corrosive decomposition products are easily and effectively absorbed by activated alumina. It is probable that with sustained power-frequency arcs far more extensive decomposition would take place, but with the use of gaseous mixtures employing nitrogen, which have electric

strengths comparable with the pure electronegative gas, the corrosive effect is likely to be considerably reduced, since the number of complex gas molecules will be smaller for a given volume.

(7.2) Vapour-Pressure Characteristics

Gases cannot be operated at pressures higher than the saturation vapour pressure corresponding to a particular temperature, and therefore when used in equipments likely to be subjected to low temperatures it is essential for the operating gas pressure to be selected so that any fall in temperature does not result in saturation. So long as a compound remains in the gas phase, the electric strength will be constant for a fixed density; if saturation occurs under constant-volume conditions, the density falls and the electric strength follows approximately the vapour-pressure characteristic. Fig. 19 gives the vapour-pressure

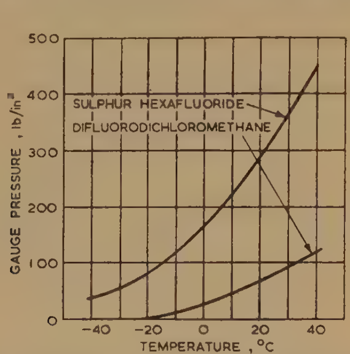

Fig. 19.—Saturated vapour pressure characteristics.

Curves can be expressed approximately as:

Sulphur hexafluoride, $\log_{10} p = 7 \cdot 28 - \frac{900}{T}$.

Difluorodichloromethane, $\log_{10} p = 7 \cdot 3 - \frac{1\,105}{T}$

where p = pressure, mm Hg.
T = absolute temperature.

characteristics (as curves and formulae) for sulphur hexafluoride (SF_6) and difluorodichloromethane (CF_2Cl_2).

On the basis of these relations sulphur hexafluoride is superior to difluorodichloromethane for applications where the temperature variation may be large, and particularly where temperatures below 0° C are likely.

The relationship between pressure and temperature over the range 10–60° C was linear, indicating that the compounds behaved as perfect gases, a fact confirmed by the consistency of breakdown of a fixed sphere-gap.

(7.3) Thermal Conductivity

Heat transfer with gases is not so rapid as with liquid insulation; as compared with transformer oil, larger cooling surfaces are required and a greater volume of dielectric must be circulated. This is partly off-set since with gaseous insulation it is possible to operate at higher temperatures; the limit for transformer oil is 90° C.

Heat conductivities are as follows:

Transformer oil	at 0° C	$7 \cdot 75 \times 10^{-5}$ joule/sec/cm² °C/cm
	at 100° C	$7 \cdot 27 \times 10^{-5}$ joule/sec/cm² °C/cm
Sulphur hexafluoride	at 25° C	$1 \cdot 7 \times 10^{-5}$ joule/sec/cm² °C/cm
Nitrogen	at 0° C	$1 \cdot 39 \times 10^{-5}$ joule/sec/cm² °C/cm
Difluorodichloro-methane	at 30° C	$0 \cdot 56 \times 10^{-5}$ joule/sec/cm² °C/cm
	at 88° C	$0 \cdot 70 \times 10^{-5}$ joule/sec/cm² °C/cm

Appendix 12.3 gives other physical properties of sulphur hexafluoride and difluorodichloromethane.

(8) ECONOMIC FACTOR

On the basis of providing the same power-frequency electric strength in a uniform field, the relative costs of oxygen-free nitrogen, transformer oil, difluorodichloromethane and sulphur hexafluoride in this country are in the ratio 1 : 6 : 7 : 94; the interesting feature is the comparable costs of transformer oil and difluorodichloromethane.

Similar figures cannot be given for non-uniform fields in general; the ratios depend upon the type of electrode arrangement and the gap.

(9) DISCUSSION

Over a wide range of pressure, sulphur hexafluoride and difluorodichloromethane have electric strengths under uniform field conditions which are more than twice that of nitrogen at the same pressure, and at approximately 3 atmopsheres absolute pressure their strengths are comparable with that of transformer oil. If they are used in place of nitrogen, equipment strength, weight and cost can be reduced; the saving in weight by dispensing with transformer oil might be more than made up by the necessity for heavier walls to withstand pressure. A valuable feature is that with uniform fields electric strengths are independent of frequency.

With non-uniform fields, the power-frequency and direct-voltage breakdown values are four or more times as great as with nitrogen under the same conditions; the performance of these gases is inferior to that of oil except for small gaps at high pressures. In the pressure regions where high electric strengths occur, breakdown is preceded by intense corona, and to make full use of the electric strengths solid insulation should be kept clear or alternatively must be capable of resisting deterioration arising from corona. If the normal practice of designing equipment to operate without discharges is maintained, working pressures of at least 45 and 35 lb/in² absolute for sulphur hexafluoride and difluorodichloromethane are required. At pressures below the critical gas pressure the breakdown voltage increases rapidly with electrode spacing, except in the case of sulphur hexafluoride under impulse conditions, but at higher pressures the positive and power-frequency breakdown voltages increase slowly with electrode separation, and a situation might well occur in which considerable increase in gap failed to give any appreciable increase in breakdown voltage. This aspect requires further study. The concentric cylinders are a particular non-uniform field condition, and for large ratios of diameters the voltage characteristics conform to those of the point-sphere arrangement.

For general outdoor use, only sulphur hexafluoride in the undiluted state has a suitable vapour-pressure/temperature characteristic, but both, in undiluted form, are suitable for indoor applications. The dilution of the gases with nitrogen, which does not seriously affect the electric strength of either in uniform or non-uniform fields, has the advantages of saving in cost, lowering of the saturation temperature for a given total gas pressure, and reducing the severity of the effects arising from the dissociation of the gas molecules when subjected to corona or flashover. For a total gas pressure of 60 lb/in² absolute, dilution of difluorodichloromethane with nitrogen to give a partial electron-negative gas pressure of 15 lb/in² lowers the saturation temperature from 9° C to −29° C; the lowering of the electric strength in a uniform field is approximately 20%.

The surface flashover data show that the flashover voltage of solid insulation benefits from the electric strength of the gas. In practical series insulation arrangements involving gaseous and solid dielectrics, since the dielectric constants of solid insulation are much greater than those of gases, the voltage

distribution is worse than it would be in similar transformer-oil/solid-insulation arrangements; data must therefore be accumulated for practical gaseous/solid-insulation combinations.

With the use of absorbents, such as activated alumina, the dissociation of electronegative gases should not be a serious problem. Camilli and others[35] have shown that the pressure rise associated with electrical breakdown (power arc) in sulphur hexafluoride is only a fraction of that developed in liquid-filled equipment; unlike liquid dielectrics the pressure rise appears to be from thermal expansion of the gas rather than from the formation of large amounts of dissociation products.

The various negative-ion-forming reactions which influence the electric strength of electronegative gases are briefly discussed in Appendix 12.2. A semi-quantitative treatment to explain much of the experimental breakdown data in uniform and divergent fields will be the subject of a further communication.

(9.1) Conclusions

Two gases, sulphur hexafluoride and difluorodichloromethane, seem to be worth considering for high-voltage insulation. It is not possible to state without qualification the best gas, gas mixture and ideal pressure, since the choice depends upon the size and the geometry of the gap, and whether the surface flashover of solid insulation is involved. In general, sulphur hexafluoride (SF_6) has the better physical, chemical and electrical properties and is to be preferred to difluorodichloromethane (CF_2Cl_2).

(10) ACKNOWLEDGMENTS

The work described above has been carried out as part of the research programme of the National Physical Laboratory, and the paper is published by permission of the Director of the Laboratory.

(11) REFERENCES

(1) Warren, J. W., Hopwood, W., and Craggs, J. D.: 'On Dissociation Processes in certain Gases of High Dielectric Strength', *Proceedings of the Physical Society* (B), 1950, **63**, p. 180.

(2) Warren, J. W., Marriott, J., and Craggs, J. D.: 'Negative-ion Formation in Gases of High Dielectric Strength', *Nature*, 1953, **171**, p. 514.

(3) Massey, H. S. W.: 'Negative Ions' (Cambridge University Press, 1950).

(4) Hurd, D.: 'Mechanism of Dielectric Breakdown', *General Electric Review*, Dec., 1948, **51**, p. 26.

(5) Harrison, M. A., and Geballe, R.: 'Simultaneous Measurement of Ionization and Attachment Coefficients', *Physical Review*, 1953, **91**, p. 1.

(6) Geballe, R., and Reeves, M. L.: 'A Condition on Uniform Field Breakdown in Electron-Attaching Gases', *ibid.*, 1953, **92**, p. 867.

(7) Hochberg, B., and Sandberg, E.: 'Investigation of the Electric Strength of Gases', *Journal of Technical Physics*, 1942, **12**, p. 65.

(8) Hochberg, B.: 'Elegas—Gas Electrical Insulation', *Elektrichestvo*, 1947, **3**, p. 15.

(9) Geballe, R., and Linn, F. S.: 'Electrical Breakdown in CSF_8', *Journal of Applied Physics*, 1950, **21**, p. 592.

(10) Charlton, E. E., and Cooper, F. S.: 'Dielectric Strength of Insulating Fluids—Part I, Gases and Gas-Vapour Mixtures', *General Electric Review*, 1937, **40**, p. 438.

(11) Neubert, U.: 'The Breakdown of Electronegative Gases at Breakdown Field Strengths', *Archiv für Elektrotechnik*, 1952, **40**, p. 370.

(12) Nonken, G. C.: 'High-Pressure Gas as a Dielectric', *Transactions of the American I.E.E.*, 1941, **60**, p. 1017.

(13) McCormick, N. R., and Craggs, J. D.: 'Some Measurements of the Relative Dielectric Strength of Gases', *British Journal of Applied Physics*, 1954, **5**, p. 171.

(14) Camilli, G., and Chapman, J. J.: 'Gaseous Insulation for High-Voltage Apparatus', *Transactions of the American I.E.E.*, 1947, **66**, p. 1463.

(15) Hudson, C. M., Hoisington, L. E., and Royt, L. E.: 'Dielectric Strengths of CCl_2F_2–Air and SO_2–Air Mixtures', *Physical Review*, 1937, **52**, p. 664.

(16) Weber, N.: 'The Electrical Behaviour of Electronegative Gases', *Archiv für Elektrotechnik*, 1942, **36**, p. 166.

(17) Unpublished I.C.I. Report.

(18) Trump, J. G., Safford, F. J., and Cloud, R. W.: 'D.C. Breakdown Strength of Air and of Freon in a Uniform Field at High-Pressure', *Transactions of the American I.E.E.*, 1941, **60**, p. 132.

(19) Gross, M. J.: 'Gas Insulation—A New Trend in Roentgen Ray Apparatus', *American Journal of Roentgenology and Radium Therapy*, 1951, **65**, p. 103.

(20) Skilling, H. H., and Brenner, W. C.: 'The Electric Strength of Nitrogen and Freon under Pressure', *Transactions of the American I.E.E.*, 1942, **61**, p. 191.

(21) Banks, H. A., and Rudge, J. A.: 'Selenium Hexafluoride: Dielectric Strength and Some Chemical Properties', *Nature*, 1953, **171**, p. 390.

(22) Nonken, G. C.: Discussion on paper by Camilli, G., and Chapman, J. J., 'Gaseous Insulation for High Voltage Apparatus', *Transactions of the American I.E.E.*, 1947, **66**, p. 1463.

(23) Gänger, B.: 'High-Frequency Disruption of Compressed Gases', *Archiv für Elektrotechnik*, 1943, **37**, p. 267.

(24) Bright, A. W.: 'High-Frequency Discharges in Gases', *Nature*, 1950, **165**, p. 811, and The British Electrical and Allied Industries Research Association Report No. L/T229, 1950.

(25) Gibson, J. W., and Miller, C. F.: 'The Electric Strength of Sulphur Hexafluoride at Radio Frequencies', *Journal of the Electrochemical Society*, 1953, **100**, p. 265.

(26) Uhlmann, E.: 'The Electrical Breakdown of Air between Concentric Cylinders', *Archiv für Electrotechnik*, 1929, **23**, p. 323.

(27) Trump, J. G., and Andrias, J.: 'High-Voltage D.C. Flashover of Solid Insulators in Compressed Nitrogen', *Transactions of the American I.E.E.*, 1941, **60**, p. 987.

(28) Midgeley, T., and Henne, A. L.: 'Organic Fluorides as Refrigerants', *Industrial and Engineering Chemistry*, 1930, **22**, p. 543.

(29) Schumb, W. C., Trump, J. C., and Priest, G. L.: 'Effect of High-Voltage Electrical Discharges on Sulphur Hexafluoride', *ibid.*, 1949, **41**, p. 1348.

(30) Thornton, N. V., Burg, A. B., and Schlesinger, H. I.: 'The Behaviour of Dichlorofluoromethane and Chlorotrifluoromethane in Electrical Discharges,' *Journal of the American Chemical Society*, 1933, **55**, p. 3177.

(31) Wilson, W. A., Simmons, J. H., and Brice, T. J.: 'The Dielectric Strength of Gaseous Fluorocarbons', *Journal of Applied Physics*, 1950, **21**, p. 203.

(32) Dibeler, V. H., and Mohler, F. L.: 'Dissociation of SF_6, CF_4, and SiF_4 by Electron Impact', National Bureau of Standards, Washington, 1948, **40**, p. 25.

(33) Baker, R. F., and Tate, J. T.: 'Ionization and Dissociation by Electron Impact in CCl_2F_2 and CCl_4 Vapours', *Physical Review*, 1938, **53**, p. 683.

(34) MASSEY, H. S. W., and BURHOP, E. H. S.: "Electronic and Ionic Impact Phenomena' (Oxford University Press, 1952).

(35) CAMILLI, G., GORDON, G. S., and PLUMP, R. E.: 'Gaseous Insulation for High-Voltage Transformers,' *Transactions of the American I.E.E.*, 1952, **71**, Part III, p. 348.

(12) APPENDICES

(12.1) Probable Impurities in the Gaseous Compounds

The impurities are shown in decreasing order of magnitude for each compound, and where no precise figures are given the impurities, in the opinion of the manufacturer, are not present in detectable amounts.

Carbon tetrafluoride CF_4 (Arcton 0)	(1) C_2F_6 (2) C_3F_8
Trifluoromethane CHF_3 (Arcton 1)	(1) CHF_2Cl (2) $CHFCl_2$ and CH_2F_2 (3) $CHCl_3$ and CH_2Cl_2
Trifluorochloromethane CF_3Cl (Arcton 3)	(1) CF_2Cl_2 (2) $CFCl_3$ and CCl_4
Difluoromonochloromethane CHF_2Cl (Arcton 4)	(1) CH_2F_2 (approximately 0·05%) (2) $CHFCl_2$ (traces detected) (3) CHF_3
Difluorodichloromethane CF_2Cl_2 (Arcton 6)	(1) CF_3Cl (approximately 0·01%) (2) $CFCl_3$ (very slight traces)
Monofluorodichloromethane $CHFCl_2$ (Arcton 7)	(1) CHF_2Cl and $CHCl_3$
Monofluorotrichloromethane $CFCl_3$ (Arcton 9)	(1) CF_2Cl_2 and CCl_4
Sulphur hexafluoride SF_6	(1) Air (0·29% w/w) (2) Water (10 w/w p.p.m.) (3) S_2F_{10} (less than 1 w/w p.p.m.) (4) Hydrolysable impurities expressed as SF_4 (6 w/w p.p.m.)
Nitrogen	(1) Neon (approximately 0·1%) (2) Helium (approximately 0·03%) (3) Argon (less than 50 v.p.m.) (4) Carbon dioxide (20 v.p.m.) (5) Oxygen (less than 10 v.p.m.)

(12.2) Properties of Difluorodichloromethane and Sulphur Hexafluoride

Difluorodichloromethane (CF_2Cl_2).

Molecular weight	120·92
Melting point	−158°C
Boiling point	−29·8°C
Critical temperature	111·5°C
Critical pressure	582 lb/in² absolute
Critical density (liquid)	0·555 g/cm³
Density 20°C (gas)	5·65 g/litre
Specific heat of vapour in calories/cm/°C at 0°C	0·145
Dielectric constant (760 mm Hg and 20°C)*	$1\cdot0032_5$

Sulphur Hexafluoride (SF_6).

Molecular weight	146·06
Melting point	−50·8°C
Boiling point	−68·1°C
Critical temperature	45°C
Critical pressure	540 lb/in² absolute
Critical density (liquid)	0·79 g/cm³
Density 20°C (gas)	6·16 g/litre
Specific heat of vapour in calories/cm/°C at 0°C	0·148
Dielectric constant (760 mm Hg and 19·4°C)	$1\cdot0021_1$

* Determined at 9 200 Mc/s by Dr. L. Essen, N.P.L.

(12.3) Factors influencing the Electric Strength of Electronegative Compounds

For the complex molecular compounds, correlation between various physical properties such as molecular weight and electric strength has been attempted, but with little success. Although correlation has been obtained for the fluoro-carbons hexafluorethane (C_2F_6), octofluoropropane (C_3F_8) and decafluorobutane (C_4F_{10}) in the form of simple linearity between electric strength and increasing gas density,[31] this does not apply to the two halogenated methane families considered, and there are other notable exceptions. Hochberg and Sandberg[7] compared measurements of α/p (α = Townsend's first ionization coefficient, p = gas pressure) as a function of E/p and electric strengths; the results showed that high values of breakdown voltage were associated with low values of α/p. They suggested that these low values of α were due to high electron-energy losses arising from non-ionizing inelastic collisions which should be more frequent with complex than with simple molecules. There are, however, complex gases with higher values of α than a simple gas like nitrogen. The more recent work of Harrison and Geballe[5] with CF_2Cl_2 and CF_3SF_5 shows that in fact the ionization coefficient α is about an order of magnitude greater than the values previously reported; it attributes the apparently low values of α previously determined to a neglect of attachment processes leading to the formation of negative ions; thus, in general, higher electric strengths would be expected for compounds having appreciable electron attachment. The case of chlorine, which has a low relative electric strength (1·5 that of nitrogen) is covered by the data provided by Harrison and Geballe; the attachment coefficient is observed to be larger for the halogen-containing molecules than for the same halogens when free.

Many types of ion-producing reactions have been observed (principally through the use of mass spectrographs), and the relative significance of the various reactions coupled with the effect of inelastic non-ionizing collisions control the electric strength.

The main reactions which take place under electron impact can be summarized for SF_6 and the CF_yCl_z family of compounds as follows:

(i) Capture of a free electron by a molecule accompanied by vibrational excitation of the molecule and subsequent stabilization. The reverse reaction takes place yielding once more the molecule and electron unless the excess energy is quickly removed in some way (as kinetic energy of a third body).

$$SF_6 + e \rightarrow SF_6^{-*} \rightarrow SF_6^-$$
$$CF_yCl_z + e \rightarrow CF_yCl_z^{-*} \rightarrow CF_yCl_z^-$$

(ii) Capture of a free electron by a molecule with dissociation of the molecule. Where fluorine and chlorine atoms occur together in the molecule the most abundant ion is that produced when the parent molecule loses a chlorine atom.

$$SF_6 + e \rightarrow SF_5 + F^-$$
$$CF_yCl_z + e \rightarrow CF_yCl_{z-1} + Cl^-$$

(iii) Dissociation of the molecule into positive and negative ions.

$$SF_6 + e \rightarrow SF_5^+ + F^- + e$$
$$CF_yCl_z + e \rightarrow CF_yCl_{z-1}^+ + Cl^- + e$$

(iv) Electron multiplication.

(a) $SF_6 + e \rightarrow SF_6^+ + 2e$

$$CF_yCl_z + e \rightarrow CF_yCl_z^+ + 2e$$

and (b) $SF_6 + e \rightarrow SF_5^+ + F + 2e$

$$CF_yCl_z + e \rightarrow CF_yCl_{z-1}^+ + Cl + 2e$$

Data on the dissociation products associated with electron bombardment for carbon tetrafluoride (CF_4) and sulphur hexafluoride (SF_6)[32] and difluorodichloromethane (CF_2Cl_2)[33] show that there is little or no tendency for the formation of the primary ion (CF_4^+, SF_6^+ and $CF_2Cl_2^+$); reaction (iv*a*) is therefore unlikely. Reactions (i) and (ii) result in actual capture and therefore tend to prevent or quench electron-avalanche formation, while reaction (iii) leading to ion-pair formation makes no contribution to an avalanche. Variations in electric strengths are therefore dependent upon the relative probabilities of the reactions (i), (ii), (iii) and (iv*b*), and for gases having high electric strengths reaction (iv*b*) would be relatively improbable.

Stabilization of excited molecules leading to stable XY^- ions can occur by radiation and by super-elastic impact. Massey and Burhop[34] state that radiation occurs over a relatively long period and can usually be ignored, but stabilization by third-body collisions may be important if the pressure is not too low; the rate of formation of the stable XY^- ion by third-body collisions is proportional to pressure at low pressures but is likely to become independent of pressure at higher pressures. At pressures where electric strength measurements are made this reaction might be important. Electron energies will be higher for reaction (ii) than for (i), and reaction (iii) which starts at a definite energy level and persists to quite high energies, is less likely than the others, since electron energies greater than ionization energies, i.e. of the order of 20 eV, are required.

The high electric strength obtained by the addition of small quantities of electronegative gases, such as CF_2Cl_2 and SF_6, to nitrogen arises from the increased probability of inelastic non-ionizing collisions and from the processes already detailed, with the exception of reaction (iii); the processes occur at potentials below the ionization potential of nitrogen.

DISCUSSION ON THE ABOVE PAPER AND ON 'THE ELECTRIC STRENGTH OF HIGHLY COMPRESSED GASES'* BEFORE THE MEASUREMENT AND CONTROL SECTION, 6TH NOVEMBER, 1956

Mr. R. Davis: The papers treat special aspects of the problem of the gas discharge—one of the most fundamental and fascinating in physics. It is fascinating because of the number of processes which may be involved, and fundamental because some of these processes may have relevance to solid, liquid and nuclear physics. In many gases at normal temperature and pressure electrical failure is preceded by electron multiplication leading to the so-called avalanche; electrons are accelerated in the applied field, collide with neutral atoms and produce new electrons, the increase in the number of electrons being exponential. This primary process is not, in general, sufficient to produce breakdown. For breakdown to occur secondary processes are needed to maintain the process of avalanche formation. These secondary processes may occur in the gas, by collisions between positive ions and neutral particles or photo-ionization, or at the cathode by impact of photons or positive ions. Recently a further secondary process has been invoked† involving collisions between electrons and excited atoms. The mathematical formulation of these ideas leads to the equation of Townsend, which indicates that the current through the gas can increase indefinitely to a value limited only by the external circuit resistance. By applying this equation it is possible to predict the breakdown voltage of a number of gases for both uniform and a range of non-uniform fields where the field divergence is not too great. With highly divergent fields, partial breakdown or corona precedes complete breakdown, and space charges are produced which modify the applied field; polarity effects become more significant. In any particular case of gas, field form or polarity, the problem is one of assessing the significance of any particular process, either primary or secondary.

Dr. Holt in his paper shows that the primary process of avalanche formation is unlikely to be significant for breakdown because of the low ionizing efficiency of the electron at the gas pressures investigated. The main source of the current required for breakdown is attributed to electron emission from the cathode in the high fields prevailing near breakdown, this current increasing rapidly with the field.

Dr. Howard describes work with electronegative gases which have the property that electrons readily attach to neutral particles to form negative ions, thus reducing the availability of electrons for multiplication. The breakdown strength of these gases may be expected to be high, as experiment shows. In a companion paper Dr. Howard claims that, for much of his experimental data, the breakdown field represents a limiting condition where the attachment and ionizing conditions approach equality. If this is truly the case, it would seem, as with Dr. Holt's work at high pressures, that for the two special cases considered in these papers, an electron avalanche of a certain magnitude is not a necessary prerequisite for breakdown.

Mr. F. S. Edwards: In Section 4.2 of the paper by Dr. Holt it is stated that the breakdown potential of air is directly proportional to the gap length, whereas Bruce (in Reference 7 of the paper) and many other investigators have shown that the breakdown potential of air in a uniform field is not proportional to the gap length. Could the author reconcile these two contradictory statements?

In Table 4 of the paper by Dr. Howard the power-frequency breakdown voltage of sulphur hexafluoride is shown to be proportional to the spacing to within less than 1% over the range of spacings tested, in spite of the fact that 5 cm spheres were used and not uniform field electrodes. This proportionality is in disagreement with the published data on 5 cm spheres in air, for which the mean breakdown gradient decreases by about 6% over the same range of spacings. Perhaps the theoretical studies of the authors will enable them to suggest reasons for the difference.

In Section 8 of the paper the case is excluded in which the impulse test voltage is much higher than the power-frequency test voltage and where, in consequence, the impulse ratio of the insulation becomes important.

In Table 2 the impulse ratio of oil is given as 2·44, which is double the highest value quoted for sulphur hexafluoride, and in the column headed 'negative impulse 0·5 cm', it can be seen that, for this spacing, the impulse breakdown voltage of oil is over 50% higher than that of sulphur hexafluoride at 4 atm pressure. Hence the cost of sulphur hexafluoride, instead of being about 16 times that of oil, would be very much greater if the impulse breakdown voltage were the decisive factor in the design.

Mr. H. C. Hall (*communicated*): Both authors have expressed

* Holt, E. H.: Paper No. 1922 M, February, 1956 (see 103 A, p. 57). Dr. Holt is at the University of Illinois: at the meeting his paper was read by Dr. H. Tropper.

† Francis, G., and von Engel, A.: 'The Origin of Streamers in Spark Discharges', *Zeitschrift für Physik*, 1956, 145, p. 560.

all data in terms of breakdown voltage, and although the reason is appreciated, it may be that they are over-cautious and thus have stopped short of making interesting generalizations using the concept of electric stress. Dr. Holt in Section 4.1 of his paper does, in fact, justify 'normalization' to a 1 mm gap by quoting linear relationships which have been found between gap length and breakdown voltage. He thus seems implicitly to use the idea of a critical breakdown stress.

There are many instances in both papers where the notion of breakdown stress could be used with advantage and simplification, although, of course, I do not imply that stress is the only criterion for breakdown. In the paper by Howard especially, the presentation of the data in Section 5.3 not only lacks generality but may be misleading. A striking feature of all the curves in Figs. 13, 14 and 15, on which the author does not comment, is the clearly defined maxima in those of (breakdown-voltage)/(ratio of the diameters of conductors). These maxima all occur at a diameter ratio of about 2·7, and, as is well known, this ratio is that for which, for a given maximum stress in the region between electrodes (occurring at the surface of the inner electrode), the voltage between them is a maximum. It is therefore clear that, using the concept of a critical breakdown stress, the maxima shown in the Figures are merely consequences of the system geometry.

The data show that, over a range of diameter ratios from about 2 to 5, breakdown stresses at the inner electrode tend to be constant, but increase as the diameter ratio is further increased; this is consistent with the development of corona—at least at power frequencies—actually tending to inhibit complete breakdown.

THE AUTHORS' REPLIES TO THE ABOVE DISCUSSIONS

Dr. E. H. Holt (*in reply*): I would like to record my deep appreciation of the service which Dr. H. Tropper of Queen Mary College, London University, rendered me in presenting the paper in my unavoidable absence. His interest in the work has been a great encouragement.

Mr. Davis points to the main conclusion of the paper on the subject of the spark mechanism. The steps in the analysis depend upon the use of the concept of the breakdown gradient of the gap.

I am therefore in full sympathy with Mr. Hall's comment about the insight gained by thinking in terms of the breakdown gradient in preference to the breakdown voltage in uniform field work.

In reply to Mr. Edwards, I would point to the agreement between the present results and those of Zeier, Howell and Trump quoted in Section 4.1 of the paper. It should be emphasized that the gap-length range quoted is between 0·1 and 25 mm (the work described in the paper is in the range 1–3 mm), and the work referred to in this range was done at pressures well above atmospheric. Bruce, in Reference 7 of the paper, was concerned with a much greater range of gap lengths, and records only one measurement in the spacing 0–9 mm (in fact at 2·39 mm). Further, his work was carried out at atmospheric pressure. Nevertheless, his measurements in the gap-length range 2·39–25 mm show a linear relationship with the breakdown voltage to within the 10% accuracy which can be achieved in the higher-pressure work.

Dr. P. R. Howard (*in reply*): Paper No. 2260 M on the next page shows that the condition for which the ionization and attachment coefficients, α/p and η/p, are equal sets a limiting value on the field/pressure ratio E/p below which the onset of discharges, either incomplete (corona) or complete (breakdown), are not possible. This is not quite the same as Mr. Davis's interpretation that 'the breakdown field represents a limiting condition where the attachment and ionizing conditions approach equality'. In the equation of the current between parallel plates for electronegative gases the limiting value of E/p is actually characterized by the condition η/p slightly greater than α/p, which means that, in the build-up of the pre-breakdown current, electrons are diminishing and being replaced by negative ions as charge carriers. It is difficult to imagine breakdown occurring under these conditions, and it is probable that, for the passage of a spark, the condition $\alpha/p > \eta/p$ must hold. This would be achieved with a very small increase of voltage, since, in the region of the limiting value of E/p, α/p is increasing rapidly with field strength and η/p is generally decreasing.

The difference, pointed out by Mr. Edwards, between the accepted decrease in mean breakdown gradient with sphere spacing with air and the apparent constant mean breakdown gradient for the same range of spacings with sulphur hexafluoride cannot, as yet, be explained by theoretical considerations. The decrease in mean breakdown gradient with increasing spacing for sulphur hexafluoride only becomes significant at gaps in excess of 6 mm.

Mr. Hall suggests that, if the results had been given in the form of breakdown stress at the inner conductor against diameter ratio, a greater degree of generalization would have been achieved. One difficulty in carrying out the suggestion is to derive the stress at the inner conductor when corona precedes breakdown.

621.315.618.9.015.5:621.3.013

Paper No. 2260 M
Apr. 1957

PROCESSES CONTRIBUTING TO THE BREAKDOWN OF ELECTRONEGATIVE GASES IN UNIFORM AND NON-UNIFORM ELECTRIC FIELDS

By P. R. HOWARD, Ph.D., B.Sc.(Eng.), Associate Member.

(*The paper was received* 21*st September*, 1956.)

SUMMARY

In the paper it is suggested that for electronegative gases, where both ionizing and attachment processes occur, the condition for breakdown in uniform fields and the onset of discharges, which may lead to complete breakdown in certain circumstances, in non-uniform fields (with the positive electrode in the high-field region) is that the ionizing and attachment coefficients have the same value.

In non-uniform fields and above a certain critical pressure p_c the breakdown and discharge inception stresses coincide, but below p_c they differ; the gaps processes operating in these regions are briefly discussed.

(1) INTRODUCTION

Some gases possess electric strengths which are much higher than those for air and nitrogen in uniform fields, and exhibit unusual breakdown-voltage/gas-pressure characteristics for non-uniform fields with a highly stressed electrode of positive polarity. These features, which are dealt with in an earlier paper,[1] are ascribed to the formation of negative ions, the modes of which can be expressed in general terms by the following reactions:

Direct attachment $XY + e \rightarrow XY^-$ .. .. (i)

Dissociative attachment $XY + e \rightarrow X + Y^-$ .. .. (ii)

Dissociation into ions $XY + e \rightarrow X^+ + Y^- + e$ .. (iii)

where X is usually an atom of carbon or sulphur and Y is a halogen atom, usually chlorine or fluorine or a combination of both.

Reactions (i) and (ii) result in actual electron capture and therefore tend to prevent or quench electron avalanche formation, while reaction (iii), leading to ion-pair formation, makes no contribution to an electron avalanche.

According to the Townsend theory of electrical breakdown in simple gases, the steady-state current flowing in a uniform-field gap is given by

$$I = I_0 \frac{\varepsilon^{\alpha d}}{1 - (\omega/\alpha)(\varepsilon^{\alpha d} - 1)} \quad . \quad . \quad . \quad . \quad (1)$$

where I_0 = Initial photo-electric current.
d = Electrode separation.
α and ω/α = Primary and generalized secondary ionization coefficients.

If the attachment processes (i) and (ii) are defined by the parameter η (mean number of attachments per centimetre drift in the field direction in analogy to Townsend's primary ionization coefficient), and the rate of the reaction (iii) is defined by the parameter λ, it can be shown that

$$I = I_0 \frac{\dfrac{\alpha+\lambda}{\alpha-\eta}\varepsilon^{(\alpha-\eta)d} - \dfrac{\lambda+\eta}{\alpha-\eta}}{1 - (\omega/\alpha)\dfrac{\alpha+\lambda}{\alpha-\eta}[\varepsilon^{(\alpha-\eta)d} - 1]} \quad . \quad . \quad . \quad (2)$$

In eqns. (1) and (2) the coefficients α, ω/α, η and λ are functions of the applied field strength E. More generally α/p, etc., are functions of E/p (where p is the gas pressure in mm Hg).

When for non-attaching gases the growth of the initial current I_0 follows eqn. (1) the electrode spacing d_s at which the current becomes self-maintaining and independent of I_0 is given by

$$d_s = \alpha^{-1}\log_\varepsilon\left(\frac{1+\omega/\alpha}{\omega/\alpha}\right) \quad . \quad . \quad . \quad . \quad (3)$$

and from this the sparking potential V_s ($= Ed_s$) can be evaluated; it is not necessarily the same as that at which a high short-circuit current passes or intense luminosity develops. The condition $(\omega/\alpha)(\varepsilon^{\alpha d} - 1) = 1$ represents the threshold for instability, and this accounts for the close agreement, within the limits of experimental error, between the observed sparking voltages and values obtained from theory, as shown by Llewellyn Jones *et al.*[2, 3] For, since α increases rapidly with E in the region near $(\omega/\alpha)(\varepsilon^{\alpha d} - 1) = 1$, the rate of change of the product $(\omega/\alpha)(\varepsilon^{\alpha d} - 1)$ as a function of voltage gradient is large. Hence, although $(\omega/\alpha)(\varepsilon^{\alpha d} - 1)$ may have to increase well beyond unity before breakdown ensues, the observed change in V_s for breakdown may be indistinguishably small.

If the Townsend criterion is valid for breakdown in electronegative gases, the threshold for a self-maintaining current is obtained when the denominator of eqn. (2) is zero,

i.e. $$(\omega/\alpha)\left(\frac{\alpha+\lambda}{\alpha-\eta}\right)[\varepsilon^{(\alpha-\eta)d} - 1] = 1 \quad . \quad . \quad . \quad (4)$$

Geballe and Reeves[4] have already pointed out that, if $\alpha \geqslant \eta$, for sufficiently large values of d breakdown is possible irrespective of the values of α, η, λ and ω/α; thus, in common with non-attaching gases, breakdown for a particular field strength is dependent upon d. For $\eta > \alpha$, however, eqn. (4) approaches, with increasing values of d, an asymptotic form

$$-(\omega/\alpha)\left(\frac{\alpha+\lambda}{\alpha-\eta}\right) = 1$$

or $$\alpha = \frac{\eta - \lambda(\omega/\alpha)}{1 + (\omega/\alpha)} \quad . \quad . \quad . \quad . \quad . \quad . \quad (5)$$

This is a condition which depends only upon E, and sets a limit for E below which no discharges should be possible whatever the value of d. If ω/α and λ are small compared with unity and η, respectively, the limiting value of E for electronegative gases can be derived from the relationship

$$\alpha = \eta \quad . \quad . \quad . \quad . \quad . \quad . \quad . \quad . \quad (6)$$

Mass-spectrograph studies indicate that the probability of λ is low, and experiments in non-attaching gases suggest that ω/α is in the region of 10^{-4}.

(2) UNIFORM FIELD BREAKDOWN

The existence of a limiting value of E has been observed for a number of gases. For example, the breakdown voltage with gap

Written contributions on papers published without being read at meetings are invited for consideration with a view to publication.
The paper is an official communication from the National Physical Laboratory.

length for air at atmospheric pressure has been expressed by a number of investigators[5,6,7] by the equation

$$V = Ad + Bd^{1/2}$$

or $$E\,(= V/d) = A + B/d^{1/2} \quad . \quad . \quad . \quad . \quad (7)$$

where A and B are constants and d is the gap length. The limiting value of E is given by the constant A.

From ionization and attachment data for air, difluorodichloromethane and sulphur hexafluoride, communicated privately by Geballe, the values of E/p for which $\alpha/p = \eta/p$ [subsequently referred to as $(E/p)_{\alpha=\eta}$] are, respectively, 31·5,* 117 and 127 volts/cm per mm Hg pressure. At atmospheric pressure the corresponding voltage gradients are 23·9,* 89 and 96·2 kV/cm. Experimental confirmation requires breakdown measurements to be made in a very uniform field and for sufficiently large gaps in order to obtain a reliable limiting value of E/p; non-uniformity of field would give too low a value. For air, the experimental data of Bruce,[5] Ritz[6] and Holzer[7] give limiting voltage gradients of 24·22, 24·55 and 23·85 kV/cm. From the data previously published,[1] the limiting voltage gradients for difluorodichloromethane and sulphur hexafluoride are 82 and 87 kV/cm, respectively; these results were obtained with sphere electrodes, which probably accounts for the greater part of the difference between theoretical and experimental values. Devins and Crowe[11] obtained excellent agreement for difluorodichloromethane and sulphur hexafluoride; in each case, with increasing values of pd, E/p approached asymptotically the limiting value predicted from measurements of α/p and η/p.

The measurement of α/p as a function of E/p made by Sandberg and Hochberg, neglecting attachment, for sulphur hexafluoride are in fairly close agreement with the figures of $(\alpha/p - \eta/p)$ determined by Geballe; they also failed to record any ionization coefficient below $E/p \simeq 116$ volts/cm per mm Hg pressure. It is probable that their data for other electronegative gases could be used to determine values of $(E/p)_{\alpha=\eta}$.

The limiting value of E/p is characterized, in eqn. (5), by the condition that η/p is slightly greater than α/p, which means that, in the build-up of the pre-breakdown current, electrons are diminishing and being replaced by negative ions as charge carriers. Although there is still considerable uncertainty about the spark mechanism, it is difficult to imagine breakdown occurring under these conditions. Eqn. (5) provides the condition for self-maintaining current, and therefore, as discussed for non-attaching gases, it is probable that, for the passage of a spark, the following condition must hold:

$$\alpha > \frac{\eta - \lambda(\omega\alpha)}{1 + (\omega/\alpha)}$$

This would be achieved with a very small increase of voltage above the limiting value, since, in the region of $(E/p)_{\alpha=\eta}$, η/p is decreasing, and α/p is increasing, rapidly with field strength.

(3) NON-UNIFORM FIELD BREAKDOWN

For field conditions where the region of high stress is in the vicinity of the positive electrode, Fig. 1 illustrates typical corona onset and breakdown-voltage/gas-pressure characteristics for an electronegative compound. All such compounds have a critical pressure p_c at and above which the corona onset and breakdown voltages coincide; at a lower pressure p_m, the breakdown voltage is a maximum.

With two electrodes of different sizes, well separated, the corona mechanisms which are active centre on the region of intense field. Electron avalanche formation, with the build-up of positive-ion space charge is only possible so long as $\alpha > \eta$, and therefore the condition $(E/p)_{\alpha=\eta}$ should give the limiting value of the field at the more highly stressed electrode for the onset of discharges either incomplete (corona) or complete (breakdown).

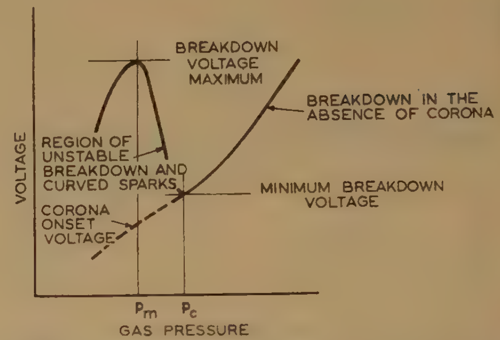

Fig. 1.—Typical breakdown-voltage/gas-pressure characteristics for positive point-to-plane electrodes.

Table 1 gives the values of E/p_c at the highly-stressed electrode, derived from the breakdown-voltage data recorded by a number of workers for electronegative compounds and air, and $(E/p)_{\alpha=\eta}$ derived from ionization and attachment data. The electrode arrangements used were either point-to-plane or point-to-sphere types, and it has been assumed that the field at the point is the same as that given by the formula for the field between a hyperboloidal point and plane, namely

$$E = \frac{2V}{R \log_\varepsilon 4x/R} \quad . \quad . \quad . \quad . \quad . \quad (8)$$

where R = radius of curvature of the point tip.
x = Point-to-plane spacing.
V = Point potential.

Complete ionization and attachment data are only available for sulphur hexafluoride, difluorodichloromethane and air, and so it has been assumed that the values of $(E/p)_{\alpha=\eta}$ for the other compounds are proportional to their relative electric strengths, with nitrogen as the datum. For example, in the case of carbon tetrafluoride[1] the relative electric strength is approximately 1·2, and that for difluorodichloromethane $[(E/p)_{\alpha=\eta} = 127$ volts/cm per mm Hg pressure$]$ is 2·75; the assumed value for carbon tetrafluoride is therefore $127 \times 1{\cdot}2/2{\cdot}75 = 56$ volts/cm per mmHg pressure.

Agreement between the values of E/p_c derived from breakdown-voltage data and $(E/p)_{\alpha=\eta}$ is reasonably good in a number of instances, particularly under irradiated conditions. The low values of E/p_c derived from the data of Pollock and Cooper for irradiated conditions may be due to too intense pre-ionization, since use was made of an X-ray tube; the possibility of lowered spark potentials from this cause is well known. The high values of E/p_c, when there is no irradiation, probably reflect time-lag effects, but the reason for the considerable disagreement in the case of the work of Foord is not clear; he did, however, experience considerable difficulty, not reported by the others, in obtaining reproducible results. The high values reported by Foord[8] could not be attributed to the degree of divergence of the field between the electrodes, since the ratio of the field at the point to the average field was 9·5 compared with values between 3·4 and 9·2 for the authors' arrangements, 6·2 and 13·2 for those of Pollock and Cooper[9] and Works and Dakin.[10]

Fig. 2 gives, for sulphur hexafluoride, difluorodichloromethane and carbon tetrafluoride, the positive static breakdown voltage—

* Recent measurements by the author give $(E/p)_{\alpha=\eta} = 31{\cdot}9$ volts/cm per mm Hg and $E = 24{\cdot}2$ kV/cm for air.

Table 1

$(E/p)_{\alpha=\eta}$ DERIVED FROM IONIZATION AND ATTACHMENT DATA COMPARED WITH E/p_c AT THE POSITIVE-POINT TIP CALCULATED FROM BREAKDOWN-VOLTAGE DATA

Compound	$(E/p)_{\alpha=\eta}$ derived from ionization and attachment data	Values of E/p_c from breakdown-voltage measurements							
		From Reference 1		From Reference 8		From Reference 9		From Reference 10	
		Irradiated gap	No irradiation	Irradiated gap	No irradiation	Irradiated gap	No irradiation	Irradiated gap	No irradiation
	V/cm per mm Hg	V/cm per mm Hg	V/cm per mm Hg		V/cm per mm Hg	V/cm per mm Hg	V/cm per mm Hg		V/cm per mm Hg
Sulphur hexafluoride, SF_6	117	114	129		171	81	141		128
Difluorodichloromethane, CF_2Cl_2	127	126	126		261	101	140		
Trifluorochloromethane, CF_3Cl	71	84	96						
Carbon tetrafluoride, CF_4	56	57	79						
Air	32				53		36		

Reference 1 applies to point-to-sphere gaps of 5–20 mm with a hemispherically ended point 1·98 mm in diameter and a 5 cm-diameter sphere.
Reference 8 applies to a point-to-plane gap of 10 mm with a hemispherically ended point 0·47 mm in diameter.
Reference 9 applies to a point-to-plane gap of 3 mm with a hemispherically ended point 0·5 mm in diameter.
Reference 10 applies to a point-to-plane gap of 25·4 mm with a hemispherically ended point 1·59 mm in diameter.

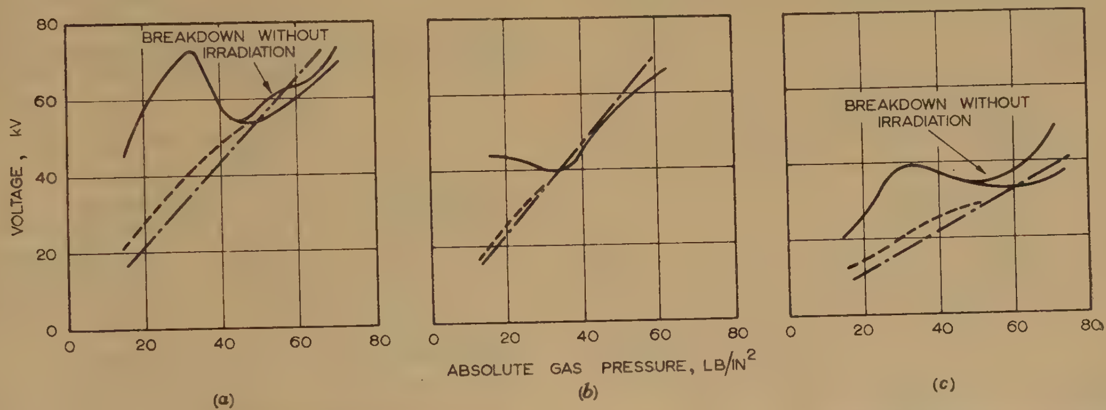

Fig. 2.—Comparison between theoretical and experimental corona-onset and breakdown-voltage/gas-pressure characteristics.

For a 10 mm gap between a hemispherically ended point and a 5 cm-diameter sphere.
——————— Breakdown voltage.
- - - - - - - Corona onset voltage.
— - — - — Point potential corresponding to $(E/p)_{\alpha=\eta}$.

(a) Sulphur hexafluoride.
(b) Difluorodichloromethane.
(c) Carbon tetrafluoride.

i.e. gradually increased—and corona onset voltage as a function of gas pressure, and the variation of the point potential with gas pressure corresponding to a field at the point of $(E/p)_{\alpha=\eta}$. Agreement between the theoretical and experimental characteristics is reasonably good; the breakdown-voltage characteristic at pressures below the critical value cannot be subjected to quantitative analysis and is subsequently discussed on a qualitative basis. The measured corona onset voltage in any electrode arrangement is a function of the sensitivity of the recording technique, and this is probably reflected in the fact that the experimental corona onset voltages are slightly higher than the theoretical values.

Breakdown-voltage measurements with point-to-sphere electrodes have shown[1] that at pressures above the critical value considerable increase in the gap at constant pressure often fails to give any appreciable increase in breakdown voltage. This is readily explained if breakdown occurs when the field at the point is $(E/p)_{\alpha=\eta}$. The field at the point is given by eqn. (8), and if this is constant and equal to $(E/p)_{\alpha=\eta}$, the point potential is a function of $\log_\varepsilon x$. Calculations based upon practical electrode arrangements show that, if V is the breakdown voltage for a 10 mm gap at a gas pressure p (above p_c), the breakdown voltages for 15, 20 and 25 mm gaps at the same pressure would be 1·11, 1·19 and 1·26 volts, respectively.

Although the foregoing analysis permits the prediction of the corona-onset-voltage/gas-pressure curve and the breakdown voltage above the critical pressure for the positive point, several features in this type of field, which have been previously reported,[1] require explanation. They include the following:

(a) The fact that the impulse breakdown voltage is lower than the static value at pressures below the critical value, and the necessity for the applied field at the point to be greater than $(E/p)_{\alpha=\eta}$ for breakdown in this region.

(b) The negative slope in the breakdown-voltage/pressure curve and curved breakdown paths in the range p_m–p_c, and the occurrence of a critical pressure where the corona-onset and breakdown voltages coincide.

(3.1) Breakdown Voltages at Pressures below the Critical Value

The significance of the experimental fact that generally with electronegative gases the positive static breakdown voltage, is higher than the impulse value suggests that field modification involving time is an important factor in determining the breakdown voltage. As soon as the field in the vicinity of the point exceeds $(E/p)_{\alpha=\eta}$ electron avalanches are formed, and because of their high mobility the electrons generated are swept immediately into the point. The positive and negative ions do not move any significant amount. However, if the applied field is maintained for a comparatively long time, separation of the positive and negative ions occurs and ultimately all the negative ions move into the point. Thus, with impulses only, electrons contribute to the lowering of the field at the point, whilst with static breakdown, there is an additional contribution by negative ions. From this it follows that, if time-lag effects could be eliminated, breakdown with very-steep-fronted impulses would occur with the applied field equal to $(E/p)_{\alpha=\eta}$.

The difference between the static and impulse breakdown voltages for a compound, on the basis of a simplified treatment, should be a function of $\alpha/(\alpha - \eta)$; the difference being greater for large values of $\alpha/(\alpha - \eta)$. With static breakdown the lowering of the field at the point is a function of α and with impulses a function of $(\alpha - \eta)$. Fig. 3 gives plots of $\alpha(\alpha - \eta)$

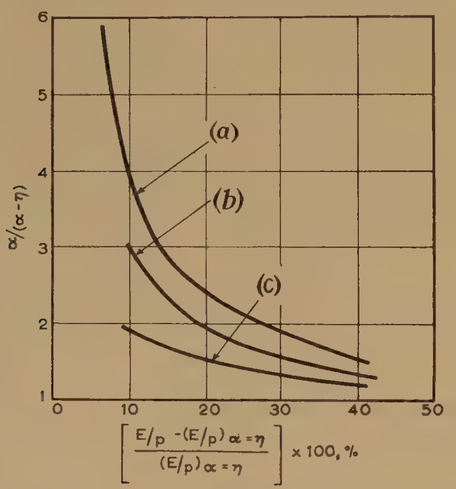

Fig. 3.—Curves of $\alpha/(\alpha - \eta)$ plotted against percentage E/p above $(E/p)_{\alpha=\eta}$.
(a) Sulphur hexafluoride.
(b) Difluorodichloromethane.
(c) Air.

for sulphur hexafluoride, difluorodichloromethane and air against the percentage of (E/p) above $(E/p)_{\alpha=\eta}$. Experimental data indicate that the difference between the static and impulse voltages is greater for sulphur hexafluoride than for difluorodichloromethane. For air, the impulse breakdown voltage exceeds the static value, but as the difference is small, this may be a manifestation of time-lag effects.

(3.2) Negative Slope, Critical Pressure and Curved Breakdown Paths

For the negative slope to occur in the breakdown-voltage curve, there must be a secondary mechanism dependent only upon pressure. The two possibilities are diffusion and photon absorption. Since curved breakdown paths have been observed with impulse voltages of duration too short for appreciable diffusion to take place, the more likely possibility is an increase of photo-absorption with increasing pressure.

The higher field in the mid-gap region arising from the net positive space charge near the point (Section 3.1) would enhance electron avalanche activity in the gap and near the cathode if photo-absorption became significant in the region of p_m. The movement of electrons and negative ions formed in these avalanches into the volume of the gap near the point would tend to cancel the space-charge field and bring about a fall in breakdown voltage; in the limit, with the space-charge field completely neutralized at p_c, breakdown would occur in the absence of corona. The curved breakdown paths probably arise from the random initiation in the gap volume of electron avalanches by photon absorption; the space charge which they each create could lead to localized intensification of field producing non-axial breakdown paths. Since breakdown at the critical pressure occurs in the absence of space charge, the breakdown paths in this region would be axial.

(4) ACKNOWLEDGMENTS

The work described has been carried out as part of the research programme of the National Physical Laboratory, and the paper is published by permission of the Director of the Laboratory.

(5) REFERENCES

(1) Howard, P. R.: 'Insulation Properties of Compressed Electro-negative Gases', see page 123.

(2) Llewellyn Jones, F., and Parker, A. B.: 'Electrical Breakdown of Gases—I. Spark Mechanism in Air', *Proceedings of the Royal Society* A, 1952, **213**, p. 185.

(3) Dutton, J., Haydon, S. C., and Llewellyn Jones, F.: 'Electrical Breakdown of Gases—II. Spark Mechanism in Nitrogen', *ibid.*, 1952, **213**, p. 203.

(4) Geballe, R., and Reeves, M. L.: 'A Condition on Uniform Field Breakdown in Electron-Attaching Gases', *Physical Review*, 1953, **92**, p. 867.

(5) Bruce, F. M.: 'Calibration of Uniform-Field Spark-Gaps for High-Voltage Measurements at Power Frequencies', *Journal I.E.E.*, 1947, **94**, Part II, p. 138.

(6) Ritz, H.: 'Breakdown Field Strengths for Homogeneous Fields in Air', *Archiv für Elektrotechnik*, 1953, **26**, p. 219.

(7) Holzer, W.: 'Impulse Breakdown of Air', *ibid.*, 1932, **26**, p. 865.

(8) Foord, T. H.: 'Some Experiments on Positive Point-to-Plane Corona and Spark Breakdown of Compressed Gases', *Proceedings I.E.E.*, Paper No. 1568 M, December, 1953 (**100**, Part II, p. 585).

(9) Pollock, H. C., and Cooper, F. S.: 'The Effect of Pressure on Positive Point-to-Plane Discharges in N_2, O_2, SO_2, SF_6, CCl_2F_2, A, He, and H_2', *Physical Review*, 1939, **56**, p. 170.

(10) Works, C. N., and Dakin, T. W.: 'Dielectric Breakdown of Sulphur Hexafluoride in Non-Uniform Fields', *Transactions of the American I.E.E.*, 1952, **71**, Part I, p. 682.

(11) Devins, J. C., and Crowe, R. W.: 'The Electric Strength of Polyatomic Gases', *ibid.*, Paper No. 56–326.

621.315.09 : 621.016.35

Paper No. 2035 S
May 1956

THE AUTOMATIC SOLUTION OF POWER-SYSTEM SWING-CURVE EQUATIONS

By COLIN ADAMSON, M.Sc.(Eng.), Associate Member, L. BARNES, M.Sc.Tech., Graduate, and B. D. NELLIST, M.Sc.Tech., Graduate.

(*The paper was first received* 17*th November*, 1955, *and in revised form*, 5*th January*, 1956. *It was published in May*, 1956, *and was read before the* SUPPLY SECTION 18*th November*, 1956.)

SUMMARY

The paper details the problem of transient stability in electrical power systems and divides the methods used to date into four categories. These categories, with the relevant literature, are briefly reviewed.

The paper then describes the theory, method of construction and mode of operation of an automatic step-by-step computer for power-system swing curves; the machine has facilities for two generators only but may be extended in scope by the addition of equipment similar to that already employed. The limitations of this machine are discussed and a direct-analogue method for use with the generator units of a network analyser is then described.

The procedure for calibration of the direct analogue is given, and difficulties in the setting up of the analogues of damping power and inertia constant are mentioned. Comparison of the results of a simple swing-curve problem by integraph, step-by-step and analogue appears at the end of the paper.

Automatic generator-unit operation on a network analyser is possible with this type of direct-analogue equipment.

LIST OF PRINCIPAL SYMBOLS

A = Gain of motor field amplifier, mA/volt.
G_r = Gear ratio between velodyne and phase-shifter.
I = Output current of network analyser generator unit.
K_T = Tachometer constant, volts/deg/sec.
M_n = Inertia constant for the nth machine.
M = Inertia constant for the special case of a machine operating against an infinite busbar.
$(N-1)$, N, $(N+1)$, etc. = Subscripts denoted the steps of a calculation.
p = Feedback control setting, operating on feed-back voltage v_p.
P_a = Net rotor accelerating power for a machine connected to an infinite busbar.
P_d = Damping coefficients for the special case of a machine operating against an infinite busbar.
P_{dn1}, P_{dn2}, etc. = Coefficients for the damping power between machines n and 1, n and 2, etc.
P_{en} = Electrical power output coefficient of the nth machine.
P_{mn} = Mechanical power input for the nth machine.
V = Output voltage of network analyser generator unit.
V_1 = Machine internal voltage.
V_2 = Voltage at infinite busbar.
v_p = Velodyne generator voltage ⎫
v_r = Reference voltage ⎬ measured at the field amplifier input terminals.
v_w = Wattmeter output voltage ⎭
X = Total reactance up to infinite busbar.
δ = Angular displacement of V_1 with respect to V_2, and also the angular displacement of the phase-shifter shaft of the analogue corresponding to synchronous-machine shaft displacement.
δ_n = Rotor angle in electrical radians, of the nth machine, with respect to a common reference axis.
θ = Velodyne shaft displacement, deg.

(1) INTRODUCTION

The fundamental theory underlying power-system stability is well known, as also are the means most commonly adopted for ensuring the maintenance of stability. Systematic work on this type of problem dates from about 1924 and was at first mainly American.[1] Historically, studies of system stability commenced with the analytical determination of the power limits of two synchronous machines connected together through an impedance, and this is still the model used to-day for illustrating the general principles. It has been shown, for example, by Crary,[2] that the two-machine system may be represented by a single machine connected to an infinite busbar of inertia constant $M_1M_2/(M_1 + M_2)$. The equation of power balance for such a system is the basis for all methods of assessment of transient stability.

Early studies were mainly concerned with the determination of system layouts which were satisfactory from the standpoint of maximum steady-state power transfer, and only later was it realized that satisfactory operating characteristics under conditions of sudden disturbances were of greater importance. In order of increasing severity the major disturbances are as follows:

(*a*) Sudden large load increases.
(*b*) Switching operations.
(*c*) Faults with subsequent isolation of the faulty section and with, or without, subsequent operation of auto-reclosing circuit-breakers.

Several different types of stability have been considered from time to time, but of these it is *steady-state* and *transient* stability which are the generally accepted and major classifications. Steady-state stability is concerned with the operation of a power system under all normal conditions, this being taken to include the effects of governors, automatic voltage regulators, load fluctuations, etc. Transient stability is said to exist in a power system if, after an aperiodic disturbance, the individual parts of the system remain in synchronism. The well-known 'equal-area criterion' may be applied directly to a study of the transient stability of an equivalent two-machine system, but this suffers from the defect that the duration of disturbance is expressed in terms of changes of rotor angular displacement; this approach is impracticable, and it is necessary to determine the curves of generator load-angle against time. These latter are the so-called *swing curves.*

Transient stability only is considered here. Possible methods of solving the power-balance equations for the synchronous generators of a system are briefly reviewed, and two methods arising out of recent experimental work are described. One of these is an automatic equipment for performing step-by-step calculations when associated with the phase-angle control of an a.c. impedance-type network analyser; the other is an analogue method using essentially an electromechanical phase-modulator.

The first method uses a step-by-step process for solving the power-balance equation of the synchronous machine(s) and is

The authors are in the Power Systems Laboratory, Department of Electrical Engineering, Faculty of Technology, University of Manchester.

fully automatic in its operation. Although it is satisfactory in operation, its use has now been discontinued in favour of the direct-analogue method, but it is thought to be of sufficient interest and educational value to merit inclusion. The analogue method, which is essentially a device for the solution of the second-order non-linear differential equation governing the power balance of a synchronous machine, has applications other than to the solution of stability problems; it may be applied, for example, to problems of hunting or to making the processes of network-analyser operation more automatic. The simulation of other phenomena associated with synchronous machines, such as governor and automatic-voltage-regulator operation, may subsequently be associated with this device.

(2) A REVIEW OF THE PROBLEM AND METHODS OF SOLUTION

The general formulation of the swing-curve equations, after Dahl,[3] is as follows:

$$M_n \frac{d^2\delta_n}{dt^2} + P_{dn1}\frac{d(\delta_n - \delta_1)}{dt} + P_{dn2}\frac{d(\delta_n - \delta_2)}{dt} + \ldots + \ldots P_{en} f[(\delta_n - \delta_1), (\delta_n - \delta_2), \ldots] = P_{mn} \quad . \quad (1)$$

For the purpose of discussion of the various methods available for the solution of this problem, eqns. (1) may be simplified, and consideration given to the case of a single synchronous machine connected through a reactance to an infinite busbar. On making the usual assumptions that the machine and busbar voltages are constant in magnitude, and that the angular velocity of the voltage vector at the infinite busbar is unchanged throughout any disturbance, the power-balance equation for the generator may be written

$$M\frac{d^2\delta}{dt^2} + P_d\frac{d\delta}{dt} + \frac{V_1V_2}{X}\sin\delta = P_m \quad . \quad . \quad . \quad (2)$$

The equation has no explicit solution for δ but forms the basis of several methods of treating the transient stability problem, which, in effect, consist of performing a double integration of the power difference:

$$P_a = (P_m - \frac{V_1V_2}{X}\sin\delta) \quad . \quad . \quad . \quad . \quad (3)$$

$$= P_m - P_e \quad . \quad . \quad . \quad . \quad . \quad . \quad . \quad (3a)$$

in order to determine δ as a function of time.

Solution by this technique involves the assumption of constant inertia constant $M = H/180f$, where H is expressed in kilowatt-seconds per kilovolt-ampere rating. It is possible to allow for the change in M with instantaneous frequency of the rotor, although this effect is slight.

The methods available for solution may be classified into four main groups: (*a*) step-by-step methods, (*b*) digital-computer methods, (*c*) differential-analyser methods, (*d*) direct-analogue methods.

(2.1) Step-by-Step Methods

Step-by-step methods employ double numerical integration. The period of swing is divided into a number of discrete time-intervals of length Δt, whose value is of considerable significance to the accuracy of the result; in general, a time interval of 50 millisec may be expected to give an accuracy of 5%. Standard texts[2,3] give the procedure, making the following assumptions:

Machine Assumptions.

(i) The input power to each generator remains constant.
(ii) Damping power is negligible.
(iii) Each machine may be represented by a constant reactance in series with an e.m.f. of fixed magnitude and variable phase.

Convenient Analytical Assumptions.

(iv) The acceleration of the rotor is constant from the middle of one interval to the middle of the next.
(v) The rotor velocity is constant during each interval.

Assumptions (iv) and (v) involve the approximation that both the acceleration and the velocity diagrams are represented by stepped curves.

The simplified machine equation from eqns. (2), (3) and (3*a*) is

$$\frac{d^2\delta}{dt^2} = \frac{P_a}{M} \quad . \quad . \quad . \quad . \quad . \quad . \quad . \quad . \quad (4)$$

The angular position at the end of the Nth interval may be shown to be

$$\delta_N = \delta_{(N-1)} + \Delta\delta_N \quad . \quad . \quad . \quad . \quad . \quad (5)$$

where

$$\Delta\delta_N = \Delta\delta_{(N-1)} + \frac{P_a(\Delta t)^2}{M} \quad . \quad . \quad . \quad . \quad (6)$$

By means of eqns. (5) and (6), the swing curve of each of the machines in the system may be plotted, the accuracy of the method depending upon the number of points taken.

It will be seen that great accuracy is not obtainable if only on account of the sweeping assumptions which are made. However, the error is biased to the estimation of a conservative stability limit.

The above analysis has to be modified during the intervals in which the onset and clearance of a fault occur. If a discontinuity occurs at the beginning of an interval, the average value of P_a for the adjoining intervals may be used. If the discontinuity occurs in the middle of an interval, no modification is needed; and if it occurs at any other point in the interval, a weighted average P_a in both that and either the succeeding or preceding interval is used.

Similar methods of analysis, but with different assumptions, may be used,[3] but the routine given is the most convenient one for automatic working.

Stability problems may be solved with the aid of an a.c. network analyser using eqns. (4), (5) and (6). However, without additional computing aids the work is tedious. Mortlock[4] has described a semi-automatic computer which uses potentiometers for carrying out the double integration; a network analyser gives the appropriate values of power and the generator-unit phase-shifters are set by hand. A development of this apparatus has been described by Jones;[5] another form of semi-automatic computer for the same purpose has been described by Peterson.[6] It has been reported by Squires and Harder[7] that an automatic step-by-step calculator has been added to the Westinghouse network analyser.

(2.2) Digital-Computer Methods

Bennett, Dakin and Knight[8] have described the use of the high-speed digital computer at the University of Manchester for the solution of stability problems. Visual display of swing curves may be obtained with this method, whose utility for power-system engineers is equalled only by a continuous-recording direct-analogue computer. A disadvantage arises in the computing time which is necessary for the machine to obtain the equivalent network of the system. The existing machine at Manchester will derive the necessary matrix coefficients, i.e. the driving point and transfer admittances, for 50 independent node pairs and 10 synchronous sources in approximately half an hour. For example, if these figures are doubled, then for the same number of generators the time taken would be of the order of 7 hours. This method of solution of the swing-curve equations has been described by Gill.[10] Further information on the application of

digital analysis to power-system problems has been given by Bills.[9]

The disadvantage mentioned above has been overcome by using a network analyser for the derivation of the necessary driving-point and transfer admittances, and has been mentioned by Rothe,[11] and Squires and Harder;[7] it is of course, self-evident that the network analyser must be sufficiently large for the purpose. It should be noted that the situation may alter in the near future when digital machines approximately ten times faster in operation than that at present installed in Manchester become available.

(2.3) Methods Involving the Use of Differential Analysers

The physical size of differential analysers limits their application to the problem; however, several attempts have been made to apply a combination of differential-analyser techniques, using either mechanical or electronic integrators and an a.c. network analyser. Although the earliest suggestions were made by Kimbark,[14] the first such application was due to Boast and Rector.[12] The use of a network analyser with a normal instrument system read by a human operator, who inserted information into a differential analyser used as an auxiliary computing device, has been described by Bekey and Schott.[15]

Van Ness[22] has described a method involving the use of double integration, in which the first integrator is electronic and the second, which drives the network-analyser phase-angle control, is electro-mechanical. There is no allowance for damping, and the inertia constant is inserted at the input of the first integrator. A modification of the method allows for the representation of saliency.

(2.4) Direct-Analogue Methods

The servo and electronic techniques, dating from the later years of the Second World War, made possible the use of direct-analogue methods associated with a.c. network analysers. Electronic phase-modulating systems have been described by Kaneff[17] and Shen and Packer.[18] Electro-mechanical methods have been proposed by Kusko,[13] Watkins,[16] Bauer,[20] Mortlock,[21] and very recently by Kaneff.[23]

All these methods, together with the one independently developed by the authors, determine automatically the net accelerating power, P_a, of the system, and use it in a servo system to control the angular position of the generator-unit phase-shifters and thereby determine the swing curves.

(3) AN AUTOMATIC STEP-BY-STEP COMPUTER FOR STABILITY STUDIES

(3.1) Essential Elements of the Computer

The components of a machine to solve eqns. (4), (5) and (6) are indicated in the block diagram of Fig. 1 and are four in number, namely

(*a*) A wattmeter to measure the quantity P_a.

(*b*) Two step-by-step integrators for the evaluation of the integral of P_a [eqn. (3)].

(*c*) A store into which is inserted initially the value of P_m, the electrical equivalent of the prime-mover input power.

(*d*) A mechanism for the sequential control of the operations of the machine.

For multi-machine problems items (*a*) and (*d*) may be centralized with consequent saving of equipment, but items (*b*) and (*c*) must be provided for each generator unit. If the wattmeter is centralized, it must be shared sequentially among the generators during each step of the calculation with consequent sacrifice of speed of operation. From Fig. 1 it will be seen that each generator has access to the wattmeter in turn through the banks of a uniselector. The integrators take the form of two storage locations between which information can be exchanged, with the facility of adding in a third quantity in one direction only.

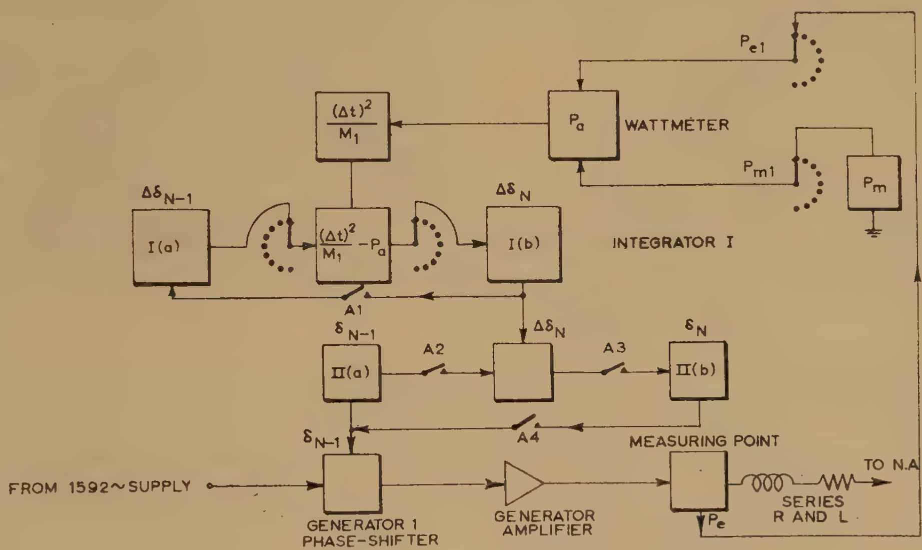

Fig. 1.—Schematic of computer.

Considering the Nth step of the calculation, with the uniselector wipers resting on the first bank contact corresponding to generator 1, the operation is as follows:

(i) The generator measuring points are connected to the wattmeter through one set of wipers and the P_m store through another. The wattmeter measures $P_m - P_e = P_a$.

(ii) The quantity P_a multiplied by the constant $(\Delta t)^2/M$ is inserted into integrator I, and added to $\Delta\delta_{(N-1)}$ to form $\Delta\delta_N$ in store I(*b*).

This solves eqn. (6) for this step.

(iii) $\Delta\delta_N$ is carried also into integrator II, where it is added to the quantity $\delta_{(N-1)}$ to form δ_N in store II(*b*). This solves eqn. (5) for this step.

(iv) The uniselector steps to the next contact and the above three steps are repeated for generator 2, *et seq.*

(v) When steps (i), (ii) and (iii) have been carried out for all the generators, and the quantities $\Delta\delta_N$ and δ_N stored in each I(b) and each II(b) respectively, step N is complete and relay A is operated. This has the effect of transferring the contents of each store I(b) and II(b) into the associated I(a) and II(a) stores, setting the integrators for the next step, and also setting the phase angles δ_N on to the phase shafts of the generators.

(vi) The uniselector is now reset to generator 1 and the above five steps are repeated with all the suffixes increased by one, i.e. the $(N + 1)$ step is now carried out.

To avoid the complex operation of taking average values for P_a for intervals which contain discontinuities, Δt is so arranged as to make all discontinuities fall in the middle of a period. The faults are applied and cleared by the machine through the banks of a second uniselector which counts the number of steps in the calculation and operates relays for this purpose at the appropriate times.

(3.2) Physical Arrangement of the Computer

(3.2.1) The Wattmeter.

The wattmeter was developed from an original idea by Bradshaw and Watkins; the first model was built by Watkins[23] during early work on a step-by-step computer at the Manchester College of Technology, but not using a velodyne as described below (Fig. 2).

The wattmeter is servo-driven and is built round a single-dynamometer movement. The instrument is deflected by amplified voltage and current signals V_v and V_i, derived from a network analyser, but is restored to a null position by a torque produced in its coils at a second frequency which differs by about 50 c/s from

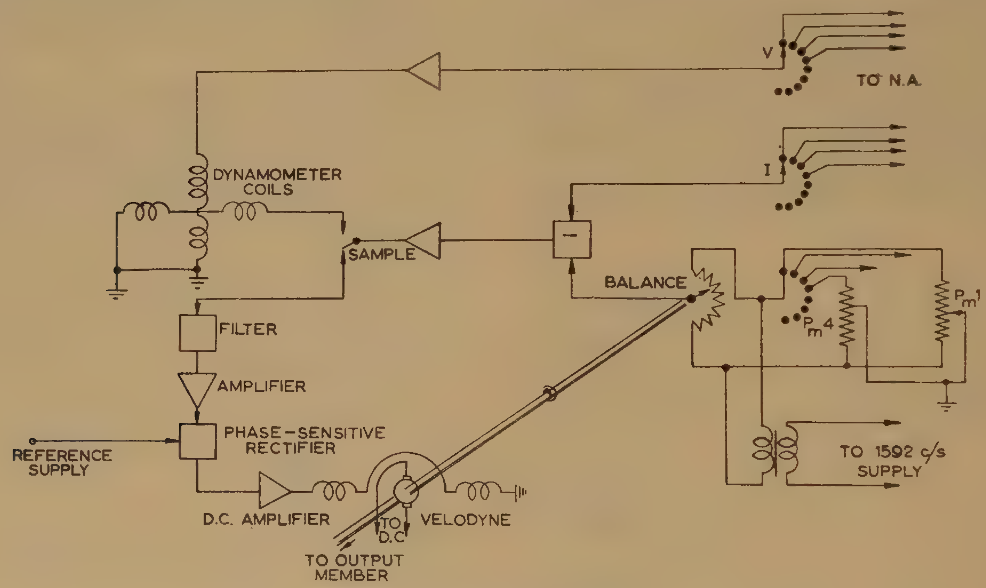

Fig. 2.—Schematic of wattmeter.

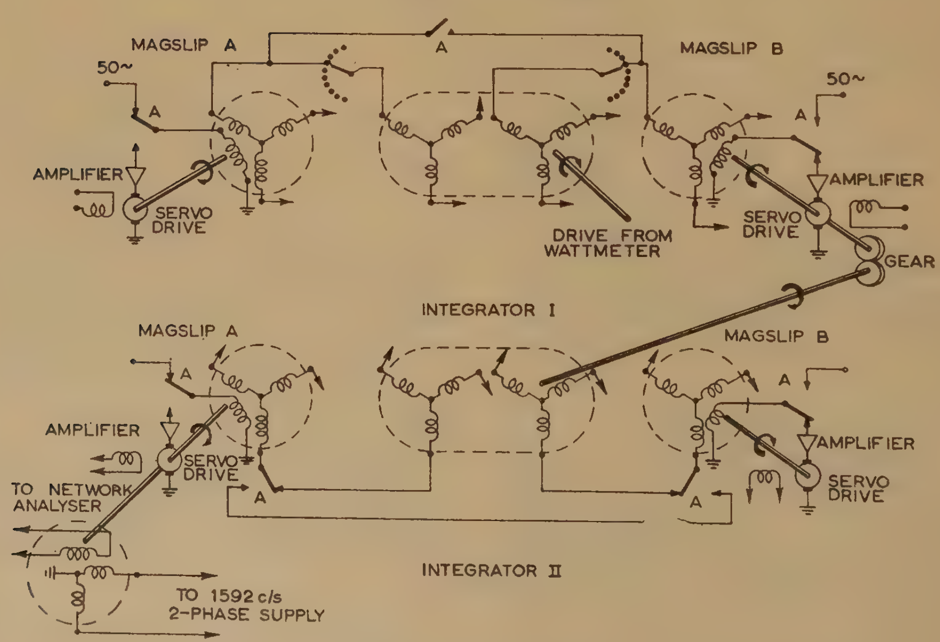

Fig. 3.—Integrator units.

the network-analyser frequency, which is 1 592 c/s. The null position is then taken to be the position of zero mutual inductance between fixed and moving coils. The angular deflection of the instrument can be measured at any instant by the magnitude and phase of the induced e.m.f., v_m, in the moving coil. The moving coil is periodically, i.e. 50 times a second, disconnected from its driving amplifier and connected instead to the input terminals of a servo system; v_m is first amplified, then detected by a phase-sensitive rectifier, and the resulting signal used to drive a velodyne. The velodyne shaft carries a potentiometer (called the 'balancing potentiometer') which controls the magnitude and direction of the second frequency-restoring torque. The servo system will thus set the wattmeter to the null position, where v_m is zero, when the power measured is proportional to the angular deflection of the balancing potentiometer.

(3.2.2) **The P_m Stores.**

The quantity P_m is subtracted from P_e by shifting the zero point of the balancing potentiometer. This is effected by putting a potentiometer in parallel with the balancing potentiometer and connecting its slider to earth. The P_m potentiometer for each appropriate generator is selected through one of the banks of the wattmeter uniselector.

(3.2.3) **The Integrators.**

The integrators use conventional magslip adding circuits (Fig. 3), but in this application information is transmitted in both directions so that magslip (*A*) and (*B*) each require to be servo-driven in turn; the direction of transmission of information is determined by relay A. Insertion of the quantity $(\Delta t)^2 P_a/M$ into integrator I is effected by switching the follow-through transmitter associated with the wattmeter into the circuit by means of six banks on the wattmeter uniselector U. $\Delta\delta_N$ is carried into integrator II by connecting its follow-through transmitter mechanically to magslip I(*B*).

The flow of information in a typical adding circuit for the first three steps of a calculation is shown in Fig. 4.

(3.2.4) **The Controller.**

The controller is responsible for the sequence of operations during the solution of the problem. It consists of several relays and two uniselectors. One uniselector connects the wattmeter sequentially to the generators whilst the other counts the number of steps in the problem. This latter is responsible for applying faults and stopping the machine, etc., on the requisite step.

(3.3) Accuracy

The accuracy of the machine is limited to that of the network analyser, the integrators and the wattmeter. It is possible to make the last two accurate to better than 1%, but the network analyser will probably be no better than to 2·5%. The accuracy of wattmeter and integrators will be worst for small angles, and so provision is made for multiplying the quantities handled by the wattmeter and integrator I by 1, 5 or 10, the angle being reduced to its correct size by a gear connecting integrators I and II (Fig. 3).

(3.4) Setting up the Apparatus

The constant $(\Delta t)^2/M_{mn}$ and the magnification factor of 1, 5 or 10 mentioned above are inserted at each generator measuring-point on the network analyser by adjustment of a potential divider. P_m is inserted initially by backing off the steady-state power on the P_m potentiometer; this is done manually by stepping the uniselector round the various generators with only the wattmeter energized.

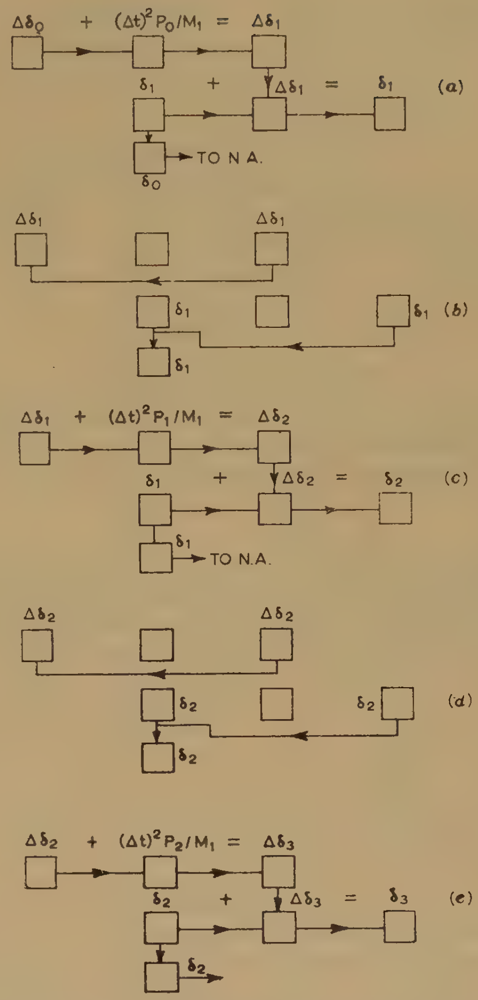

Fig. 4.—Flow of information for the first three steps of a calculation.

(*a*) Step 0.
(*b*) Transfer at end of step 0.
(*c*) Step 1.
(*d*) Transfer at end of step 1.
(*e*) Step 2.

(4) AN ANALOGUE METHOD FOR THE AUTOMATIC PHASE-ANGLE CONTROL OF NETWORK-ANALYSER GENERATOR UNITS

(4.1) Principle of the Analogue

Eqn. (2) may be written

$$M\frac{d^2\delta}{dt^2} + P_d\frac{d\delta}{dt} + (P_e - P_m) = 0 \quad . \quad . \quad . \quad (7)$$

This equation is similar in form to that of a second-order servo system with derivative feedback. The analogue described employs an electronic wattmeter and a velodyne[25] in a d.c. servo system driving a generator-unit phase-shifter. The arrangement of components is shown in the block diagram of Fig. 5. It will be seen that the wattmeter supplies a signal proportional to power output P_e and, after subtraction from a reference voltage proportional to P_m, the signal controls the velodyne motor; negative derivative feedback, proportional to P_d, the damping power, is applied from the velodyne generator. The loop is completed by coupling the velodyne mechanically to the phase-shifter. Under transient conditions, the system obeys an equation of the

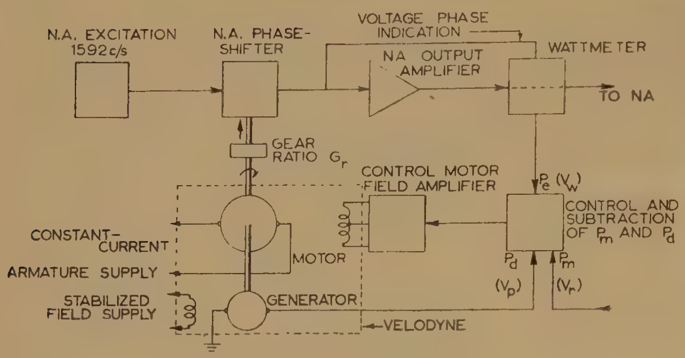

Fig. 5.—Schematic of simulator.

same form as the machine power relation, with the coefficients pre-set by adjustment of the controls.

Referring to Fig. 7, the motor field current is

$$I_f = A(v_r - v_w - pK_T\frac{d\theta}{dt}) \quad . \quad . \quad . \quad . \quad (8)$$

Since the inertia of the moving parts is constant, a parameter α may be introduced defining the acceleration (deg/sec^2) for a step in the field current of 1 mA. For the machines used in the apparatus α has a value of 8. Hence the equation of the loop is

$$\frac{d^2\theta}{dt^2} = A(v_w - v_r - pK_T\frac{d\theta}{dt}) \quad . \quad . \quad . \quad . \quad (9)$$

This may be written as

$$\frac{G_r}{\alpha A}\frac{d^2\delta}{dt^2} + pG_rK_T\frac{d\delta}{dt} + (v_w - v_r) = 0 \quad . \quad . \quad (10)$$

It is seen that the analogue of power is simulator voltage.

(4.2) Time Scaling

It is not necessary for the time of duration of the swing curve on the actual power system to be reproduced on the simulator. If only on account of the inertia of the drive to the phase-angle control of the network-analyser generator unit, it is convenient to scale time and decrease the swing-curve frequency. If the system equation is expressed in the form of eqn. (7), a scaling factor s may be introduced such that $t' = st$, where t' is the scaled time of the simulator. The simulator equation may be written

$$M'\frac{d^2\delta}{d(st)^2} + P'_d\frac{d\delta}{d(st)} + P_e = P_m \quad . \quad . \quad . \quad (11)$$

i.e.
$$\frac{M'}{s^2}\frac{d^2\delta}{dt^2} + \frac{P'_d}{s}\frac{d\delta}{dt} + P_e = P_m \, . \quad . \quad . \quad . \quad (12)$$

Thus, if the analogue inertia constant M' is made equal to s^2M, and the analogue damping constant P'_d is made equal to sP_d, the division of the simulator time-scale by s converts the curve derived from the simulator to that of the system equation.

If k_w is the wattmeter output voltage per unit power input, then eqn. (10) may conveniently be written with per-unit coefficients; this permits direct comparison with the coefficients of the machine eqn. (7), in order to satisfy the conditions above. If δ in eqn. (7) is expressed in electrical degrees, and the coefficients are in per-unit values, comparison of eqns. (7), (10) and (12) yield the following relationships:

$$\frac{G_r}{k_w\alpha A} = M = M'/s^2 \quad . \quad . \quad . \quad . \quad . \quad (13)$$

$$\frac{pG_rK_T}{k_w} = P_d = P'_d/s \quad . \quad . \quad . \quad . \quad . \quad (14)$$

in which all quantities except A and p are constants.

(4.3) Analogue Equipment

(4.3.1) The Measurement of P_e.

The requirements for the power-measuring device are that the response should be fast and that negligible burden should be imposed on the network analyser. The wattmeter measures power corresponding to the internal power of a synchronous machine which, for transient studies, is the power behind the transient reactance. Since the voltage at this point is usually assumed constant throughout the study, a phase-sensitive rectifier circuit may be employed: the arrangement is indicated in Fig. 6(*a*).

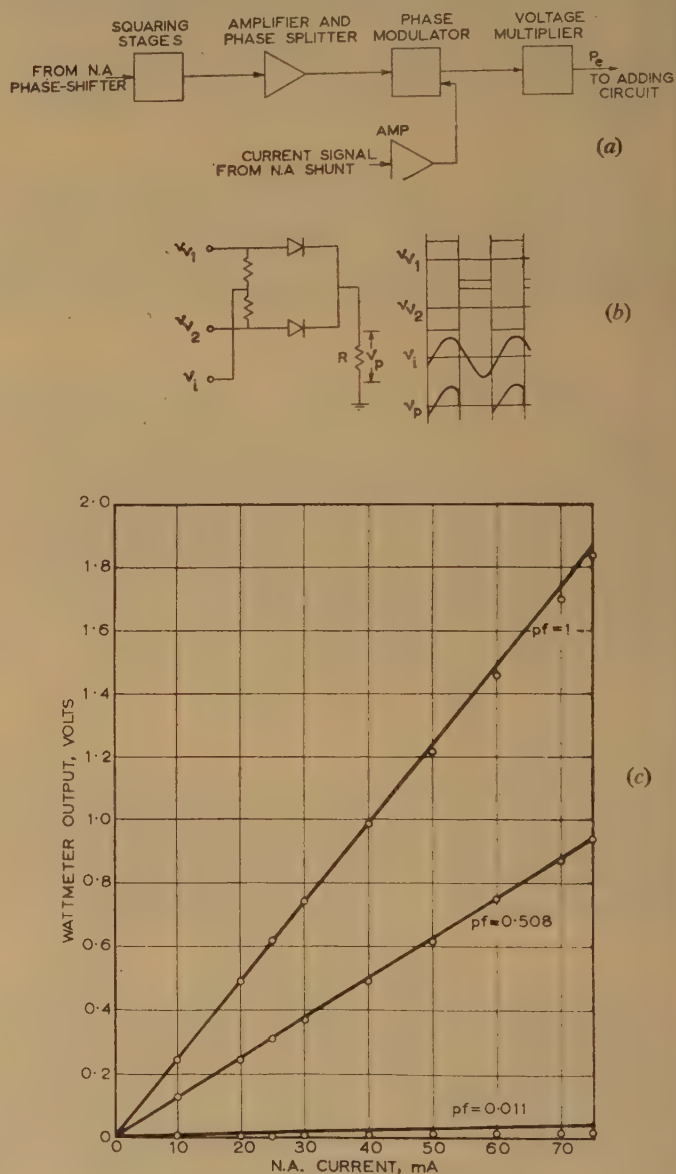

Fig. 6.—(*a*) Schematic of wattmeter.
(*b*) Operation of phase modulator.
(*c*) Wattmeter performance.

The straight lines indicate the expected performance calculated from the experimental point (25 mA, 0·620 volt). Other experimental points are encircled.

In Fig. 6(*b*) the square waves v_{v1} and v_{v2} are in phase and anti-phase, respectively, with the analyser voltage at the metering point. The passage of current due to the signal v_i, which is proportional to, and in phase with, the generator current, is governed by the sign of the voltage across the rectifiers, i.e. by the polarities of the square waves. While v_{v1} is positive and v_{v2} negative, current

due to v_i flows and develops a voltage v_p in the load R. The d.c. output, being the average value of v_p, is a function of the magnitude of v_1 and the phase difference between v_i and v_{v1}, i.e. the power-factor angle.

Let $v_i = V\sin\theta$ and let ϕ be the power-factor angle. Then, if the square waves v_v have sensibly vertical sides and high amplitude compared with v_i, the d.c. output of the wattmeter is given by

$$\frac{k}{\pi}\int_{\varphi}^{(180+\varphi)} V\sin\theta d\theta = \frac{2kV}{\pi}\cos\phi \quad . \quad . \quad . \quad . \quad (15)$$

where k depends on the circuit constants.

It is seen that the wattmeter output is proportional to analyser current and power factor, but independent of analyser voltage. With constant voltage at the metering point, the multiplication $V \times I\cos\phi$ may be effected on a potentiometer calibrated in terms of per-unit analyser voltage and connected at the output of the wattmeter; this requires manual adjustment of the control prior to each swing-curve study. The output of the wattmeter is smoothed by an RC filter. The time-constant of this filter determines the speed of response of the wattmeter and is approximately 7 millisec, i.e. 10 cycles of base frequency. Performance of the wattmeter is illustrated in Fig. 6(c).

(4.3.2) **Generator-Unit Phase-Shifter Drive.**

The type 73 velodyne is suitable for the purpose of driving the 3 in magslip phase-shifter of the network analyser and the precision potentiometer necessary for presentation of angular information to either a cathode-ray or Duddell oscillograph.

The split field of the motor is supplied in push-pull from a three-stage negative-feedback amplifier, with the linear range extending up to rated field current in order to have maximum torque available. The circuit and performance of the amplifier are shown in Figs. 7 and 8 respectively. The necessary stabiliza-

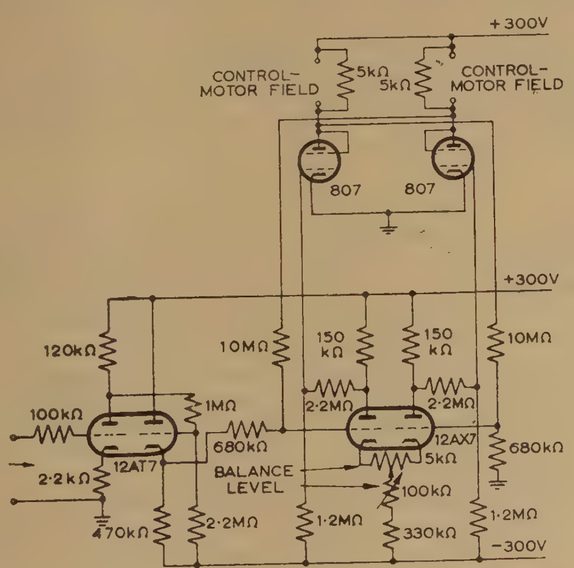

Fig. 7.—Control-motor field amplifier.

tion of motor armature current is effected with a simple degenerative circuit using one series valve and a shunt amplifier by which the current regulation at rated speed is reduced below 2%.

The velodyne tachometer-generator field is fed from a stabilized source which reduces the effect of supply-voltage variations by a factor of 10. The availability of derivative feedback also affords a means of neutralizing the effect of friction in the moving parts

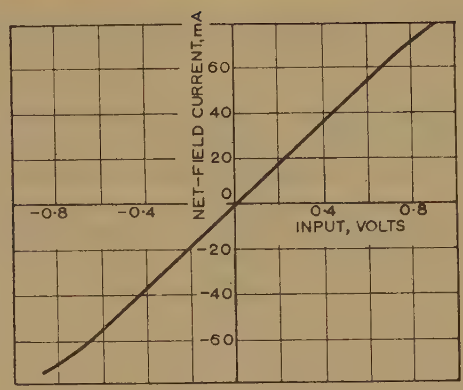

Fig. 8.—Gain characteristic of control-motor amplifier.

of the simulator. An approximate expression often employed for friction torque is

$$T = f'\frac{d\delta}{dt}$$

where T is friction torque, f' a friction coefficient and δ angular displacement. Thus, the effect of friction is to produce error in the first-order term of eqn. (10) and to impose a definite lower limit to the damping which occurs when the feedback control is at zero setting. The limitation can be removed by applying positive derivative feedback in a way similar to that employed for the simulation of damping power.

(4.3.3) **Reference Voltage and Adding Circuits.**

In transient-stability studies, the consideration of first-swing stability is of prime importance. For this reason, and owing to the delay in prime-mover governor operation subsequent to a sudden disturbance, the prime-mover input power may be assumed constant for transient-stability work with the simulator. Hence it is sufficient to represent P_m by an adjustable voltage which, according to eqn. (10), must be subtracted from the wattmeter output voltage corresponding to P_e.

Several methods of subtraction are available, but with a careful choice of circuit values, both the operation mentioned above and the addition of the voltage corresponding to asynchronous damping power may be carried out conveniently and with adequate accuracy by resistor networks.

(4.4) Simulator Operation

(4.4.1) **Simulator Controls.**

The adjustable analogue quantities are as follows:

Analogue quantity		*System quantity*
v_r	controls	P_m
A	controls	M
P	controls	P_d

The various controls of the simulator must be calibrated to facilitate rapid adjustment of system quantities and synchronous-machine parameters to the required values prior to swing-curve studies.

Most of the tests involved in the calibration have been carried out with the simulator in a static condition, the exception being the derivation of an acceleration constant for the control motor of the phase-shifter. The sequence of steps in the calibration is as follows:

(i) The maximum setting of the wattmeter voltage-multiplier is assigned a value equal to the highest relevant generator voltage likely to occur in normal problems. Intermediate points are immediately defined, since the setting is linear and proportional to the magnitude of the voltage to be represented. The control is adjusted to 1 per-unit voltage for the remaining steps in the calibration.

(ii) A static load is connected to the generator unit associated with the simulator. Adjustment of the P_m control to give zero difference power defines a point on the P_m calibration, and this is repeated for several values of the load.

(iii) Calibration of the M control is accomplished in two stages. First, the acceleration of the phase-shifter control motor is determined as a function of its field current. The relationship is linear and yields a constant giving the acceleration of the phase-shifter per milliampere step in the motor field current. Secondly, with a known and constant difference power at the input to the inertia-constant control, the setting of the control is varied and a graph of output against motor field current is obtained. Using the constant α, and the value of difference power, the scale of motor field current may be converted to per-unit power/deg/sec². By reference to the graph, the inertia-constant control may be calibrated in terms of these units.

A more direct method would be to perform run-up tests with constant power differential and with variation of the inertia-constant setting: subsequent modifications, or other changes in any part of the apparatus, would entail a repetition of the acceleration-constant tests.

(iv) The tachometer armature is disconnected and a constant voltage is applied to the damping-factor control. With the prime-mover power set to balance the electrical power, the output from the damping-factor control is varied and plotted against motor field current. The scale of the latter may be converted to power using the results of one of the tests in (iii) above. It may further be modified to read per-unit power/deg/sec² by dividing by a speed: this speed corresponds to the test voltage applied to the damping-power control and is obtained from the tachometer-voltage/speed curve.

(4.4.2) **The Use of the Simulator in Steady-State and Transient-Stability Studies.**

Normally, the setting-up on the network analyser of the equivalent sequence networks of a power system is followed by the tedious manual process of adjusting the analyser generator units until the required values of power and voltage, obtained from system information, are attained. The simulator described may be employed for this purpose as a preliminary to either load-flow or transient-stability studies, with the following procedure:

The supplies to the control motors are switched off, the equivalent inertia constants are set to minimum values and the damping factors to maximum values. The P_m controls and the generator-voltage magnitude controls are adjusted to the required values, and after the setting-up of the network analyser and interconnection of the generator units, the supplies to the control motors are switched on. Owing to their low equivalent inertia and high damping, they immediately position the phase-shifters to give the correct phase-angle and system conditions, provided an additional generator is available for supplying the system losses.

The accuracy of the automatic setting-up process is governed by the sensitivity of the motor to small field-current changes, as there is a dead band of field-amplifier inputs within which no change of phase angle results. Positioning accuracy may be increased quite simply by providing a gain switch which enables the amplifier to be saturated by small inputs, in which case the accuracy is limited only by the accuracy of the wattmeter [Fig. 6(*c*)].

When transient-stability studies are to follow the setting-up of the generator units, it is only necessary to adjust the inertia-constant and damping-factor controls to correspond to predetermined values before carrying out the switching operations on the analyser network.

(5) RESULTS

A suitable problem without damping, which had previously been analysed by means of an integraph, was chosen from Park and Bancker[26] and is shown in Fig. 9.

The problem was solved step by step and by the simulator and was checked against the published integraph solution. The step-by-step and integraph solutions were identical and are shown in curve A (full line). The analogue solution is shown as curve A (dotted line), and it will be observed that the simulator is pessimistic both as regards peak angle of swing and rate of change of angle. Thus the simulator shows an overswing of approximately 3° before recovery and attains peak angle of swing approximately 3 cycles (at system frequency) earlier in the case of the other solutions. The same problem, with allowance for damping power, $P_d = 0{\cdot}758 \times 10^{-4}$ per deg/sec, was then considered, the determination of P_d being an approximation due to Park.[27] The results are shown as curves B.

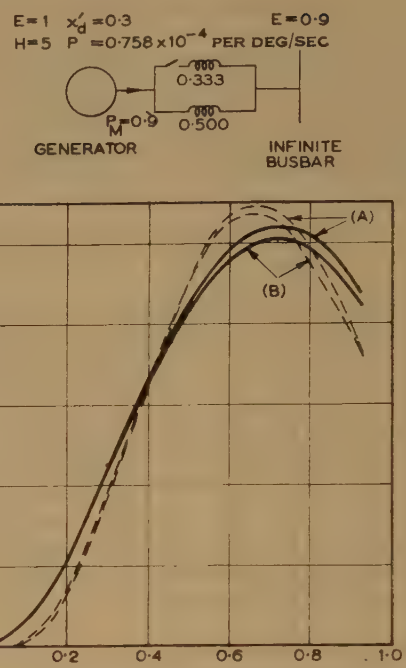

Fig. 9.—Calculated and simulator curves.

(A) Zero damping.
(B) Including damping.

(6) ECONOMY OF APPARATUS

Precise information from other workers in the field is difficult to obtain, but it appears that the direct-analogue equipment developed by the authors is competitive economically with other schemes of automatic generators for use with a.c. impedance-type network analysers. The equipment described in the second part of the paper, if manufactured commercially, would consist of an electronic chassis with wattmeter and velodyne controls and supplies, an electro-mechanical chassis containing voltage control setting, phase control, velodyne and gear-box, and a power-unit chassis. A large-scale commercially-produced network analyser could be thus equipped for the solution of swing curves, at a cost per generator not exceeding 1% of the cost of the complete installation. The accuracy obtainable would be within that normally required for power-system stability studies.

(7) CONCLUSIONS

The discrepancies in the results recorded may be attributed to the calibration of the damping and inertia controls; further work will be carried out on this aspect now that three automatic generators have been delivered for the large power-system simulator under construction at the College of Technology, Manchester. Provided that simulator operation is carried out on a

slow time-scale (e.g. of the order of real time), voltage regulator action could be represented; circuits to this end involve simulation of the performance of the generator field circuit and regulator and the derivation of appropriate modulating signals. This work, as yet, is unpublished.

The automatic step-by-step method of solution of stability problems described in the paper is time-consuming, although it is faster than normal methods of desk computation with information derived from a network analyser. Two generators have been built using, in the main, suplus equipment, and would have been expensive if new equipment had been used. Furthermore, the machine is applicable only to transient-stability studies and, without further elaboration, cannot be used for saving time and setting up a network analyser for steady-state studies. The continuous-analogue method is rapid in operation and presents information in a convenient form; with heavy damping and increased external gain, the apparatus may be used as an auxiliary to a network analyser.

(8) ACKNOWLEDGMENTS

The authors wish to acknowledge the encouragement given to the work by Professor E. Bradshaw, and the advice of their colleagues in the Department of Electrical Engineering, Manchester College of Technology, particularly that of Mr. V. H. Attree.

(9) REFERENCES

(1) Evans, R. D., Bergvall, R. C., Sels, H. K., Fortescue, C. L., Wagner, C. F., Hanker, F. C., Shand, E. B., Thomas, P. H.: Symposium of Six Papers on Electrical Power Transmission, *Transactions of the American I.E.E.*, 1924, **43**, p. 16.

(2) Crary, S. B.: 'Power System Stability' (Wiley, 1945), **1** and **2**.

(3) Dahl, O. G. C.: 'Electric Power Circuits—Theory and Applications' (McGraw-Hill, 1938), **2**.

(4) Mortlock, J. R.: 'A Computer for Use in Power-System Transient Stability Studies', *Journal I.E.E.*, 1948, **95**, Part II, p. 751.

(5) Jones, K. M.: 'An Eight-Machine Transient Stability Computer', *BTH Activities*, 1950, **21**, No. 3, p. 81.

(6) Peterson, H. A.: 'Electric Computer', U.S. Patent, Number 2489106, 1949.

(7) Squires, R. B., and Harder, E. L.: Discussion of Reference 15, *Transactions of the American I.E.E.*, 1954, **73**, Part 3–A, p. 241.

(8) Bennett, J. M., Dakin, F. V., and Knight, U. G.: 'Digital Computers and their Application to Some Electrical Engineering Problems', C.I.G.R.É., Paris, 1952, Paper No. 304.

(9) Bills, G. W.: 'Application of Digital Analysers to Power System Problems', American Power Conference, Chicago, 1954.

(10) Gill, S.: 'A Process for the Step-by-Step Integration of Differential Equations in an Automatic Digital Computing Machine', *Proceedings of the Cambridge Philosophical Society*, 1950, **47**, Part 1, p. 96.

(11) Rothe, F. S.: Discussion of 'System Stability, Load and Frequency Control', C.I.G.R.É., 1954, **1**, p. 564.

(12) Boast, W. B., and Rector, J. D.: 'An Electric Analogue Method for the Direct Determination of Power System Stability Swing Curves', *Transactions of the American I.E.E.*, 1951, **70**, Part 2, p. 1833.

(13) Kusko, A.: Discussion of Reference 12, p. 1835.

(14) Kimbark, E. W.: Discussion of 'A New A–C Network Analyser', *ibid.*, 1938, **57**, p. 419.

(15) Bekey, G. A., and Schott, F. W.: 'Analyser Interconnections for Direct Determination of Power-System Swing Curves', *ibid.*, 1954, **73**, Part 3–A, p. 238.

(16) Watkins, B. O.: Discussion of Reference 15, p. 241.

(17) Kaneff, S.: 'A High-Frequency Simulator for the Analysis of Power Systems', *Proceedings I.E.E.*, Paper No. 1497 M, August, 1953 (**100**, Part II, p. 405).

(18) Shen, D. W. C., and Packer, J. S.: 'Analysis of Hunting Phenomena in Power Systems by Means of Electrical Analogues', *ibid.*, Paper No. 1565 S, February, 1954 (**101**, Part II, p. 21).

(19) Shen, D. W. C., and Lisser, S.: 'An Analogue Computer for Automatic Determination of System Swing Curves', *Transactions of the American I.E.E.*, 1954, **73**, Part 1, p. 475.

(20) Bauer, H.: Discussion of 'System Stability, Load and Frequency Control', C.I.G.R.É., 1954, **1**, p. 542.

(21) Mortlock, J. R.: *ibid.*, p. 546.

(22) Van Ness, J. E.: 'Synchronous Machine Analogues for Use with the Network Analyzer', *Transactions of the American I.E.E.*, 1954, 73, Part 3–B, p. 1054.

(23) Kaneff, S.: 'Dynamic Operation of an A.C. Network Analyser', *Proceedings I.E.E.*, Paper No. 1847 S, October, 1955 (**102** A, p. 597).

(24) Watkins, R. D.: 'The Development of an Automatic Swing Curve Computer', unpublished thesis for the degree of Master of Technical Science, submitted to the University of Manchester, 1952.

(25) Williams, F. C., and Uttley, A. M.: 'The Velodyne', *Journal I.E.E.*, 1946, **93**, Part IIIA, p. 1256.

(26) Park, R. H., and Bancker, E. H.: 'System Stability as a Design Problem', *Transactions of the American I.E.E.*, 1929, **48**, p. 170.

(27) Park, R. H.: 'Two Reaction Theory of Synchronous Machines—2', *ibid.*, 1933, **52**, p. 352.

[The discussion on the above paper will be found on page 161.]

621.313.322

Paper No. 2015 S
June 1956

ELECTRONIC-ANALOGUE-COMPUTER STUDY OF SYNCHRONOUS-MACHINE TRANSIENT STABILITY

By A. S. ALDRED, M.Sc., Graduate, and P. A. DOYLE, B.E.

(*The paper was first received* 3*rd August, and in revised form* 28*th November*, 1955. *It was published in June*, 1956, *and was read before the* SUPPLY SECTION 18*th November*, 1956.)

SUMMARY

The paper describes a method of solution of synchronous-machine transient-stability problems by a more exact electronic analogue representation of the system equations than has hitherto been employed. In the machine analysis emphasis is placed on the variation of field flux linkage during transient disturbances, and reasons are given why this is necessary. The equations of performance are derived in the most convenient form for analogue computing.

The equivalent analogue interconnections are given both for time-varying and for constant field flux linkage. The components required for these analogues are considered briefly.

The section on computer control deals with the control of integrators with reference to the introduction of 'initial conditions', 'hold' and 'compute' states. A delay unit is described which enables the switching out of a faulted transmission line to be simulated.

The results of various problems solved by the computer are presented in graphical form as boundaries between stable and unstable states. It is shown how instability subsequent to the first rotor oscillation may occur, and an explanation is proposed to account for this phenomenon.

Synchronous-machine and transmission-line analysis are excluded from the main text for clarity and are presented in detail in the Appendices.

LIST OF PRINCIPAL SYMBOLS

M = Inertia constant.
δ = Rotor angle.
T_d = Damping coefficient.
P_i = Power input.
T_{do} = Field time-constant.
i_d = Direct-axis current.
i_q = Quadrature-axis current.
X_d = Direct-axis self-inductance (synchronous reactance).
X_d' = Direct-axis transient reactance.
X_q = Quadrature-axis self-inductance (synchronous reactance).
X_t = Transmission-line series inductance (reactance).
v_d = Direct-axis terminal voltage.
v_q = Quadrature-axis terminal voltage.
P_0 = Power output.
v = Terminal voltage of infinite system.
v_{fd} = Field impressed voltage.
R_{fd} = Field resistance.
i_{fd} = Field current.
X_{fd} = Field self-inductance.
X_{ad} = Mutual inductance (reactance) between field and direct-axis armature.
ψ_d = Direct-axis flux linkage.
ψ_q = Quadrature-axis flux linkage.
ψ_{fd} = Field flux linkage.
R = Resistance of quadrature-axis or direct-axis circuit.
$p\theta$ = Speed.

Mr. Aldred and Mr. Doyle are in the Electrical Engineering Department, University of Liverpool.

(1) INTRODUCTION

The problems associated with the maintenance of stability of synchronous machines in power systems, and the factors affecting stability during transient disturbances, have received considerable attention in recent years.

The methods of physical reasoning applied by engineers to the steady-state analysis of the relatively simple cylindrical-rotor synchronous machine were extended by Blondel in his two-reaction theory to the case of the more complex salient-pole field structure. The mathematical generalization and extension to transient analysis of Blondel's two-reaction theory are due to R. H. Park,[1,2,3] and it is on Park's equations that this investigation of synchronous-machine stability has been based.

Hitherto, the application of Park's equations to system stability has involved a number of assumptions in addition to the idealization of the machine. These assumptions are used to make the expression for the transient power of a machine a function of its rotor angle only and not of time as well. The most fundamental of these assumptions, known as the constant-flux-linkage theorem, states that the flux linking the field circuit of a synchronous machine remains constant following a disturbance, not only initially but indefinitely. The use of this assumption reduces a system-stability problem to the solution of a number of simultaneous second-order non-linear differential equations which equate the product of the moment of inertia and angular acceleration to the accelerating torque.

Equations of this type have been solved by a number of methods, namely

Mechanical model simulator.[4,5,6]
Step-by-step and graphical analysis.[7,8,9]
General differential-analyser application.[10,11]
Special analogue simulator.[12,13,14]

Because of the difficulties of measurement on actual systems, most synchronous-machine-system transient analysis has been carried out using analogue methods. An alternative approach has been developed in France with model machines and miniature transmission systems.[15] While this method is more realistic and more likely to approach the practical case, it is not as flexible as a general mathematical study with the aid of computers.

The object of the work described in the paper has been to take into consideration some of the effects previously neglected in synchronous-machine stability studies. The inclusion of these effects has necessitated the development of rapid methods of solution of the equations which describe more accurately the performance of synchronous machines in power systems. In particular, attention has been paid to the effects of variations of field flux linkage during transient disturbances. This is necessary for three reasons.

First, it is desired to find how the damping characteristics of the machine are affected by the rejection of the assumption of constant-field flux linkage.

Secondly, voltage regulators and excitation systems are being developed and widely used at present to improve power-system

performance. The use of voltage regulators excludes the assumption of constant-field flux linkage. This work is therefore the first step towards more detailed investigation of voltage-regulator action on synchronous-machine stability.

Thirdly, from the results of these and associated studies it is required to make some generalizations concerning the relationship between system parameters and allowable assumptions.

Before commencing the design of the apparatus required to solve these problems, experiments were conducted on three prototype analogue computers: a combined electric, electro-mechanical and electronic simulator, an electro-mechanical analogue computer, and a purely electronic analogue computer.

The conclusion reached was that the most suitable approach would be to use an analogue computer of the d.c. electronic type. The prime factors influencing this decision were (*a*) the need for flexibility in setting system parameters, (*b*) rapid solution and re-solution of system equations to enable boundaries between stable and unstable states to be derived quickly, and (*c*) the possibility of using the apparatus in conjunction with real components of a system, e.g. a synchronous-machine exciter. When this project was commenced, conventional analogue computers were not readily available. It was also envisaged that such computers would not be suitable for the solution of the problems involved because of the non-linearities and the need for simultaneous switching of several system parameters at prescribed times during a computation. The latter operation is necessary to simulate the switching of faulted transmission lines.

The design of the computer is briefly described in Section 3.

(2) POWER-SYSTEM STABILITY

The simplest power-system configuration which may be investigated for stability is that of a single synchronous generator, driven by a prime mover, and connected by a transmission line of series inductive reactance to an infinite system.

(2.1) Simplified Stability Problem

It can be shown (see Appendix 8.3) that the equation of motion for this system in terms of power becomes

$$P_i = M\frac{d^2\delta}{dt^2} + T_d\frac{d\delta}{dt} + P_m \sin\delta \quad . \quad . \quad . \quad (1)$$

if the following assumptions are made:

(*a*) The machine is ideal.
- (i) The armature flux wave is sinusoidally distributed in space.
- (ii) The saturation is negligible.
- (iii) The effect of eddy-current and hysteresis loss is negligible.

(*b*) The percentage speed change during a transient which results in the machine remaining in synchronism is negligible, i.e. the component of generated voltage due to the rate of change of rotor angle is negligible compared with the voltage generated at fundamental speed.

(*c*) The voltages induced in the armature by the rate of change of the armature flux linkage, namely $p\psi_d$ and $p\psi_q$, are negligible compared with the voltages $\psi_q p\theta$ and $\psi_d p\theta$ generated by the fluxes ψ_q and ψ_d rotating at fundamental speed. This is because $p\psi_d$ and $p\psi_q$ are rates of change of slowly varying quantities, whereas $\psi_q p\theta$ and $\psi_d p\theta$ are large because $p\theta$ is large.

(*d*) The armature and line resistances are negligible.

(*e*) The field flux linkage remains constant following a disturbance, not only initially but indefinitely.

(*f*) The direct-axis transient reactance is equal to the quadrature-axis transient reactance (i.e. there is zero transient saliency).

(*g*) The action of the prime-mover governor is not sufficiently fast to change the mechanical input power following a small change in speed, so that the mechanical input is constant.

This equation has been solved by a number of methods, as indicated in References 4–14. If these simplifying assumptions are made for systems containing many generators a number of equations arise, each equation being similar in form to eqn. (1), which must be solved simultaneously.

(2.2) Time-Varying Field Flux Linkage

The equations which describe the system, if assumptions (*e*) and (*f*) are not made, are as follows:

Field $$\Psi_{fd} = \frac{V_{fd} - I_{fd}}{T_{do}p} \quad . \quad . \quad . \quad . \quad . \quad . \quad (2)$$

$$I_{fd} = \Psi_{fd} - i_d(X_d - X_d') \quad . \quad . \quad . \quad . \quad (3)$$

Direct axis $$v_d = -X_q i_q \quad . \quad . \quad . \quad . \quad . \quad . \quad (4)$$

Derived quantity $$V_Q = I_{fd} + i_d(X_d - X_q) \quad . \quad . \quad . \quad . \quad (5)$$

Quadrature axis $$v_q = I_{fd} + X_d i_d \quad . \quad . \quad . \quad . \quad . \quad (6)$$

Power output $$P_0 = V_Q i_q \quad . \quad . \quad . \quad . \quad . \quad . \quad . \quad (7)$$

Equation of motion $$P_i = M\frac{d^2\delta}{dt^2} + T_d\frac{d\delta}{dt} + P_0 \quad . \quad . \quad . \quad . \quad (8)$$

where $$v_d = v\sin\delta \quad . \quad . \quad . \quad . \quad . \quad . \quad . \quad (9)$$

and $$v_q = v\cos\delta \quad . \quad . \quad . \quad . \quad . \quad . \quad . \quad (10)$$

These equations have been derived in Appendix 8.1, namely eqns. (51), (47), (39), (54), (49), (55), (37).

The introduction of the per-unit system makes the speed $p\theta$ equal to unity in the above equations, and the inductances become numerically equal to the reactances. The standard form of the system equations is as follows:

Field $$v_{fd} = R_{fd}i_{fd} + X_{fd}pi_{fd} + X_{ad}pi_d \quad . \quad . \quad . \quad (11)$$

Direct axis $$v_d = -X_q i_q p\theta \quad . \quad . \quad . \quad . \quad . \quad (12)$$

Quadrature axis $$v_q = (X_d i_d + X_{ad}i_{fd})p\theta \quad . \quad . \quad . \quad . \quad (13)$$

Power $$P_0 = [(X_{ad}i_{fd} + X_d i_d)i_q - X_q i_q i_d]p\theta \quad . \quad . \quad (14)$$

Equation of motion $$P_i = M\frac{d^2\delta}{dt^2} + T_d\frac{d\delta}{dt} + P_0 \quad . \quad . \quad . \quad . \quad (15)$$

The former set has been derived in the most convenient form for analogue computation, and it possesses the following advantages:

(*a*) If the field time-constant is varied no other compensating changes need be made in the parameter-changing equipment or impressed voltages.

(*b*) Points are made available to record I_{fd}, Ψ_{fd}, i_q, i_d, δ and P_0.

(*c*) A simple disconnection in the analogue loop and the application of a constant voltage enables the system to be operated under conditions of (i) constant field-flux linkage and (ii) constant field current. These two conditions correspond to the extreme limits of T_{d0}, i.e. $T_{d0} = \infty$, $T_{d0} = 0$. Since these extreme cases are not physically realizable the equipment could not simulate them without changes. These changes are most easily accomplished in the equivalent analogue connection defined by these equations.

(*d*) The change from cylindrical-rotor to salient-pole machine is easily made, and the degree of saliency is easily adjusted.

(*e*) The introduction of the quantity V_Q reduces the number of multipliers required from two to one.

(3) THE ELECTRONIC ANALOGUE COMPUTER

(3.1) Equivalent Analogue Interconnection

The equations given in Section 2.2 are simulated by the interconnection of elements shown in Fig. 1.

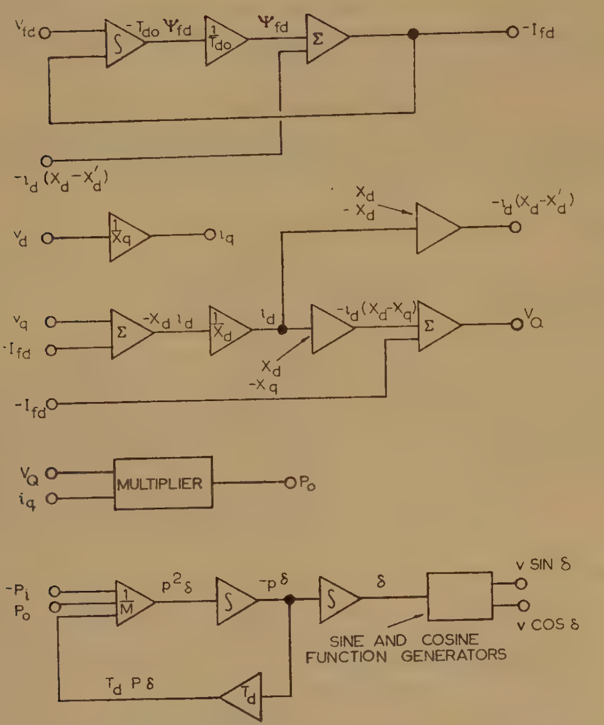

Fig. 1.—Equivalent analogue connections for eqns. (2)–(10).

This can be shown to satisfy the relationships defined by the equations.

Consider the first section which simulates eqns. (2) and (3). V_{fd} is an impressed voltage known from the system data. Assume temporarily that $-I_{fd}$ is known. Then if V_{fd} and $-I_{fd}$ are added and the sum integrated and multiplied by -1, $-T_{d0}\Psi_{fd}$ is obtained as given by eqn. (2). Multiplication of $-T_{d0}\Psi_{fd}$ by $-1/T_{d0}$ gives Ψ_{fd}. From eqn. (3), if $i_d(X_d - X_d')$ is added to Ψ_{fd} and the sum is multiplied by -1 the result is equal to $-I_{fd}$. This supplies $-I_{fd}$, which was assumed to be known initially. In a similar manner the complete set of equations is simulated.

(3.2) Computing Elements

It can be seen that the elements in this interconnection perform the following operations:

(*a*) Addition of two or more variables.
(*b*) Integration of a variable with respect to time.
(*c*) Simultaneous addition and integration.
(*d*) Multiplication by a constant coefficient.
(*e*) Multiplication of two variables.
(*f*) Generation of non-linear functions of a variable.

The basic elements used for performing operations (*a*), (*b*), (*c*) and (*d*) are direct-coupled amplifiers. The techniques by which they are employed are now well known.[16] For addition and scaling, low-gain amplifiers are used, each consisting of two stages of amplification terminated by a cathode-follower output giving an overall gain of 800. The first stage tends to compensate for changes in heater voltage. The above operations were carried out with an accuracy of 1%.

Multiplication by a constant is a frequent operation, and where it is necessary to vary accurately and conveniently the value of the constant, the circuit of Fig. 2 is used.

With the switch in position 1

$$V_0 = -\frac{1}{\beta}\frac{R_2}{R_1}V_i \text{ if } R_2 \gg R_3$$

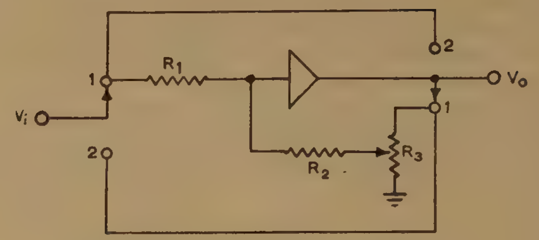

Fig. 2.—Circuit for parameter variation.

If $R_2 = R_1$, then $\quad V_0 = -\dfrac{1}{\beta}V_i$

With the switch in position 2

$$V_0 = -\beta V_i$$

R_3 is a ten-turn helical potentiometer and β, which is the ratio of the resistance between the slider and ground to the total potentiometer resistance, can be accurately observed from the calibrated dial. This enables the scaling value to be continuously varied and set with an accuracy of 0·1%.

For integration, amplifiers having gains of 10^5 are used. These amplifiers have an improved drift-compensation circuit which limits the short-time drift. When integrating zero input voltage, with $RC = 0{\cdot}25$ sec the drift is of the order of 0·15 mV per hour referred to the input.

(3.3) Multiplication

The multiplier shown in Fig. 1 is required to produce a direct-voltage output equal to the product of two input direct voltages. It is a four-quadrant multiplier based on the principle of sum and difference squaring using the identity

$$xy = \tfrac{1}{4}[(x + y)^2 - (x - y)^2]$$

The problem is therefore resolved into processes of addition, scaling and squaring. The first two are easily performed with amplifiers and associated networks. Squaring may be carried out by means of linear interpolation using diodes.[17] The more convenient method used employs non-ohmic resistors, although this limits the attainable accuracy. The overall accuracy is of the order of 1% of the maximum output voltage. The circuit of the multiplier is shown in Fig. 3.

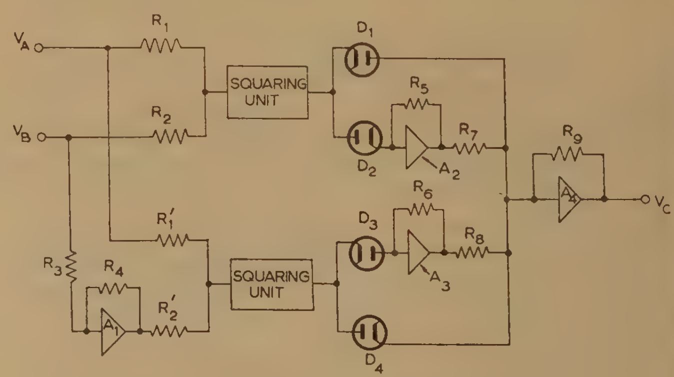

Fig. 3.—Four-quadrant multiplier.

Since the non-ohmic-resistor squaring circuits provide only the square of the magnitude and not of the sign of the inputs, the diode circuits in conjunction with the sign-reversing amplifiers are used to ensure that the outputs are of correct sign. The diodes D_1 and D_2 with the amplifier A_2 ensure that $(V_A + V_B)^2$

is always negative, and the diodes D_3 and D_4 with the amplifier A_3 ensure that $(V_A - V_B)^2$ is always positive. Therefore the output of A_4 is $+kV_AV_B$, where k is a suitable scaling factor, in this case one-tenth.

(3.4) Function Generation

The analogue forms of eqns. (9) and (10) require sine and cosine function generators. These provide direct voltages proportional to the sine and cosine of a variable input direct voltage. The generation of these functions is by linear interpolation using diodes.[17] The accuracy required determines the number of line segments and hence the number of diodes. Eight diodes are used for each function over the range 0–π, and the accuracy is within 1%.

(3.5) Computer Control

In order that a definite solution may be obtained from a set of differential equations, it is necessary to know the values of the variables at the start of a disturbance. The number of initial conditions required is equal to the number of integrators, and these initial conditions are set in by charging the integrating capacitors while the computer is inoperative.

It is desirable, by introducing a 'hold' condition, to be able to stop the computer during the course of a computation in such a manner that all the variables are held to the values they had at the instant the computation was stopped. This is necessary so that different coefficients may be set in while the computer is inoperative and the solution then continued. If switching action takes place in a transmission system following a fault, new coefficients must be introduced to represent the effect of the switching action on the system parameters.

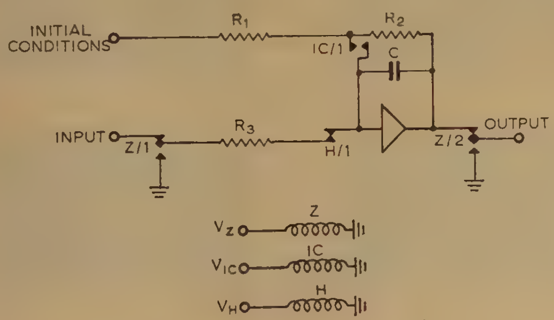

Fig. 4.—Integrator control circuit.

These facilities are incorporated by controlling the integrators as shown in Fig. 4.

(3.5.1) Integrator Control.

If voltages V_{IC} and V_H are applied to the relays IC and H respectively, the integrator becomes a scaling circuit. By applying a voltage from a variable source to the terminal marked 'initial conditions' the output voltage may be set to any desired value. If V_{IC} is removed the integrator will be reduced to an amplifier with a capacitor connected across it. This capacitor will remain charged to hold the output voltage at the value it had when V_{IC} was removed. Computation is initiated by removing V_H and releasing the H relay. By operating this relay during a computation the output voltage will remain at the value it had when the relay operated.

Operation of the Z relay places the integrator in a condition in which the rate of drift can be adjusted to a minimum by a fine control. The integrator control voltages are provided from a main control unit.

(3.5.2) Delay Unit.

In addition, a delay circuit is used to enable problems involving the switching of transmission lines to be solved. This delay circuit (Fig. 5) consists of a cathode-coupled multivibrator giving a voltage step of variable delay depending on the setting of R_2, which is a ten-turn helical potentiometer, and the capacitance of C_2. This voltage step triggers the following bi-stable multivibrator, which operates the relay L in the cathode of V_3 by changing the grid voltage of V_3 from negative to positive. This delay circuit is triggered simultaneously with the initiation of a computation, and after the preset time delay, the operation of the relay L applies a voltage V_H to the integrators which sets the computer in the 'hold' condition. It also operates a set of relays located in the various scaling units, which make the necessary changes in the coefficients. Completion of the switching action generates a signal which re-initiates the computation. Computation is therefore suspended only for the operating time of a fast relay. This facility is desirable when the optimum value of a parameter is being obtained from observation of the computer solutions, and is not usually incorporated in conventional computers.

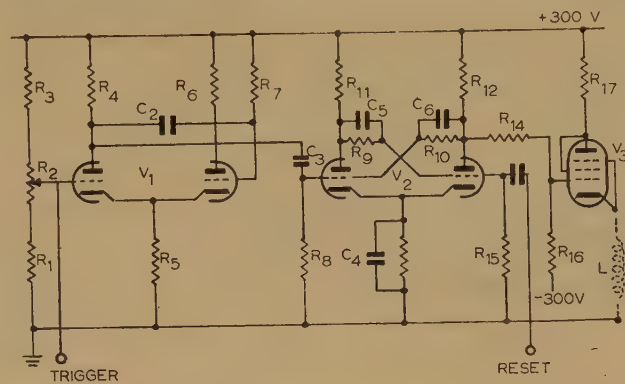

Fig. 5.—Delay-pulse generator.

(4) EXPERIMENTAL RESULTS AND DISCUSSION

The problems which are solved are divided into two sections as follows:

(a) Solutions of simplified transient-stability problems (Section 2.1) for comparison of the results with those obtained by previous investigators.

(b) Solutions of transient-stability problems with varying-field flux linkage and constant-field flux linkage to show the effect of the former.

(i) In response to a step function of mechanical power input.
(ii) In response to a disturbance caused by a transmission-line fault without clearing by circuit-breakers.
(iii) In response to a similar disturbance with clearing by circuit-breakers.

(4.1) Simplified Stability Problems

It is shown in Appendix 8.3 that the equation of motion of a synchronous machine connected by a transmission line to an infinite system is

$$P_i = M\frac{d^2\delta}{dt^2} + T_d\frac{d\delta}{dt} + P_m \sin\delta \quad . \quad . \quad . \quad (16)$$

This equation is put into a dimensionless form by means of the following substitutions:

$$t = t'\sqrt{\frac{M}{P_m}} \quad . . . . \quad (17)$$

$$p_i = \frac{P_i}{P_m} \quad . . . . \quad (18)$$

$$K_c = \frac{T_d}{\sqrt{(MP_m)}} \quad . . . . . . \quad (19)$$

Using these relationships eqn. (16) becomes

$$p_i = \frac{d^2\delta}{dt'^2} + K_c\frac{d\delta}{dt'} + \sin\delta \quad . . . . \quad (20)$$

Now p_i may be divided into two parts—the initial load ratio p_{00} and the abrupt load ratio p_L—given by

$$p_{00} = \frac{P_{00}}{P_m} \quad . . . . \quad (21)$$

$$p_L = \frac{P_L}{P_m} \quad . . . . \quad (22)$$

where $P_L + P_{00} = P_i$

and $P_{00} = P_m \sin\delta_0$

Eqn. (20) then becomes

$$p_L + p_{00} = \frac{d^2\delta}{dt'^2} + K_c\frac{d\delta}{dt'} + \sin\delta \quad . . . \quad (23)$$

This equation has the advantage of being independent of the inertia constants of the machines and of the constants of the transmission network. Eqn. (23) is solved by connecting computing elements as shown in Fig. 6. First with $K_c = 0$, the

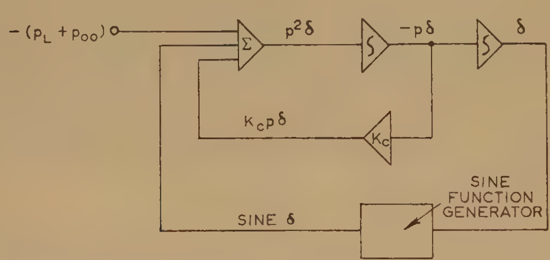

Fig. 6.—Analogue interconnection for simplified stability problem.

maximum value of p_L which results in a stable solution is found for various values of δ_0. Summers and McClure[10] have given solutions of eqn. (23) with $K_c = 0$ in the form of curves of δ plotted against time for values of δ_0 from $\sin\delta_0 = 0$ to $\sin\delta_0 = 1$, the sines being at intervals of 0·1. Hence, for a given value of $\sin\delta_0$, the highest value of $p_L + p_{00}$ which gives a stable solution, is known, and a succeeding value $p_L + p_{00} + 0{\cdot}05$ which gives an unstable solution is also known. Since p_{00} is known, two values of p_L as outlined can be plotted for each value of $\sin\delta_0$ (Fig. 7). The line joining all the upper points gives a boundary on and above which the solution is unstable, and the line joining the lower points gives a boundary on and below which the solution is stable. The values of p_L obtained from the computer are also plotted, and these lie on the lower boundary or between the two. This indicates that the computer is operating correctly. The line joining the points obtained from the computer is approximately straight. This feature, which has also been used to check the accuracy of the computer, is dealt with in Reference 18.

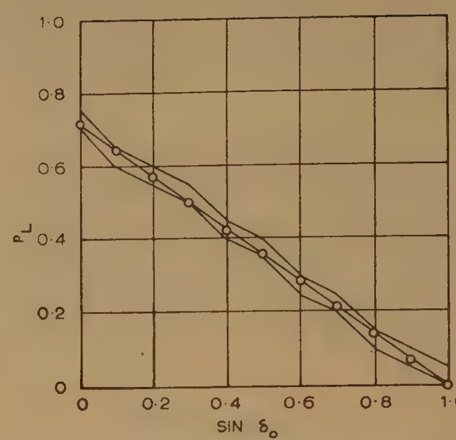

Fig. 7.—Stability boundary with no damping, compared with results in Reference 10.

The solutions of eqn. (23) for a range of values of K_c and p_L have also been published.[11] A comparison of these results and those obtained from the computer is given in Fig. 8.

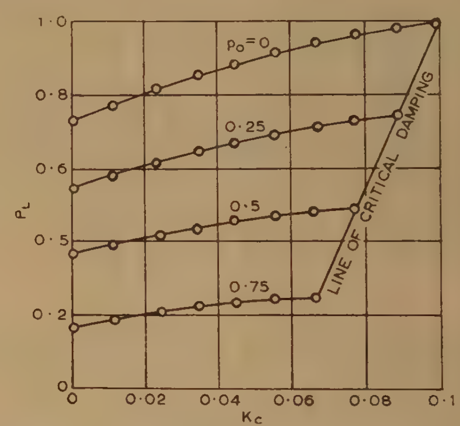

Fig. 8.—Stability boundaries with damping, compared with results in Reference 11.
—— Reference 11.
⊙ Computer.

(4.2) Time-Varying Field Flux Linkage

A series of problems has been solved allowing for the variation of field flux linkage with time. The results are obtained by solving eqns. (2)–(10) using the interconnection of computing elements shown in Fig. 1. The system parameters have the following values: $X_d = 1$; $X_q = 1$; X'_d variable; T_{d0} variable; T_d variable; M, variable.

In addition, the following relationships, based on the design constants of the computer, exist between computer quantities and system quantities:

$$t_c = \frac{0{\cdot}0396}{\sqrt{M}}t_s$$

$$T_{dc} = \frac{6{\cdot}32}{\sqrt{M}}T_{ds}$$

$$T_{d0c} = \frac{0{\cdot}158}{\sqrt{M}}T_{d0s}$$

where the suffixes c and s refer to the computer and system, respectively. It is shown that system and computerquantities

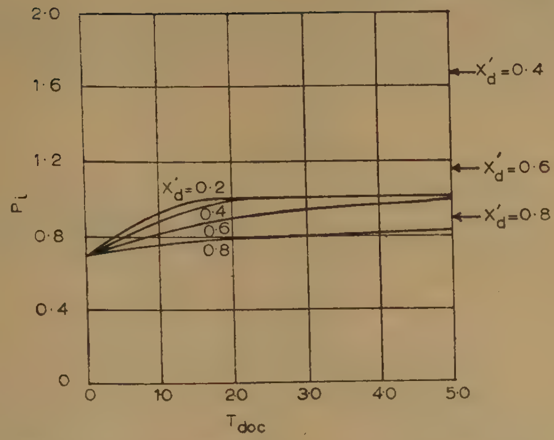

Fig. 9.—Effect of field time-constant on stability limit.
←— Constant-flux-linkage boundaries.

are related by $\sqrt{M}$. Fig. 9 shows the maximum values of P_i which may be impressed so that the system remains stable. From this graph it is evident that the stability limit decreases with decreasing values of field time-constant, i.e. the stability limit with varying-field flux linkage is less than that with constant-field flux linkage. The oscillogram [Fig. 10(*a*)] shows the variation of δ with time during a transient in which the field flux linkage remains constant, and Fig. 10(*b*) shows the variation of δ when the field flux linkage is variable. In addition to lowering the stability limit as seen from Fig. 9, it can be seen from Fig. 10(*b*) that another effect of the varying field flux linkage is to introduce damping.

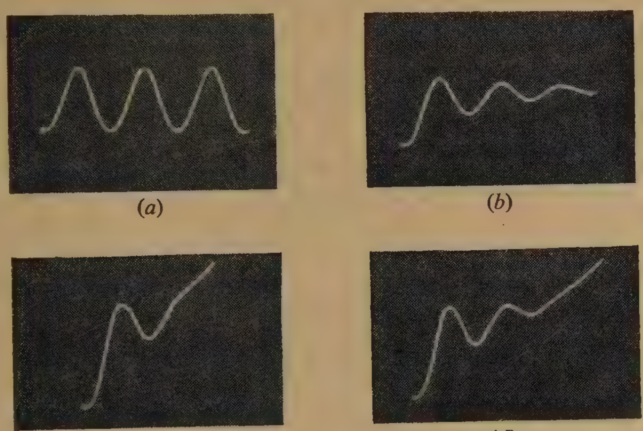

(*a*) (*b*) (*c*) (*d*)

Fig. 10.—Oscillograms of rotor oscillations.
(*a*) Constant flux linkage.
(*b*) Damping effect of field winding.
(*c*) Instability subsequent to first swing.
(*d*) Instability subsequent to second swing.

In obtaining these results it was observed that, for values of P_i greater than those shown by the boundaries in Fig. 9, instability did not always occur on the first swing, but also subsequently, as shown in Figs. 10(*c*) and 10(*d*). This result is of considerable interest, and an approximate explanation is proposed in Section 4.3, to account for this phenomenon.

(4.3) Instability Subsequent to the First Swing

It is shown in eqn. (60) that the power output of a machine in terms of flux and terminal voltage is

$$P_0 = \frac{\Psi_{fd} v \sin\delta}{X'_d} - \frac{v^2(X_q - X'_d)}{2X_q X'_d}\sin 2\delta \quad . \quad . \quad (24)$$

Neglecting the second term on the right-hand side for simplicity, the graph of P_0 against δ is a sine function, having a maximum value of $\Psi_{fd}v/X'_d$. If the initial value of δ_0 is zero, then, from Fig. 7, P_i can have a value of $0·7\Psi_{fd}v/X'_d$ without causing instability. In the steady state which follows the disturbance, the power output becomes

$$P_0 = \frac{V_{fd} v \sin\delta}{X_d} - \frac{v^2(X_q - X_d)}{2X_q X_d}\sin 2\delta \quad . \quad . \quad (25)$$

or, neglecting the second term,

$$P_0 = \frac{V_{fd} v}{X_d}\sin\delta \quad . \quad . \quad . \quad . \quad . \quad . \quad (26)$$

Assuming that the field-circuit time-constant is sufficiently large to maintain the initial flux constant for the duration of one swing, the value of Ψ_{fd} in eqn. (24) will be equal to the initial value of Ψ_{fd0} at the start of the disturbance.

From eqn. (59),

$$\Psi_{fd0} = v\cos\delta_0\left(1 - \frac{X'_d}{X_d}\right) + V_{fd}\frac{X'_d}{X_d} \quad . \quad . \quad (27)$$

Hence $$\frac{\Psi_{fd0}}{X'_d} = v\cos\delta_0\left(\frac{1}{X'_d} - \frac{1}{X_d}\right) + \frac{V_{fd}}{X_d} \quad . \quad . \quad . \quad (28)$$

Since $\delta_0 = 0$, $\cos\delta_0 = 1$

Therefore $$\frac{\Psi_{fd0}}{X'_d} = \frac{V_{fd}}{X_d} + v\frac{(X_d - X'_d)}{X_d X'_d} \quad . \quad . \quad . \quad . \quad (29)$$

Since by definition [eqn. (46)], $X'_d < X_d$

then $$\frac{V_{fd}}{X_d} < \frac{\Psi_{fd0}}{X'_d}$$

Hence if $0·7\Psi_{fd0}/X'_d > V_{fd}/X_d$ the system cannot ultimately be stable, and since it is stable for the first swing, it must become unstable subsequently. Increasing X'_d reduces the value of $0·7\Psi_{fd}/X'_d$, and when this becomes less than V_{fd}/X_d, instability on swings subsequent to the first cannot occur. From the values of the parameters, this occurs for $X'_d > 0·7$.

Fig. 11 shows continuous-line boundaries of P_i for various values of X'_d, above which instability occurs on the first swing. For values of P_i below these boundaries, instability occurs on the second or subsequent rotor oscillations until the dotted boundaries for the corresponding values of X'_d are reached. For these

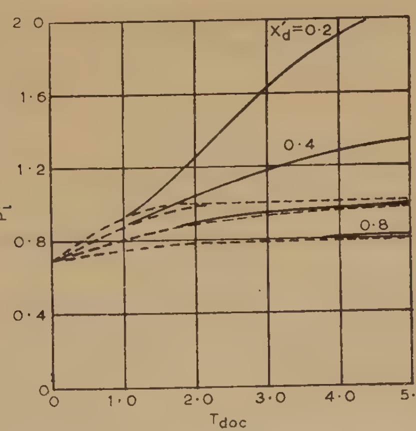

Fig. 11.—Boundaries for second-swing instability.

values of P_i the system is ultimately stable. From Fig. 11 it can be seen that the extent of the region in which instability subsequent to the first swing can occur decreases as X_d' increases. For $X_d' = 0{\cdot}8$ the region has almost vanished, which is in accordance with the approximate theoretical explanation presented above.

(4.4) Damping Proportional to Rate of Change of Rotor Angle

It is desirable to determine the amount of damping proportional to $d\delta/dt$ necessary to make the stability limit with varying-field flux linkage equal to that with constant-field flux linkage.

To illustrate this, the value of X_d' in the computer was adjusted so that the maximum value of P_i which resulted in a stable solution with constant-field flux linkage was not greater than the maximum power which could be transmitted under steady-state

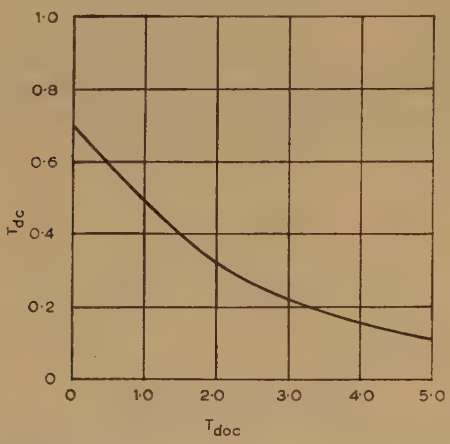

Fig. 12.—Amount of damping necessary to maintain stability.

conditions. Fig. 12 shows the amount of damping which was necessary to maintain stability as the field time-constant was decreased.

(4.5) Transmission-Line Faults

The problems which follow are more closely related to actual system operation. Fig. 13 shows the amount of power which

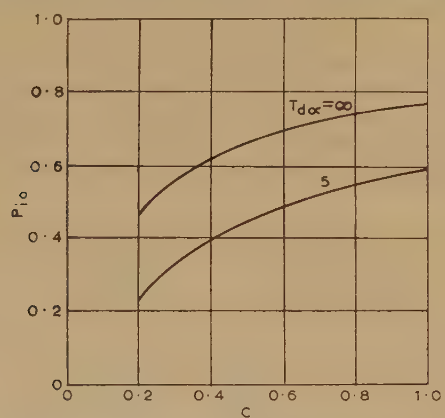

Fig. 13.—Maximum power transmitted by faulted transmission system —no clearing.

can be transmitted by two transmission lines in parallel, when a 3-phase earth fault occurs on one of them, so that stability is maintained. The parameter c is a measure of the distance of the fault from the machine terminals, c being zero at the machine terminals and unity at the infinite system. It is therefore a measure of the intensity of the disturbance, since faults at the machine terminals are most severe.

Computation is commenced with the values of the parameters under the fault conditions set in. These values are obtained by applying Thévenin's theorem to the transmission system shown

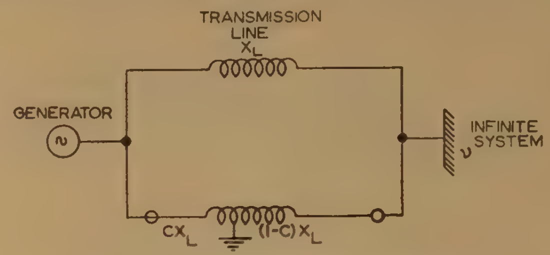

Fig. 14.—Faulted transmission system.

in Fig. 14, which reduces to a series reactance X_t connected to an equivalent bus voltage kv. The values of X_t are given by

$$X_t = \frac{c}{1+c}X_L$$

and

$$k = \frac{c}{1+c}$$

The values of X_d and X_q are summarized as follows:

(*a*) *Before a fault*

$$X_d = X_{dm} + \frac{X_L}{2};\ k = 1$$

$$X_q = X_{qm} + \frac{X_L}{2}$$

(*b*) *During a fault*

$$X_d = X_{dm} + \frac{c}{1+c}X_L;\ k = \frac{c}{1-c}$$

$$X_q = X_{qm} + \frac{c}{1+c}X_L$$

(*c*) *Subsequent to clearing*

$$X_d = X_{dm} + X_L;\ k = 1$$

$$X_q = X_{qm} + X_L$$

The values of the system parameters used are $X_{dm} = 0{\cdot}6$, $X_{qm} = 0{\cdot}4$, $X'_{dm} = 0{\cdot}2$, $X_L = 0{\cdot}8$.

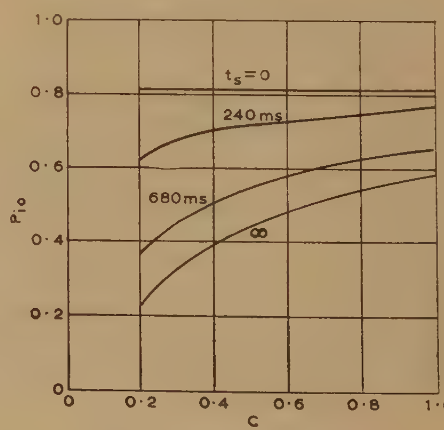

Fig. 15.—Effect of switching time on power transmitted.

$T_{doc} = 5.$
t_s = Switching time.

Fig. 15 shows the power which can be transmitted under the same conditions as before, when circuit-breakers are used to clear the faulted line section. The power which can be transmitted increases with faster operation of the circuit-breakers.

(5) CONCLUSIONS

The use of a d.c. electronic analogue computer is an ideal method of simulating synchronous machines in power systems for stability studies. The authors have reached the stage of allowing for variations in the field flux and have shown that this can have an appreciable effect on stability. It has also been shown that instability subsequent to the first rotor oscillation can occur. In cases where changes in field flux linkage and saliency effects are not important, the simple analogue provides accurate and rapid evaluation of system swing curves. Where these factors are important, e.g. in the study of voltage-regulator action on stability, the more exact representation is useful. An additional analogue for the voltage-regulator loop can be added to the equipment to provide the field terminal voltage. Similarly effects due to speed governing of the prime mover could be determined by an additional analogue.

An additional function of the machine analogue would be its use in connection with a network analyser, which would allow investigations of more complex transmission systems to be carried out. This involves a transformation of d.c. quantities to a.c. quantities; the control in magnitude and phase of the voltages applied to the network analyser would be exercised by the magnitudes of the field voltage and the prime-mover torque.

(6) ACKNOWLEDGMENTS

The authors are grateful to Dr. J. R. Mortlock for his comments on the first draft of the paper. They wish to thank Professor J. M. Meek for his interest in the work and for facilities provided in laboratories of the Electrical Engineering Department of Liverpool University. They are also indebted to Mr. J. W. Lynn for his advice and to the Central Electricity Authority for financial support.

(7) REFERENCES

(1) PARK, R. H.: 'Definition of an Ideal Synchronous Machine and Formula for the Armature Flux Linkages', *General Electric Review*, 1928, **31**, p. 332.

(2) PARK, R. H.: 'Two Reaction Theory of Synchronous Machines, Generalised Method of Analysis, Part I', *Transactions of the American I.E.E.*, 1929, **48**, p. 716.

(3) PARK, R. H.: 'Two Reaction Theory of Synchronous Machines, Part II', *ibid.*, 1933, **52**, p. 352.

(4) GRISCOM, S. B.: 'A Mechanical Analogy of the Problem of Transmission Stability', *Electric Journal*, 1926, **23**, p. 230.

(5) BERGVALL, R. C., and ROBINSON, P. H.: 'Quantitative Mechanical Analysis of Power System Transient Disturbances', *Transactions of the American I.E.E.*, 1928, **47**, p. 915.

(6) GREENWOOD, A.: 'A Simple Mechanical Analogue for Solving Certain Power-System Stability Problems', *Electrical Engineering*, 1954, **73**, p. 879.

(7) BYRD, H. L., and PRITCHARD, S. L., JR.: 'Solution of Two Machine Stability Problem', *General Electric Review*, 1933, **36**, p. 81.

(8) LONGLEY, F. R.: 'The Calculation of Alternator Swing Curves—The Step-by-Step Method', *Transactions of the American I.E.E.*, 1930, **49**, p. 1129.

(9) PRESCOTT, J. C.: 'The Transient Stability of Alternators: A Graphical Solution of the Two-Machine Case', *Proceedings I.E.E.*, Monograph No. 48 S, September, 1952 (**99**, Part IV, p. 367).

(10) SUMMERS, J. H., and MCCLURE, J. B.: 'Progress in the Study of System Stability', *Transactions of the American I.E.E.*, 1930, **49**, p. 132.

(11) LYON, W. V., and EDGERTON, H. E.: 'Transient Torque Angle Characteristics of Synchronous Machines', *ibid.*, 1930, **49**, p. 686.

(12) BOAST, W. B., and RECTOR, J. D.: 'An Electric Analogue Method for the Direct Determination of Power System Stability Swing Curves', *ibid.*, 1951, **70**, p. 1833.

(13) MORTLOCK, J. R.: 'A Computer for Use in Power-System Transient Stability Studies', *Journal I.E.E.*, 1948, **95**, Part II, p. 751.

(14) KANEFF, S.: 'A High-Frequency Simulator for the Analysis of Power Systems', *Proceedings I.E.E.*, Paper No. 1497 M, August, 1953 (**100**, Part II, p. 405).

(15) ROBERT, R.: 'Micromachines and Micronetwork Study of the Problems of Transient Stability by the Use of Models Similar Electromechanically to Existing Machines and Systems', C.I.G.R.É., Paris, 1950, Paper No. 338.

(16) KORN, G. A., and KORN, T. M.: 'Electronic Analogue Computers' (McGraw-Hill, 1952).

(17) BURT, E. G. C., and LANGE, O. H.: 'Function Generators based on Linear Interpolation', R.A.E. Technical Note No. G.W., 244.

(18) PARTON, J. E.: 'A note on the Equal Area Stability Criterion', *Proceedings I.E.E.*, Monograph No. 31 S, March, 1952 (**99**, Part IV, p. 187).

(8) APPENDICES

(8.1) Derivation of the Equations of a Synchronous Machine connected by a Transmission Line to an Infinite System when Constant Flux Linkage is not assumed

Park's equations[2] for the system are as follows:

$$v_{fd} = R_{fd}i_{fd} + p\psi_{fd} \quad . \quad . \quad . \quad . \quad . \quad (30)$$

$$v_d = R_d i_d + p\psi_d - \psi_q p\theta \quad . \quad . \quad . \quad . \quad (31)$$

$$v_q = R_q i_q + p\psi_q + \psi_d p\theta \quad . \quad . \quad . \quad . \quad (32)$$

where

$$\psi_{fd} = X_{fd}i_{fd} + X_{ad}i_d \quad . \quad . \quad . \quad . \quad . \quad (33)$$

$$\psi_d = X_d i_d + X_{ad}i_{fd} \quad . \quad . \quad . \quad . \quad . \quad . \quad (34)$$

$$\psi_q = X_q i_q \quad . \quad . \quad . \quad . \quad . \quad . \quad . \quad . \quad (35)$$

and

$$v_d = v \sin \delta, \; v_q = v \cos \delta$$

X_d is the total inductance in the direct axis, being the sum of the machine direct-axis self-inductance X_{dm} and the transmission-line series inductance X_t. Similarly

$$X_q = X_{qm} + X_t$$

These equations apply to an ideal machine with no quadrature-axis rotor circuits or amortisseur windings.

The equation of motion of the machine in terms of torque is

$$T_i = I\frac{d^2\delta}{dt^2} + T'_d\frac{d\delta}{dt} + T_0 \quad . \quad . \quad . \quad . \quad (36)$$

It is assumed that the speed change during a transient which results in the machine remaining in synchronism is a negligible percentage of fundamental speed; then $p\theta$ is constant. The equation of motion of the machine in terms of power is then

$$P_i = M\frac{d^2\delta}{dt^2} + T_d\frac{d\delta}{dt} + P_0 \quad . \quad . \quad . \quad . \quad (37)$$

where $$P_0 = (\psi_d i_q - \psi_q i_d)p\theta \quad . \quad . \quad . \quad . \quad . \quad (38)$$

It is assumed that the voltages induced in the armature by the rate of change of armature flux linkages are negligible compared with the voltages generated by these fluxes rotating at fundamental speed, i.e. $p\psi_d$ and $p\psi_q$ are negligible.

Armature and transmission-line resistance is assumed to be negligible, and thus $R_d i_d$ and $R_q i_q$ are zero.

Eqns. (31) and (32) become

$$v_d = -\psi_q p\theta = -X_q i_q p\theta \quad . \quad . \quad . \quad . \quad (39)$$

$$v_q = \psi_d p\theta = (X_d i_d + X_{ad} i_d)p\theta \quad . \quad . \quad . \quad (40)$$

From eqn. (33),

$$i_{fd} = \frac{\psi_{fd} - X_{ad} i_d}{X_{fd}} \quad . \quad . \quad . \quad . \quad . \quad . \quad (41)$$

then $$X_{ad} i_{fd} = \frac{X_{ad}}{X_{fd}}(\psi_{fd} - X_{ad} i_d) \quad . \quad . \quad . \quad . \quad (42)$$

Define $$I_{fd} = X_{ad} i_{fd} p\theta \quad . \quad . \quad . \quad . \quad . \quad . \quad (43)$$

and $$\Psi_{fd} = \frac{X_{ad}}{X_{fd}}\psi_{fd} \quad . \quad . \quad . \quad . \quad . \quad . \quad (44)$$

Substitution of eqns. (43) and (44) in eqn. (42) gives

$$\frac{I_{fd}}{p\theta} = \Psi_{fd} - \frac{X_{ad}^2}{X_{fd}} i_d \quad . \quad . \quad . \quad . \quad . \quad . \quad (45)$$

But $$X_d - \frac{X_{ad}^2}{X_{fd}} = X'_d \quad . \quad . \quad . \quad . \quad . \quad . \quad (46)$$

where X'_d is defined as the total direct-axis transient inductance. Therefore, from eqn. (46), eqn. (45) becomes

$$\Psi_{fd} = \frac{I_{fd}}{p\theta} + (X_d - X'_d)i_d \quad . \quad . \quad . \quad . \quad (47)$$

Also from eqns. (43) and (34),

$$\psi_d = X_d i_d + \frac{I_{fd}}{p\theta} \quad . \quad . \quad . \quad . \quad . \quad . \quad (48)$$

which, from eqn. (40), gives

$$v_q = X_d i_d p\theta + I_{fd} \quad . \quad . \quad . \quad . \quad . \quad . \quad (49)$$

Multiplying eqn. (30) by $\dfrac{X_{ad}}{X_{fd}}$ gives

$$p\Psi_{fd} = v_{fd}\frac{X_{ad}}{X_{fd}} - \frac{R_{fd}}{X_{fd}} I_{fd} \quad . \quad . \quad . \quad . \quad (50)$$

When the machine is on open-circuit and operating under steady-state conditions, i.e. $i_d = i_q = p = 0$

$$v_d = 0$$

$$v_q = \frac{v_{fd}}{R_{fd}} X_{ad} p\theta$$

Hence the magnitude of the machine terminal voltage, which is given by $\sqrt{(v_d^2 + v_q^2)}$, is $\dfrac{v_{fd}}{R_{fd}} X_{ad} p\theta$

This quantity is denoted by V_{fd}.

Hence eqn. (50) becomes

$$p\Psi_{fd} = \frac{V_{fd} - I_{fd}}{T_{d0} p\theta} \quad . \quad . \quad . \quad . \quad . \quad (51)$$

where $T_{d0} = \dfrac{X_{fd}}{R_{fd}}$, which is the field time constant.

The power output of the machine is, from eqns. (34), (35) and (38),

$$P_0 = [(X_d i_d + X_{ad} i_{fd})i_q - X_q i_q i_d]p\theta \quad . \quad . \quad (52)$$

or $$P_0 = i_q[I_{fd} + i_d(X_d - X_q)p\theta] \quad . \quad . \quad . \quad (53)$$

Define a quantity V_Q such that

$$V_Q = I_{fd} + i_d(X_d - X_q)p\theta \quad . \quad . \quad . \quad . \quad (54)$$

then eqn. (53) becomes

$$P_0 = V_Q i_q \quad . \quad . \quad . \quad . \quad . \quad . \quad . \quad (55)$$

Eqns. (51), (47), (39), (54), (49), (55) and (37) are simulated in the analogue computer and are summarized in Section 2.2. In summarizing these equations the per-unit system is introduced, so that $p\theta$ becomes equal to unity and inductances are numerically equal to the reactances.

(8.2) Derivation of Equations for Ψ_{fd} and P_0 in Terms of Operating Conditions and System Parameters

For the problems involving faulted transmission lines, more convenient expressions for Ψ_{fd} and P_0 are required than those given by eqns. (47) and (55).

Solving for i_d from eqn. (49) gives

$$i_d = \frac{v_q - I_{fd}}{X_d} \quad . \quad . \quad . \quad . \quad . \quad . \quad (56)$$

Substituting eqn. (56) in eqn. (49),

$$\Psi_{fd} = v_q\left(1 - \frac{X'_d}{X_d}\right) + I_{fd}\frac{X'_d}{X_d} \quad . \quad . \quad . \quad . \quad (57)$$

In the steady state at the instant before a disturbance, from eqn. (51),

$$I_{fd} = V_{fd} \quad . \quad . \quad . \quad . \quad . \quad . \quad . \quad (58)$$

and since $$v_q = v\cos\delta_0$$

$$\Psi_{fd0} = v\cos\delta_0\left(1 - \frac{X'_d}{X_d}\right) + V_{fd}\frac{X'_d}{X_d} \quad . \quad . \quad . \quad (59)$$

Solving eqn. (55) in terms of Ψ_{fd} and δ gives

$$P_0 = \frac{\Psi_{fd}}{X'_d} v\sin\delta - v^2\frac{(X_q - X'_d)}{2X_q X'_d}\sin 2\delta \quad . \quad . \quad (60)$$

or in terms of I_{fd}

$$P_0 = \frac{I_{fd}}{X_d} v\sin\delta - v^2\frac{(X_q - X_d)}{2X_q X_d}\sin 2\delta \quad . \quad . \quad (61)$$

In the steady state, since $I_{fd} = V_{fd}$

$$P_0 = \frac{V_{fd}}{X_d} v\sin\delta - v^2\frac{(X_q - X_d)}{2X_q X_d}\sin 2\delta \quad . \quad . \quad (62)$$

(8.3) Equation of Motion for Simplified Stability Problem

If it is assumed that the field flux linkage ψ_{fd} remains constant during a disturbance and that the quadrature-axis synchronous reactance is equal to the direct-axis transient reactance, i.e. $X_q = X'_d$, then from eqn. (60),

$$P_0 = \frac{\Psi_{fd0}}{X'_d} v\sin\delta = P_m\sin\delta \quad . \quad . \quad . \quad . \quad (63)$$

where Ψ_{fd0} is proportional to the initial field flux linkage. The equation of motion then becomes

$$P_i = M\frac{d^2\delta}{dt^2} + T_d\frac{d\delta}{dt} + P_m\sin\delta \quad . \quad . \quad . \quad (64)$$

DISCUSSION ON THE ABOVE TWO PAPERS AND ON 'DYNAMIC OPERATION OF AN A.C. NETWORK ANALYSER'* BEFORE THE SUPPLY SECTION, 28TH NOVEMBER, 1956

Mr. A. Chorlton: The major inaccuracy in the machine simulator described by Mr. Kaneff would seem to arise from representation of the machine impedance by a static network. Although the author promises to account for the effects of saturation by modifying the machine impedance with time, the method still rests on the validity of the constant-flux theory. The representation might be satisfactory for the first-swing conditions, but the inaccuracies might increase in the study of subsequent behaviour, and stability problems involving fluctuating loads would entail studies beyond the first swing. Adjustment of the machine impedance would be required for the study of asynchronous operation, otherwise precalibration would be necessary. In such circumstances the merit of including second-order effects such as voltage regulation, exciter response and governor action would become questionable. If asynchronous operation can be simulated, can the equipment also be used for the study of transient behaviour of induction motors, since problems of this character are becoming increasingly significant?

Sub-transient effects and machine losses are not mentioned, yet these would probably have the greatest effect on accuracy during the first swing. I agree, however, that the absolute error should be small enough for all practical purposes, the most important requirement in my view being consistency in the results obtained.

The device should prove suitable for application to most a.c. network analysers and useful where only first-swing conditions are required and asynchronous phenomena can be studied, particularly since the actual steady-state conditions are set automatically.

The analogue method described by Messrs. Aldred and Doyle seems to suffer from the same limitations as Mr. Kaneff's instrument in requiring a time scale which differs from actual time and using constant impedance for machine representation. While future work is promised to allow for voltage control, it would be interesting to know whether the use of actual components is envisaged or whether it is intended to simulate regulator action.

Mr. T. M. Whitelegg: The problems associated with synchronous machines can be divided into two groups, namely those in which the performance of the machine and its control systems are of prime interest and in which the effects of the external system are of second-order importance, and those in which the system is of primary importance, and whereas a reasonably accurate representation of the machine is required not too much detail is necessary. When the machine itself is of prime interest, the equipment described by Messrs. Aldred and Doyle is more flexible and probably offers more scope for development; but when the system is of prime interest, the electro-mechanical analogue would seem to be more appropriate. In any case, there must be an exchange of information and results between the various types of equipment; and results based on more accurate representation of machines must be made available, to ensure that the assumptions made in using network analysers are related to the truth.

The inherent accuracy required for the apparatus could be debated at great length, but the most important feature is repeatability and day-to-day accuracy. An analyser used commercially must be immediately available every day. We should not have to calibrate various items of the apparatus every morning —once a month, or every six months, should suffice: repeatability of accuracy is therefore most important.

In the past we have been satisfied with one or two swing curves on a system, and by means of interpolations and, in certain cases, extrapolations, we have estimated the stability limit. When the machine analogue devices are available, we should be able to determine the stability limit accurately and produce our results in the form, not of swing curves, but of boundary conditions for critical stability. I should like to add a note of warning that, when the simulators are available, we shall require rather more data on the systems than before. There is still in some parts a feeling that a problem can be set up on a network analyser without knowing what the problem is. This is not so, and the introduction of machine simulators will not change the situation. The more accurate data there are, the more accurate will be the results.

Mr. P. G. Kendall: A further gain in accuracy over step-by-step methods to be obtained from the use of the simulator is the avoidance of errors in calculation and in the reading of meters and setting of dials which results from the ordinary hand operation of a network analyser for the purpose.

Although it is necessary to have repeatable results (one can have no faith in a machine that gives different answers on different occasions), it is essential that the results when repeated should reasonably relate to the truth. Thus the paper by Messrs. Aldred and Doyle is very valuable in that it investigates the influence of some factors which are normally ignored in these investigations.

Section 4.3.1 of the paper by Messrs. Adamson, Nellist and Barnes states that the d.c. output of the wattmeter has a certain function if the square waves have sensibly vertical sides and high amplitude. Another very necessary condition is that the square waves have unity mark/space ratio. This may, by the occurrence of even harmonics in the waveform, not always be quite true.

The authors state that the potentiometer which multiplies the $I \cos \phi$ factor by V requires manual adjustment of the control prior to each swing-curve study. If the amplitude adjustment of the generator e.m.f. is by means of a potentiometer, this further potentiometer might reasonably be ganged to it and so be adjusted automatically.

Mr. G. Lyon: The step-by-step method of plotting swing curves for transient stability studies has two disadvantages, namely uncertain accuracy and excessive duration. It would be convenient, but it is not necessary, to eliminate both drawbacks by one method.

Theoretical comparison and field experience both suggest that the errors in conventional solutions are substantially less than those in the data, and a more refined method is not needed for the bulk of stability surveys. On the other hand, the assessment of the merits of different designs of synchronous machine, and of different control schemes, does require the more refined representation of one or two machine groups. The apparatus for this purpose, which is likely to be complicated and expensive, therefore needs to cater for only two or three machine groups, provided that the rest of the system and machines can be included with normal accuracy. The single machine against an infinite busbar serves to demonstrate a method, but it does not permit an economic assessment of the relative value of alternative machine designs in the development of a complete system.

In conventional stability surveys both the swing-curve calculations and the analyser readjustments occupy much time. Automatic generator simulators (even a simple design) would reduce the time sufficiently to enable adequate surveys to be made as a routine matter, and most analyser owners would consider justified

* KANEFF, S.: Paper No. 1847 S, October, 1955 (see 102 A, p. 597).

an extra equipment cost of about 10% (as quoted by Mr. Adamson and also in some of the references). I do not believe that this cost would cover equipment providing an accuracy higher than is obtained at present.

About six years ago I suggested that network analysers were ripe for the introduction of automatic elements. The prototype simulators have tended to be disappointingly complicated, but I am convinced that future simulators will be more elegant and compact, and thus cheaper and more easily maintained. Static analysers will give surprisingly satisfactory service with perfunctory maintenance, but this is unlikely to be true of high-precision dynamic elements.

It is desirable that further work should produce, on the one hand, the most simple and economical device for routine surveys—perhaps a simulator or a digital auxiliary computer—and, on the other hand, the most comprehensive and accurate device for special studies and control problems—perhaps an elaborate simulator or an analogue-computer addition for network analysers. Recognition of a division of interest at present could well lead to a corresponding division of labour during the next stage of development.

Mr. P. D. Aylett: There seems to be no satisfactory definition of what we mean by 'stability following a disturbance'. After a fault the system oscillates in some way, and at a chosen time we see whether the relative angles are diminishing. But there is no definite criterion available for multi-machine systems. The use of analogues may increase our difficulties, for systems may appear stable and then become unstable later; because of the long periods being covered in an extended study, we may be unable to tell whether there has been some drift in an amplifier or whether a component is giving trouble.

Recent analysis of the non-linear differential equations simulated shows that one can establish an integral whose values for the velocities and angles of the machines at a particular time determine whether the system is stable. This may make digital computers more useful than analogue computers, in that only the value of the integral need be obtained from the digital machine to determine stability. The problem of transient stability is essentially that of deciding, when looked at in the phase space of velocities and angles, whether the system as a whole will tend towards stable or unstable equilibrium.

Fig. 9 of the paper by Messrs. Aldred and Doyle gives the starting point between 0·4 and 0·8; recent experiments with the N.P.L. differential analyser gave 0·7242, the calculated value being 0·7246.

It is most important that the damping of synchronous machines should be included in the analogue. Tests show that turbo-alternators have damping-torque coefficients of 100–200 (in per-unit-kVA/per-unit-slip). This leads one to believe that whatever the fault, provided that the system after a fault has a position of steady-state stability and damping exceeds a critical value, the machine will always resynchronize. The problem of transient stability then becomes one of deciding whether the machine has adequate damping. Since the damping is as much a function of the system parameters as the synchronous torque, if we are to construct accurate analogues it is essential to have an accurate representation of the induction generator characteristics.

Mr. R. A. Hore: The availability of these simulators brings us to a position where we can with reasonable labour—though not, perhaps, at very reasonable expenditure—take into account the majority of refinements in synchronous-machine representation, but since the refined simulation is expensive, it is important to appreciate its significance.

The precise answer one requires from a transient-stability study is usually the critical load which the system will carry, without loss of synchronism, following a system disturbance. Of the three types of disturbance listed by Messrs. Adamson, Barnes and Nellist, the fault is the most serious, and Table A relates to this type of disturbance. The effects of neglecting saliency, etc., can be expressed as errors in the estimate of critical power; a positive error means that the estimate exceeds the correct value.

Table A

Factor	Typical error	Maximum error	Type
	%	%	
Integration errors ..	+2 to −5		Random
System reactance (errors in data)	±4	±8	Random
Neglecting saliency	−3·5	−14	Assessable
Neglecting damping	−1	−3	Assessable
Neglecting air-gap flux decrement	+3·5	+17	Assessable

The typical errors can, of course, be added, and it appears that, in general, the use of the constant-flux-linkage theorem results in negligible errors (about 1%). The maximum errors cannot be added, since they occur under different conditions. Occasionally, therefore, it may be desirable to take into account one or more refinements in representing a machine.

Simulator units or accurate numerical methods can eliminate integration errors, but in considering refinements one must bear in mind system reactance, and the question of load. The prediction of the loads for planning analysis cannot be made more accurately than, say, ±10%, or, to put it another way, ±1 year in the date at which a certain load will be reached.

The above estimates are confirmed by Figs. 9, 13 and 15 of the paper by Messrs. Adamson, Nellist and Barnes and Figs. 8 and 9 of that by Messrs. Aldred and Doyle. In Fig. 8 of the latter K_c is not likely to exceed 0·03, and in Fig. 9 T'_{d0} is usually between 6 and 12 sec (even B.S. 2658 uses T'_{d0}; to use T_{d0} with T_d for a damping coefficient invites confusion).

The possibility of overlooking second-swing instability does not seem very serious. Steady-state studies ensure that the system is stable when the decay of flux is complete. Even if such stability depends on voltage-regulator action, it is an easy matter to find the minimum flux (and the time at which it occurs) and then to determine the worst condition for the machine to maintain synchronism, representing the machine as a voltage behind a reactance.

Mr. K. M. Jones: The high-speed features of the simulators described will be welcomed by those concerned with network analysis on a commercial basis. I recall a study of a relatively simple system involving only four machine groups for which it was considered worth while to make about 80 swing-curve calculations to determine system limits. However, it is not only transient-stability studies which take a long time: the initial load balance on an analyser may take 2–3 hours, and subsequent balances about an hour each, depending on the number of generators in the system and the skill of the operator. As much time will be saved on load-flow problems as on transient-stability problems when simulators become available.

It is known that the method of representing loads can have a distinct bearing on the stability between generation sources on a power system. Particular types of load comprising large synchronous motors, if not too numerous, could be represented by the simulators described, and it should not be long before an induction-motor simulator is available. However, it will not be economical to use these simulators for all major load points in

the network, and it would therefore appear that there will be a demand for a simple device to represent the power/voltage characteristic of composite loads. Such a device should simulate the action of under-voltage relays, since this has an important effect on system stability.

Much has been said about extending the basic simulator to include the complete electrical characteristics of the synchronous machine. I agree that this should be treated as a separate problem, but one must be reasonably certain that the basic design of the simulator is capable of extension, if this is desired ultimately. I believe that the development of analogue devices for composite loads and induction motors should precede any further development of the synchronous-machine simulator required to include electrical effects.

In the simplified simulator described by Mr. Kaneff the saving in apparatus is not so great as would appear at first sight. If the load-voltage and current amplifiers can be dispensed with, this would apply to the original simulator also. However, I doubt whether the feed to the wattmeter current coil could come directly from a Selsyn, but it could be derived from the main buffer amplifier which will be required with either scheme to feed the analyser. I feel that, having regard to tachometer ripple and general noise effects, the use of the differentiator is the main disadvantage in the simplified scheme.

THE AUTHORS' REPLIES TO THE ABOVE DISCUSSION

Messrs. C. Adamson, L. Barnes and B. D. Nellist (*in reply*): The square wave to which Mr. Kendall refers is derived from the input to the generator output amplifier, where the total harmonic content is less than 1%: we are thus not concerned with variation in the mark/space ratio of the square wave. The V-multiplying potentiometer is ganged to the amplitude-adjusting potentiometer of the generator unit: this was omitted on the diagram for the sake of simplicity.

While we agree with Mr. Lyon's comments, we would point out that for routine work a simple analogue device is all that is required for stability studies or load-angle setting; for the more complex special studies and control problems, however, a digital computer, by virtue of its universality, when associated with a network analyser is likely to have much greater versatility than any complex analogue device. This approach is at present under investigation at the Manchester College of Science and Technology.

We agree with Mr. Hore that additional complexity and cost is hardly justified, in general, for assessing the performance of systems with regard to second-swing instability. This is an interesting problem, but we feel that additional expenditure would not be attractive to the owners of commercially operated network analysers.

In our laboratory, considerable attention has been paid to simulation of the electrical characteristics of synchronous machines. Whereas we would agree that simulation of composite loads and induction motors has priority from the aspect of commercially operated analysers, we would disagree for more general reasons. There are not enough workers considering these problems of simulation, and to state a particular priority in an arbitrary fashion is inappropriate, particularly since the transient performance of a synchronous machine cannot be determined conveniently by normal analytical method for cases other than connection to a single lossless reactance.

In our view, from the standpoint of a commercial analyser, the most important considerations are simplicity and low cost: recent experience in Manchester* has shown that simulators for the electrical transients on synchronous machines can be built for the same order of cost as the equipment described in our paper above. Furthermore, a very preliminary estimate of the cost of load-simulating devices shows that these would be of the same order also.

Mr. A. S. Aldred and **Dr. P. A. Doyle** (*in reply*): We would point out to Mr. Chorlton that, in the electronic analogue-computer representation of a synchronous machine, the analogue is not restricted to operate with a time scale different from unity. One main advantage is that the time scale can be changed with little difficulty, except when operating in conjunction with a real component of a system, when it must be fixed at unity. The inclusion of the field circuit in the analogue and the link between the field circuit and the direct-axis circuit [namely $-i_d(x_d - x_d')$ in Fig. 1] automatically allows the direct-axis reactance to change from its transient value to its synchronous value during a disturbance. Provided that information relating the variation of reactances with saturation is available, these non-linear effects could be simulated. In its present form, however, no attempt has been made to allow for saturation in the analogue. The work on the effects of continuous fast-acting voltage regulators on synchronous-machine performance is being carried out using a simulated regulator loop. Some results have already been obtained which should be available for publication shortly.

We agree with Mr. Whitelegg that the electronic analogue approach is most useful in providing information about how a machine behaves, as opposed to a complete system. It is more difficult to obtain information about system behaviour, because of the extreme complexity of complete system equations. Further work is necessary to establish satisfactory methods of coupling a machine analogue to a conventional a.c. network analyser, in order that the advantages of both analogues can be fully realized.

In common with Mr. Lyon we envisage a repetitive dynamic system analyser operating with a high base frequency with a repetition rate of, say, 20–30 solutions per second for continuous visual display. The initial high cost of electronic analogue equipment would to some extent be offset by the reduction in size of the network-analyser components. Research work along these lines is being carried out at Liverpool University, and a model 2-machine system is nearing completion. It is hoped to report on the results of this experiment in the near future.

We agree with Mr. Aylett that it is necessary to introduce damping characteristics in any analogue representation of a synchronous machine. This can be done either by including in the initial analysis equations for the windings which contribute to damping, or by the introduction of a quantity $T_d p\delta$ as a damping torque in the dynamic equation of motion of the machine. The first method would increase the size of the analogue considerably, but would have the advantage of accuracy: the second method is more simple, but is an approximation, since it appears that the coefficient T_d is not constant during a disturbance. This makes it difficult to assign the correct value to the damping coefficient, except for small disturbances, when damping torques can be evaluated by the method of small oscillations.

Mr. S. Kaneff (*in reply*): The problem of synchronous-machine representation, whether for power-system investigations or machine design purposes, is necessarily complex. The more factors that require representation and independent control, the greater the complexity and cost; moreover, higher cost must

* ADAMSON, C., and EL-SERAFI, A. M. S.: 'Simulation of the Transient Performance of Synchronous Machines on an A.C. Network Analyser', *Proceedings I.E.E.*, Monograph No. 222 S, February, 1957 (104 C).

accompany higher precision. These facts are sufficiently well known and should cause no surprise or dismay.

Compared with other computing aids (such as general-purpose analogue or digital computers), the number of electronic components used in the synchronous-machine simulation is very small. Moreover, the components are entirely practicable from the standpoint of reliability, and the desire to have apparatus which need not be calibrated every morning, but only every month or so, is met by suitable design.

In reply to Mr. Chorlton, it certainly is inaccurate to employ a static network to represent machine impedance: this was done merely to follow normal network-analyser practice. If a study requires more accurate representation, it is quite practicable in a simple manner to switch from subtransient to transient to synchronous impedance (and also to include machine losses). Certainly the method still rests on the validity of the constant-flux-linkages theory, again because this has been normal practice. It is hoped eventually to simulate regulator action.

In reply to Mr. Jones, the load-voltage and current amplifiers can be dispensed with in the original simulator; they were used originally because of the current requirements of the wattmeter. The feed to the wattmeter current coil could come directly from the Selsyn, so long as this had good regulation and could satisfactorily supply all current requirements, and so long as the wattmeter current coil had sufficiently low impedance. The advantage of the simplified scheme is that it requires no accurate Velodyne; its disadvantage is the noise effects on the differentiator, as suggested.

It should, perhaps, be mentioned that the purpose of the simulator under discussion has been to produce a device which can speed the setting-up and solution of present-day power-system problems, and at the same time be capable of adaptation to existing a.c. network analysers. Accordingly, there must necessarily be limitations in the representation of synchronous machines. The principle, however, may be employed for a much more detailed representation of synchronous machines, and recent work has indicated the possibility of representing induction machines by an extension of the methods. If purely electronic methods of representation are employed,* the simulator can operate on a cycle-to-cycle basis in the same manner as the actual machine. As stated by Mr. Whitelegg, there are two classes of problem, those involving power systems as a whole and those involving machines in particular: these classes require different degrees of simulation, and it is reasonable to expect that the methods of simulation may develop in different ways.

As has been suggested in the discussion, the inadequacies in power-system studies are at present in the degree of accuracy with which network and machine parameters are known, and not in the accuracy of solution. A simulator (or any computing aid) cannot be more accurate than the information available about the units being simulated, and the major problem seems to be in obtaining such information, rather than in devising more accurate computing aids. In the meantime, methods are available for speeding up solutions based on available information, so allowing a more thorough investigation of problems. For these reasons, is not the cost of added equipment justified?

* KANEFF, S.: 'A High-Frequency Simulator for the Analysis of Power Systems', *Proceedings I.E.E.*, Paper No. 1497 M, August, 1953 (100, Part II, p. 405).

621.3:656.25

Paper No. 2301
Apr. 1957

THE APPLICATION OF ELECTRICITY TO RAILWAY SIGNALLING

A Review of Progress

By R. DELL, Member.

(1) INTRODUCTION

The last review of progress on railway signalling* was made in 1949, and covered the period from the introduction of electricity into railway signalling to the time of publication. The present review can therefore conveniently continue from that date up to the present time.

The application of electricity to railway signalling has continued to make increasing progress, and the conversion from mechanical signals to colour-light signals, with power-operated systems making for the elimination of signalmen or the simplification of the signalman's work, has been growing.

(2) COLOUR-LIGHT SIGNALS

The standard system of aspects in use throughout British Railways provides for four indications: *red*, stop; *yellow*, proceed at caution, prepared to stop at the next signal, which is at danger; *double yellow*, proceed at caution, next signal at yellow and insufficient braking distance from the yellow light to the signal at red beyond; *green*, proceed.

Indication of the direction in which the points are set at junctions is given by means of a junction indicator, which comprises a line of lunar white lights mounted above the colour-light signal. The line of white lights may be at an angle of 45°, or at greater angles if there is more than one diverging route at the junction, and the plan of the lights is arranged either to the left or to the right of the colour-light signal, indicating the direction in which the train is to be diverted. A colour-light signal alone indicates that the train is signalled on the straight track, and a colour-light signal with the addition of a junction indicator indicates that the train is being diverted, generally over a lower-speed route.

Shunting movements are governed by subsidiary signals, which are of the position-light type or of the movable-disc type.

The two types of colour-light signals in use are

(*a*) *Searchlight signals.*—A single lamp and reflector, together with a clear projecting lens, are used, and a small moving member carries three small colour filters, which can be moved by means of the electrically operated mechanism to cause the beam to be coloured red, yellow or green.

(*b*) *Multi-lens signals.*—A separate lens and lamp are used for each colour, and the circuits for lighting the appropriate lamps are closed by contacts on the relays.

The searchlight-type signal permits lower-powered lamps to be used, because an elliptical reflector can be employed and the efficiency of collection of the light from the lamp is higher than with a lens. With the multi-lens type of signal a reflector cannot be employed, because of the risk of phantom lights from reflections of the sun or other sources. The lamps in multi-lens signals are almost invariably of the double-filament type, rated at 25 watts, although in some instances a lamp rated up to 33 watts is in use.

Methods of proving that the colour-light signal is alight vary. In some instances, reliance is placed on the use of the double-filament lamp and no other proving circuit is employed, but there is a tendency for proving circuits to be introduced. These generally comprise a circuit whereby a relay is energized in series with the filament of the lamp, and when the filament fails the relay causes a proving circuit to operate, which may cut in an auxiliary lamp or the auxiliary filament of a double-filament lamp. In some instances it is arranged to prevent the previous signal showing a clear aspect after the failure of the lamp filament.

(3) POINT OPERATION

Two methods of power operation of points continue to be used: in one an electric motor drives the point mechanism through gears, the direction of the rotation of the motor being reversed for the alternate movement of the points; in the other the power for the point operation is provided by compressed air acting on a piston in a cylinder, the admission of the air to the cylinder being controlled by electrically operated valves. Although electro-pneumatic operation of points dates back to the earliest installations of power signalling, there has been in subsequent years a tendency for the electric-motor-driven machine to be more favoured, since it avoids the need to provide a compressed-air supply. In more recent years, however, the greater simplicity of the electro-pneumatic system has again brought it into favour, and several large installations employing electro-pneumatic operation of points have been installed.

The complete security of the points against inadvertent operation while a train is passing over them is of great importance, and the fitting of an additional and separately operated lock to the point mechanism is becoming increasingly favoured. This ground track-lock is controlled by the track circuit, and because it is provided with an entirely separate circuit from that used for operating the points, it is a great safeguard in maintaining the points securely locked during the passage of a train. This track-lock (Fig. 1) is generally operated entirely electrically, an electromagnet withdrawing the lock, which is normally held in

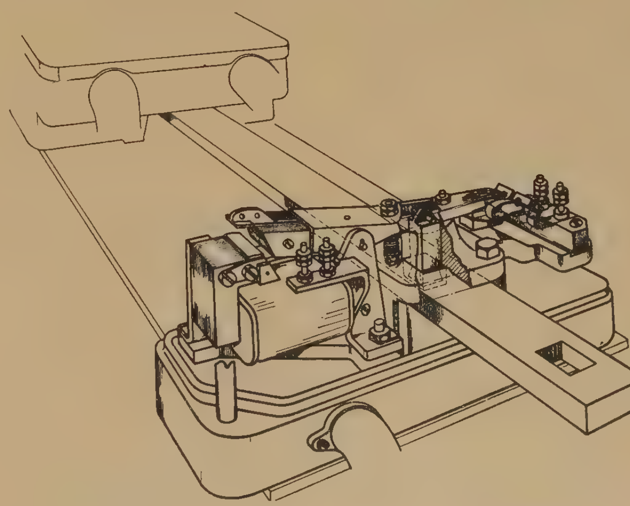

Fig. 1.—Ground track-lock fitted to points mechanism.

* Wood, W.: 'The Application of Electricity to Signalling for Railway Transport', *Proceedings I.E.E.*, 1949, 96, Part I, p. 34.

Mr. Dell is with the London Transport Executive.

position by gravity. Proving contacts are provided to ensure that the lock is secured before the signals are cleared. Recently, experiments have been in progress with the design of an electro-pneumatically operated lock for use where compressed air is available, since this type of equipment is better able to withstand the vibration experienced on the track.

(4) TRACK CIRCUITS

Most modern signalling installations include a.c. track circuits and, generally speaking, the design has been standardized in two forms. Where the demands of the d.c. return through the running rails are not too heavy, so that one rail will suffice for this purpose, or where the running rails are not used for traction return, the single-rail condenser-feed track circuit is employed. This circuit comprises a supply of power, generally at 100 or 110 volts, feeding in series through a tapped condenser to the track-circuit rail, with a relay connected at the far end of the track-circuit section; it gives a high train shunt—1 ohm or slightly more is generally achieved—and is extremely simple to adjust.

Where both running rails are required for the traction current return, impedance bonds must be provided at each end of the track circuit to enable the rails to be insulated into sections but to maintain a continuous path for the d.c. traction return. Fig. 2

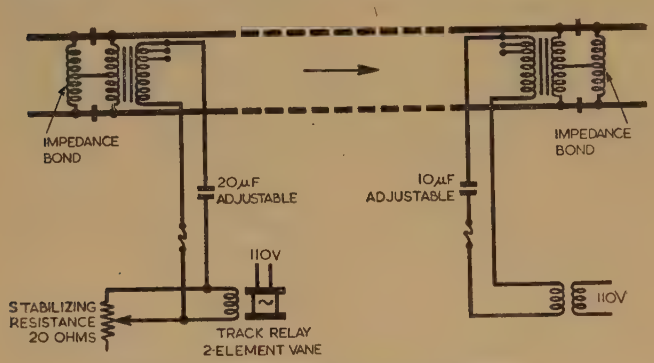

Fig. 2.—Track circuit for third-rail system.

shows a typical track circuit employing impedance bonds for the return current. The main winding of the bonds is connected directly between the two running rails, and although a large iron core is provided, only a few turns can be arranged on this winding, so that its impedance to the track-circuit current is low. It is thus the practice to provide additional windings, giving a step up in voltage, to which condensers are applied, producing a resonating effect on the impedance bonds and greatly increasing the impedance as affecting the track circuit operation. Advantage is taken of this winding to provide the connection for the feed and the relay, and as shown in Fig. 2, the condenser at the feed end performs the double purpose of resonating the circuit of the impedance bond and controlling the current entering the circuit from the 110-volt supply. At the relay end of the track circuit the relay is connected to the secondary winding on the impedance bond in series with the resonating condenser, and the comparatively high voltage of this circuit enables the relay to be placed at any convenient point, such as in the signal-cabin relay room, without serious loss in the cable from the track circuit. The use of resonated impedance bonds has rendered the track circuit sensitive to frequency variations, and the post-war variations in frequency of the Grid supply have been troublesome and have resulted in special machines being installed to correct the frequency of the power supply used for signalling.

For use with single-rail a.c. track circuits, where an improvement in train shunt is desired, a special arrangement using an

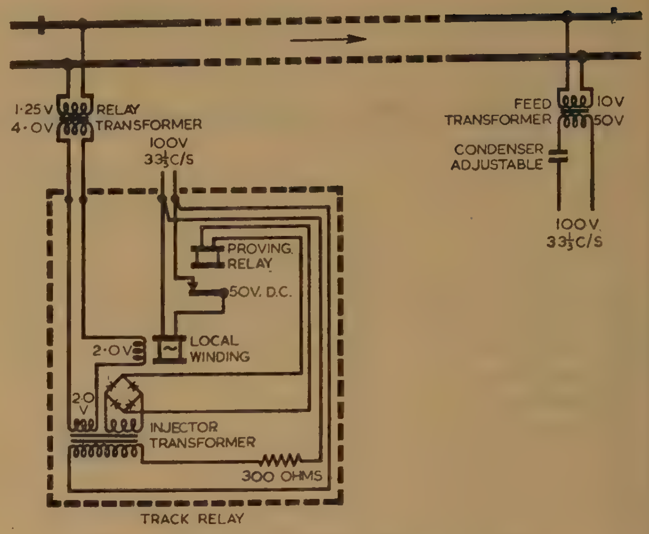

Fig. 3.—Track circuit with injector-type relay.

injector-type relay has been introduced. The injector relay contains a small transformer, the secondary of which is connected in series with the track winding, but the polarity is the opposite to that required to energize the relay. This opposing e.m.f. has to be overcome by the e.m.f. from the track circuit before the relay can be energized. In effect, this raises the percentage release value of the relay, which results in much higher train shunt being obtained, even with long track circuits. Fig. 3 shows a track circuit using an injector-type relay.

(5) RELAYS

The relays used for signalling circuits must meet stringent requirements with regard to reliability of operation, for there must never be any possibility of a relay failing to open its contacts when it is de-energized.

In some power signalling equipment, particularly for anything having moving parts, proving circuits are used to ensure the correct response under all conditions and to prevent any accident arising, even though it should fail to function as normally intended. Up to the present, however, it has not been possible to devise a really satisfactory proving circuit for many signalling relays, particularly the track-circuit relays, and the integrity of the signalling system therefore continues to depend entirely on the proper working of these relays.

Basically, the design of signalling relays has not changed very greatly over the last 30 years. The d.c. relay is of the attracted-armature type, with gravity release, the contact springs being mounted directly on the armature. A.C. relays are of the type with an aluminium vane working in the air-gap of one or more magnetic circuits. In a relay required only for circuit work a single-element winding suffices, and a typical relay, which would have six contacts to make when the relay was energized, would operate on 24 VA. In the track relay, however, the sensitivity must be much higher than can be obtained by a single-element magnetic circuit: a double winding is therefore used, one winding producing no torque in the aluminium vane but most of the power for its operation when the flux is combined with a flux produced by a control winding. A typical a.c. track relay, with six contacts making when the relay is energized, would use 33 VA on its local winding, but the control winding would give full operation of the relay on 0·5 VA.

A particular feature of the contacts used for signalling relays is that there must be an absolute safeguard against the possibility

of contacts welding together. For this purpose, one of each pair of contacts is always made of carbon, the usual material for the second at present being silver.

With the introduction of larger signalling installations, ready means of disconnecting the relays for servicing became necessary, and detachable terminal tops have thus been introduced to permit all the wire connections to be left in place while the relay is removed. With a similar objective, plug-in relays have also been introduced recently, the connections being brought out to plugs inserted into a socket mounted in a vertical position on the relay rack, so that the relay can be drawn out and a spare inserted without disconnecting the wires from their permanent connections on the relay rack. Plug-in relays have been designed for both d.c. and a.c. circuits.

As a result of the use of circuit interlocking, special relays adapted to work with this system have been introduced. One particular design not only carries a large number of contacts for operation of the appropriate signalling circuits, but is provided with electrically operated locks acting on the main armature of the relay, these locks having their own operating coils. The main movement of the relay is thus prevented from responding, even though the main coil is energized, until the lock holding the armature has been released, thus performing some of the interlocking functions within the relay.

(6) CABLES

Signalling cables work under extremely arduous conditions, and the utmost reliability is required. For this reason, special cables are generally used, manufactured to specifications drawn up by British Railways. Those connecting the signal cabin to signal and points are generally lead-covered, with oiled paper or rubber insulation. Multi-core cables are sometimes connected to terminal boxes fitted beside the line, where it is required to make connections, while on the railways of London Transport, individual lead-covered cables are used for each circuit, with the lead sheath used as an earthed screen between circuits.

A new form of screened cable has recently been introduced for signalling circuits, providing a very high degree of security derived from its screening. Each pair of conductors comprises a central conductor, insulated by rubber or Neoprene, and a concentric conductor outside this insulation, in the form of a braided screen, this, in turn, being insulated by a thin layer of p.v.c. Each circuit is arranged so that its live side is connected to the inner conductor and its return side to the outer conductor or screen. In this way, the live conductors are entirely screened from one another and the possibility of any stray current, through a fault in the insulation, passing from one circuit to another is eliminated. A number of these screened conductors are made up in a cable, which is lead sheathed.

In the wiring of relay rooms associated with signal cabins, very large quantities of wire are used, and the avoidance of any risk of fire is important. For some years, therefore, considerable attention has been given to the development of a flameproof wire for this purpose, largely depending on a non-inflammable lacquer on the outside of the braiding. More recently, however, a wire having much higher fire-resisting properties has been introduced, on which the Neoprene insulation is covered on the outside with a braiding of glass fibre, the outside of this being coated with a non-inflammable lacquer. Should an external fire damage the wire, the glass braiding will maintain the insulation between the conductors, and the risk of current passing from one circuit to another under these conditions is greatly minimized.

The cables for connection to the track have particularly difficult working conditions, and rubber insulation is customary. Recently, however, a cable with a very substantial sheath of Neoprene has been developed for this purpose; it requires no protection other than its sheath and can therefore meet the difficult conditions of movement of the track more readily than cables mounted in steel pipes or concrete troughing. Fig. 4 shows details of these special cables.

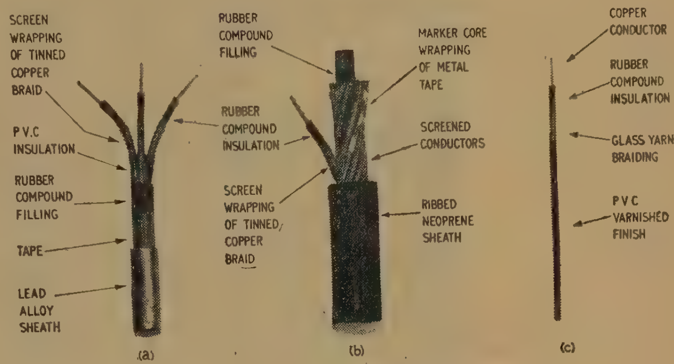

Fig. 4.—Signalling cables.

(*a*) 1/·064 in 3-core screened.
(*b*) 1/·064 in 10-core screened.
(*c*) 1/·052 in glass-braided flameproof.

An important feature introduced into the cables for connection to the track, and one making for long life, is the vulcanizing of the ends of the cable with a metal-to-rubber bond on to a suitable metal fitting forming part of a junction box or the case of the apparatus on the track. The vulcanizing yields an extremely waterproof joint and strengthens the cable at the point of entry to the case, which, without some such arrangement, tends to be a weak spot at which vibration is concentrated.

(7) SIGNAL-CABIN CONTROL METHODS

The use of power operation for signal cabins has now become almost the recognized standard, and mechanical signalling is installed only in the less important places. Progress has been towards the provision of easier operation by the signalman, and although power frames have continued to be installed in quite considerable numbers employing interlocked levers, most of which have adopted electrical interlocking, the tendency has been to provide most of the larger installations with thumb switches or pushbutton control for the signalman. Most of these employ circuit interlocking, although one trial installation has been made where the interlocking is achieved by means of rotary shafts carrying contacts, very similar to one form of automatic telephone exchange. It is claimed for this type of equipment that the interlocking tends to be simplified, since conflicting functions can be connected through contacts spaced at different positions on the same shaft, and interlocking between these circuits then becomes automatic, according to the position in which the shaft has stopped. More commonly, however, the equipment is provided with circuit interlocking by means of appropriate electrical circuits. With these, route control is usually employed, in which the setting of one thumb switch causes an entire route between two points on the layout to be set up, including the correct setting of the points and clearing the appropriate signals. In one form of installation, the route setting is done by pushbuttons instead of thumb switches, one at each end of the route having to be operated in order to determine the route to be set up. The thumb switches can be arranged either in a geographical layout by combining them with the illuminated diagram or on a separate panel. Both types continue to be installed, and while the geographical layout has some attractive features, mainly on the score of simplicity of learning the operation, the separate

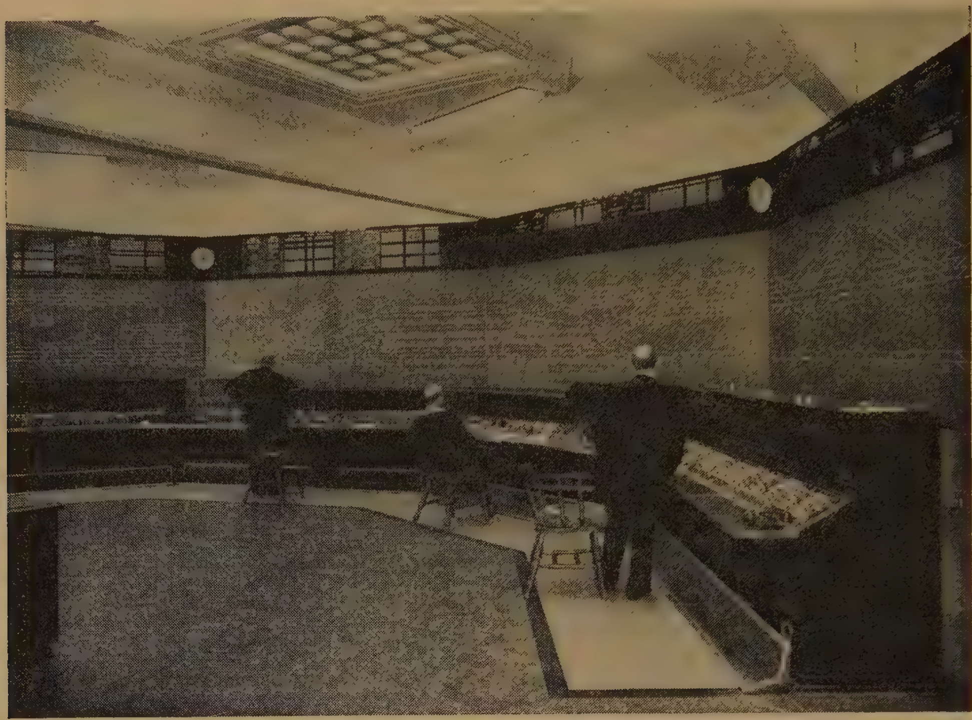

(a)

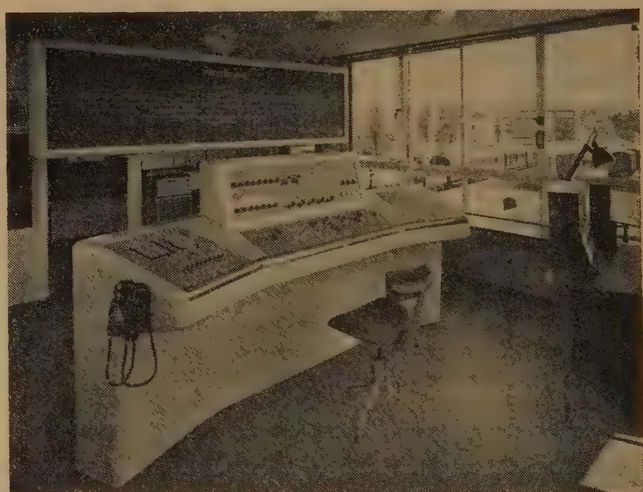

(b)

Fig. 5.—Contrast in control panels and illuminated diagrams.

(a) York: operating thumb-switches on separate panel.
(b) Potters Bar: thumb switch at route entrance, pushbutton at route end.

panel enables the thumb switches to be arranged more conveniently within the signalman's reach.

Fig. 5(*a*) shows the control panel at York, which is the largest circuit-interlocking installation in existence, and, in contrast, Fig. 5(*b*) shows the much smaller set at Potters Bar.

On London Transport, an interlocking machine has been introduced in place of circuit interlocking: it is controlled from a desk equipped with self-resetting pushbuttons, only one button movement being required for each route set up, and preselection has also been adopted, provision being made for storage of one movement ahead of the actual train movement in progress. The interlocking machine has mechanical interlocks and is arranged so that each shaft is operated through an angle appropriate to make or break the signalling contacts by one of a pair of small compressed-air cylinders controlled by electro-pneumatic valves actuated by the control circuits initiated by the pushbuttons. Such a machine enables much of the complicated circuit work to be carried out with less trustworthy, and therefore cheaper, equipment while maintaining the fullest integrity of the signalling circuits between the interlocking machine and the signalling equipment, such as points or signals.

(8) AUTOMATIC JUNCTION OPERATION

The automatic operation of points is not a new feature, and the automatic operation of a single crossover at the terminus of a line has been in operation at several places for as long as 30 years. More recently, much attention has been given to the possibility of the automatic setting of junctions where the route of the train has to be determined. In the United States a considerable amount of work has been done on a system of automatic indication of its destination from the train itself. This comprises a tuned coil carried on a train which, when it passes a coil mounted beside the track, causes an oscillation to be set up at the frequency of the train coil; thus, with train coils tuned to different frequencies, it is possible to indicate the different destinations, and junctions can be automatically set by this means. In this country, a noteworthy installation of automatic junction setting was installed by London Transport at Camden Town. The route to be taken by the train is signalled ahead of the train by means of the train describer used to advise passengers of the train's destination and was previously used to advise signalmen of the route to be set. In the Camden Town installation, the train describer is connected to the signalling equipment, so that the destination indicated for each train automatically causes the junction points to be set to the corresponding route and the signals cleared. There are four such facing junctions at Camden Town, all train-describer operated. The converging junctions cannot be operated from the train describer, but they are arranged to be set automatically on the

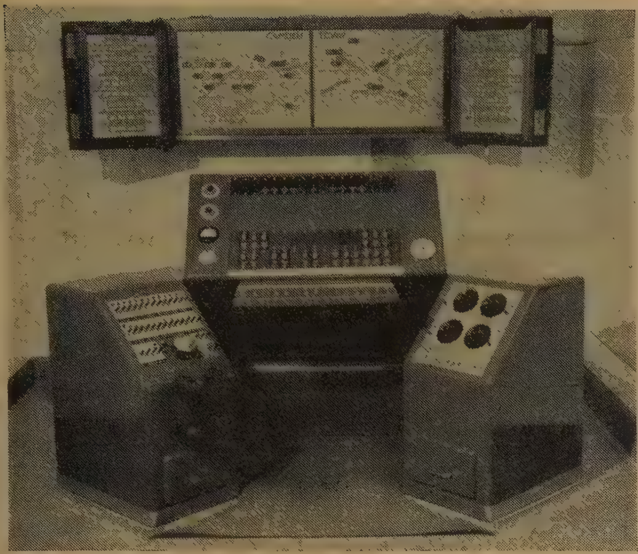

Fig. 6.—Auxiliary control desk with pushbutton operation, preselection and provision for full automatic junction working.

approach of the train, the first train to approach them causing the points to be set and the signals to be cleared for it. This installation is provided with an auxiliary panel of pushbuttons, so that, in the event of it being necessary to arrange the route of the train differently from that shown on the train describer or to change its destination, this can be done by manual operation of the pushbuttons.

Fig. 7 shows a typical circuit for automatic junction control by train-describer operation, the interlocking machine being represented by a single shaft near the centre of the diagram. All circuits to the right of this must be of the highest integrity, since the safety of the train operation depends upon them, but all circuits to the left only operate the compressed-air cylinder rotating the interlocking machine shaft, and thus, although reliable, do not need to be so highly trustworthy, the full protection for the traffic being provided by the interlocking machine.

The plan at the top of Fig. 7 shows the particular portion of track governed by this section of the signalling, and it will be observed that it is a simple diverging movement, the points being No. 19 and the signal No. 4. The signal is provided with a junction indicator, indicating to the driver the direction he will take over the points.

For full automatic operation a contact is provided, actuated by the train describer, and in this case, a Golders Green or Edgware description sets the points to the left, and an Archway, High Barnet or Finchley description sets the points to the right.

The relays 4LXR and 4RXR are the two governing the preselection of movement of the shaft of the interlocking machine, and these are controlled by the contact on the train describer, or by the contact of the pushbutton, if this is switched in by the key. Contacts on these two relays complete the appropriate circuit to energize either the normal or the reverse shaft cylinders.

(9) AUTOMATIC TRAIN CONTROL

In England automatic train control remains very much in the development stage. The mechanical system installed throughout the Western Region continues to operate successfully, but intensive trials are being carried out with an alternative system employing magnetic communication from the track to the train, and it is probable that this system will, in time, be adopted for British Railways generally. A noteworthy installation of auto-

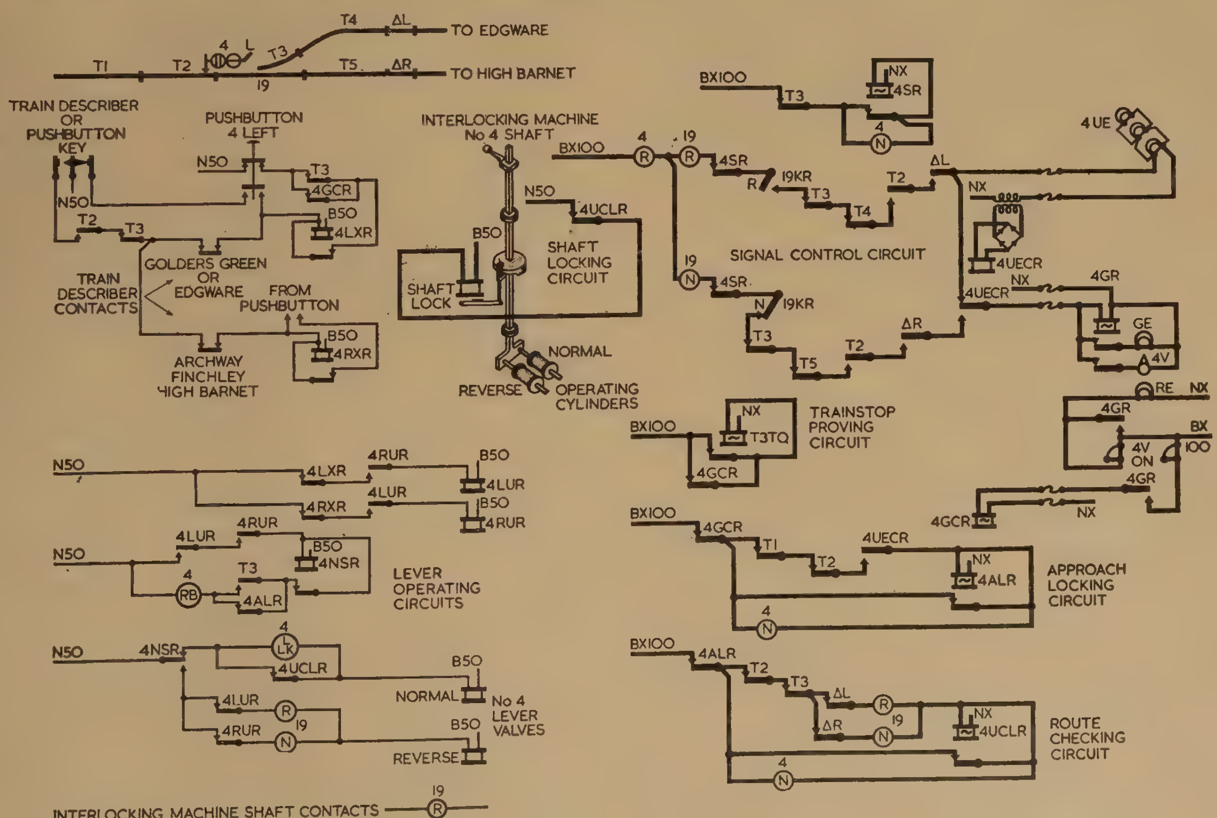

Fig. 7.—Typical circuits for train-describer and pushbutton control of automatic junction working.

matic train control, with cab signalling, has been installed in the subways at Stockholm; wayside signals have not been provided, except where there are junctions, and the trains run entirely under the control of the cab signalling system. The cab signal is a continuous one, operated by induced currents carried in the running rails and picked up by coils mounted on the front of each train and just above the running rails. The basic 75 c/s signalling supply is interrupted so as to provide a varying frequency of pulses or codes, the high-speed cab signal corresponding to 180, and the medium-speed signal to 75, pulses/min; the low-speed signal is given either by a steady supply at 75 c/s or by no current at all. The train is provided with a speed governor having settings at two speeds corresponding to the cab-signalling indication: if its speed exceeds the value indicated by the cab signal, an automatic brake is applied and the speed of the train reduced. Thus the driver can normally control his train in accordance with the indications of the cab signalling system, but the equipment automatically applies the brakes if he fails to observe these indications.

(10) SPEED-CONTROL SIGNALLING

A special form of signalling in which provision is made for measuring the speed of trains has been introduced by London Transport. This is a special arrangement and applicable only to an electrified railway having a very close service of passenger trains. Basically, the principle involves measuring the speed of an oncoming train, and if the speed has been reduced the signals are cleared so that the train may approach closer to a stationary train in front than would be safe unless the speed of the oncoming train had been so reduced.

The original installation provided for the measurement of train speed by timing it over a measured length of track circuit, by means of a specially designed time control relay. Very recently, a new method of measuring the speed has been introduced, in which the cast-iron shoe of the train, in passing over an inductor fixed on the track, generates a small current whose frequency is proportional to the speed of the train. After amplification, this current is used to operate a frequency-sensitive relay arranged to respond to any frequency below a set value, which generally corresponds to 25 or 20 m.p.h.

(11) TRAIN DESCRIPTION

Train describers are a necessary adjunct to power signalling, especially when the latter is used to reduce the number of signalmen required. A train describer is used to advise the signalman of the destination of a train approaching the signal box, and it can also be arranged to display signs for the information of passengers. Train describers were first introduced on the Underground Railways of London nearly 50 years ago, but since that time, improved designs have been used on the main-line railways.

The essential feature of a train describer is some means of storage of the descriptions. The earliest type used a mechanical drum capable of indicating up to 15 different descriptions and storing 32; it required four line wires and rail return, and was d.c. operated on a code-of-four system. Later designs used pulse codes for transmitting the descriptions from point to point, and hence only two line wires were required. In one system, storage is carried out by means of telephone-type uniselector switches combined with telephone-type relays: the number of descriptions stored is dependent upon the number of uniselectors provided, and in order to keep the amount of equipment reasonably low, it is the practice to retransmit automatically the descriptions from point to point as the train progresses. Another type employs a paper tape for storage. Holes are punched into the tape over a section, the punching of the holes determining the description to be given; no difficulty arises in providing facilities for a large number of train descriptions to be stored. Transmission by the signalman of the train descriptions is carried out either by operating a pushbutton or by setting a pointer on a dial. It is at present common practice for retransmission for a train passing a signal box to be carried out automatically, and in this instance the line on to which the transmission shall take place is determined by the set of the junction.

(12) AUTOMATIC TRAIN ANNOUNCER

On the Eastern Region an automatic train announcer has been installed and is arranged to reproduce standard announcements to coincide with the arrival of trains, without the operator having to continue to repeat the same message. The announcements are recorded on a loop of magnetic tape 3 in wide, and the reproducing head is moved across the tape by a selector mechanism so as to reproduce the appropriate announcement. The tape has a capacity of 25 recording tracks and is in the form of a continuous loop, 30 ft in length, driven at 7·5 in/sec. The joint in the tape is formed by a metal jointing piece, which also acts to close a contact as the joint passes, thus indicating that one complete announcement has been made and that the tape is at the beginning of any fresh announcement.

The apparatus is set by an operator pressing the appropriate button on a control panel, and storage is provided so that announcements can be preselected as trains approach. The announcement is set in operation when the train occupies suitably positioned track circuits, and it is normally in two parts—a 'train approaching' announcement and, after a suitable delay to permit the train to stop at the platform and the doors to open, a 'train standing' announcement. During a busy service, when there is not time for a double announcement, the 'train approaching' portion is automatically cut out.

An experimental installation was also made, some years ago, of an automatic train announcer operated direct from the train describer. Such an installation needs no operator.

(13) MECHANIZATION OF MARSHALLING YARDS

The introduction of mechanization into marshalling yards for goods wagons is a feature of growing importance in the operation of railways, and it has caused the introduction of a number of electrical devices to aid the operation of the sorting of the wagons.

A mechanized marshalling yard is constructed with a hump at the entrance to a fan of sidings, providing a down gradient of about 1 in 20 on which the trucks run by gravity. Track brakes or retarders are provided just below the hump, so that control can be exercised on the speed of wagons running down the slope. Points leading into the sidings are operated either electrically or electro-pneumatically and are specially arranged to move very quickly.

The method of working is that a train of goods wagons, which is being sorted according to the destination of the wagons, is first uncoupled so that the individual wagons or groups of wagons for the same destination are free to run separately, and then with a locomotive at the rear, the train is slowly propelled over the hump. As each wagon passes over the hump on to the down gradient, it begins to run by gravity and separately from the wagons behind. The wagons are directed into the appropriate siding according to their destination by operating the points between the wagons. The speed with which the wagons run down the incline must be sufficient to carry them to the extreme end of the siding, but as the sidings become filled with wagons, the speed of the wagon down the incline must be checked by the retarder, so that the wagon runs only to the required spot in the siding comparatively gently.

The procedure for dealing with the wagons through the marshalling yard can be divided into three main groups, namely

(*a*) The gathering of information as to the make-up of the train, so that the wagons can be directed into the appropriate sidings.
(*b*) The efficient operation of the points between the wagons or the groups of wagons, so that the wagons are directed to the appropriate siding.
(*c*) The control of the speed of the wagons, so that they will run to the correct point in the siding and not collide too violently with the wagons already standing there.

The first operation necessitates the reading-off of the destination of each of the trucks comprising a train from the ticket which is clipped on the side of each truck. One of the essentials is the rapid transference of this information to the control tower from which the points are operated, and a number of methods have been used for improving this operation. In some installations, the man who stands beside the track and reads the tickets on the wagons is provided with a microphone, so that he can repeat the destinations of the wagons as they pass, and this information is written down by an operator listening to a loudspeaker. An improvement on this arrangement provides for a tape recorder to take down the original message from the man reading beside the track, and then by means of a teleprinter circuit, an operator transcribes from the record on the tape to the teleprinter, which produces a printed list of the destinations at the control tower. In some very recent installations, particularly in the United States, the use of a closed-circuit television equipment has been introduced for reading the tickets on the wagons. A camera is placed at a suitable point beside the track and the receiving set placed in a convenient office. This enables the wagon details to be read direct from the office, without the man standing beside the track.

The points for switching the wagons are controlled from a tower near the top of the hump, by thumb switches or push-buttons, generally arranged on a sloping table and in geographical form in accordance with the plan of the lines. The points themselves must be operated very quickly, and this is done either by electro-pneumatic operation or by special high-speed point machines driven by electric motors. The operation of the points is controlled by rail circuits, connected in a similar manner to a track circuit, but arranged on the normally-de-energized principle, instead of the normally-energized principle, of the track circuit. This different circuit is necessary to obtain the high-speed response required for this type of work, and the high degree of safety of the normally-energized track circuit is not required.

In addition to the operation of the point machines direct from the control panel, provision is nearly always made for storage of the required arrangement. The provision of a suitable storage device enables the operator to set up the point movements required for a whole train, and thereafter the operation of the points is automatically controlled by the appropriate rail circuits as the wagons pass over them. Various methods of storage are in use, the most common being sets of relays, but in France special machines are in use, operated by steel balls which run down trackways and are released, step by step, to correspond to the progress of the wagons and making contact at each step for the operation of the appropriate points.

Communication between the operator in the control tower and the driver of the locomotive propelling the wagons over the hump is of considerable importance, and v.h.f. radiotelephones providing both-way communication are provided for this purpose.

The retarders (Fig. 8) for the control of wagon speed have generally been operated by a special operator, and this requires extremely good judgment to determine the correct braking effect necessary on each of the wagons. Recently, experimental installations have been carried out to provide for

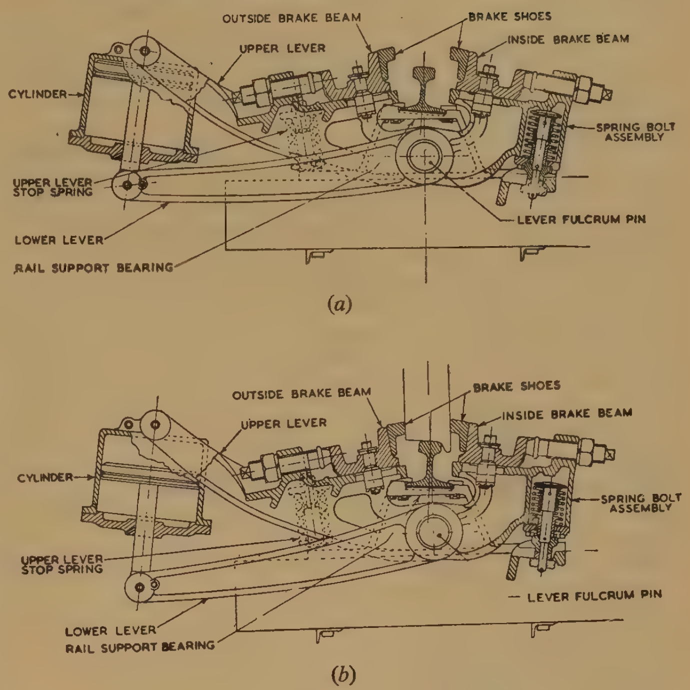

Fig. 8.—Cross-section of track retarder.
(*a*) Open position.
(*b*) Braking position.

automatic operation of the retarders, actuated from devices that measure the speed and weight of the approaching wagon. Two methods of measuring the speed have so far been introduced. In one, the rails are divided into a series of extremely short insulated lengths and each piece of rail is connected to a separate rail circuit, which, in turn, is connected to a series of relays for measuring the time the wheels of the wagon take to pass over the short lengths of rail; from this, the speed of the wagon is indicated. In another arrangement the speed of the approaching wagon is measured by a device fixed to the track which emits a supersonic sound in the direction of the wagon; the sound is reflected from the front of the wagon back to a microphone and the reflected sound thus picked up, after amplification, is used, by means of the Doppler effect, to indicate the speed at which the wagon is moving. This information is then used to control the retarder and can be used to bring the wagon to a set speed, as indicated by the operator.

(14) CODED CENTRALIZED TRAFFIC CONTROL

Although it has not at present been in use on British Railways, coded centralized traffic control is a feature of signalling which has made very great strides in recent years throughout the world, and much of this equipment has been manufactured in England.

Coded centralized traffic control (c.t.c.) equipment was first designed and manufactured in the United States in 1927, and since then its use has continued to expand. It was originally designed for the control of the signalling of long sections of single line having passing loops, but its use has recently been extended to other purposes, including the control of reversible signalling on double lines, where this reversible signalling has been provided to enable more efficient use to be made of the tracks and permitting trains to be signalled in either direction over either of the tracks; the train movements throughout are safeguarded by the normal power signalling arranged beside

the track. Track circuits are employed throughout to detect the presence of the trains and to control the signals and points in each of the areas appropriate to the particular sections of track, and these provide the full safeguards for protecting all the train movements.

The c.t.c. system provides a medium for sending controls from a central office to operate the appropriate signals and points, and thus to determine the precedence of the trains. A coded system is also used for the return indications, which provide on the control panel in the central office a complete indication of the positions of track circuits occupied by the trains and the positions of points and signals. This coded indication and control is carried out over two line wires, the code comprising a series of pulses. In one system, 16 pulses provide the necessary codes, both for control and for indication. Codes from the central office are transmitted to field stations connected to the common pair of line wires and located at suitable points for providing the control and indication from the local signalling. The number of field stations which can be connected in one circuit is limited by the number of pulses in the code, and is 35 field stations in the 16-pulse system; however, it is possible to add further groups of 35 field stations by means of carrier channels superimposed on the d.c. line wires. When this carrier system is employed, each group is operated by d.c. pulses. A carrier of suitable frequency is then superimposed on the d.c. circuit and, at the end of the first d.c. circuit, the carrier pulses are converted to d.c. pulses, which operate the circuit for the next group. If further stations are required, a second carrier frequency is superimposed on the first d.c. circuit and carried on to the second d.c. circuit, at the end of which the carrier pulses on the second carrier frequency are converted to d.c. pulses and actuate the third d.c. circuit. The carrier frequencies are generally in the range 10–45 kc/s, with a separation of about 5 kc/s.

The distances over which a c.t.c. signalling system can control are very extensive. D.C. circuits themselves are generally limited to about 50 miles, although some extend to 150–250 miles. With the addition of the carrier, the distance covered by the system will include everything that could be reasonably required to be controlled from one office.

The c.t.c. equipment is adapted to perform additional functions. For example, in areas where an electricity supply is not available provision can be made for a small local Diesel-engine generator to be started and stopped by means of the c.t.c. controls. In addition, provision is made for telephone communication over the common line wires to the various points at which signals are located, and this provides communication with the central control office when required.

(15) CONCLUSION AND ACKNOWLEDGMENTS

The indications are that power signalling will continue to be introduced on the railways of this country at an increasing rate. The projected electrification of much of the main-line railways will greatly accelerate the rate of this progress.

The author wishes to express his thanks to the Signal Engineers of British Railways, Messrs. L. J. Boucher, L. J. M. Knotts, A. Moss, A. F. Wigram, S. Williams and A. W. Woodbridge, and also to Mr. T. J. Aldridge, for their assistance in supplying him with information.

(16) REFERENCES

(1) PETER, L. H.: 'Modern Developments in Railway Signalling', *Journal I.E.E.*, 1936, **78**, p. 353.
(2) GOLDING, A. J.: 'Relay Interlocking', *Proceedings of The Institution of Railway Signal Engineers*, 1937–8, Part II, p. 232.
(3) CHALLIS, E. W.: 'A Comparison between Relay and Electric Interlocking', *ibid.*, 1938–9, Part II, p. 256.
(4) MOTT, J. E.: 'Train Describers', *ibid.*, p. 218.
(5) DELL, R.: 'Power Worked Lever Remote Control Signalling System', *ibid.*, 1942, p. 87.
(6) TATTERSALL, A. E. L.: 'Railway Signalling and Communications', *Journal of The Institution of Civil Engineers*, 1942–3, p. 3.
(7) DELL, R.: 'Development in Railway Signalling on London Transport', *Journal I.E.E.*, 1944, **91**, Part II, p. 400.
(8) COLEY, J. P., and MACGREGOR, R. M.: 'Coded Track Circuits, their Theory and Application', *Proceedings of The Institution of Railway Signal Engineers*, 1944, p. 39.
(9) MOTT, J. E.: 'Automatic Train Control (The link between the track and moving locomotive)', *ibid.*, 1948, p. 166.
(10) 'Sequence Switch Interlocking and Signalling at Doncaster South', *Modern Transport*, 1949, **60**, p. 15.
(11) '40 Years of Automatic Train Control—The Western Region', *Journal of The Institution of Locomotive Engineers*, 1949, **39**, p. 3.
(12) OWEN, W.: 'Speed Control Signalling for Close Headway Working', *Proceedings of The Institution of Railway Signal Engineers*, 1949, p. 212.
(13) COLEY, J. P.: 'Relay Standardisation', *ibid.*, p. 66.
(14) VENNING, C. F. D.: 'All Electric Interlocking Lever Frames versus Relay Interlocking Control Panels for Large Installations', *ibid.*, p. 194.
(15) HADAWAY, H. W.: 'Improvements in Track Circuit Shunt (Injector Track Circuits)', *ibid.*, 1950, p. 43.
(16) 'A Southern Region Colour Light Signalling Scheme', *Engineer*, 1950, **190**, p. 461.
(17) 'Signalling of E.R. Electrification (Part I)', *Railway Gazette*, 1950, **93**, p. 544.
(18) 'Signalling of E.R. Electrification (Part II)', *ibid.*, p. 573.
(19) 'S.R. Colour Light Signalling—First Stage', *ibid.*, 1951, **94**, p. 41.
(20) S.R. Colour Light Signalling—Second Stage', *ibid.*, 1952, **97**, p. 434.
(21) DELL, R.: 'Control Desk Signalling Operation at Ealing Broadway', *ibid.*, p. 599.
(22) 'Power Signalling at Euston—L.M.R.', *ibid.*, p. 684.
(23) 'Modern Signaling in New Subways in Stockholm, Sweden,' *Railway Signaling and Communications*, March, 1954, **47**, p. 32.
(24) 'In Southern Yard at Chattanooga . . . Efficient is Key Word', *ibid.*, July, 1956, **49**, p. 30–40.

656.05:621.34

Paper No. 2346
Apr. 1957

THE APPLICATION OF ELECTRICITY TO SIGNALLING FOR ROAD TRANSPORT

A Review of Progress

By J. STRINGER, M.A., and A. T. WILFORD, B.Sc.

(1) INTRODUCTION

When the previous review was written* very little installation of new traffic signals had taken place since before the war, and—in London, at least—the lack of regular maintenance combined with the extensive use of substitute war-time materials had led to a comparatively low standard of reliability.[1] In the intervening eight years, not only has the performance of signals improved, but there have been a number of new installations incorporating novel features dictated by the complex traffic patterns at the respective sites. The outward form of signals has undergone no change since the present sequence of aspects,[2] i.e. *red*, *red* plus *amber*, *green*, *amber*, *red* came into general use about 1930 (see also British Standard 505: 1939). Advances have been made, however, in the means for detecting the presence of a vehicle and in the automatic adjustment of signal timings to suit the ever-changing pattern of traffic as detected.[3,4] So-called 'vehicle-actuated' traffic signals[5] have long been the rule in this country, and installations must now be of this type to attract a grant from the Ministry of Transport. A new specification for traffic signals is at present being drawn up by the Ministry to cover developments now considered necessary for optimum traffic control, including those described in the present review; it will also provide for greater standardization and convenience of manufacture.

The successful application of automatic traffic signals to the solution of traffic-control problems depends, not only on the ingenuity displayed in the design of the electrical apparatus, but on the correct choice of cycle timings and other operational details. The problem of ensuring that delay to traffic is minimized without loss of safety is a difficult one, particularly where the volume of traffic is high in proportion to the capacity of the road or intersection, for in such circumstances random fluctuations in the amount and character of traffic may lead to the formation of queues of waiting vehicles, greatly increasing the overall delay. In such circumstances the average delay can be expressed only in a statistical form, and suitable values of the operating parameters cannot be established by deterministic methods. In practice, an acceptable mode of operation for a particular traffic signal is found by approximate calculation and subsequent adjustment on site, both when signals are first installed and at other times when the traffic pattern or volume may have altered. It is of interest to note, however, that studies are being made of the theoretical aspects of heavily loaded intersections. In research being carried out by the Road Research Laboratory of the Department of Scientific and Industrial Research the electronic digital computer Ace has been employed to calculate the average delay to vehicles as affected by the various parameters of a signal and by the volume of traffic.[6,7] The results of this research, which have not yet been published in detail, may be expected to help in securing the optimum adjustment of traffic control systems. One result demonstrated, as shown in Fig. 1, is that when an intersection is heavily loaded the average delay

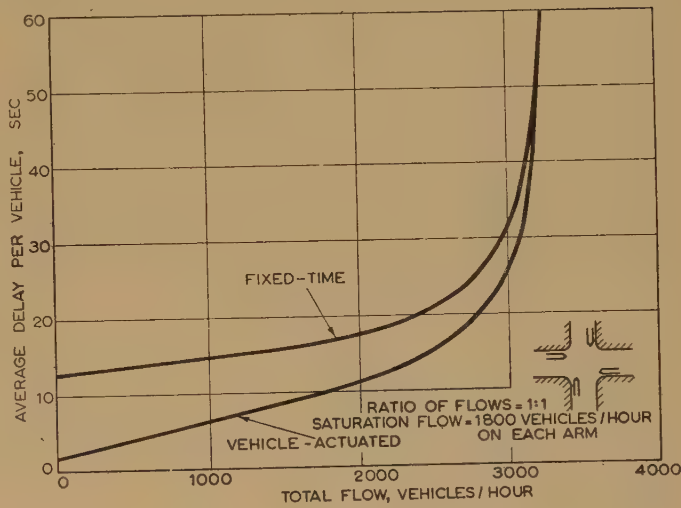

[*Crown Copyright*

Fig. 1.—Average delay as a function of volume of traffic.

Fixed time
'Green' time = 40 sec/phase.
Cycle time = 86 sec.

Vehicle actuated
Maximum 'green' period = 40 sec/phase.
Vehicle interval = 4 sec.

For inset diagram
Ratio of flows = 1 : 1.
Saturation flow = 1 800 vehicles/hour in each lane.

is very sensitive to the degree of saturation (the actual flow divided by the maximum possible flow or capacity). It follows that at an intersection which is barely capable of handling the traffic which offers, a comparatively small improvement in capacity may result in a quite large alleviation of delay. This demonstrates the importance of schemes for increasing the effective capacity of an intersection and for ensuring that none of the time available for vehicles movement is wasted because of inability of the signals to respond to changes in the traffic pattern.

(2) VEHICLE-ACTUATED SIGNALS

As a background to appreciation of the electrical problems arising in the design of vehicle-actuated signals it is first necessary to describe the operating features which may be incorporated. The simplest form of signal is one which caters for two conflicting traffic movements, or 'phases' as they are termed. Such a signal is used at a normal crossroad intersection where the eastbound and westbound streams of traffic receive right of way alternately with the northbound and southbound streams. The principles of operation, and the features incorporated in the 2-phase system described in this Section, apply similarly to systems in which three or more phases are given right of way in succession.

The control mechanism arranges the timing of the 'green' periods and ensures that 'amber' is displayed for the standard

* Sinclair, G. F.: 'Application of Electricity to Signalling for Road Transport', *Proceedings I.E.E.*, 1949, 96, Part I, p. 178.

Mr. Wilford is, and Mr. Stringer was formerly, with the London Transport Executive. Mr. Stringer is now with the Central Electricity Authority.

3 sec. The 'red' and 'red-amber' periods of one phase are determined, of course, by the 'green' and 'amber' periods of the other. The 'green' period consists of two parts. There is a fixed minimum preset to such length that vehicles standing between the stop line and the detector pad in the road can start up and safely cross the intersection before the signals change again. Any further vehicle, by striking the detector, extends the 'green' period for a number of seconds known as the 'vehicle interval' or 'vehicle extension' period, at the end of which time, if no further vehicle arrives and there are vehicles waiting on the other phase, the right-of-way passes to that phase. The vehicle interval can be made to vary in accordance with the speed of the approaching vehicle by the use of an electro-pneumatic system which is sensitive to the length of time during which the wheels are in contact with the detector. This means that, while a sufficient period is afforded for a slow-moving vehicle approaching a crossing, there is no time wasted with faster vehicles. A continuous stream of vehicles, with no spaces greater than the vehicle interval, could hold the right of way indefinitely, were it not for the provision of a maximum setting, which causes the signals to change when a vehicle on the phase which is at 'red' has been halted for a predetermined period. Thus a vehicle which has operated the detector in such a way as normally to extend the 'green' period, may nevertheless be stopped arbitrarily by operation of the maximum feature. It could happen that a vehicle, caught in this way between the detector pad and the stop line without further chance for its presence to be detected, would be held stationary for a considerable time. It is therefore necessary to provide for injection of an artificial demand, so that the phase which has lost right of way by operation of the maximum setting reverts to it at the earliest opportunity.

A further development which will be included in the new Ministry of Transport specification concerns adjustments to the 'minimum green' period. In existing installations this is set to a time which is sufficient to enable a column of four or five vehicles, accommodated between the stop line and the detector pad, to clear the intersection. At slack periods this interval is unnecessarily long for the release of isolated vehicles. It is therefore the intention to make the 'minimum green' period vary, between preset limits in accordance with a count of the vehicles which have crossed the detector(s) during the 'red' period.

The various time settings may be adjusted by means of hand-set switches within the controller box, so that the needs of individual intersections can be met with standard equipment. There is also provided a switch for each phase, by means of which a permanent artificial demand can be introduced, primarily for testing purposes. This artificial demand may be used to cause right of way to revert to the more important road without awaiting the operation of the detectors by an approaching vehicle. The feature may also be used to compensate for a faulty detector until the fault can be remedied. It will be apparent, however, that some loss of efficiency results from the use of an artificial demand which is not related to the realities of the traffic situation.

A signal system such as has been described will satisfy the needs of a straightforward crossing of normal proportions. With more complicated layouts, and where right-turning traffic or pedestrian movements are heavy, special provisions must be made.[8] The clearance period between opposing 'greens', when right of way is being transferred from one phase to the other, normally lasts 3 sec, for which time 'amber' and 'red-amber' indications are simultaneously displayed on the two phases respectively. Where this period is not sufficient to clear the junction of vehicles before the new movement is released, and to cater, where necessary, for pedestrians, additional clearance time must be provided. In present equipment the 'amber' and 'red-amber' periods are both controlled by a common timer. As a result, they may be concurrent or sequent, but they cannot overlap. New developments will allow for separate timers, so permitting overlapping of the 'amber' and 'red-amber' adjustable in 1 sec steps. Where more time is required, it is arranged for all signals to show 'red' between the end of 'amber' and the start of 'red-amber'. Such extensions of the clearance period naturally increase the lost time during which no vehicles are moving into the intersection from its approaches. It will therefore be appreciated that, if the clearance period exceeds the minimum needed to prevent conflicting movements of traffic, the capacity of the intersection is reduced. As was explained in the Introduction, this can only have the effect of increasing the average time which vehicles spend in the queue waiting for the lights to change in their favour. It is therefore important that means should be provided for restricting the 'all red' clearance period to the minimum necessary. At a complicated intersection it may be controlled by extra 'extending' detectors placed in the middle of the intersection, and it can be automatically suppressed if no vehicles have been detected on any phase in a predetermined time.

A useful application of extendable 'all red' periods occurs in the case of a long narrow bridge or tunnel, wide enough for only one lane of traffic. The approaches are detected and right of way is allocated in a manner similar to that at a road crossing, but further vehicle-detector pads are placed on the bridge, so that if a vehicle enters immediately before a signal change, its progress is followed and the 'all red' period extended until the last detector is passed, when the opposing traffic is released. By these means the 'all red' period is adjusted to suit the speed of the vehicle on the bridge.[9]

Further features may be incorporated in the central mechanism to deal with the particular traffic problems of individual intersections.[10] An example is the use of green arrows to permit the left-turning traffic to filter during part of a period when the straight-through traffic is halted. Another case is the use of 'late start' or 'early cut off' applied to only one of the streams of traffic making up a particular phase. This facility is used, where the layout of the intersection allows it, to enable right-turning traffic to clear from the stream then running alone. Where, as in the centre of a large town or city, signalled intersections are close together, it is often advantageous for their functioning to be governed to some extent by a common control which can take account of conditions over a wider area. The operation of such systems can best be described by reference to actual installations, and details of two recent examples of special interest are given later in this review.

(3) PROVISION FOR PEDESTRIANS

At a simple cross-road intersection, pedestrians can normally cross the road in comparative safety by obeying the signals applicable to the parallel stream of traffic. Where pedestrian traffic is heavy, however, or where the traffic includes a high proportion of vehicles turning across the pedestrians' path, serious interference with the smooth flow of traffic can result and, in the confusion, accidents are more likely to occur, to the particular danger of pedestrians. An 'all red' period can be included in the cycle to allow the pedestrians free movement.

The disadvantages of a fixed 'all red' period in reducing capacity of an intersection has already been stressed, and some benefit is gained by making the signal control responsive to pedestrian actuation, so that the pedestrian phase is omitted when there is no demand. Where this feature is incorporated, well-defined pedestrian lanes are marked on the road and 'Cross Now' signals are located facing inwards across them. Push-buttons are mounted on the signal poles by means of which a

demand for inclusion of the pedestrian phase in the cycle can be registered. Normally this pedestrian phase does not have the same variation as vehicle actuation, i.e. its length is fixed. Another difference is that, while the 'red' aspect is mandatory to drivers, obedience to traffic signals is not legally required of pedestrians.

A similar application of traffic lights to meet the needs of pedestrians is the pushbutton-operated signal situated on a main road, not at an intersection, but where both pedestrian and vehicular traffic are heavy. In the absence of pedestrian demands, the 'green' signal is displayed to traffic in both directions. When the button is pressed, traffic is stopped by the usual 'amber-red' sequence, and a fixed period allowed for pedestrian movement. As normally arranged, further pressure on the button does not extend the period of pedestrian right of way, and, once the traffic is again moving, a definite period must elapse before it can be halted. These operational requirements can be met with a form of controller simpler than the fully-traffic-actuated pattern, the apparatus used being a standard fixed-time controller such as is manufactured in this country for application abroad, where in some places the lower cost of the simpler apparatus is an attraction and the operational disadvantages of fixed-time cycles can be tolerated. The circuit of this type of controller is adaptable and provides for separate adjustment of the timing of each phase by means of a plug-board. The apparatus can be employed in a variety of ways, short of full vehicle actuation. For instance, the pedestrian controller can be linked with any signalling scheme, so that pedestrians are not invited to cross at a time when a body of traffic has been released from an adjacent traffic light.

A recent innovation in the road-signalling field is the flashing Belisha beacon used to mark pedestrian crossings. The need for some form of illumination of these beacons arose with the introduction of 'zebra' striping, which is often not conspicuous to approaching drivers when viewed under street lighting, particularly if the road is wet. Increased use of the striped crossings by pedestrians made it more than ever necessary for a motorist to have advance warning, by night as well as by day, that he is approaching a pedestrian crossing. Experiments carried out under the auspices of the Ministry of Transport and of the Road Research Laboratory of the Department of Scientific and Industrial Research pointed to the flashing beacon as being the most satisfactory form of illumination to attract the attention of drivers.[11,12] Simplicity and reliability are important requirements for the flashing unit, particularly in view of the large number—approximately 12000—of pedestrian crossings in the country. The unit must be capable of controlling a tungsten-filament lamp or lamps up to a total load of 200 watts (though normally 40 or 60 watts is used per beacon) to give on and off periods of $\frac{1}{2}$ sec each, timed to an accuracy within $\pm 10\%$—approximately 20×10^6 switching cycles per year. Early experience showed that, with beacons independently controlled, irritating light patterns could be produced where several pedestrian crossings in a street were visible at the same time. It was therefore found necessary to arrange for the two beacons at a crossing to flash in synchronism with each other and in some cases with other adjacent beacons.

The basis of one control mechanism is a synchronous motor driving a cam-operated contact. Synchronization of adjacent beacons is achieved by the simple device of advancing or retarding the making and breaking of the main contacts, so that, with one of the beacons flashing, the remainder can each be adjusted visually to flash at the same time. The accuracy achieved is claimed to be within $\frac{1}{25}$ sec, which is sufficient to eliminate the irritating light patterns which might prove a distraction to drivers. By providing a separate control for each light and using this method of synchronization, no interconnection between beacons is required other than that all are connected to the a.c. mains. The flasher unit is arranged to plug into its mounting, so providing for easy removal and replacement for maintenance. It is usual for beacons to be illuminated by day and by night, but a time switch can be included in the circuit so that the beacon lamp flashes only during a predetermined period. In this case the synchronous motor of the flasher unit remains running continuously, so that adjacent beacons do not lose synchronism. Fig. 2 is a circuit diagram of the complete flasher unit with time-

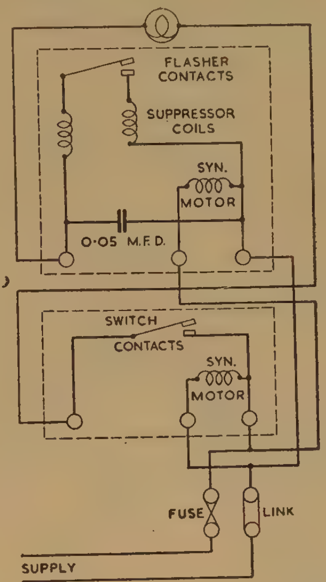

[*Venner Times Switches, Ltd.*

Fig. 2.—Flasher unit, with time switch.

switch operation and radio and television interference suppressors. With d.c. mains and in some other cases where convenient, several beacons may be connected to one flasher.

All the pedestrian beacon equipment was subject to approval by the Ministry of Transport; it was thus possible to arrange that housings and components of any manufacturer may be readily interchanged with those of other makes.

(4) CONTROL EQUIPMENT

The equipment of a vehicle-actuated traffic-signal installation consists of

(*a*) Detectors, to pick up the arrival of each vehicle.
(*b*) A controller, receiving impulses from the detectors, storing and sorting them in accordance with the phases and timing circuits, and switching the signals at the appropriate time.
(*c*) The signal heads, conveying instructions to drivers.

At the time of the previous review (1948) the pressure-sensitive detector had been generally adopted in this country: this type has since continued in exclusive use, but has been improved so as to simplify installation and maintenance.

Two rubber strips are now employed in place of the former broad rubber mat, which contained two longitudinal air passages and was set in a cast-iron or steel frame. With either type, the passage of a vehicle over the detector causes an increase of pressure in the air, which actuates a pneumatically-operated contactor. In one make,[13] the two strips are held in dovetail channels in a mild-steel frame of unit construction, made up in 2ft lengths. For installation, an appropriate number of frame sections are coupled together and supported by temporary

battens at the correct height in a prepared trench, and they in turn support reinforcing rods. Concrete is then poured, thus forming a beam of great strength, tailored to the contour of the road. When replacement is necessary the rubber strips are readily pressed into place in the dovetail channels. In another make, separate rubber tubes are held flush with the road surface in a fabricated steel framework. The tubes are securely located by a spring bar which passes through the length of each and, being under tension, exerts a downward pressure at all points. To replace a tube it is necessary merely to remove four studs and lift out the spring bar and tube; the spring bar is then inserted into a new rubber tube and the assembly replaced. The operational requirements for a detector are exacting: it must be sensitive to any pressure, from a bicycle to a heavy lorry, and must discriminate between vehicles entering and leaving the junction; in the event of a vehicle parking on its surface, the detector must remain able to detect vehicles passing round the obstruction (this is achieved by so shaping the rubber sections that the air passage cannot be entirely closed); an air leak is also provided, so that the original impulse of the parked vehicle decays. As a result of development work in recent years, the reliability of detectors and their associated pneumatic contactors has improved considerably, while replacement of a faulty pneumatic unit in the street takes only a matter of minutes, so that the interference with traffic flow is minimized.[14]

Unidirectional detection may be achieved either mechanically, by interlocking the movement of the bellows, or electrically, using the two impulses obtained from the separate tubes of the detector. A diagram[15] of a unidirectional switching is given in Fig. 3, in which the normal sequence of operation of the

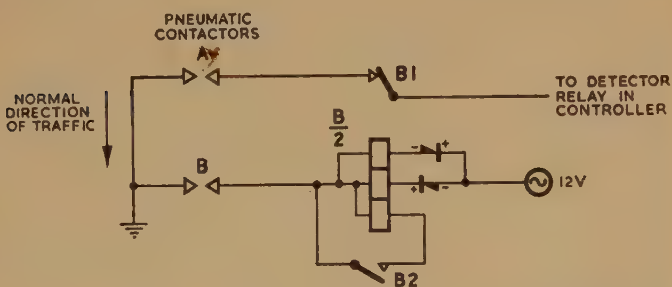

[*Electrical Times*

Fig. 3.—Circuit for unidirectional detection.

pneumatic contactors is A–B. Should B be energized first, by a vehicle leaving the junction, the controller circuit from A is opened by relay B and does not operate. Contact B_2 provides a slow-release feature to cover the transit time of the vehicle between the detector tubes, which in this make is about 60 millisec at 5 m.p.h.

The value of a signal-detector system sensitive to vehicle speed is that the vehicle interval can be automatically adjusted so that a slow-moving vehicle is allowed adequate time, while a fast-moving vehicle does not claim more time than is necessary for it. Speed timing will, in future, be called for in all vehicle-actuated systems, and will be achieved from the time interval between the pulses from the two strips of a detector. A circuit[9] used in the latter case is shown in Fig. 4, the method of operation being as follows:

> Contact S_1 is normally open and C_1 is free to assume a voltage on the grid side which is substantially zero, owing to the combined effects of the current through R_1 and grid current which flows if the grid is even slightly positive, and in such circumstances the previously operated relay, ST, would release immediately contact S_2 closes. S_1, however, is operated by vehicles traversing the detectors in the roads which have right of way, and upon the closure of its

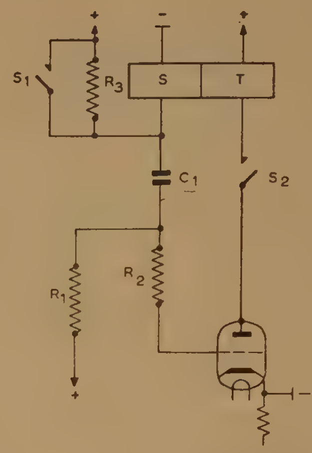

[*G.E.C. Journal*

Fig. 4.—Basic speed-timing circuit.

> contact C_1 will start to charge, although it is prevented from taking a full charge instantly by R_2. In fact, the amount of charge which is taken is now dependent upon the length of time for which S_1 is closed. R_1 and R_2 are so chosen that the charge will have been modified to its zero value by the time the vehicle which had caused the actuation of S_1 has reached a predetermined point, or zone, at the crossing. Contact S_2 is on the demand relay, and indicates by its closure that a vehicle or vehicles are calling for a change of right of way.

This circuit is a simple modification of the valve timing circuit described in the previous review; such circuits are now frequently used in place of the former neon-tube circuit.

The controller employs telephone-type relays to store the demands for right of way. Control relays are also used in one make for dividing the cycle, although in another make a solenoid-operated cam switch is used, the position of which determines the signal aspects displayed. Operation of these relays or stepping of the switch is controlled by the timing circuit, modified by the position of the demand relays. For example, at the end of the initial interval of the 'green' period, the camshaft is stepped on, and timing of the vehicle interval commences, being recommenced each time the demand relay is energized. Timing of the 'amber' periods is initiated by the control relays or by the cam switch itself as soon as 'green' terminates. An interlock is provided to prevent 'green' being shown to conflicting traffic streams in the event of a fault. The control relays are so switched that when one phase shows 'green' the timing circuits relating to the other phases are broken. Developments of this basic circuit can become quite complex, as in the two integrated systems now to be described.

(4.1) Two Recent Examples

Two examples of complex traffic-light systems recently brought into operation in London will illustrate, not only the special conditions peculiar to each new application, but also the versatility of the standard basic equipment which has been used in each case.

In Oxford Street a new vehicle-actuated progressive system replaced in November, 1954, a fixed-time linked system, which was installed in 1930 and originally controlled 18 crossings in the 1¼-mile stretch from Marble Arch to St. Giles Circus (Tottenham Court Road). At the Monument in the City of London, vehicle-actuated signals have been installed to control a main intersection in which five roads converge, together with a nearby junction, all lying in a compact area, and previously controlled by a police sergeant and six constables.

(4.1.1) Oxford Street.

Under the old fixed-time system the signals at each of the 18 crossings were switched individually by a local controller, but subject to the overriding influence of a master controller, which ensured a constant cycle time throughout the system. The start of each local cycle was subject to a phase shift, whereby right of way appeared progressively at successive crossings, so that vehicles travelling at the speed of this progression would meet a majority of 'green' signals.

In practice, it is not possible so to link the signals that vehicles travelling in both directions have a clear passage throughout. Ideal linkings can be achieved only in a one-way system or, for two-way traffic, where the intersections are appropriately spaced at a sufficient distance apart, as in some cities abroad. In the latter case, the cycle time cannot be altered without altering the progressive speed which vehicles must maintain if they are to have an uninterrupted journey. In the original Oxford Street installation the cycle time, and hence the progressive speed, could be altered manually at the master controller, but since the effect was to alter also the proportion of 'green' time allocated to each side road, the amount of variation in cycle time was limited, and in practice only two cycles were used, for heavy and light traffic respectively. It will be apparent that this limited variation could not cater efficiently for the wide range of traffic volume and speeds between peak hours and evenings or week-ends. The system now in operation uses an electronic master controller to generate a master cycle time, which is conveyed by tie lines to the local controllers. The progressive phase-shift feature is again incorporated, but the proportion of time given to the side roads is now determined by vehicle actuation, so that the cycle time can be varied over a much greater range than hitherto.

To deal with the entirely different forms of traffic under week-day and week-end or night-time conditions, two distinct patterns are provided for co-ordinating the progressive switching, one suitable for light traffic and the other for slower and denser week-day traffic. Selection of the appropriate pattern can be by time switch, or by an integrator, which estimates the density of traffic from the demands registered at the detector pads. The integrator is also used to vary the cycle time as generated by the master controller, in accordance with the general traffic density. In addition, at times when traffic normally reaches a higher density, artificial demands are introduced on the main and side roads at the local controllers, so as to overcome difficulties which arise when traffic is unable to move over the detectors because of the large numbers of pedestrians. At these times of most dense traffic, the insertion of artificial demands means that the system works to a fixed-time cycle.

The traffic integrator uses the vehicle detectors in five approach roads to Oxford Circus, which are considered to give a reliable measure of the average traffic density over the whole area under control. The impulses from all detectors are summed initially by an electronic circuit which passes impulses to the stepping solenoid of a uniselector switch. After 5 min of counting, the result is compared with that obtained and stored previously: if the two results vary by more than a certain amount, the old result is replaced by the new. Thus the master controller, acting under the influence of the integrator, dictates a cycle time in accordance with the trend of traffic density but ignores short-term fluctuations. Additional tie lines between the master and local controllers convey impulses signalling the change of progressive pattern or the introduction of artificial demands when the traffic density reaches predetermined levels.

Special arrangements are provided to bring the other control systems in the vicinity (i.e. Wigmore Street, Mortimer Street and Regent Street) under the general direction of the Oxford Circus controller, which therefore ultimately controls some 40 local controllers. In view of its importance, the master controller has duplicate impulse generators and a monitoring device to switch in the standby if the working unit fails. The units are otherwise interchanged daily.

(4.1.2) Monument.

The Monument system serves the busy area at the north end of London Bridge, consisting of the main junction of King William Street with Cannon Street, Gracechurch Street and Eastcheap, and the nearby junction of King William Street with Arthur Street and Monument Street.

Lorries from Billingsgate Fish Market, emerging from Monument Street, complicate the traffic pattern in the early part of the day, including the morning peak period. Thus the minor junction is provided with signals linked to those at the main junction. The link between the two controllers operates only during the busy part of the day-time. During the night and on Saturday afternoons and Sundays, when traffic is very light, both controllers operate as isolated units, the change-over being arranged by a time switch. Even so, there is still an element of linking, since both controllers are responding to the traffic offering on the common route. Such a natural linking would not be evident when traffic was heavy, because of the effect of demands on the other phases.

Provision is made in the design of the controllers for several alternative control schemes by varying the sequence of the phases and by varying the application of clearance periods. Each control scheme has its associated night scheme designed to suit the smaller volume of traffic. One of these is illustrated in Fig. 5, which shows six stages in the traffic pattern. Stages 1, 3 and 5 are the major movements, and stages 2, 4 and 6 are simple modifications of them; under light-traffic conditions, stages 4 and 6 are omitted and stage 2 is also omitted if, owing to the absence of demand, stage 1 has not been inserted in the cycle. As in all controllers, a manual control feature is included, so that, under unusual circumstances, operation by a police official

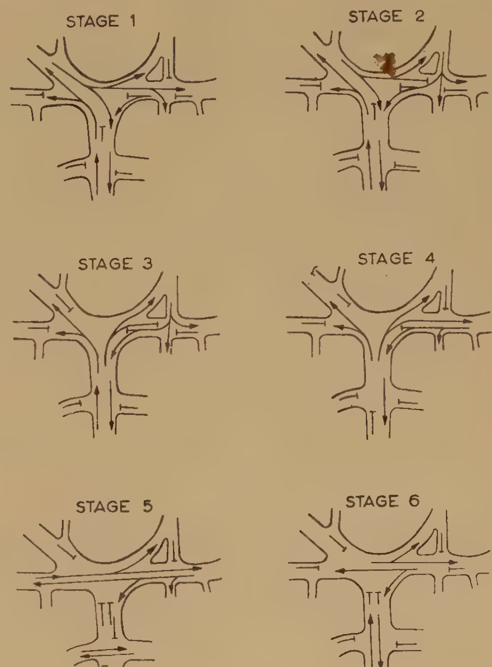

[*Automatic Telephone and Electric Co., Ltd.*

Fig. 5.—Stages of traffic flow at Monument, London.

is possible; but in the Monument installation additional arrangements are provided so that the 'red' and 'green' signals of the main phases are repeated on a display panel; operation of a toggle switch both preselects the next phases to receive right of way and gives effect to the change of phase previously selected. It is not possible inadvertently to give right of way to conflicting streams of traffic at the same time.

(6) SIGNALLING AT LEVEL CROSSINGS

Under existing statutory regulations in Great Britain, level crossings must be protected by gates and an attendant must be present to operate them. In a very few instances traffic signals have been installed in conjunction with gates controlled from a signal cabin within 100yd of the crossing. The traffic signals follow the usual sequence, a change from 'green' to 'red' being made by the railway signalman prior to initiating action to allow the passage of a train. After 3sec have elapsed the signalman starts to move the gates. The signal remains at 'red' until the train has passed, and changes to 'red-amber' as the signalman starts to reopen the gates, becoming 'green' when they are fully open. Sanction has been obtained for the use of lifting barriers operated on site, each case being considered on its merits. One is already in experimental use at a level crossing in the north of England and is, of course, manually controlled. Further relief from the statutory obligation is being sought, and if obtained would permit the protection of crossings by lifting barriers operated either automatically by track circuits or remotely controlled from the nearest signal box, thus coming into line with Continental practice.

(6) INNOVATIONS IN THE U.S.A. AND ON THE CONTINENT OF EUROPE

A pilot radio control system[16] costing $50000 was introduced in Chicago in November, 1955. Traffic signals at all intersections on La Salle Avenue and at two other outlying intersections are controlled by a programme radiated from a central point by a single transmitter. The programme dictates details of cycle time and allocation of 'green' time appropriate to each intersection. An aerial decoder and receiver have been fitted to the existing equipment at each intersection, the decoder accepting only signals intended for that intersection. The system enables the timing of all signals to be in accordance with the prearranged pattern, which may be varied by time of day and day of week. There is provision for switching to manual control in the event of bad weather or other unusual occurrence. The system is capable of expansion to include other intersections in the city, and is claimed to be much less costly than the alternative conventional method of linkage. It has been reported that a similar system is to be installed in Los Angeles.

Radar is being employed for detection of vehicles in Seattle.[17] A system was required for controlling vehicle-actuated signals at an intersection situated at one end of a railway bridge. Installation of conventional detectors in the surface of the bridge would have entailed mechanical difficulties. In addition, since the bridge formed a funnel in the city's traffic pattern, serious delays would have resulted from interference with even one lane of traffic flow while the constructional work was in progress. Magnetic detection from the underside of the bridge was rejected, because of the thickness of concrete and the presence of a high-voltage cable. The detection device finally adopted depends on the Doppler effect between the transmitter beam and the beam reflected from the vehicle beneath. Each detector is approximately the same size as a street lamp and is suspended over the traffic lane in the same way. By adjustment of the sensitivity, detection may be restricted to vehicles in one lane or may be extended to include vehicles in three lanes. A separate detector of appropriate sensitivity is provided for controlling a single lane of left-turning vehicles (equivalent to right turning in Great Britain).

It may be noted that a radar speed-meter, also employing the Doppler effect in measuring the speed of vehicles from the roadside, has been in use for some time in the United States, both for traffic research and for speed-limit enforcement purposes. A similar device has recently been employed in this country for experimental purposes by the Road Research Laboratory,[18] and by the police in advising motorists of excessive speed.

An experiment is being conducted in Detroit with the use of television cameras at important intersections.[19] By this means a watch may be kept for breakdowns or other causes of congestion by monitoring television screens at a distance control point.

An innovation in the control of pedestrians in the United States is the 'scramble' period.[20,21] During a substantial part of the cycle at an intersection, all vehicle movement is stopped by the signals and pedestrians are given complete priority. The normal rule that pedestrians should cross one street at a time with the lights is waived, and they may cross diagonally. It was found in San Francisco that, although both pedestrians and motorists liked the system, delays to vehicles were much increased.

In Munich a device for detecting the approach of, and giving priority to, a tram requiring to turn right at an intersection has been installed.[22] Difficulty in starting was often encountered when a tram was halted by the signals at this intersection, which is on a steep hill. A separate set of rails has now been provided for right-turning trams, and the device situated at the points ensures that the tram will not be held on the hill. A device to serve a similar purpose is also employed in San Francisco.

Mention may also be made of a scheme in Dusseldorf whereby, at tram stops near intersections, traffic lights applicable only to trams are placed at the crossings, those for other traffic being situated some 30yd to the rear. The lights are so phased that the trams reach the crossing ahead of other traffic. Passengers can thus board and alight in comparative safety, and at the same time the public vehicle is given priority at the crossing.[23]

Signals are widely used on the Continent for controlling level crossings. On German railways in particular, remotely operated barriers are equipped with a loudspeaker intercommunication system, so that the road user may communicate with the signalman.[24] With its aid the signalman can detect the approach of vehicles and pedestrians and the position of trains, and can also speak to road users in the vicinity of the crossing.

(7) MAINTENANCE AND RELIABILITY

As mentioned in the Introduction, the reliability of traffic signals has undergone a notable improvement since the previous review was written. The conditions under which the apparatus is required to operate are far from ideal, and the improvement is largely due to the special attention given to preventive maintenance and the elimination of war-time substitute materials.

Each time a vehicle passes over a detector pad, a relay is caused to operate, and at a busy intersection the number of operations may be 12–15×10^6 per year. By contrast, the hardest worked comparable relay in telephone service operates approximately 2×10^6 times a year. Moreover, the traffic-signal relays must operate under a wide range of temperatures and in the presence of dust and moisture. In the United Kingdom both routine maintenance and fault clearing are normally attended to, under contract, by the manufacturers of the equipment.[25] The normal practice is for inspections, cleaning and general attention at intervals of about 3 months, plus 'beck and call' service for any troubles in the interim. The work done at

each visit is recorded and subsequently analysed. Statistics are also maintained of the consumption of various piece parts, so that the effects of any modifications may be determined in terms of the average life before replacement. Statistical information obtained from operating experience in this way plays an important part in improving both the design of the equipment and the methods of maintaining it, leading to greater reliability.

(8) ACKNOWLEDGMENTS

The authors wish to express their thanks to Mr. E. Bailey, Chief Signal Engineer, Automatic Telephone and Electric Co. Ltd., Mr. H. J. N. Riddle, Design and Development Engineer, Siemens and General Electric Railway Signal Co. Ltd., Mr. W. Hadfield, Senior Engineer, Ministry of Transport and Civil Aviation, and to Venner Time Switches, Ltd., for the help and information they have provided.

Acknowledgment is also due to the Controller of H.M. Stationery Office for permission to reproduce Fig. 1.

(9) REFERENCES

(1) Ministry of Transport: 'London Traffic Congestion', Report by the London and Home Counties Traffic Advisory Committee (H.M. Stationery Office, London, 1951), p. 39.

(2) B.S. 505 : 1939, 'Road Traffic Control (Electric): Light Signals'.

(3) Preist, T. P.: 'Traffic Signal Sequences', *A.T.E. Journal*, 1953, **9**, p. 163.

(4) Range, A. L.: '50 V Road Signal Timer', *ibid.*, p. 96.

(5) Tyack, F. G.: 'Street Traffic Signals, with particular reference to Vehicle Actuation', *Journal I.E.E.*, 1938, **82,** p. 125.

(6) Road Research Laboratory: 'Road Research 1953', Report of the Road Research Board (H.M. Stationery Office, London, 1954), p. 33.

(7) Road Research Laboratory: 'Road Research 1954', Report of the Road Research Board (H.M. Stationery Office, London, 1955), p. 26.

(8) Thorpe, E.: 'Electromatic Vehicle-Actuated Traffic Signals at the "Bank Complex", London', *Strowger Journal*, 1948, **6**, p. 99.

(9) Riddle, H. J. N.: 'Vehicle-Actuated Road Traffic Signals', *G.E.C. Journal*, 1949, **16**, p. 216.

(10) Green, R. C.: 'Ludgate Circus Traffic Signals', *A.T.E. Journal*, 1953, **9**, p. 242.

(11) Road Research Laboratory: 'Road Research 1952', Report of the Road Research Board (H.M. Stationery Office, London, 1953), p. 20.

(12) 'Lighting the Zebra Stripes', *Imperial Review*, May, 1953, p. 44.

(13) Preist, T. P.: 'The Flat-Strip (Type FS) Road Vehicle Detector', *Strowger Journal*, 1952, **8**, p. 73.

(14) Preist, T. P., and Wallace, R.: 'Electromatic Street Traffic Control Equipment', *ibid.*, p. 128.

(15) Thorpe, E.: 'Road Traffic Control', *Electrical Times*, 1954, **126**, p. 581.

(16) 'Chicago Controls Traffic Signals with Radio', *Traffic Engineering*, 1956, **26**, p. 209.

(17) Lewarch, E. E.: 'Seattle's Radar Signal Installations', *ibid.*, 1955, **26**, p. 59.

(18) Laker, I. B., and Whiting, P. D.: 'A Speedmeter for Use at High Traffic Flows', *Electronic Engineering*, 1955, **27**, p. 284.

(19) Janicki, E.: 'Television for Traffic Control', *Public Works*, 1955, **86**, p. 82.

(20) Shoaf, R. T., and Marconi, W.: 'Scramble in San Francisco', *Traffic Engineering*, 1954, **25**, p. 53.

(21) Shoaf, R. T.: 'A Discussion of Warrants for Scramble Signals', *ibid.*, 1955, **25**, p. 261.

(22) Ulsamer, J.: 'Eine Moderne Verkehrssignalanlage', *Verkehrund Technik*, 1952, **5**, p. 229.

(23) Private communication.

(24) Schmitz, W.: 'Einrichtungen für Technische Sicherung von Webübergüngen', *Eisenbahntechnische Rundschau*, October, 1955, p. 469.

(25) Wright, D.: 'Electromatic Street Traffic Signals Maintenance Service', *Strowger Journal*, 1951, **8**, p. 44.

621.385.16:621.316.824

Paper No. 2288 M
Apr. 1957

A THERMIONIC RHEOSTAT FOR AUTOMATIC CONTROL

By E. G. HOPKINS, Ph.D., B.E.

(*The paper was first received 9th May, and in revised form 12th September* 1956.)

SUMMARY

The paper describes an experimental thermionic rheostat in which the spacing between the two thermionic cathodes is controlled by rotating the valve while one cathode is held stationary by means of an external permanent magnet. The valve has a small receiving-valve envelope and will control a.c. loads of up to 60 watts when operated as a series resistor from 240-volt mains. Three experimental closed-loop automatic-control systems are described whose electrical circuits consist simply of experimental valves actuated by mechanical error signals and controlling the current delivered to a.c. motors: the systems are a position control, a velocity-integral control for moving materials and an air-flow control.

(1) INTRODUCTION

In many closed-loop control systems the position or motion of a mechanical element driven by an electric motor is monitored with the aid of some form of pick-off device which produces an electrical error signal, which is used to control the flow of electric power to the motor. The electrical portion of such a system contains a mechanical-electrical transducer, a power amplifier and often one or more intermediate stages of amplification to increase the loop gain of the system.

In electronic control systems it is usual to amplify electrical signals with the aid of thermionic valves which introduce additional power into the system from an external source of supply. The most commonly used valves are thyratrons, which act as electrical relays, and high-vacuum thermionic valves which act as electrically controlled rheostats. The operation[1,2] of both types is usually explained in terms of variation of the space-charge-free electric field within the valve, this field being a function of control-grid potential. The source of their amplification lies in the fact that control-grid potential may be varied by a signal of very much less power than the change in anode-circuit power which it produces.

The electric field within a thermionic valve is a function of the inter-electrode spacing. It is therefore possible to control this field through the displacement of an internal electrode by a low-powered mechanical signal and thus to produce mechanical-to-electrical signal conversion accompanied by amplification. Up to the present, this possibility has been realized in practice only in the form of low-power diodes[3] and triodes[4] used for the measurement of very small mechanical displacements. A single thermionic valve is never used as a means of controlling the power delivered to a relatively large electrical load in response to a mechanical signal.

In a previous paper,[5] three 'self-heating' thermionic valves were described. One of these, the thermionic rheostat, is a high-vacuum diode having two planar oxide cathodes with variable spacing which act as a bidirectional variable resistance in a.c. circuits. The full anode dissipation of such a self-heating valve is available for heating the cathodes, which may therefore have much larger emitting areas than those of conventional thermionic valves. This fact enables the thermionic rheostat to operate efficiently when controlling the flow of power to a load from a.c. supply mains in the common range 200–250 volts. A successful thermionic rheostat might therefore be expected to perform the functions of transducer and amplifier without the necessity for the power transformers and rectifiers usually associated with conventional amplifiers. The possibility exists of obtaining satisfactory performance for certain control requirements by using only two electrical components—a thermionic rheostat and its load. That such a simplification should be appreciated is evidenced by the number of statements made during recent years emphasizing the need for greater reliability and simplicity in industrial electronic equipment.

The experimental thermionic rheostat previously described, in which the spacing was varied by tilting the valve, was intended only for the measurement of its electrical performance. Although some possible methods of effecting control of the spacing were suggested, no attempt was made at that stage to evolve a practical design. The present paper is an account of subsequent work carried out with the objects of demonstrating that an effective thermionic rheostat can be designed using conventional valve construction, and that such a valve can be made to perform operations of sufficient economic importance to justify the development of production models.

(2) THE EXPERIMENTAL VALVE

The experimental thermionic rheostat described in the paper was designed to make use of the equipment, the techniques and some of the parts used in making a small self-heating triode which has been described elsewhere.[6] It represents only one of a number of widely varying approaches which might be made to the problem of designing a practical thermionic rheostat by designers having at their disposal the full range of modern valve technique. To emphasize the particular nature of the valve, and for convenience, it will be referred to as the 'evatron' (eccentric variable-angle thermionic rheostat). The evatron may be regarded as a model whose power ratings could if necessary be increased by a factor of at least 20. Twenty individual valves of this design have been made.

(2.1) Control of Inter-Electrode Spacing

The 'moving' cathode of the evatron is mounted so as to rotate within the valve about a certain axis, while the whole valve is mounted so as to rotate about this same axis. The moving cathode may thus be fixed in space by the action of an external stationary magnet on an armature attached to the cathode. This arrangement (Fig. 1) provides a relatively rigid mechanical relationship between the angular displacement of the valve and the inter-electrode spacing.

(2.2) Construction

The valve and its working parts are illustrated in Fig. 2. The elements are mounted on a standard receiving-valve stem sealed within a standard cylindrical envelope 29 mm in diameter and 85 mm long. Both cathodes are 42 mm long and have hollow rectangular cross-sections measuring 10 mm × 1·5 mm outside

Written contributions on papers published without being read at meetings are invited for consideration with a view to publication.

Dr. Hopkins is in the School of Electrical Engineering, New South Wales University of Technology.

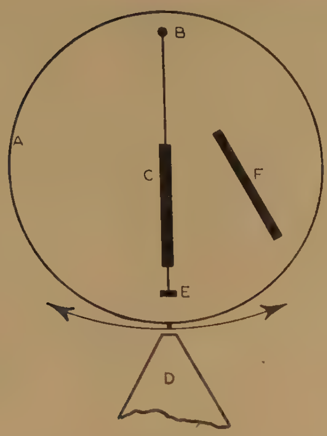

Fig. 1.—Method of controlling inter-electrode spacing.

The envelope, A, rotates about the axis, B. The moving cathode, C, is held stationary by the external magnet, D, acting on the armature, E. The fixed cathode, F, is mounted rigidly within the envelope.

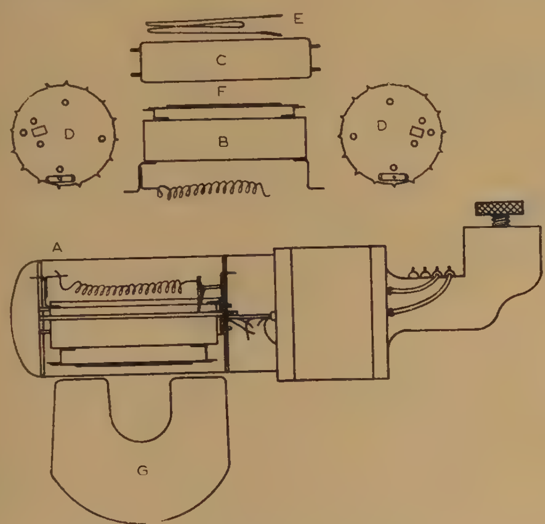

Fig. 2.—The evatron and its working parts.

A. Complete tube.
B. Moving cathode.
C. Fixed cathode.
D. Micas.
E. Heater.
F. Armature.
G. Magnet.

with a wall thickness of 0·25 mm. The fixed cathode is supported between the mica spacers by means of four 1 mm diameter nickel rods. The moving cathode is supported by means of two 0·75 mm molybdenum rods formed into the shape of cranks whose ends rotate within holes drilled in 0·12 mm × 2 mm molybdenum straps clipped to the inside surfaces of the mica spacers. The steel armature measures 30 mm × 2 mm × 1 mm and is attached to the moving cathode by two 0·17 mm tungsten wires which restrict thermal conduction from the cathode. Electrical connection is made to the moving cathode through a helix of 0·12 mm tungsten wire. Both cathodes are made from Grade A nickel and are coated on one face with barium-strontium oxide. Coating weights of from 0·5 to 4·0 mg/cm^2 of carbonates have been used successfully. The fixed cathode is fitted with an insulated starting heater rated at 10 watts, but the moving cathode has no heater. Both cathodes are heat-treated during manufacture by induction heating. A Bakelite base which fits a ¼ in diameter shaft is cemented to the envelope. The base has four hollow nickel terminals which are crimped to flexible connecting wires, the crimped junctions lying on the axis of rotation of the tube. Two internal stops set the minimum cathode-to-cathode spacing at 1 mm and the maximum angle of rotation at about 35°.

(2.3) Mechanical Characteristics

A typical valve mounted on ball races and counterbalanced requires a torque of 3 g-cm to overcome the total static friction. Without counterbalance the valve has a maximum moment due to gravity of 40 g-cm and a moment of inertia of 240 g-cm^2.

(2.4) Electrical Characteristics

The electrical characteristics of an evatron may be represented by a series of r.m.s. voltage/current curves[7] each of which corresponds to a particular angular position of the valve. Such curves are of limited value in practice, because only loads having unity power factor can be represented conveniently on them and because the limits set by cathode-heating requirements vary with the type of load and so cannot be represented as absolute boundaries. It is more convenient to represent the characteristics of the combination of a valve and a particular load connected to a specified a.c. supply as a set of experimental curves showing the significant load variables as functions of the angular position of the valve and indicating the limits set by the requirements of cathode heating.

The maximum cathode-heating power, which should not exceed the maximum permissible cathode dissipation, is a function of the supply voltage and the characteristics of the load, and occurs at a definite angular setting for a particular load[8] condition. The minimum permissible steady-state cathode dissipation is greatly affected by inter-electrode spacing, because the net heat loss from the cathodes at a given temperature increases with the spacing; moreover, the first derivative of heating power with respect to equivalent valve resistance is negative when the spacing is greater than the value corresponding to maximum heating power. Consequently, any tendency to temperature-limited operation over part of the cathode will result in a cooling of the cathode, further loss of emission and perhaps ultimate cessation of current flow. On the other hand, if this derivative is positive, changes in emission and temperature tend to be self-compensating. The above factors result in lower minimum permissible dissipations for inter-electrode spacings below the condition of maximum heating power than for spacings above this value. The effects of these factors are very pronounced with non-parallel inter-electrode arrangements such as that of the evatron.

Fig. 3 shows load power and valve dissipation as functions of angular position, for the series combination of an evatron and a 700-ohm resistive load connected to a 240-volt a.c. supply; the maximum cathode heating power is 20 watts, while the minimum permissible steady-state cathode dissipations are 10 watts in the direction of decreasing angle and 15 watts in the opposite direction with corresponding load powers of 60 watts and 9 watts. The angular sensitivity [(change of load voltage)/(change of angular position)] varies between 8·5 and 2·5 volts per degree over this range.

Fig. 4 shows the torque/speed characteristics of a universal series motor as a function of the angular position of an evatron through which the motor is connected to the 240-volt a.c. mains. The boundaries set by the minimum requirements for steady-state cathode heating are also shown. Such curves, together with the moments of inertia of the motor and the valve, constitute the necessary information for applying such a combination to a control problem, since the effective internal motor torque can be assumed in practice to be an instantaneous function of motor speed and valve position.

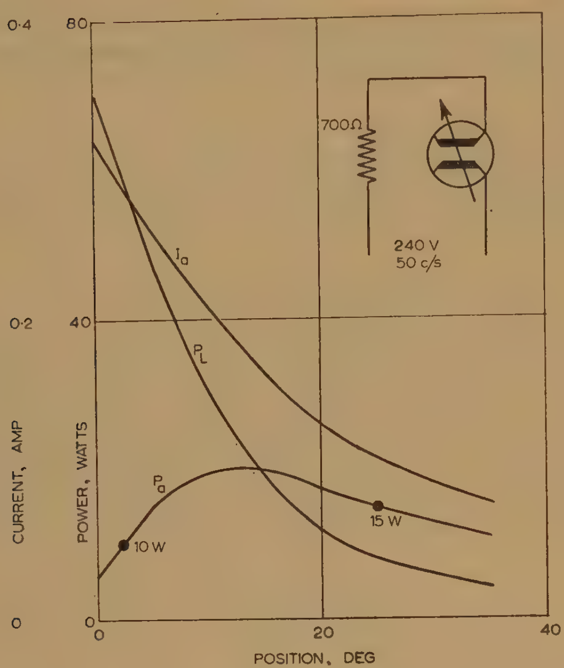

Fig. 3.—Curves of load power, P_L, cathode dissipation, P_a, and r.m.s. current, I_a, as functions of angular position for an evatron connected to a 240-volt supply through a 700-ohm resistive load.

The limits of steady-state operation lie between 10 and 15 watts cathode dissipation.

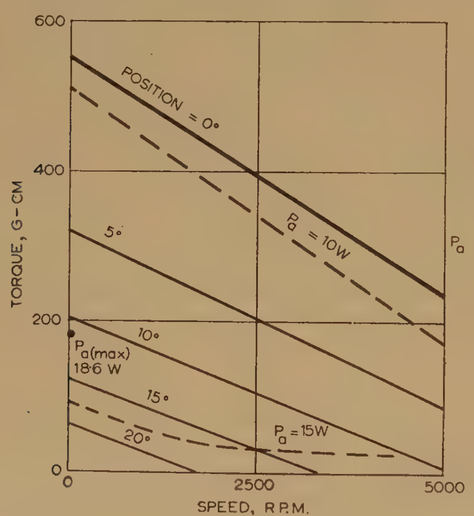

Fig. 4.—Variation of motor torque with speed at various angular valve positions for the series combination of an evatron and a series motor connected to a 240-volt supply.

A 1 μF capacitor is connected across the motor to improve its power factor. Broken lines (10 and 15 watts dissipation) define the limits of steady-state operation.

(2.5) Power Gain and Noise

In order to compare the performance of the evatron with other amplifying devices, it may be helpful to obtain an approximate figure for power gain under some typical operating condition. If the static frictional torque of 3 g-cm referred to in Section 2.3 is assumed to be constant over a sinusoidal input signal of 10° peak value, and if the power of the output signal is defined as $\frac{1}{4}$[(maximum load power) − (minimum load power)] with a 700-ohm load, the power gain can be shown to be 48 dB at 1 c/s and to fall at the rate of 3 dB per octave with increasing frequency. The effective value of the inertial torque increases with the square of frequency and will equal the assumed frictional torque at 1·6 c/s.

Because the output of the evatron is used without further amplification, the noise currents generated by the flow of space-charge-limited current through the valve are of no significance and are in any case likely to be overshadowed by noise originating in the supply mains. However, any relative displacement of the cathodes due to mechanical shock or vibration or to bearing friction during rotation will result in an amplified output signal which could possibly excite a control system in which the valve was operating. The effects of shocks and vibration on the output of the evatron have not been studied, because its unbalanced layout—which will greatly influence its vibration sensitivity—is not regarded as an essential feature (see Section 2.8). The moving cathode can be made to oscillate in the field of the magnet by the effects of a mechanical shock, a typical frequency being 20 c/s. Such oscillations are sustained only for peak amplitudes of 2° or less and do not significantly affect the characteristics of a combination of motor and valve.

(2.6) Starting

The evatron is started by heating the fixed cathode only and operates initially as a rectifier. When both cathodes are at operating temperature the heater is switched off, either manually or by a relay whose coil is in series with the cathodes. One experimental valve has a Nichrome-molybdenum bimetallic strip attached to a cathode support, the strip operating a pair of contacts within the valve to break the 240-volt supply to the heater. Automatic starting using such an internal thermal relay, together with mains-voltage heaters, appears to be practicable.

(2.7) Life Tests

Two evatrons (Nos. 6 and 9) were life tested for a period of 3 000 hours in an apparatus which subjected them to a displacement of ±15° 90 times per minute at constant angular velocity while operating in series with 240-volt 40-watt lamps. At the end of the test the bearings of both tubes had worn by approximately the journal diameter and the cathodes of No. 6 (originally sprayed with 0·5 mg/cm^2 of carbonates) were almost denuded of coating.

(2.8) Further Development

The principal weaknesses of the present design are the non-parallel cathode movement, the electron bombardment of the envelope, and the unnecessarily high moment of inertia due to eccentricity. In higher-powered valves having larger envelope diameters and multiple cathodes moving about a central axis of rotation, these weaknesses could be reduced or eliminated. The life of such valves could be improved as regards cathode erosion and bearing wear by increasing the coating weight and the bearing area. Moreover, research into cathode performance and bearing design might be expected to produce significant improvements.

Notwithstanding the present encouraging results, a survey should be made, prior to any further development, into all suggested methods of cathode suspension and control in the light of available production techniques and probable application requirements. The result of such a survey could well be a practical design having little resemblance to the present model.

(3) APPLICATIONS

It is possible to devise applications for suitably designed thermionic rheostats in many control systems where mechanical-to-electrical signal conversion and subsequent amplification are

required. However, the principal potential advantage which these valves appear to offer at present lies, not in the improvement of existing electrical controls, which are already highly developed, but rather in making possible the addition of electrically simple automatic controls to certain industrial processes where present-day electronic equipment cannot be justified because of its initial cost or because of the servicing problems which it creates. The three experimental laboratory equipments illustrated in Figs. 5, 6 and 7 are intended to typify such applications of the thermionic rheostat.

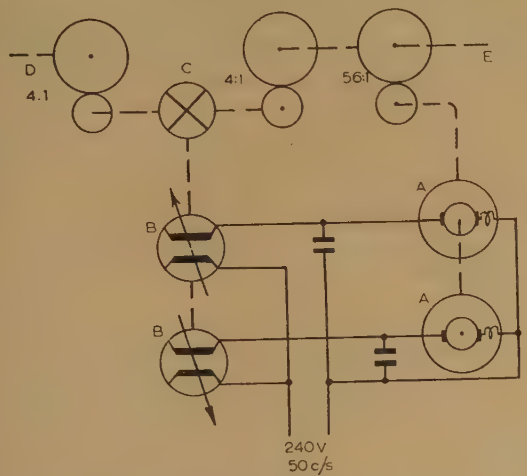

Fig. 5.—Experimental position control.

A. Series motors.
B. Evatrons.
C. Differential gear.
D. Input shaft.
E. Output shaft.

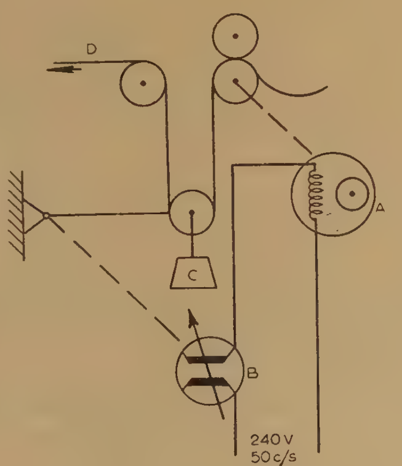

Fig. 6.—Experimental velocity integral control.

A. High-resistance shaded-pole induction motor.
B. Evatron.
C. Tensioning weight.
D. Moving thread.

(3.1) Stability

The provision of special electrical means for controlling the stability of such systems is inconsistent with the retention of their electrical simplicity. However, in systems such as those shown in Figs. 5 and 6, all mechanical inertias, including those of the motor and the valve, are inelastically coupled together, resulting in a second-order characteristic which may be damped sufficiently if the internal motor torque falls rapidly with increasing speed.[9] Higher-order systems in which a mechanical compliance exists between the motor and the valve (see Fig. 7)

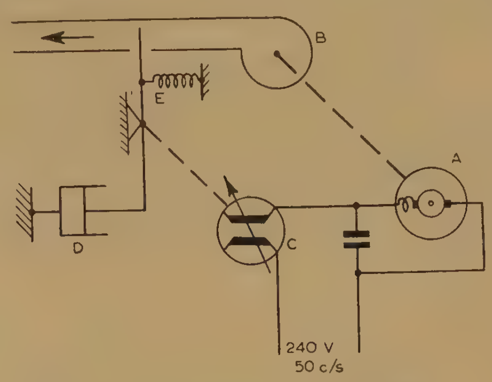

Fig. 7.—Experimental air-flow control.

A. Series motor.
B. Blower.
C. Evatron.
D. Oil dashpot.
E. Restoring force.

may be stabilized at the expense of response time by the application of mechanical damping to the valve shaft, which is normally the point of minimum signal power.

(3.2) Position Control

The position control illustrated in Fig. 5 makes use of two series motors (Fig. 4), each controlled by an evatron, which exert opposing torques on a common shaft to obtain reversible motor action.* The evatrons act in opposite directions in response to an error signal. The driven motor produces a damping of the system in addition to that of the driving motor, but also absorbs some of the shaft power of the driving motor. The following performance figures[10] were measured with the angular displacement between the valves set to give a critically damped characteristic:

Dead zone: $\pm 2°$.
Velocity misalignment coefficient: $1 \cdot 3 \times 10^{-2}$ sec.
Time-constant of step-function response: 9×10^{-2} sec.
Stiffness coefficient: 6 kg-cm/deg.

(3.3) Velocity Integral Control (Tension Control)

The velocity integral control illustrated in Fig. 6 will operate in either direction, with the controlled motor acting either as motor or as brake. The ranges of operating speeds with a typical thread tension of 100 g are 20–140 cm/sec for motoring and 20–300 cm/sec for braking. The natural frequency of the system lies between 2 and 2·5 c/s over the range, and the damping ratio is approximately 0·2.

(3.4) Air-Flow Control

The air-flow control illustrated in Fig. 7 uses the series motor shown in Fig. 4. The typical restoring torque setting of 74 g-cm acting on the valve results in a steady-state motor voltage of 170 volts and an angular valve position of 7°. At this working point the zero-frequency open-loop gain is −24, the natural frequency is 1·3 c/s and the overshoot is 10%.

* A valve containing four pairs of cathodes (see Section 2.8) connected as a 4-element bridge to supply the control winding of a 2-phase servo-motor is visualized as the most promising arrangement for reversible motor action.

(4) CONCLUSION

The construction and successful operation of a small experimental thermionic rheostat, the evatron, has shown that the theoretical possibilities of the thermionic rheostat as an element in simple automatic control systems can be realized in practice.

(5) REFERENCES

(1) SPANGENBERG, K. R.: 'Vacuum Tubes' (McGraw-Hill, New York, 1948), p. 201.
(2) COBINE, J. D.: 'Gaseous Conductors' (McGraw-Hill, New York, 1941), p. 453.
(3) RAMBERG, W.: 'Vacuum-Tube Acceleration Pick-Up', *Journal of Research of the National Bureau of Standards*, 1946, **37**, p. 391.
(4) OLSON, H. F.: 'Mechano-Electronic Transducers', *Journal of the Acoustical Society of America*, 1947, **19**, p. 307.
(5) HOPKINS, E. G.: 'Self-Heating Thermionic Tubes', *Proceedings I.E.E.* Paper No. 1604 R, March, 1954 (**101**, Part III, p. 77).
(6) HOPKINS, E. G.: 'A Self-Heating Triode for Voltage Stabilization', *Wireless Engineer*, 1954, **31**, p. 169.
(7) Reference 5, p. 79.
(8) Reference 5, p. 78.
(9) WEST, J. C.: 'Textbook of Servomechanisms' (English Universities Press Ltd., London, 1953), p. 34.
(10) 'Glossary of Terms Used in Automatic Controlling and Regulating Systems', B.S. 1523: 1954, Section 3, Sub-Section 37.

Abstract No. 2359
Apr. 1957

NORTH STAFFORDSHIRE SUB-CENTRE: CHAIRMAN'S ADDRESS

By A. T. CHADWICK, Member

(ABSTRACT *of Address delivered at* STAFFORD, 11*th February*, 1957.)

It is not within the mental capacity of one individual to become intimately conversant with the detail design and manufacture of the whole variety of equipment comprising electrical generation, distribution and application. The result is that engineers tend to become either possessed of a general acquaintance with a large part of the subject or alternatively trained to a close and intimate knowledge of an apparently very restricted field. At the start of an engineer's life (as such) the decision as to which of these impulses to follow is made—consciously or by accident or fate in the form of opportunity.

Those who consciously form a choice may be inclined to a view commonly held that the concentration on a restricted line of work is less attractive, if only by reason of its apparent narrowness, and the words 'in a groove' may be used to discourage the idea. The alternative of becoming knowledgeable over a wide range of our subject may be more alluring, in that such a course may provide means to a wider engineering life and experience and consequently a position of greater value to the community and therefore to the individual. This question, which it may be agreed presents itself with a greater or less degree of conscious torment to every young engineer, calls for an early decision. The period which may be termed training time must constitute approximately 30% of an engineer's effective working life. To be most beneficially used, it should be started with a definite view of its real purpose.

Of these two views of aims of professional engineering life, namely generalization or specialization, a choice must be made and may vary by reason of individual feeling or may be made without a proper appreciation of the inherent effects of the choice. It may be suggested that generalization will provide an interest and experience in many and varied items of engineering practice and equipment: life will be full, and variety is the spice of life; this is the tempting sequence.

The allure of generalization can, however, be deceptive. Taken to the limit, of course, it may result in knowing nothing about everything or sheer bewilderment. There is this about the specialist: provided he starts early and earnestly, he must and will find a widening of this field of essential interest the further he travels in his specialist pathway. To obtain the most effective results in his particular field, he finds himself forced to discover the characteristics of a large range of associated materials and processes. This can be done only by contact with others who are themselves specialists. It is probably true to say that specialists in different branches of engineering form a close brotherhood, where experience is shared in common acceptance of the continual effort to wrest from nature more profit and life to mankind. To become a specialist is therefore to play a vital part in a great human enterprise. This acquaintance with his fellows and the detail of their knowledge forms the basis for much of his own specialist work.

Mr. Chadwick is with the English Electric Co., Ltd.

As an instance of this wideness of essential knowledge involved in the fullest application to a single line of work, we may consider the design and construction of what is frequently referred to as the simplest and most elemental form of electrical equipment, namely the power transformer. This usually consists of an assembly of steel, copper, vegetable fibres, mineral oil and porcelain. The field of interest and detail knowledge desirable to a specialist transformer engineer involve all the materials and products which he uses; only then can he make the most effective use of the several elements of the finished transformer. Such interest will, I suggest, prove to be both broad and alluring.

To illustrate this theme, I propose to discuss under several heads the main elements used in transformer construction, namely steel for the magnetic circuit, copper for the windings, Fullerboard for the main insulation, and ceramics for terminal bushings. Finally I propose to show something of the production of the transformers themselves.

[There followed a review of the history and development of production processes applicable to the four basic materials, and a brief description of core treatment, coil winding and transformer assembly, profusely illustrated by lantern slides.]

Perhaps I should apologize for the implied limits of interest and desirable knowledge involved in relation to the design of transformers. I have only attempted to deal sketchily with the main basic materials and have made no mention of the problems of mechanical stress imposed on winding structure under system short-circuits; electrical stresses resulting from lightning imposed on transmission circuits; the involved thermal performance of the core, windings and cooling systems; and the many and varied conditions relating to the application of transformers.

I hope I have conveyed an impression that the specialist designer can and must take a wide and comprehensive view from his own corner of our industry and can therefore discover a full and rewarding demand on his utmost capacity.

621.3:614.84

Paper No. 2316 U
Apr. 1957

FIRES OF ELECTRICAL ORIGIN

By D. I. LAWSON, M.Sc., F.Inst.P., Member, and J. F. FRY, B.Sc., A.M.I.C.E.

(*The paper was first received* 10*th October, and in revised form* 10*th December*, 1956.)

SUMMARY

The incidence of electrical fires is described, and it is shown that fires due to apparatus occur at a rate of one per 10^4 MWh transmitted. Fires due to fixed installations do not appear to vary with time, although it is expected that these may increase during the coming years owing to the ageing of cables. There appears to be little evidence that fires are being caused by the overloading of cables. Details are given of a survey which is to start in 1957.

(1) INCREASING DEMAND FOR ELECTRICITY

During the last 50 years the electrical energy distributed per annum has risen steadily, and it seems that, in the future, with the development of nuclear power, electrical distribution will play an even greater part in the national economy. It is perhaps prudent, therefore, to consider how this is likely to affect the fire situation over the next decade or two.

Table 1 shows the growth in the demand for electricity with time. It will be seen that the energy distributed is expected to rise by a factor of approximately three by 1975, while the number of consumers will rise by about one-quarter.

Table 1

THE INCREASING DEMAND FOR ELECTRICITY

Year	1905	1915	1925	1935	1945	1955	1965	1975
Electrical energy transmitted, MWh × 10^6	0·5	2	6	17	35	74*	120*	200*
Electrical power generated, MW × 10^3 ..	—	1·2	4·4	8	12	20*	40*	60*
Consumers × 10^6	—	—	1·86	7·62	10·9	14·0†	16·4†	17·8†

* Estimated from Reference 1.
† Estimated.

The pattern of electrical development in the future is expected to be much the same as in the past, as can be seen from Table 2, which shows the amounts to be used in various applications. This continuity of pattern would tend to indicate that the growth in the annual rate of fires from electrical causes would be maintained.

(2) ELECTRICAL FIRES IN GENERAL

Nearly all the electrical energy generated is ultimately degraded to heat in a controlled manner, which harmlessly warms the surroundings in which the equipment is used. This is a tribute to the quality of electrical circuits and equipment. Nevertheless, sometimes small amounts of energy are inadvertently applied to combustible materials, and a fire may then ensue. The power density required to start ignition is quite small. A density of 5 watts/cm^2 is quite sufficient to cause most combustible materials to ignite spontaneously.

The chance of fires occurring would be expected to depend both on the power transmitted, and, of course, since the problem is a statistical one, on the time for which the transmission is taking place. This suggests that the number of fires should be proportional to the energy transmitted.

The chance of a fire being caused by a fixed installation will also depend on the length of circuit energized, but, as will be seen later, the large majority of fires are associated with apparatus, so that, to a first approximation, the effect of the length of the circuit can be disregarded.

It can be seen from Fig. 1 that a linear relationship exists between the number of fires annually attended by the fire brigades and the electrical energy transmitted. These fires may be divided into two categories: those due to wire and cable, and those due to apparatus. It is convenient to consider each separately.

(2.1) Fires Due to Wire and Cable

For the purpose of the paper fires due to wire and cable are defined as those originating in permanently installed electrical circuits, and they do not include fires in plugs and flexible leads to apparatus. The latter are considered in Section 2.2. It can be seen from Fig. 1 that fires due to wire and cable are independent of the amount of electrical energy transmitted—the number is about 2 400 per annum. The fact that the number of new installations is varying much less rapidly with time than the amount of electrical energy transmitted annually suggests that the fires associated with wires and cables are not due to the continuous overloading of cables, and it is interesting that

Table 2

ELECTRICITY CONSUMPTION IN GREAT BRITAIN
(Taken from Reference 1)

	1925	1950	1954	1965	1975
	MWh × 10^6	MWh × 10^6	MWh × 10^6	MWh × 10^6	MWh × 10^6
Industrial	3·7	23·4	32·0	61	107
Domestic and agricultural	0·6	14·9	19·6	37	63
Commercial	0·9	6·1	9·5	16	27
Traction	0·5	1·5	1·4	2	4

Written contributions on papers published without being read at meetings are invited for consideration with a view to publication.

Mr. Lawson and Mr. Fry are with the Joint Fire Research Organization of the Department of Scientific and Industrial Research and Fire Offices' Committee.

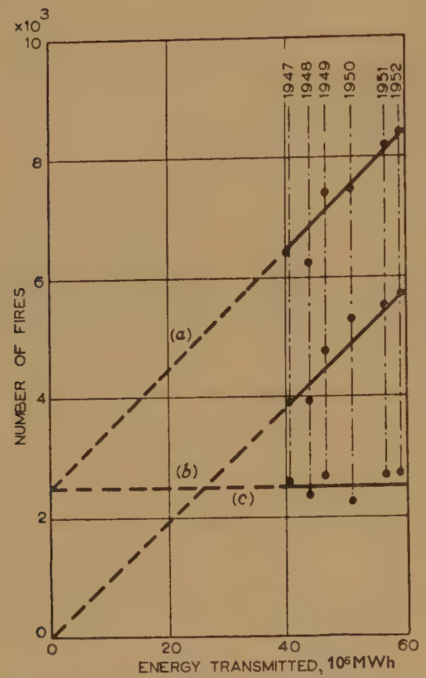

Fig. 1.—Number of fires of electrical origin occurring annually, in terms of electrical energy transmitted.

(a) Total fires of electrical origin.
(b) Fires due to electrical apparatus.
(c) Fires due to wire and cable.

Gosland[2] lists overloading as the cause of very few fires. Indeed some experiments carried out by McGuire and the author on fires due to overloaded cables (see Appendix 8.1) showed that gross overloading must take place before a fire is started.

The independence of fires due to wire and cable on the electrical energy transmitted might suggest that the faults were associated with bad connections and leakage, as these would tend to vary more with the number of installations, although the evidence is not at all conclusive. It has been stated[2] that the chance of a fire occurring in an installation increases at the rate of 7 parts per million per year, and thus the fires might be expected to increase according to the age and number of circuits in existence. This trend over the period covered by the paper would be lost in the statistical fluctuations of the data available. Some estimates of the fires caused by wire and cable may be made from Table 1. The aggregate age of the installations at present in use and those predicted in the years 1965 and 1975 is given in Table 3.

Table 3

Aggregate Age of Installations (in Consumer Years $\times 10^6$)

Year of survey	Pre-1925	1925–35	1935–45	1945–55	1955–65	1965–75	Total
1955	65	140	50	15·5	—	—	270
1965	83	201	82	46	12	—	424
1975	102	260	116	77·5	36	7	598

Thus, unless a large proportion of the fixed installations are written off in the next 20 years, it might be expected that the annual number of fires caused by fixed installations would increase to about double the present figure of 2400 per annum. The maximum number of fires would be caused by the installations connected in the period 1925–35; these would account for about one-half of the total fires due to fixed installations.

(2.2) Fires Due to Electrical Apparatus

No attempt has been made so far in the collection of statistics of fires due to electrical apparatus to ascribe the cause either to the user or to the apparatus. Thus it does not follow that the fires were necessarily due to faulty equipment; indeed, it is known that a large number were due to misuse of apparatus and might, in some cases, have occurred had other types of fuel been used.

It can be seen from Fig. 1 that the number of electrical fires occurring annually is proportional to the annual quantity of electrical energy transmitted, the rate being one fire per 10^4 MWh. Thus it might be expected from the programme of electrical power development that the number of fires per annum would be trebled unless there were a marked change in the reliability of apparatus or the habits of the general public in that time. Fig. 2 shows the total number of fires (including wire and cable) estimated for the next 20 years.

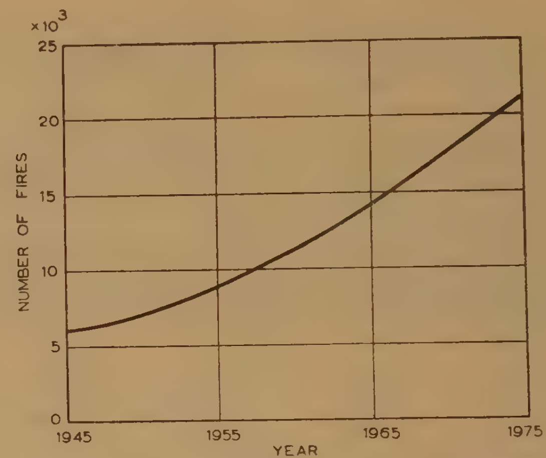

Fig. 2.—Estimated number of fires of electrical origin occurring annually in Great Britain for the period up to 1975.

This increase in the number of fires of electrical origin may, however, be accompanied by a decrease in the number of fires which would formerly have had their origin in other sources of fuel. For example, a change to electrical heating may result in an electrical fire, but at the same time it means that there is potentially one fire less due to coal or gas heating; and the increasing fire incidents associated with electric heaters, cookers and irons may be counterbalanced by a decrease in fire outbreaks due to coal, gas or oil-fired appliances. Whether this will result in the fire situation becoming better or worse will depend on the relative hazards associated with the equipment and its use.

The annual number of fires associated with various kinds of apparatus is shown in Table 4.

Some of the appliances (e.g. radio, television, etc.) can use only electricity, and for these the increasing fire rate is not counterbalanced by any decrease in the number of fires having their origins in other forms of fuel. The same applies to equipment that can use an alternative fuel but in which fires occur mainly in the electrical version. This division is shown in Fig. 3, where it can be seen that the fire rate for equipment which can use only electricity is about the same as that for electrical equipment which has its equivalent using other fuel.

(3) FUTURE ACTION

This possible large increase in the annual rate of fires of electrical origin requires the closest attention. Since the majority

Table 4

ELECTRICAL FIRES IN GREAT BRITAIN, 1947–52

Supposed cause of fires	Number of fires					
	1947	1948	1949	1950	1951	1952
Cooker	393	444	744	738	784	812
Fire, heater or radiator	1 184	889	884	1 078	1 186	1 156
Iron	378	354	436	370	360	368
Motor	429	328	200	282	336	356
Refrigerator	552	782	1 104	1 128	1 014	1 116
Sound radio	228	332	388	356	414	424
Television	12	30	52	96	134	156
Wire and cable ..	2 556	2 316	2 640	2 188	2 656	2 696
Other apparatus ..	696	712	948	1 256	1 284	1 272

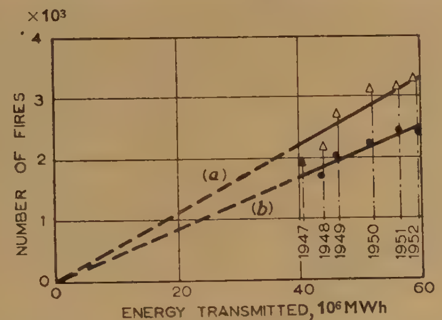

Fig. 3.—Effect of the type of electrical apparatus on the annual number of fires.

(a) Apparatus peculiar to electricity.
(b) Apparatus not peculiar to electricity.

of the fires appear to be associated with apparatus, it is necessary first to identify the types of apparatus giving most trouble and to find out whether the fires are being caused by misuse or by defective equipment.

If the fires are found to be mainly due to the misuse of electrical apparatus, it will be necessary to educate the public in the use of the apparatus concerned and to see whether it can be made more foolproof. It may be found that fires are being caused by cookers or heating appliances which are installed too near combustible materials, and this would require a change in the regulations governing the installation of such appliances.

Should it be found that a large number of fires are resulting from electrical faults, the co-operation of electrical manufacturers' associations or of individual manufacturers as appropriate would be required.

Any recurrent faults in fixed installations would, of course, be a matter for consideration by The Institution's Wiring Regulations Committee.

(4) COLLECTION OF INFORMATION

Before any action can be considered it is necessary to collect the information on which it can be based.

During the last few months a questionary has been drawn up by the Joint Fire Research Organization in consultation with members of the Electrical Research Association Sub-Committee V/B (Fire Risks), and H.M. Chief Inspector of Fire Services has agreed to ask the various fire brigades in the United Kingdom to complete it for all fires they attend which are suspected of being caused by electrical apparatus or electrical installations. In case of doubt the C.E.A. Area Board will be consulted. The form to be issued is shown in Appendix 8.2. It has been designed by the Statistical Unit of the Joint Fire Research Organization and is self-coding—the appropriate items will be ringed. Though the form looks complicated, comparatively few items are involved, a minimum of writing is necessary and it is hoped that ambiguity has been avoided.

During the first year it is expected that reports will be available for nearly 9 000 fires, and this should enable some of the broader issues to be considered.

(5) CONCLUSIONS

(a) Fires due to electrical apparatus which are attended by fire brigades are increasing proportionately to the amount of electrical energy transmitted annually. These fires occur at a rate of one fire for every 10^4 MWh transmitted.

(b) If the scheduled increase in the generation of electrical power is maintained, it is expected that the fires due to apparatus will increase from the present figure of about 6 000 per annum to 18 000 per annum in 1975.

(c) The number of fires due to fixed installations is, at present, fairly independent of the electrical energy transmitted, although Gosland[2] has shown that there is a significant increase in fire susceptibility with the age of the installation. During the next 20 years the aggregate age of installations will more than double unless a considerable proportion is written off, and it may be expected that fires due to installations will rise by 1975 to nearly 5 000 per annum.

(d) There is, at present, no evidence to suggest that the fires in fixed installations are mainly due to the overloading of cables. Laboratory experiments indicate that cables are very conservatively rated with respect to fire; this is borne out by the independence of fires in fixed installations on the energy transmitted.

(e) The first step in the solution of the problem of electrical fires is to start a survey to discover the causes. This is now being carried out.

(6) ACKNOWLEDGMENTS

The work described in the paper forms part of the programme of the Joint Fire Research Organization of the Department of Scientific and Industrial Research and Fire Offices' Committee; the paper is published by permission of the Director of Fire Research.

The authors are indebted to the members of the British Electrical and Allied Industries Research Association Sub-Committee V/B for their advice in designing the questionary on electrical fires. Mr. D. W. Millar of the Statistical Unit of the Joint Fire Research Organization advised in the difficult task of preparing the form for coding, and the Unit also provided the statistical information on which the paper is based. Mr. J. H. McGuire supervised the experiments on overloaded cables, and Miss E. M. Shakeshaft assisted with the preparation of the paper for publication.

(7) REFERENCES

(1) 'A Programme of Nuclear Power', House of Commons Command 9389 (H.M. Stationery Office, 1955).

(2) GOSLAND, L.: 'Age and the Incidence of Fires in Electrical Installations', *Proceedings I.E.E.*, Paper No. 1938 U, January, 1956 (**103** A, p. 271).

(8) APPENDICES

(8.1) Fires Due to Overloading Cables

Investigations were undertaken to find the circumstances under which the following electric cables could cause fires:

(a) Twin rubber-covered 250-volt cable (1/·044 in rated at 6·1 amp).

(*b*) Twin 660-volt p.v.c.-covered cable (3/·029 in rated at 7·8 amp).

(*c*) Single vulcanized-rubber-insulated cable (3/·029 in rated at 7·8 amp).

(*d*) Samples of old vulcanized-rubber-insulated cable installed in 1916 and withdrawn in 1952 (3/·029 in rated at 7·8 amp).

(8.1.1) Experimental Procedure.

Various overload currents were passed through the cables under test. The conductors of the twin cables, which each carried the test current, were maintained at different potentials in order to observe when the conductors touched. In the case of single cables the potential was maintained between the conductor and a foil of thin copper containing the cable. The cables were placed between ½ in-thick sheets of fibre insulating board, and observations were made of the times at which the conductors broke through the insulation to form a short-circuit and also of the times at which fires broke out.

(8.1.2) Results.

The results are shown graphically in Fig. 4, in which it is seen that the short-circuit fault in both p.v.c. insulation and rubber is

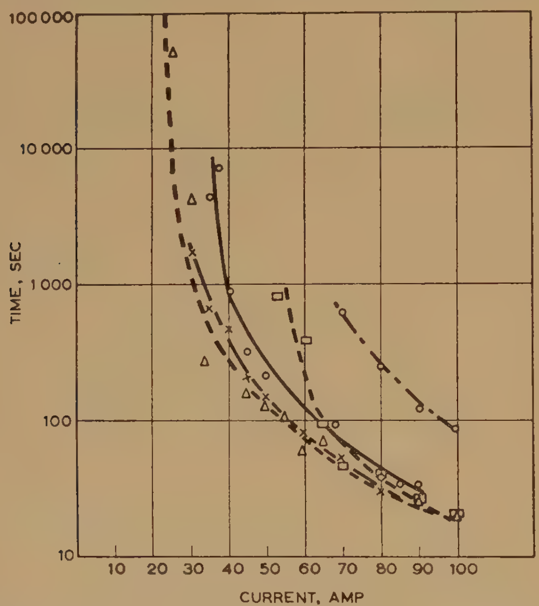

Fig. 4.—Graph showing the time for either a fire or a short-circuit to develop on a cable when carrying various currents.

×—×—× Tough-rubber-sheathed cable. Short-circuit.
○—○—○ Tough-rubber-sheathed cable. Fire.
△- -△- -△ P.V.C.-insulated cable. Short-circuit.
□- -□- -□ P.V.C.-insulated cable. Fire.
○-··-○-··-○ Vulcanized-rubber-insulated cable. Short-circuit and fire.

distinct from the beginning of the fire. These two events occurred almost simultaneously when higher currents were passed through the p.v.c. cable, although closer inspection showed that the short-circuiting of the conductors and the outbreak of fire were not related. However, with the vulcanized-rubber-insulated cable, the two occurrences appeared to be simultaneous.

From the curves it seems that there was a greater tendency for short-circuits to develop with p.v.c.-insulated conductors at lower currents than with rubber-covered cable, but a lower tendency to cause fires as the current was increased.

The minimum currents at which fires occurred in the various cables are given in Table 5.

Table 5

CURRENTS NECESSARY TO CAUSE FIRES IN VARIOUS CABLES

Type	Current	Power per run	Equivalent shunt resistance to give the same power with 230 volts between conductors
	amp	watts/ft	ohms/ft
Twin rubber-covered cable (1/·044 in)	35	13	4 100
Twin p.v.c.-covered cable (3/·029 in)	55	25	2 100
Vulcanized - rubber - insulated cable (3/·029 in)	65	17·5	3 000

Some experiments were made with cables which had been boiled in water for 15 min. With p.v.c. and tough-rubber cable the moisture evaporated on test owing to the heating of the current-carrying cable, and the insulation between the conductors remained good until the current was increased to the short-circuiting point. The water appeared to affect the resistance of the vulcanized-rubber insulation, reducing it to about 50 000 ohms/in. The insulation recovered as the cable dried.

There appeared to be no significant difference in performance between old and new vulcanized-rubber-insulated cables, although the insulation of old cable was harder and more friable.

The insulation resistance was measured before and after test for the various types of cable, and the results are shown in Table 6.

In all samples of cable investigated the currents necessary to cause fires were greatly in excess of the rated currents. A current of this magnitude would flow only if the local fuse were incorrectly rated. It is understood that the fuse rating for domestic premises is 60 amp and it is perhaps interesting that this current would cause a fire in tough-rubber-sheathed and p.v.c. insulated cables within a few minutes, but attempts to cause a fire by passing

[*continued on page 191*

Table 6

INSULATION RESISTANCE OF THE VARIOUS TYPES OF CABLE BEFORE AND AFTER TEST

Type	Insulation test before experiments	Insulation test after experiments	Remarks
Rubber and p.v.c. insulation	∞	∞	Even when the material was reduced to powder by flame, this still applied
New vulcanized rubber insulation Old vulcanized rubber insulation } ..	∞	∞	Currents of 60 amp and less
New vulcanized rubber insulation Old vulcanized rubber insulation } ..	∞	Between zero and ∞	Currents in excess of 60 amp, whether fire occurred or not

Report of Electrical Fire

[See Section 8.2, page 191]

This side of form to be used for reporting fires due to wire and cable and equipment forming part of permanent electrical supply installation, including outdoor fires but excluding fires in vehicles.

Code	Item	Cols.
	Fire Brigade	1–3
	K.433 No.	4–7
	Date	8–13
	Day of week	14
	Time of discovery	15–16
	Premises	17–18
00	House	
01	Flat built as flat	
02	Flat in converted house	
03	Club, hotel, restaurant, etc.	
04	Office	
05	Shop or showroom	
06	Warehouses, wholesale dealers	
07	School, college	
08	Hospital, home, institution	
09	Factory, workshop, other industrial premises	
	Other than above	
	Location of Failure	19
0	Indoor	
1	Outdoor	
	Part of Installation Failing	20–21
00	Cable or flex	
01	Ceiling rose	
02	Circuit-breaker	
03	Fuse box (metal)	
04	Fuse box (Bakelite, plastic)	
05	Fuse box (other than above)	
06	Joint box (compound-filled)	
07	Joint box (not filled)	
08	Plain socket	
09	Switch socket	
10	Switch	
11	Distribution board	
	Other than above	
	Age of Installation	22–23
	Age in years	
99	Unknown	
	Type of Labour Used for Installation	24
0	Professional	
1	Amateur	
2	Unknown	
	Type of Fuse	25
0	Enclosed	
1	Open	
2	Cartridge	
3	Miniature circuit-breaker	
4	Enclosed fuse with earth-leakage circuit-breaker	
5	Open fuse with earth-leakage circuit-breaker	
6	Cartridge fuse with earth-leakage circuit-breaker	
7	Miniature circuit-breaker with earth-leakage circuit-breaker	
	Other than above	
	Size of Fuse or Rating of Circuit-Breaker	26–27
	Amp	
99	Unknown	

Code	Item	Cols.
	Type of Wiring Causing Fire	28
0	V.R. lead-covered	
1	V.R. other than lead-covered	
2	T.R.S.	
3	P.V.C. or other plastic-covered	
4	Flexible cable (flex)	
5	Temporary wiring	
	Other than above	
	Protection of Cable	29
0	Unprotected	
1	Casing and capping	
2	Steel conduit	
3	Plastic conduit	
4	Ducting	
	Other than above	
	Size of Conductor (Size — Current rating, amp)	30–31
00	1/·044 — 6·1	
01	3/·029 — 7·8	
02	3/·036 — 12·0	
03	7/·029 — 18·2	
04	7/·036 — 24·0	
05	7/·044 — 31·0	
06	7/·052 — 36·8	
07	Other cables with 7 strands or less	
08	Cables with more than 7 strands	
99	Unknown	
	Defect in Main Conductors	32–33
00	Circuit overloaded	
01	Defective contact	
02	Broken conductor	
03	Insulation damaged mechanically, e.g. by chafing and piercing	
04	Insulation damaged from other causes, e.g. moisture, heat, age, chemical action	
	Other than above	
99	Unknown	
	Defect in Protective System	34–35
00	Defective contact in earthing circuit	
01	Earth-continuity conductor touching gas pipe	
02	Earth fault not associated with gas pipe	
	Other than above	
99	None	
	Seat of Generation of Heat Causing Fire	36
1	Any defect in main conductors	
2	Any defect in protective system	
	Extinction of Fire	37
1	Fire died out	
2	Fire extinguished before arrival of fire brigade	
3	Fire tackled before arrival of fire brigade, extinguished by brigade	
4	Fire not tackled before arrival of fire brigade, extinguished by brigade	

Report of Electrical Fire

[See Section 8.2 on next page]

This side of form to be used for reporting fires due to electrical apparatus, including outdoor fires but excluding fires in vehicles.

Code	Item	Cols.
	Fire Brigade	1–3
	K.433 No.	4–7
	Date	8–13
	Day of week	14
	Time of discovery	15–16
	Premises	17–18
00	House	
01	Flat built as flat	
02	Flat in converted house	
03	Club, hotel, restaurant, etc.	
04	Office	
05	Shop or showroom	
06	Warehouses, wholesale dealers	
07	School, college	
08	Hospital, home, institution	
09	Factory, workshop, other industrial premises	
	Other than above	
	....	
	Location of Failure	19
0	Indoor	
1	Outdoor	
	Apparatus Primarily Involved	20–21
00	Boiling ring	
01	Cooker, oven (domestic)	
02	Drier (other than oven)	
03	Hot-plate	
04	Kettle	
05	Oven (industrial)	
06	Fire (guarded)	
07	Fire (unguarded)	
08	Heater (convection)	
09	Heater (off-peak storage type)	
10	Radiator or tubular heater	
11	Lamp (portable)	
12	Light or light fitting (fixed)	
13	Fluorescent lighting (or choke)	
14	Immersion heater	
15	Water heater (other than immersion)	
16	Radio or radiogram	
17	Television	
18	Accumulator	
19	Blanket or bed-warmer	
20	Iron	
21	Motor	
22	Motor controller	
23	Plug, adaptor or connector	
24	Projector	
25	Refrigerator (compressor type)	
26	Refrigerator (heater type)	
27	Thermostat or thermal relay	
28	Transformer	
29	Washing machine	
30	Welding apparatus	
31	Wire or cable (lead to apparatus)	
	Other than above	
	....	
	Indicator Lamp	22
0	Pilot lamp fitted	
1	No pilot lamp	

Code	Item	Cols.
	Thermostatic Control	23
0	Thermostat fitted	
1	No thermostat	
	Power Taken by Apparatus	
	(*a*) Watts	24–27
	or (*b*) Horse-power	28–30
	Fuse in Circuit-Feeding Apparatus	31–32
	Size of fuse, amp....................	
99	Unknown	
	Make of Apparatus	33–34
	Maker's name	
	....	
99	Unknown	
	Age of Apparatus	35–36
	Age in years	
99	Unknown	
	Allocation of Fault	37
0	Fault in equipment	
1	Fault in installing or connecting equipment	
2	Improper or careless use	
	Other causes	
	....	
9	Unknown	
	Cause of Fire	38–39
00	Heating due to bad contact	
01	Heating due to defective insulation	
02	Overheating other than by overloading	
03	Overloading	
04	Short-circuit by mechanical defect or external agency	
05	Earth fault leading to generation of heat elsewhere	
06	Direct contact with combustible material	
07	Ignition of combustible material without direct contact	
	Other causes	
	....	
99	Unknown	
	Spread of Fire	40
1	Fire confined to apparatus of origin	
	Fire spread beyond apparatus of origin	
2	damaging —structure only	
3	—contents only	
4	—structure and contents	
	Extinction of Fire	41
1	Fire died out	
2	Fire extinguished before arrival of fire brigade	
3	Fire tackled before arrival of fire brigade, extinguished by brigade	
4	Fire not tackled before arrival of fire brigade, extinguished by brigade	

this current through the more traditional vulcanized-rubber-insulated cables failed.

(8.2) Reporting Forms for Electrical Fires Involving Fixed Installations and Apparatus*

Notes on Completing 'Report of Electrical Fire'

A copy of the form should be completed for every fire to which a fire brigade was called, in which either electrical apparatus or electric wire or cable was the source of ignition, including those fires in which materials were ignited not through any fault in the apparatus but because of careless usage. Electrical fires in vehicles should *not* be included.

1. Please ring the appropriate number in the column headed 'Code' (e.g. if the fire occurred in an hotel a ring should be put around the number 3 to the left of 'club, hotel, etc.').

2. Where no number is shown in the 'Code' column, please enter particulars in the space provided.

3. Please note that this form does not replace the normal form K.433.

4. The intention is that for any given fire only one side of the form, and only one item in any box should be applicable. Difficult cases may arise, but reporting officers are asked to resolve the difficulty if possible, or to send in a brief description of the circumstances.

5. The I.E.E. current rating has been included against each specified size of the conductor to help the reporting officer to judge whether the circuit is overloaded. A short table of the current-flow equivalent to various power ratings in watts at three voltage levels is given below, together with some representative power and current-consumption figures for various types of domestic apparatus.

(1) Current Flow equivalent to Various Power Ratings

Power rating of apparatus	Normal voltage of installation		
	200 volts	220 volts	240 volts
	Calculated current flow		
watts	amp	amp	amp
25	0·13	0·11	0·10
50	0·25	0·23	0·21
100	0·50	0·46	0·42
200	1·00	0·91	0·83
500	2·50	2·27	2·08
750	3·75	3·41	3·13
1 000	5·00	4·45	4·17
1 500	7·50	6·82	6·25
2 000	10·00	9·09	8·33
3 000	15·00	13·64	12·50

(2) Representative Power Ratings of Various Types of Apparatus

	Watts
Boiling ring	1 000
Hot-plate	1 000–2 000
Fire	1 000–3 000
Convector heater	1 000–3 000
Off-peak storage heater	1 500–2 000
Lamp, portable	60–150
Light or light fitting	25–150 (per bulb)
Immersion heater	2 000
Water heater (other than immersion)	2 000
Radio or radiogram	60–100
Television	Up to 150
Blanket or bed-warmer	40

* See Section 4, page 187; the forms appear on pages 189 and 190.

DISCUSSION ON 'AN ASYMMETRICAL INDUCTION MOTOR WINDING FOR 6 : 3 : 2 : 1 SPEED RATIOS'†

Mr. E. W. Krebs (*communicated*): It is interesting to note that the very ingenious 4-speed winding developed by the authors leads to the investigation of asymmetrical and unbalanced windings and their permissibility. Such types of windings are not unknown (as single-speed windings) to designers of small induction motors; they occur when stator stampings have to be used whose number of slots is a multiple of the number of phases. Instances of this kind are 3-phase windings for 6 poles in 24 or 48 slots, or 2-phase windings for 4 poles in 36 slots. The choice of such slot numbers may be dictated by existing stampings or, in the case of multi-speed motors, by the restrictions imposed by the other number of poles. The windings can be single-layer or double-layer, and the number of turns per coil may be equal or different in different phases, sometimes with the wire gauge adjusted to suit the slot filling.

The asymmetries met with such windings include the forms described and investigated in connection with the 4-speed motor. In addition to the slightly different magnitudes of the phase voltages (or their fundamental components), there may be a slight unbalance in their angles, and there may also be sub-harmonics that are more or less unbalanced. I am in complete agreement with the authors that all these types of unbalance do not appear to affect the performance too badly, so long as they are reasonably small and a mesh connection is avoided.

Prof. G. H. Rawcliffe and **Mr. B. V. Jayawant** (*in reply*): We did, of course, know that various forms of asymmetry had previously been tolerated in electrical machinery. The examples with which we are familiar, however, are like those cited by Mr. Krebs, in that the asymmetries have been small and accidental, arising from such things as a desire to use existing slot numbers, rather than an inherent part of the design.

We are glad that Mr. Krebs agrees with us that moderate unbalance does not appear seriously to affect performance, but that it is desirable to avoid a delta connection. It might, however, be noted that we have also shown that a winding which is balanced for fundamental components, but is geometrically asymmetrical, may none the less still be used in delta connection.

† Rawcliffe, G. H., and Jayawant, B. V.: Paper No. 2180 U, December, 1956 (see 103 A, p. 599).

DISCUSSION ON

'AN ELECTRONIC OVER-CURRENT RELAY FOR ELECTRICAL MACHINES'*

Mr. K. W. Goody (*communicated*): I do not agree with the authors' statements regarding the use of the relay shown in Fig. 2 in multi-phase circuits. The most common type of multi-phase working is 3 phase, and if the authors' recommendations to connect the current transformer outputs in either series or parallel are followed, then for a 3-phase symmetrical overload of any magnitude the output will be zero and the relay will not operate.

A fundamental limitation to both circuits exists in the high value of grid resistance necessary to provide a suitable time-constant for the exponential delay. With a grid resistance of several megohms the reverse grid current plays an important part in deciding the standing bias for the valve. Since this reverse grid current is of the order of $0 \cdot 5$–2μA for most valves of the type used, considerable differences in bias, and therefore in sensitivity, can be expected according to the individual reverse current characteristic.

Tests I have recently carried out on a similar circuit arrangement showed a large divergence from the unit calibration when other new valves of the same type were fitted. The alternative to a large value of discharge resistance is a higher value of capacitance, but physical size limitations may not allow this.

The authors suggest that in general their electronic device is far superior in most respects to conventional thermal and magnetic over-current relays. In my opinion a well-designed electro-mechanical over-current relay is preferable for the following reasons: lower production costs; smaller volume occupied; inherent reliability eliminates the need for self-failure protection;

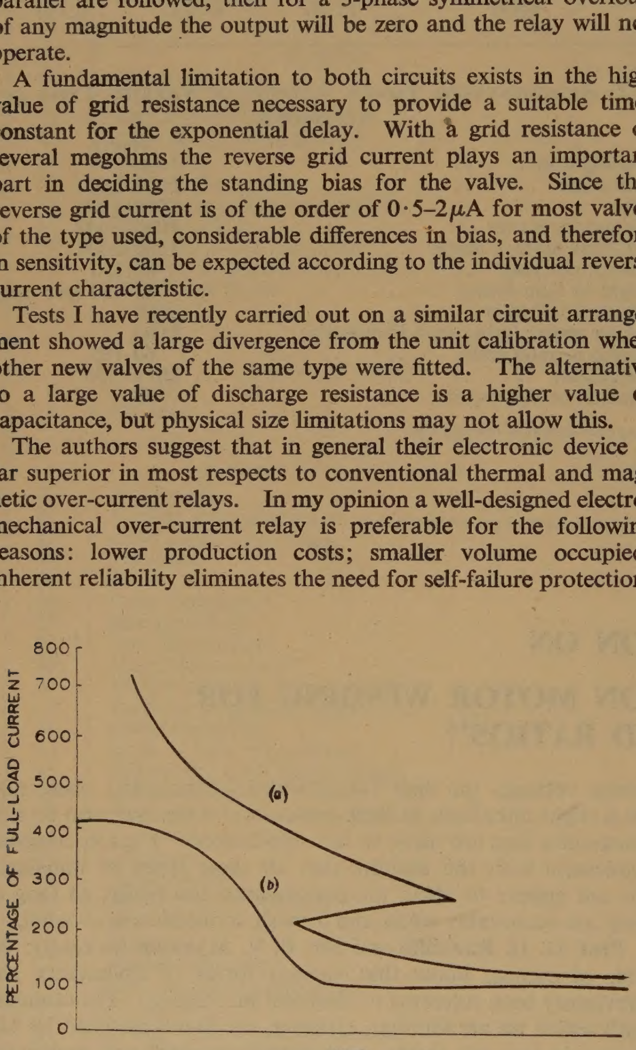

Fig. A

(*a*) Oil dashpot relay with restrainer.
(*b*) Motor starting current.

accuracy easily maintained within B.S. limits ($\pm 10\%$); automatic provision for peak starting currents (see Fig. A).

I consider that the sphere of electronic protection lies within the same bounds as electronic speed control of motors and may be considered as an expensive refinement where other devices will not fulfil the close tolerance requirements of a particular motor drive application.

Messrs. J. S. H. Goodall and **G. S. Chapman** (*in reply*): The fact that the sum of the a.c. outputs of current-sensitive elements when connected in 3-phase circuits is zero if the phases are balanced is well known, but an examination of our circuits will show that rectifiers are interposed between the outputs of the elements and the relay, and hence, owing to the high back resistance of those rectifiers, the positive half-cycles only are presented at the input of the relay. Thus a direct potential proportional to the line current appears at the input.

The reason why Mr. Goody considers a grid resistance of several megohms is necessary is not clear to us. The voltage at the input is generally not more than 50 volts, and hence components of high capacitance and small physical size such as have been developed for use in conjunction with transistors may be utilized.

With reference to Mr. Goody's comparison between electronic and electromagnetic relays we would make the following observations.

The cost of the electronic relay when mass produced is unlikely to be significantly greater than that of the electromagnetic type, since one basic unit only would be required to cover all current ranges, adjustments only being required to the values of a small number of the components in the input network.

Having regard to the large dimensions of most overload coils and their dashpots, it is unlikely that the volume occupied by the electronic relay would be greater to any marked degree.

It is our experience that, in general, the current types of magnetic and thermal overloads are far from reliable, particularly after long periods without operation. It may also be noted that failure to operate due to rusted plungers, stuck pistons in dash-pots and other mechanical failures is not apparent until it is too late. It is not generally possible to test electro-mechanical relays when in circuit, without passing full overload current, whereas the electronic type may readily be tested for both current and delay-time calibrations by use of a small dry battery, as described in the paper.

An accuracy of $\pm 10\%$ is an extremely wide tolerance, perhaps dictated by the limitation of the electromagnetic relay. With the electronic relay we would envisage a tolerance of $\pm 5\%$ on the current calibration and $\pm 2\%$ on the delay-time calibration.

Provision for peak starting current may or may not be automatic, as required. Further, instantaneous operation of the electronic relay is obtained when starting under stall conditions. Fig. A shows that there is a delay in operation of the electromagnetic relay even when it is passing 700% of full-load current, while restrained operation is obtained with as little as twice full-load current. The electronic relay may be arranged to allow say 4 times full-load current for starting, but to give instantaneous operation at 5 times full load while reverting to normal delayed protection immediately the motor current falls to its normal value after the starting-up period has passed.

We regard accurate and reliable protection of electrical machines as a necessity rather than a refinement.

* Goodall, J. S. H., and Chapman, G. S.: Paper No. 2109 U, August, 1956 (see 103 A, p. 375).

PROCEEDINGS OF THE INSTITUTION OF ELECTRICAL ENGINEERS

Part A. POWER ENGINEERING, APRIL 1957

CONTENTS

Bibliographical References.—It is requested that bibliographical reference to an Institution paper should always include the serial number of the paper and the month and year of publication, which will be found at the top right-hand corner of the first page of the paper. This information should precede the reference to the Volume and Part.

Example.—SMITH, J.: 'Overhead Transmission Systems', *Proceedings I.E.E.*, Paper No. 3001 S, December, 1954 (102 A, p. 1234).

Published by The Institution, Savoy Place, London, W.C.2. *Telephone:* Temple Bar 7676. *Telegrams:* 'Voltampere, Phone, London.'
Printed by Unwin Brothers Limited, Woking and London.